

**INVESTIGATION OF
MOLECULAR FACTORS
INVOLVED IN MYCOBACTERIAL
STRESS RESPONSES AND
NON- REPLICATING PERSISTENCE**

Thesis submitted to The University of Leicester for
degree of Doctor of Philosophy

NOR AZIAN HAFNEH

Department of Infection, Immunity and Inflammation,
College of Medicine, Biological Sciences and
Psychology, University of Leicester

October 2017

ABSTRACT

Investigation of molecular factors involved in mycobacterial stress responses and non-replicating persistence

Nor Azian Hafneh

Mycobacterium tuberculosis is a remarkably successful human pathogen due to its ability to switch into dormancy or non-replicating persistence (NRP) phase driven by the host stress microenvironments. Identifying the panoply of genes or pathways involved in dormancy will progress our understanding on latent tuberculosis infection. Rv2660c and Rv2661c (conserved hypothetical proteins) and Rv1675c (transcriptional regulator) were implicated in mycobacterial stress response and transition to dormancy, hence their biological importance in *M. tuberculosis* biology was further explored.

Rv2660c and rv2661c were highly upregulated *in vitro* starvation and *in vivo* infection model, however, recent high upregulation of a noncoding RNA, ncRv12659 in these models challenged the importance of these genes for NRP. A panel of single and double in-frame deletion mutants and over-expressing strains of rv2660c and rv2661c in *M. tuberculosis* were generated. A deletion of rv2660c and rv2661c also resulted in partial inactivation of ncRv12659 and rv2662 respectively. The deletion mutants exhibited normal growth *in vitro* and in mice. Furthermore, the strains showed unimpaired survival under nutrient starvation, hypoxia, oxidative and nitrosative stresses. Quantitative RT-PCR analysis revealed that neither target gene was highly expressed throughout starvation, oxidative and acidic pH stresses.

Rv1675c (Cmr) is a redox sensor that regulates the DosR signalling pathway. Cmr binding to DNA was severely reduced by nitrosation of the two conserved cysteine residues. The cmr mutant displayed survival advantage during exposure to nitrosative stress. The over-expression of cmr or cmr_{C2A} form (mutated cysteines) had a mild inhibitory effect on growth of *M. tuberculosis*. The over-expressing strain of cmr_{C2A} was more resistant to hydrogen peroxide, suggesting that Cmr may also control the response to oxidative stress.

Our study clarified the role of Rv2660c and Rv2661c in growth, NRP and infection, and further highlighted a novel Cmr-mediated regulatory network involved during nitrosative stress and transition to dormancy.

ACKNOWLEDGMENTS

The first person that receives my deepest gratitude is my supervisor, Dr Galina Mukamolova. Her steadfast support, understanding and intellectual guidance from start to finish has been invaluable over the years. I have learned a lot from her and it is truly a privilege to be her student.

I would like to acknowledge The Government of Brunei Darussalam that has funded my studies and the Brunei High Commission staff in London who has taken care of my welfare and stay in UK.

Many thanks to my Progress Review Panel members, Professor Peter Andrew and Professor Mike Barer for their constructive comments and guidance during our annual meetings.

I am very grateful to the past and present colleagues of Lab 213b and 136 for their advice, support and foremost friendship during the challenging years. I am so indebted to Dr Sarah Glenn and Khalid Khan for pMV261::*cmr* and pMV261::*cmr*_{C2A} plasmids, Dr Robert Buxton from NIMR for the *cmr* deletion and complemented strains, Dr Laura Smith for PGS2103 and PGS2475 plasmids, Dr Natalie Lazar and Dr. Asel for the input *in vivo* experiments, Dr Natalie Garton and Malgorzata Wegrzyn for PDIM experiment; Dr Raghad Sanyi who taught me a lot from the start of studies especially tissue culture work, Dr Amin Bakir for advice on qRT-PCR and macrophage infection experiments, Dr Andrew Bell and Jonathan Decker for microscopy work.

My deepest appreciation to my parents; Haji Hafneh and Hajjah Aznah, and parents-in-law; Pehin Haji Abdullah and Datin Hajjah Hasiah- I could not have done this without their prayers, endless advices and belief in me. Special thanks to my siblings; Amirul, Azmi, Nina, Nora, Airul and in-laws for their continuous encouragements and unwavering love.

This thesis is dedicated to my children; Siti Maisarah, Nadyah Fariezah, Mu'iz Hakeem, Muhammad Afeeq and little Aleysha Humaira. The guilt of parting with them in their vulnerable years will always be etched in my memory but above all their continuous love, patience and understanding have kept me determined and motivated.

This thesis is also truly dedicated to my husband and confidante, Firdaus Abdullah. I would have not been able to do my PhD studies without his approval and

commitment as full parent to the children in my absence but importantly for the unwavering love and moral support. Thank you again.

ABBREVIATIONS

AFB	Acid Fast Bacilli
ATP	Adenosine Triphosphate
bp	Base pairs
BCE	Before Common Era
C ₃	Category 3
C _T	Threshold Cycle
CE	Common Era
cAMP	Cyclic Adenosine Monophosphate
c-di-GMP	(3'-5')-Cyclic Dimeric Guanosine Monophosphate
CDS	Coding DNA Sequences
cDNA	Complementary Deoxyribonuclei Acid
CFU	Colony Forming Unit
CFP-10	Culture Filtrate Protein 10
ChIP-Seq	Chromatin Immunoprecipitation- DNA Sequencing
CO	Carbon monoxide
CRP	c-AMP Receptor Protein
DNA	Deoxyribonuclei Acid
DCO	Double Cross Over
DCTB	Differentially Culturable Tubercule Bacilli
DIG	Digoxigenin
DMSO	Dimethyl Sulfoxide
EMSA	Electromobility shift assay
6-FABA	2-Amino-6- Fluorobenzoic Acid
dNTP	Deoxyribonucleotide Triphosphate
EHR.	Enduring Hypoxic Responses
ESAT-6	Early Secreting Antigen Target 6
EPTB	Extra pulmonary Tuberculosis
FBS	Foetal Blood Serum
FNR	Fumarate Nitrate Reductase

GSP	Gene Specific Primers
gDNA	Genomic Deoxyribonuclei Acid
hMDMs	Human Monocytes-Derived Macrophages
H ₂ O ₂	Hydrogen Peroxide
HIV	Human Immunodeficiency Virus
HP	Hypothetical Protein
HTH	Helix turn Helix
InDels	Insertions/ Deletions
IL	Interleukin
IFN- γ	Interferon Gamma
IPTG	Isopropyl B-D-1-Thiogalactopyranoside
LARC	Large Resting Cells
LC-FA	Long Chain Fatty Acid
LOD	Limit of Detection
LPS	Lipopolysaccharide
LTBI	Latent TB Infection
MDR-TB	Multidrug Resistance Tuberculosis
MGIT	Mycobacterial Growth Indicator Tube
MHC Class II	Major Histocompatibility Complex Class II
MIC	Minimum Inhibitory Concentration
MOI	Multiplicity of Infection
MS	Malate Synthase
MSC	Microbiological Safety Cabinet
MTBC	<i>Mycobacterium tuberculosis</i> Complex
NAD	Nicotinamide Adenine Dinucleotide
NAD	Reduced Nicotinamide Adenine Dinucleotide
NBT/BCIP	Nitro Blue Tetrazolium Salt /5-Bromo-4-Chloro-3-Indolyl Phosphate
NRP	Non-replicating Persistence
NO	Nitric Oxide
NOS ₂	Nitric Oxide Synthase 2
NOX ₂	Nicotinamide Adenine Dinucleotide Phosphate-Oxidase 2

OD	Optical Density
PDIM	Phthiocerol Dimycocerosate
(p)ppGpp	Guanosine Pentaphosphate or Tetraphosphate
PBS	Phosphate Buffer Saline
PCR	Polymerase Chain Reaction
PPD	Protein Purified Derivatives
R ²	Correlation Coefficient
RAD	Rapid Anaerobic Model
RNA	Ribonucleic Acid
RNAP	Ribonucleic Acid Polymerase
RNA-Seq	RNA Sequencing
Rpf	Resuscitation Promoting Factor
RR-TB	Rifampicin Resistant Tuberculosis
RNI	Reactive Nitrogen Intermediates
ROI	Reactive Oxygen Intermediates
SD	Standard Deviation
SEM	Standard Error of Mean
SDM	Site- Directed Mutagenesis
SNP	Single Nucleotide Polymorphism
SMRC	Small Resting Cell
TAG	Triacylglycerol
TB	Tuberculosis
TCA	Tricarboxylic Acid
TCSS	Two- component Signal Transduction System
Th1	T helper Cell 1
THP-1	Human Leukemia Monocytic Cell Line
T _m	Melting Temperature
TMM	Trehalose monomycolates
Tn	Transposon
TNF	Tumour Necrotic Factor
TST	Tuberculin Skin Testing

TSS	Transcriptional Start Site
TR	Transcriptional Regulator
TRaSH	Transposon Site Hybridisation
UV	Ultraviolet
WGS	Whole Genome Sequencing
QRT-PCR	Quantitative Real Time Reverse Transcription Polymerase Chain Reaction
XDR-TB	Extreme Drug Resistance Tuberculosis
X-Gal	5-Bromo-4-Chloro-3-Indolyl-B-D-Galactopyranoside

LIST OF FIGURES

Figure 1-1: The three high-burden countries (HBC) list each consist of 30 countries used by World Health Organisation for 2016-2020.....	7
Figure 1-2: Models of dormancy or non-replicating persistence (NRP) in <i>M. tuberculosis</i>	15
Figure 3-1: Schematic representation of the <i>rv266oc</i> and <i>rv2661c</i> genomic region in <i>M. tuberculosis</i>	46
Figure 3-2: Strategy for generation of deletion mutants in <i>M. tuberculosis</i> using homologous recombination approach.	60
Figure 3-3: Physical map of <i>rv2661c-rv266oc</i> region with positions of flanking region and primers used for construction of deletion strains.....	61
Figure 3-4: Overview of Southern Blot hybridisation.	63
Figure 3-5: Gel analysis showing PCR products of wildtype and deletion strain genomic DNA using test primers.	68
Figure 3-6: Southern blot of digested wild-type and deletion strains genomic DNA. .	69
Figure 3-7: Gel analysis showing PCR products of control (empty plasmid) and over-expressing strains using pMV261 primers.	71
Figure 3-8: Growth curve <i>M. tuberculosis</i> deletion strains of <i>rv266oc</i> and <i>rv2661c</i>	74
Figure 3-9: Colony morphology of <i>M. tuberculosis</i> wild-type and deletion strains <i>rv266oc</i> and <i>rv2661c</i>	75
Figure 3-10: Colony morphology of over-expressing strains <i>rv266oc</i> and <i>rv2661c</i> in <i>M. tuberculosis</i>	76
Figure 4-1: Survival of <i>rv266oc</i> and <i>rv2661c</i> deletion strains of <i>M. tuberculosis</i> H37Rv during nutrient starvation.	95
Figure 4-2: Growth and survival of <i>M. tuberculosis</i> wild-type and $\Delta rv2661c:rv266oc$ in Wayne's Hypoxia Model.....	97
Figure 4-3: Effect of oxidative stress on the survival of both deletion and over-expressing of <i>rv266oc</i> and <i>rv2661c</i>	99
Figure 4-4: Effect of nitrosative stress on the survival of both (A) deletion and (B) over-expressing of <i>rv266oc</i> and <i>rv2661c</i>	102
Figure 4-5: Intracellular replication in naïve J774.1 macrophages.....	104

Figure 4-6: Effect of Amikacin on intracellular replication of <i>M. tuberculosis</i> H37Rv during resting THP-1 macrophage infection.....	106
Figure 4-7: Intracellular growth of <i>M. tuberculosis</i> H37Rv infected with different MOIs in resting THP-1 macrophage infection.	107
Figure 4-8: Intracellular replication in THP-1 macrophages using MOI 2.	109
Figure 4-9: Intracellular replication in THP-1 macrophages using MOI 0.5.	110
Figure 4-10: Microscopy images of internalised mycobacterial strains in resting THP-1 cells.	111
Figure 4-11: Intracellular growth of <i>M. tuberculosis</i> wild-type and $\Delta rv2661c:rv2660c$ deletion strain during BALB/c mice infection.	113
Figure 5-1: Genomic organisation of <i>rv1675c (cmr)</i> in <i>M. tuberculosis</i>	133
Figure 5-2: A proposed model for Cmr-mediated nitrosative and oxidative stress responses in regulation of the DosR regulon.	134
Figure 5-3: Whole genome sequencing (WGS) and workflow analysis.	137
Figure 5-4: Gel analysis showing PCR products of control (empty plasmid) and <i>cmr</i> over-expressing strains using pMV261 primers.	139
Figure 5-5: Colony morphology of over-expressing strain of <i>cmr</i> and its mutant variant in <i>M. tuberculosis</i>	140
Figure 5-6: Effect of nitrosative stress on the survival of <i>cmr</i> mutant.	141
Figure 5-7: Normalised expression of <i>cmr</i> during nitrosative stress.	143
Figure 5-8: Effect of oxidative stress on the survival of <i>cmr</i> mutant.	144
Figure 5-9: Effect of cold shock on the survival of <i>cmr</i> over-expressing strain.	145
Figure 5-10: Effect of oxidative stress on the survival of pre-cooled <i>cmr</i> over-expressing strains.	146

LIST OF FIGURES IN APPENDICES

Figure- 1: Plasmid construct for $\Delta rv2660c$ deletion delivery vector, p $\Delta rv2660c$	167
Figure- 2: Plasmid construct for $\Delta rv2661c$ deletion delivery vector, p $\Delta rv2661c$	167
Figure- 3: Plasmid construct for $\Delta rv2661c:rv2660c$ delivery vector, p $\Delta rv2661c:rv2660$ (16,199bp)	168
Figure- 4: Plasmid construct for pMV261:: <i>rv2660c</i>	169
Figure- 5: Plasmid construct for pMV261:: <i>rv2661c</i>	169

Figure- 6: Plasmid construct for pMV261:: <i>rv2661c+rv2660c</i>	170
Figure- 7: Plasmid construct for pMV261:: <i>rv1675c</i> / pMV261:: <i>cmr</i>	171
Figure- 8: Plasmid construct for pMV261:: <i>rv1675_{C2A}</i> / pMV261:: <i>cmr_{C2A}</i>	171
Figure- 9: Sequence map of region amplified with gene specific primers for <i>rv2660c</i> and nCrV12659.....	172
Figure- 10: Melting curves for <i>rv2660c</i> and <i>rv2661c</i> over-expressing and control strains including No-RT and gDNA standard samples using MYCO 16s primers.....	176
Figure- 11: Melting curves for <i>rv2660c</i> and <i>rv2661c</i> over-expressing and control strains including No-RT and gDNA standard samples using RT2660 primers	176
Figure- 12: Melting curves for <i>rv2660c</i> and <i>rv2661c</i> over-expressing and control strains including No-RT and gDNA standard samples using RT2661 primers	177
Figure- 13: Melting curves for <i>rv2660c</i> and <i>rv2661c</i> over-expressing and control strains including No-RT and gDNA standard samples using RT12659 primers	177
Figure- 14: Melting curves for <i>M. tuberculosis</i> wild-type strain including No-RT and gDNA standard samples using MYCO 16s primers from nutrient starvation experiment.....	177
Figure- 15: Melting curves for <i>M. tuberculosis</i> wild-type strain including No-RT and gDNA standard samples using RT2661 primers from nutrient starvation experiment.....	178
Figure- 16: Melting curves for <i>M. tuberculosis</i> wild-type strain including No-RT and gDNA standard samples using RT2662 primers from nutrient starvation experiment.....	178
Figure- 17: Melting curves for <i>M. tuberculosis</i> wild-type strain including No-RT and gDNA standard samples using RT12659 primers from nutrient starvation experiment.....	178
Figure- 18: Melting curves for <i>M. tuberculosis</i> wild-type strain and gDNA standard samples using RT2660 primers.....	179
Figure- 19: Melting curves for <i>M. tuberculosis</i> wild-type strain including No-RT and gDNA standard samples using MYCO 16s primers from oxidative stress (5mM H ₂ O ₂) experiment.....	180

Figure- 20: Melting curves for <i>M. tuberculosis</i> wild-type strain including No-RT and gDNA standard samples using RT2660 primers from oxidative stress (5mM H ₂ O ₂) experiment.....	180
Figure- 21: Melting curves for <i>M. tuberculosis</i> wild-type strain including No-RT and gDNA standard samples using RT2661 primers from oxidative stress (5mM H ₂ O ₂) experiment.....	180
Figure- 22: Melting curves for <i>M. tuberculosis</i> wild-type strain including No-RT and gDNA standard samples using RT2662 primers from oxidative stress (5mM H ₂ O ₂) experiment.....	181
Figure- 23: Melting curves for <i>M. tuberculosis</i> wild-type strain including No-RT and gDNA standard samples using RT12659 primers from oxidative stress (5mM H ₂ O ₂) experiment.....	181
Figure- 24: Melting curves for <i>M. tuberculosis</i> wild-type and $\Delta rv2661c:rv2660c$ strain including No-RT and gDNA standard samples using MYCO 16S primers from oxidative stress (25mM H ₂ O ₂) experiment	182
Figure- 25: Melting curves for <i>M. tuberculosis</i> wild-type and $\Delta rv2661c:rv2660c$ strain including No-RT and gDNA standard samples using RT2660 primers from oxidative stress (25mM H ₂ O ₂) experiment	182
Figure- 26: Melting curves for <i>M. tuberculosis</i> wild-type and $\Delta rv2661c:rv2660c$ strain including No-RT and gDNA standard samples using RT2661 primers from oxidative stress (25mM H ₂ O ₂) experiment	183
Figure- 27: Melting curves for <i>M. tuberculosis</i> wild-type and $\Delta rv2661c:rv2660c$ strain including No-RT and gDNA standard samples using RT2662 primers from oxidative stress (25mM H ₂ O ₂) experiment	183
Figure- 28: Melting curves for <i>M. tuberculosis</i> wild-type and $\Delta rv2661c:rv2660c$ strain including No-RT and gDNA standard samples using RT12659 primers from oxidative stress (25mM H ₂ O ₂) experiment	183
Figure- 29: Melting curves for <i>M. tuberculosis</i> wild-type strain including No-RT and gDNA standard samples using MYCO 16S primers from acid stress experiment	184
Figure- 30: Melting curves for <i>M. tuberculosis</i> wild-type strain including No-RT and gDNA standard samples using RT2660 primers from acid stress experiment ...	184

Figure- 31: Melting curves for <i>M. tuberculosis</i> wild-type strain including No-RT and gDNA standard samples using RT2661 primers from acid stress experiment....	184
Figure- 32: Melting curves for <i>M. tuberculosis</i> wild-type strain including No-RT and gDNA standard samples using RT2662 primers from acid stress experiment ...	185
Figure- 33: Melting curves for <i>M. tuberculosis</i> wild-type strain including No-RT and gDNA standard samples using RT12659 primers from acid stress experiment..	185
Figure- 34: Melting curves for <i>cmr</i> and <i>cmr_{C2A}</i> over-expressing and control strains including No-RT and gDNA standard samples using MYCO 16s primers.....	186
Figure- 35: Melting curves for <i>cmr</i> and <i>cmr_{C2A}</i> over-expressing and control strains including No-RT and gDNA standard samples using RT1675 primers.....	186
Figure- 36: Melting curves for <i>M. tuberculosis</i> wild-type, <i>cmr</i> deletion and complemented strains and gDNA standard samples using MYCO 16S primers from nitrosative stress experiment.....	187
Figure- 37: Melting curves for <i>M. tuberculosis</i> wild-type, <i>cmr</i> deletion (green lines) and complemented strains and gDNA standard samples using RT1675 primers from nitrosative stress experiment.....	187

LIST OF TABLES

Table 2-1- <i>M. tuberculosis</i> bacterial strains and plasmids used in the study (mentioned in Chapter 3, 4 and 5).....	32
Table 3-1: Expression of <i>rv2660c</i> , <i>rv2661c</i> and <i>rv2662</i> in various <i>in vitro</i> NRP and stress models analysed by microarray. T	51
Table 3-2: Expected sizes for each PCR products using respective test and ‡gene specific primers	68
Table 3-3: Expected band sizes of <i>HindIII</i> and <i>NheI</i> digested wildtype and deletion strains hybridised with DIG-labelled 2660FR2 DNA fragment.....	69
Table 3-4: Relative expression of <i>rv2660c</i> and <i>rv2661c</i> in control and respective over-expressing strains.....	72
Table 3-5: Growth parameters of wildtype and deletion strains of <i>rv2660c</i> and <i>rv2661c</i> grown in standard culture media.....	75
Table 4-1: Compilation of relative expression induction ratio of <i>rv2660c</i> , <i>rv2661c</i> , <i>rv2662</i> and ncRv12659 transcripts in <i>M. tuberculosis</i> compared to exponential growth.. ..	116
Table 4-2: Comparison of <i>rv2660c</i> , <i>rv2661c</i> , <i>rv2662</i> and ncRv12659 transcripts detected between published studies and the current study.	118
Table 5-1: Relative expression of <i>cmr</i> in control and respective over-expressing strains.	139
Table 5-2: Comparison of the genomic sequences of <i>M. tuberculosis</i> wildtype H37Rv and <i>cmr</i> mutant strain	150

LIST OF TABLES IN APPENDICES

Table - 1: List of primers used for construction and confirmation of deletion and over-expressing strains in <i>M. tuberculosis</i>	165
Table - 2: List of gene specific primers used in qRT-PCR	166
Table - 3: QRT-PCR assay performance for confirmation of over-expressing strains of <i>rv2660c</i> and <i>rv2661c</i> in <i>M. tuberculosis</i> (Chapter 3)	173
Table - 4: QRT-PCR assay performance for nutrient starvation experiment (Chapter 4)	173

Table - 5: QRT-PCR assay performance for oxidative stress experiment (Chapter 4)	174
Table - 6: QRT-PCR assay performance for acidic pH, pH5.3 (Chapter 4)	174
Table - 7: QRT-PCR assay performance for confirmation of over-expressing strains of <i>cmr</i> and <i>cmr</i> _{C2A} strains	175
Table - 8: QRT-PCR assay performance for nitrosative stress experiment	175

TABLE OF CONTENTS

ABSTRACT	I
ABBREVIATIONS.....	IV
LIST OF FIGURES.....	VIII
LIST OF TABLES.....	XIII
CHAPTER 1 INTRODUCTION.....	2
1.1 Tuberculosis as an ancient disease with modern problems.....	2
1.2 Global status of Tuberculosis threat.....	5
1.3 General characteristics of <i>Mycobacterium tuberculosis</i> complex.....	8
1.4 Overview of the TB disease process.....	10
1.5 Dormancy and non-replicating persistence.....	13
1.6 Experimental systems for generation of dormant mycobacteria.....	15
1.6.1 <i>In vitro</i> models.....	15
1.6.2 <i>In vivo</i> models.....	21
1.7 Mycobacterial factors involved during non-replicating persistence.....	23
1.7.1 Transcriptional regulators (TRs).....	23
1.7.2 Non-coding RNA (ncRNA).....	24
1.8 Aims and specific objectives.....	26
CHAPTER 2 GENERAL METHODS AND MATERIALS.....	28
2.1 Reagents and growth media.....	28
2.1.1 Reagents and chemicals.....	28
2.1.2 Growth media and supplements.....	28
2.2 Bacterial strains.....	29
2.3 Preparation of bacterial stocks for <i>in vitro</i> experiments and infection....	33
2.3.1 Starter culture.....	33
2.3.2 Preparation of frozen stocks of mycobacterial strains.....	33
2.4 Optical density measurements.....	33
2.5 Colony forming unit counts.....	34
2.6 General <i>In vitro</i> stress assays.....	34

2.6.1	Oxidative stress	34
2.6.2	Nitrosative stress.....	34
2.6.3	Microdilution Resazurin Assay.....	35
2.7	Heat Inactivation of mycobacteria for PCR.....	35
2.8	Deoxyribonucleic acid (DNA) Manipulations	36
2.8.1	Polymerase chain reaction (PCR).....	36
2.8.2	Agarose gel electrophoresis	37
2.8.3	DNA and plasmid purification.....	37
2.8.4	Restriction enzyme digestion	37
2.8.5	Ligation	38
2.8.6	Transformation	38
2.8.7	Electroporation	38
2.9	Isolation of Genomic DNA from <i>M. tuberculosis</i> strains	39
2.10	Ribonucleic acid (RNA) Manipulations	39
2.10.1	Preparation of Guanidine Thiocyanate (GTC) solution	39
2.10.2	RNA extraction from <i>M. tuberculosis</i>	40
2.10.3	RNA cleanup and purification	40
2.10.4	Measuring RNA concentration	41
2.10.5	Reverse transcription.....	41
2.10.6	Quantitative Real Time PCR (qpcr).....	41
2.10.7	Analysis of qRT-PCR	42
2.11	Statistical analysis	44
CHAPTER 3	INITIAL INVESTIGATIONS ON DETERMINING THE ESSENTIALITY OF <i>RV266oC</i> AND <i>RV266iC</i> IN <i>MYCOBACTERIUM TUBERCULOSIS</i>	46
3.1	Introduction.....	46
3.1.1	Construction of genetic deletions in <i>M. tuberculosis</i> H37Rv	52
3.1.2	Construction of over-expressing strains in <i>M. tuberculosis</i>	55
3.2	Methods	58
3.2.1	Bacterial strains.....	58
3.2.2	Generation of single and double deletion of <i>rv266iC</i> and <i>rv266oC</i> strains in <i>M. tuberculosis</i>	58

3.2.3	Southern Blot Hybridisation	62
3.2.4	Generation of single and double over-expressing strains of <i>rv2661c</i> and <i>rv2660c</i> strains in <i>M. tuberculosis</i>	64
3.2.5	qRT-PCR.....	64
3.2.6	<i>In Vitro</i> growth analysis.....	64
3.2.7	Determination of MIC using 2-amino-6- fluorobenzoic acid (6-FABA) ..	65
3.3	Results.....	66
3.3.1	Confirmation of <i>rv2661c</i> and <i>rv2660c</i> deletion strains in <i>M. tuberculosis</i> H37Rv	66
3.3.2	Confirmation of the over-expressing strains of <i>rv2661c</i> and <i>rv2660c</i> in <i>M. tuberculosis</i> H37Rv	70
3.3.3	<i>In vitro</i> growth of <i>rv2660c</i> and <i>rv2661c</i> deletion strains in standard culture medium	73
3.3.4	<i>In vitro</i> growth of over-expressing strains of <i>rv2660c</i> and <i>rv2661c</i> in standard culture medium	76
3.3.5	Sensitivity of <i>rv2660c</i> and <i>rv2661</i> deletion mutants to 6-FABA compound	77
3.4	Discussions	78
3.4.1	Successful generation of deletion and over-expressing strains of <i>rv2660c</i> and <i>rv2661c</i> in <i>M. tuberculosis</i>	78
3.4.2	Deletion and over-expression of <i>rv2660c</i> and <i>rv2661c</i> in <i>M. tuberculosis</i> have not affected growth <i>in vitro</i>	80
3.4.3	Deletion of <i>rv2660c</i> and <i>rv2661c</i> do not affect sensitivity of <i>M. tuberculosis</i> to 6-FABA.....	81
3.5	Conclusions	82
CHAPTER 4	INVESTIGATING THE ROLE OF <i>RV2660C</i> AND <i>RV2661C</i> IN <i>MYCOBACTERIUM TUBERCULOSIS</i> DURING INFECTION.....	84
4.1	Introduction.....	84
4.2	Materials and methods.....	87
4.2.1	<i>In vitro</i> non-replicating persistence models and stress experiments.....	87

4.2.2	Thin Layer Chromatography (TLC) of phthiocerol dimycocerosate (PDIM) analysis.....	88
4.2.3	Macrophage infection and microscopy.....	89
4.2.4	Murine infection	92
4.3	RESULTS.....	94
4.3.1	Phenotypic characterisation of <i>rv266oc</i> and <i>rv2661c</i> deletion and over-expressing strains of <i>M. tuberculosis</i> H37Rv during <i>in vitro</i> non-replicating persistence and under stress exposure	94
4.3.2	Intracellular replication and survival of <i>rv2661c</i> and <i>rv266oc</i> deletion strains in macrophages.....	103
4.3.3	Replication of <i>rv2661c</i> and <i>rv266oc</i> deletion strains in BALB/c mice.....	112
4.3.4	Gene Expression Profiling of <i>rv266oc</i> , <i>rv2661c</i> , <i>rv2662</i> and ncRv12659 by qRT-PCR.....	114
4.4	DISCUSSIONS.....	117
4.4.1	The <i>rv2661c</i> and <i>rv266oc</i> genomic region does not influence <i>M. tuberculosis</i> survival in PBS	117
4.4.2	The <i>rv2661c</i> and <i>rv266oc</i> genomic region does not influence <i>M. tuberculosis</i> survival during hypoxia.....	119
4.4.3	Deletion and over-expressing <i>rv2661c</i> and <i>rv266oc</i> did not affect the ability of <i>M. tuberculosis</i> to survive during oxidative and nitrosative stress.....	120
4.4.4	Low transcriptional response of <i>rv266oc</i> , <i>rv2662</i> and ncRv12659 in <i>M. tuberculosis</i> when exposed to acidic pH 5.3.....	123
4.4.5	Macrophage infection	124
4.4.6	Replication of double <i>rv2661c</i> and <i>rv266oc</i> mutant in mice	127
4.5	Conclusions	129
CHAPTER 5	INVESTIGATING THE ROLE OF <i>RV1657C</i> (<i>CMR</i>) IN <i>MYCOBACTERIUM TUBERCULOSIS</i> DURING <i>IN VITRO</i> STRESS CONDITIONS.....	131
5.1	Introduction.....	131
5.2	Materials and methods.....	135
5.2.1	Bacterial strains.....	135

5.2.2	Construction of over-expressing strains of <i>cmr</i> and <i>cmr</i> mutant variant	135
5.2.3	Combined cold and oxidative stress experiments.....	136
5.2.4	qRT-PCR.....	136
5.2.5	Whole genome sequencing	136
5.3	Results.....	138
5.3.1	Confirmation of the identity of the <i>cmr</i> over-expressing strains in <i>M. tuberculosis</i> H37Rv	138
5.3.2	<i>In vitro</i> growth of the <i>cmr</i> over-expressing strains	140
5.3.3	Investigating the role of <i>cmr</i> in survival of <i>M. tuberculosis</i> in response to <i>in vitro</i> stress (Published in Smith et al., 2017).....	141
5.3.4	Oxidative Stress	143
5.3.5	Whole genome sequencing of <i>M. tuberculosis</i> strains	147
5.4	Discussions.....	151
5.4.1	<i>Cmr</i> plays a significant role in the survival of <i>M. tuberculosis</i> during nitrosative stress	151
5.4.2	The lack of complementation was not caused by SNPs in either wild-type or <i>cmr</i> mutant strain.	152
5.4.3	Phenotypic characterisation of <i>cmr</i> and <i>cmr</i> mutant variant (<i>cmr</i> _{C2A}) over-expressing strains in <i>M. tuberculosis</i>	154
5.5	Conclusions	156
CHAPTER 6 FINAL CONCLUSIONS AND FUTURE PERSPECTIVES.....		158
APPENDICES		164
Appendix 1.	List of primers used for construction and confirmation of deletion and over-expressing strains	164
Appendix 2.	Gene specific primers used in qrt-pcr	166
Appendix 3.	Deletion delivery plasmid vectors of <i>rv2660c</i> and <i>rv2661c</i> constructed using flexible cassette method.....	167
Appendix 4.	Plasmid constructs used for generation of over-expressing strains	169

Appendix 5. Sequence map of region amplified using gene- specific primers for <i>rv2660c</i> and <i>ncrv12659</i>	172
Appendix 6. qrt-pcr assay performance	173
Appendix 7. Melting curves.....	176
Appendix 8. Target gene copy numbers and relative expression values.....	188
Appendix 9. Publication	191
REFERENCES.....	191

CHAPTER 1

Introduction

CHAPTER 1 INTRODUCTION

1.1 TUBERCULOSIS AS AN ANCIENT DISEASE WITH MODERN PROBLEMS

Tuberculosis (TB) is an ancient scourge and has plagued humankind with the surge of great epidemics and then receded. However, it remains a significant public health challenge (Daniel, 2006). TB spondylitis that leads to Pott's disease, one of the oldest described diseases, is characterised by spinal deformity with progressive changes of the vertebral column (kyphosis) leading to damage and eventual paralysis (Boachie-Adjei and Squillante, 1996, Spiegel et al., 2005). Paleopathological studies of human skeletal remains with these spinal characteristics have led to suggestions that TB existed from the Neolithic period (3200-2300 BCE) and was culturally associated with the earliest cattle breeders and also Egyptian mummies dating back from 1000 BCE to 400 CE (Zimmerman, 1979, Crubézy et al., 1998). A combination of biomolecular techniques using lipid biomarkers and DNA analysis of human remains excavated from Atlit Yam in the Eastern Mediterranean, has shown that the earliest case of human TB was in the pre-Neolithic period (6200-5500 BCE) (Galili et al., 1993). Evidence of TB in other geographical sites in Ain Ghazal, Jordan that dated back to 7250 BCE (El-Najjar et al., 1996, Hershkovitz et al., 2015). Further analysis of Atlit Yam's remains indicated infection with 'ancestral' *Mycobacterium tuberculosis* lineage with TbD₁¹ deletion that existed approximately 9000 years ago (Hershkovitz et al., 2015, Brosch et al., 2002). Some studies have suggested that *M. tuberculosis* emerged 40,000 years ago and this coincided with the expansion of "modern" human populations (*Homo sapiens*) migrated out of Africa (Wirth et al., 2008, Mellars, 2006). However, the time scale and geographical origin of TB remain uncertain.

TB was also reported as *phthisis* by the prominent Greek physician Hippocrates (460-370 BCE) who gave a clear description of post-traumatic kyphosis, presentation of

¹ Human-adapted *M. tuberculosis* strains are grouped into seven main lineages, each of which is primarily associated with distinct geographical distribution. *M. tuberculosis* specific deletion, TbD₁ indicates the deletion event specific for *M. tuberculosis* lineages 2 (East Asia), 3 (India and East Africa) and 4 (Europe and America) (Galagan et al., 2014)

hard tubercles in lungs and abscesses found around the lumbar region (Vasiliadis et al., 2009, Herzog, 1998). During the 17th century, scrofula (TB of lymph nodes) also known as 'the King's-Evil' was reported and believed to be cured by the monarch's touch. Through the 18th and 19th centuries, the TB epidemic had spread across Europe and America coinciding with western urbanisation and industrialisation. 'Consumption', 'the white death' and 'the graveyard cough' were names describing TB during this catastrophic period (Frith, 2014).

The first breakthrough in TB research was in 1865 by Jean Antoine Villemin, a French military surgeon who demonstrated that TB from man or cow was transmissible into rabbits or guinea pigs (Frith, 2014). Robert Koch's discovery of the methylene blue stained-bacilli- '*tubercule bacillus*' grown in medium containing cattle serum in 1882 finally elucidated that an infectious bacterium, *Mycobacterium tuberculosis*, detected in sputum samples, caused TB (Blevins and Bronze, 2010, Sakula, 1982). In 1890, Koch proposed an application of tuberculin obtained from *M. tuberculosis* culture filtrates as a new cure for TB. However, tuberculin failed to demonstrate any positive therapeutic effect (Sakula, 1982). Koch's discovery later paved the way for the development of the Pirquet (von Pirquet, 1909) and Mantoux (Mantoux, 1912) tuberculin skin tests (TST) and Albert Calmette and Camille Guérin's BCG vaccine (Hawgood, 2007).

BCG is a live vaccine derived through attenuation of *Mycobacterium bovis*. It is the only licensed vaccine against TB, and this vaccine has been used as part of national childhood immunisation programmes for more than 80% of neonates and infants in countries over the last 80 years (WHO, 2015). The post-vaccination protection is not life-long and only lasts for 10-20 years (Sterne et al., 1998). The efficacy varies from none to 80%, where the lowest protection is conferred in the highest TB burden countries (Fine, 1995). The difficulty in establishing the protective efficacy of the vaccine is due to the limitation of TST. The purified protein derivative (PPD) that contains numerous *M. tuberculosis* antigens can cross-react with BCG and non-tuberculosis mycobacteria (NTM) producing a positive TST result (O'Garra et al., 2013). TST involves intradermal administration of PPD also called tuberculin (Nayak and Acharjya, 2012) and a delayed-type hypersensitivity response develops within 24–48 hours in the form of swelling and reddening at the site of injection (Andersen and Doherty, 2005). TST has been replaced with the recently developed Interferon

Gamma Release Assays (IGRA). QuantiFERON-®TB GOLD is an IGRA test that measures a release of interferon-gamma (IFN- γ) by T-cells following stimulation by *M. tuberculosis*-specific secreted antigens, ESAT-6 (early secretory antigenic target 6) and CFP-10 (culture filtrate protein 10) (Mazurek and Villarino, 2002). These antigens are absent in BCG and found in very few NTM strains (LoBue and Castro, 2012), making it more specific in BCG- vaccinated individuals. Due to the poor efficacy of BCG vaccine, development of novel and effective vaccination strategies against pulmonary TB has become a priority in TB research.

The global TB incidence started to decline with the introduction of streptomycin in 1944 until most of the infected patients later developed streptomycin-resistant strains with minor improvement in mortality over untreated patients (Medical Research Council Streptomycin in Tuberculosis Trials Committee, 1948). Nevertheless, it was only in the early 1990s that drug-resistant TB began to receive global attention as a public health threat. In line with the emergence of multi-drug resistant (MDR) and extremely drug-resistant (XDR) TB strains, the recommended antibiotic treatment was prolonged and included an extended cocktail of anti-TB drugs regime for an effective cure (Mitchison, 2005). The combination of the toxic and lengthy treatment resulted in poor patient adherence to treatment further decreasing the progress of TB elimination (Quenard et al., 2017). In addition, the slow progress is contributed by the advent of human immunodeficiency virus (HIV) as well as poverty, weak TB control programs and the small investments in research and development (Ormerod, 2005, Chadha, 1997, Mayer and Hamilton, 2010). Furthermore, the challenges posed by resource-limited countries, which are usually the high TB burden areas, include lack of funding or expertise to implement a rapid and accurate point-of-care TB diagnostic settings. In most cases, they have to resort to sputum microscopy, the commonly used diagnostic method which is insensitive for HIV co-infected patients and children as the bacillary load is much reduced (Getahun et al., 2007). An estimated investment of 1- 3 trillion US dollars will be required to cover the cost of global TB treatment for the next ten years, presenting significant financial strains for developed and especially developing countries (Global TB Alliance).

1.2 GLOBAL STATUS OF TUBERCULOSIS THREAT

The World Health Organisation (WHO) declared TB as a global emergency in 1993 (WHO, 2016). In 2015, WHO reported an estimated 10.4 million new (incident) TB cases world wide (WHO, 2016). A global population growth to over 7 billion in 2014 corresponds to the increase of TB burden. The six countries with the highest human population (India, Indonesia, China, Nigeria, Pakistan and South Africa) account for 60% of the global TB cases (WHO, 2016, Economic et al., 2015). Countries with an absolute number of TB incident cases of 10000 or 1000 MDR, or TB-HIV cases per year, are classified as high TB burden countries as shown in Figure 1-1 (WHO, 2016). The number of TB deaths fell by 22% between 2000 and 2015, but TB remained one of the top ten causes of death worldwide in 2015 (WHO, 2016).

In 2014 approximately 1.7 billion individuals, a quarter of the global population, were considered as latently infected (Houben and Dodd, 2016). Latent TB infection (LTBI) is characterised by the absence of clinical and radiological signs of active disease, with evidence of immune sensitisation to mycobacterial antigens (Barry et al., 2009). LTBI patients are believed to be clinically non-infectious, and infected individuals have a 10% lifetime risk of TB reactivation (Nahid and Daley, 2006), resulting in the spread of *M. tuberculosis* to close contacts (Lillebaek et al., 2002).

HIV co-infection is the major risk factor for progression of latent *M. tuberculosis* infection to active disease and increases the risk of TB reactivation by 20-fold (Getahun et al., 2010, Selwyn et al., 1989). Likewise, TB has been reported to exacerbate HIV infection (Whalen et al., 1995, Modjarrad and Vermund, 2010), accounting for about 26% of AIDS-related deaths (Getahun et al., 2010). In 2015, people living with HIV accounted for 1.2 million (11%) of all new TB cases (WHO, 2016).

In 2015, there were an estimated 480 000 new cases of MDR-TB, TB caused by *M. tuberculosis* strains resistant to at least isoniazid and rifampicin, the two most effective anti-TB drugs. The statistic includes an additional 100 000 people with rifampicin-resistant TB (RR-TB) who were also eligible for MDR-TB drug regimen. RR-TB is defined as TB resistant to rifampicin, with or without resistance to other drugs including MDR-TB, and are referred to as MDR/RR-TB (WHO, 2017). Unfortunately, 250 000 deaths from MDR/RR-TB were reported in 2015 (WHO, 2016) with worldwide

treatment success of almost 50% (Zumla et al., 2015). By 2050, the number of deaths by MDR-TB is estimated to approach 2.5 million (TB Alliance, 2017).

The increase of XDR-TB in 92 countries where 9.5% of MDR-TB strains have XDR-TB, has exacerbated the global TB burden. This strain has an additional resistance to any of the fluoroquinolones (such as levofloxacin or moxifloxacin) and at least one of the three injectable second-line drugs (amikacin, capreomycin or kanamycin). Treatment of patients infected with MDR-TB is expensive and requires a longer duration of more than two years (WHO, 2016). Total Drug-Resistant Tuberculosis (TDR-TB) is a generic definition for TB resistant to all first and second line drugs (Velayati et al., 2009). TDR-TB cases were reported in Italy (Migliori et al., 2007), India (Udwadia et al., 2012) and South Africa (Klopper et al., 2013) where reports raise further public health concern as it indicated current regimen failure.

To eliminate TB, WHO has developed a global TB strategy with a perspective beyond 2015 in line with the Millennium Development Goals and the Stop TB Partnership targets (WHO, 2010, WHO, 2014). TB elimination is defined as a reduction of TB to less than one case per million population (WHO, 2014). The goal is to reduce global TB incidence from more than 1000 cases per million population today, to less than 100 cases per million by 2035 (Raviglione and Ditiu, 2013). The STOP TB strategy launched in 2006 includes expansion of high quality directly observed treatment, short-course (DOTS) (WHO, 2010). DOTs strategy aims to detect at least 70% of the existing sputum smear-positive TB cases and to cure at least 85% of these newly detected ones (WHO, 2002).

The strategy also addresses TB-HIV, MDR-TB, the needs of poor and vulnerable populations and development of new diagnostic tools, drugs and vaccines (WHO, 2010).

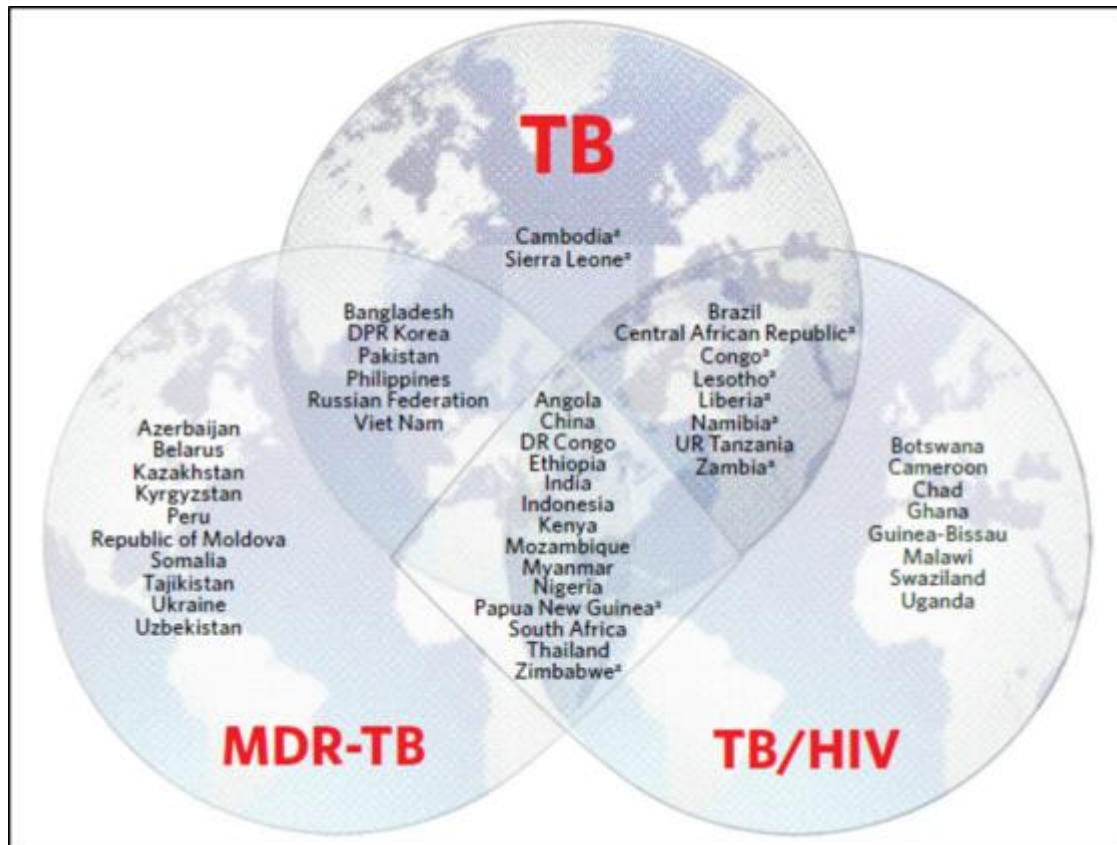


Figure 1-1: The three high-burden countries (HBC) list each consist of 30 countries used by World Health Organisation for 2016-2020. The three new HBC lists each account for 85-89% of global burden. There are 14 countries (shown in central diamond in the figure) that are burdened not only with TB but MDR-TB (multidrug-resistant TB) and TB/ HIV co-infection (WHO, 2016)

1.3 GENERAL CHARACTERISTICS OF *MYCOBACTERIUM TUBERCULOSIS* COMPLEX

Human and animal TB are caused by the *Mycobacterium tuberculosis* complex (MTBC) which includes *Mycobacterium africanum*, *Mycobacterium bovis*, *Mycobacterium microti*, *Mycobacterium caprae*, *Mycobacterium orygis*, *Mycobacterium pinnipedii*, *Mycobacterium mungi* (van Ingen et al., 2012, Brosch et al., 2002, Alexander et al., 2010). In addition, the actual host range for *M. cannettii*, the 'smooth colony' bacilli remain unknown (Gutierrez et al., 2005, Koeck et al., 2011). The members of MTBC exhibit more than 99.9% similarity in DNA sequences (Cole et al., 1998). Despite the high overall genetic relationship, the MTBC species show variability in their phenotypes, host range and importance for human TB. *M. bovis* and phylogenetically related strains have a lower transmissibility for the human host compared to *M. tuberculosis*, and mutations of two-way component regulation system PhoP/PhoR (PhoPR) are believed to be contributing factors to this attenuation (Gonzalo-Asensio et al., 2014).

The genus of mycobacteria belongs to class Actinomycetales that includes genera Actinomyces and Nocardia. The name *myco* has the meaning fungus-like alluding to the observation that mycobacteria grow in a filamentous manner on the surface of liquid culture media (Kerr and Barrett, 1917). The mycobacterial cell wall has a complex structure and consists of three distinct macromolecules; peptidoglycan, arabinogalactan and mycolic acids which are surrounded by a non-covalently linked outer membrane of proteins and polysaccharides. The high-density lipid formation gives a characteristic thick waxy lipid coat that contributes to virulence (Barry et al., 2007, Domenech and Reed, 2009). Mycobacteria are classified as acid-fast bacilli as they can retain the Carbol fuchsin dye (such as in Ziehl-Neelson stain) and resist decolourisation with acid. Mycolic acids are predominately covalently bound to the arabinogalactan polysaccharide, and some are found as trehalose monomycolates (TMM) and dimycolates, reviewed in (Minnikin et al., 2002). The TMM contributes to the distinct 'rope-like form' or serpentine cords produced by virulent *M. tuberculosis* strains (Besra and Chatterjee, 1994).

Members of genus *Mycobacterium* were also earlier classified by their growth rates (Stahl and Urbance, 1990). Fast-growing mycobacteria form colonies within seven

days, such as *M. smegmatis*. Slow growing mycobacteria are mostly pathogenic and include *M. tuberculosis* (generation time of 15-20 hours) (Haas and Des Prez, 1995) and *M. leprae*, take from weeks to months to form colonies (Stahl and Urbance, 1990). *M. tuberculosis* grows on liquid broth (such as Middlebrook 7H9, Dubos or Sauton's medium) or egg-based solid medium such as Lowenstein-Jensen (LJ) (Lee et al., 2004) (Lee et al., 2004) medium. Colonies are usually dry, non-pigmented and have a rough surface. Due to slow growth of colonies in LJ medium (3 weeks to 3 months) (Naveen and PeeraPur, 2012, Mayer and Hamilton, 2010), WHO has recommended the use of liquid culture systems such as BD mycobacteria growth indicator tube (MGIT) system (Becton Dickinson, USA) to increase culture positivity. The clinical samples are incubated in a modified Middlebrook's medium and supplemented with MGIT PANTA antimicrobial mixture (Polymyxin B, Amphotericin B, Nalidixic acid, Trimethoprim and Azlocillin) to suppress the growth of contaminants. The MGIT tube contains a fluorochrome, 4, 7-diphenyl-1, 10-phenanthroline ruthenium chloride pentahydrate that is embedded in a silicone base, fluorescence is quenched by the free oxygen present in the tube. Bacterial growth results in oxygen consumption which would proportionally increase in the intensity of fluorescence. The monitoring of fluorescence is done automatically every 60 minutes, and any detectable increase in fluorescence will alert the operator (Siddiq and Rusch-Gerdes, 2006). The sensitive and rapid culture detection system also provides a more accurate susceptibility testing assay for isoniazid, rifampicin, streptomycin, ethambutol and pyrazinamide (first line anti-TB drugs) (WHO, 2007) rather than conventional agar method (Tortoli et al., 2002). Nevertheless, one of the drawbacks of this system is that the positive culture requires further investigations such as microscopy to confirm the presence of AFB bacilli and not due to growth of contaminants.

1.4 OVERVIEW OF THE TB DISEASE PROCESS

M. tuberculosis infection is complex, and the classification of TB infection as active disease and LTBI had always been conceptualised simply for clinical definitions and treatment choices (Barry et al., 2009). The diagnosis of *M. tuberculosis* infection has been made through laboratory investigations such as microscopy and culture of clinical samples, TST and chest X-ray (Piccazzo et al., 2014, Esmail et al., 2014). In fact, TB is viewed as a continuous spectrum of infection which extends from sterilising immunity, to the presentation of subclinical disease, through active fulminant disease (active disease) characterised by a range of lesions to support bacterial replication, persistence or killing (Barry et al., 2009). Each stage stated above depends on the host immune status and infection can remain quiescent for decades (LTBI) (Schnappinger and Ehrt, 2016) to be later disrupted resulting disease reactivation (Barry et al., 2009). This section provides an overview of the different stages of events during the infection process from a cellular perspective for both bacilli and its host.

Early stages- Approximately 95% of those exposed to *M. tuberculosis* will be able to control infection, and the rest will develop pulmonary pathology in the first year (O'Garra et al., 2013). Infection is usually initiated by inhalation of aerosolised *M. tuberculosis* expectorated by patients with active pulmonary TB and is much effectively transmitted through coughing (Yates et al., 2016). Infection develops in the apices of lungs (area of high oxygen tension) (Im et al., 1995). The inhaled bacilli are phagocytosed and differentially distributed by resident alveolar macrophages, recruited interstitial macrophages, monocytes, dendritic cells, and neutrophils (Srivastava et al., 2014). The phagocytosis of the pathogen is the first line of host defence against the pathogen. Most of the internalised bacilli are subjected to killing, and a proportion of the pathogen can adapt to the intraphagosomal environment making it a niche in which to reside and proliferate. Corresponding to this event, the host releases proinflammatory cytokines and chemokines such as IFN- γ and Interleukin (IL)- 2 and macrophages will be activated (Srivastava et al., 2014). These immune effector cells will then shift in their function to accommodate microbicidal activity and antigen presentation (Russell et al., 2009). The cellular immunity is initiated and mediates formation of the granuloma shortly after infection (Davis et al., 2002, Braian et al., 2015). The response will also lead to recruitment of lymphocytes

(Th₁ cells and CD8⁺ cytotoxic T cells) and migration of infected dendritic cells to local lymph nodes in the lungs (Sia et al., 2015).

The ability of *M. tuberculosis* to persist intracellularly is contributed to by a portfolio of survival strategies adopted *in vitro*. The inhibition of phagosome-lysosome fusion was proposed as central to the survival of *M. tuberculosis* within human macrophages. Inhibition of the fusion is achieved by pathogen-mediated manipulation of host signalling pathways, which ensures that the bacteria remain in early endosome (Podinovskaia et al., 2013, Ehrt and Schnappinger, 2009) and thus prevents delivery of the bacilli to an acidic (~ pH5.2) and hydrolytic compartment (Tan and Russell, 2015, Ramachandra et al., 2001). Other strategies used by the pathogen involved phagosomal rupture mediated by the ESX-1 type VII secretion system (ESX-1 SS) (Simeone et al., 2015) and this was further enhanced by presence of phthiocerol dimycocerosates (PDIM), a mycobacterial cell wall lipid (Augenstreich et al., 2017). The ESX-1 SS is a critical secretion system in both *M. tuberculosis* and *M. marinum* that delivers at least four virulence factors such as ESAT-6, CFP-10, EspA, and EspB to the host macrophages during infection (McLaughlin et al., 2007, Xu et al., 2007, Fortune et al., 2005, Sasseti and Rubin, 2003). The rupture can lead to a cytosolic translocation of *M. tuberculosis*, a dynamic process that was speculated to facilitate the escape of the pathogen from intracellular environment (Jamwal et al., 2016).

Survival of *M. tuberculosis* is not only attributed by manipulating the host cell processes but also the ability to resist stresses induced from immunologically activated macrophages. Generation of reactive oxygen intermediates (ROI) and reactive nitrogen intermediates (RNI) are the main mechanism activated in the mature macrophage phagosome that inhibit *M. tuberculosis* proliferation *in vivo* (MacMicking et al., 1997a, Ehrt and Schnappinger, 2009). ROI are oxygen-derived small molecules, including oxygen radicals [superoxide (O₂⁻), hydroxyl (·OH), peroxy (RO₂·), and alkoxy (RO·)] which are further converted to oxygen derivatives such as hydrogen peroxide (H₂O₂). Nitrogen-containing oxidants, such as nitric oxide (NO·) are called RNI (Bedard and Krause, 2007). Together with ROI, NO generates peroxynitrite (a strong oxidant), and collectively these molecules damage mycobacterial biomolecules such as DNA, lipids and proteins. The two phagosomal enzymes; phagocyte NADPH oxidase, NOX2 and inducible nitric oxide synthase, iNOS

produce ROI and RNI respectively (Ehrt and Schnappinger, 2009). It was found that the iNOS-deficient mice are more susceptible to TB infection rather than NOX2-deficient mice, however, this still indicates the vital role of both enzymes in defence against the pathogen (Adams et al., 1997, MacMicking et al., 1997b, Cooper et al., 2000). Mycobacteria will initially induce transcriptional factors and approximately 70 non-coding RNAs (ncRNAs) (Voskuil et al., 2011) (Namouchi et al., 2016) where these responses are required for the regulation of plethora genes responsible for sensing redox signals (den Hengst and Buttner, 2008), detoxifying and metabolising these intermediates (Voskuil et al., 2011) (Namouchi et al., 2016).

Later stages- As cellular immunity develops, infected macrophages are killed, and this results in the formation of the caseous centre of the granuloma. This is surrounded by a cellular necrotic zone formed by blood-derived monocytes, epithelioid cells (differentiated macrophages) and multinucleated giant cells (also known as Langhans giant cells) with a rim of the T- and B-cell lymphocytes (Dannenberg Jr and Rook, 1994). The granuloma is considered as the hallmark of TB and can be presented in different formation ranging from non-necrotising granulomas, necrotic neutrophilic granulomas and completely fibrotic granulomas (Canetti, 1955, Flynn et al., 2011). A sufficient accumulation of host lipids and mycobacterial cells was proposed to trigger necrosis causing a cavity. This destructive fusion of liquefying granuloma with an adjacent pulmonary airway will allow *M. tuberculosis* to escape and infect new host cells followed by formation of new lesions (Hunter, 2016). Usually, there is a delay of 1–2 years between an individual being infected with *M. tuberculosis* and onset of clinical pulmonary TB where tissue destruction is observed (Salgame et al., 2015). Otherwise, *M. tuberculosis* can persist for decades within the granuloma structure and remain dormant until host immune response is compromised or other contributory factors trigger bacterial reactivation (Guirado and Schlesinger, 2013).

M. tuberculosis is a 'dual intracellular/extracellular bacterial pathogen' (Silva, 2012) and is able to cause extracellular infections (systemic dissemination) after an initial intracellular infection (Dannenberg Jr and Rook, 1994, Cardona, 2007). Hence, *M. tuberculosis* infection is not confined only to the lungs (pulmonary TB) but can be disseminated to other organs and tissues via haematogenous and lymphatic spread

known as extrapulmonary TB (EPTB) (as reviewed by Ramírez-Lapausa, 2015 #877). EPTB represents 20-25% of all TB cases (Lee, 2015).

1.5 DORMANCY AND NON- REPLICATING PERSISTENCE

The dynamics of granuloma formation and pathology in TB represent stages of a pathophysiological continuum. This also corresponds to different stages of *M. tuberculosis* growth or metabolic adaptation and can further spread to the next host following granuloma disruption (Ehlers and Schaible, 2012). An important aspect of this life cycle that has been receiving attention in *M. tuberculosis* research is the ability for the actively replicating pathogen to switch into dormancy driven by the hostile stress microenvironments encountered during infection.

Dormancy is termed as a reversible state of low metabolic activity, in which cells can persist for extended periods without division (Kaprelyants et al., 1993). Dormant bacilli are usually accompanied by development of phenotypic drug resistance, adoption of specific metabolic pathways and inability to grow in standard media (Wayne and Sohaskey, 2001, Shleeve et al., 2002, Gengenbacher and Kaufmann, 2012). Wayne and Sohaskey introduced a definition of “non-replicating persistence” (NRP) (Wayne and Sohaskey, 2001) which also describes a prominent characteristic of the dormant bacilli without assuming the various mechanisms involved. Hence, both terminologies are used interchangeably in this thesis.

Dormant mycobacteria have a high medical importance. The coexistence of the ‘antibiotic tolerant’ or ‘persister’ subpopulations of dormant mycobacteria pose an additional challenge to be eradicated and hence, are responsible for the need for prolonged chemotherapy. Such bacilli could tolerate more than 50 times the minimal inhibitory concentrations (MICs) of isoniazid and rifampicin *in vitro* (Ojha, 2008 #885). In fact, it was shown in a *in vivo* NRP model such as Cornell’s mice model (McCune et al., 1966) (discussed in next section) that an application of higher dose of rifampicin (50mgkg^{-1}) in combination of standard doses of isoniazid and pyrazinamide was required to eradicate these persister cells (Hu et al., 2015b). The authors have suggested that the high concentration of rifampicin used was very efficient to inhibit proliferation of the persisters by disrupting the ongoing RNA synthesis of molecular factors required for the survival of these bacteria *in vivo* (Hu et al., 2015b). *In vivo*

existence of persister cells were documented by Lenaerts and colleagues who isolated these cells within the acellular rim of necrotic granulomas from guinea pig lungs (Lenaerts et al., 2007). However, the scope of antibiotic tolerance in persister cells has not been fully explored due to the narrow spectrum of antimicrobials tested, different models of dormancy and various susceptibility methods were employed *in vitro* (Lipworth et al., 2016).

Drug-tolerant bacilli have also been isolated in humans. Gomez and McKinney have reviewed some of the classical studies that proposed specific microenvironment conditions present in close TB lesions and treated TB patients as a niche for the survival of this subpopulation of bacilli in humans (Gomez and McKinney, 2004). In particular, the persister cells were predominately found in human tuberculous sputum samples suggesting a role during TB infection (Garton et al., 2002). In addition, these cells are lipid body positive (Garton et al., 2008) and display a differential culturable phenotype (Mukamolova et al., 2010) (Chengalroyen et al., 2016) implicating the heterogeneity of the NRP bacilli population. The presence of lipid body positive (containing triacylglycerols (TAGs) and wax esters) mycobacteria was demonstrated under *in vitro* NRP conditions such as stationary phase (Garton et al., 2008), hypoxia (Low et al., 2009) and during macrophages incubated in hypoxia (Daniel et al., 2011). The clinical relevance of lipid body- positive mycobacteria with drug tolerance was demonstrated recently in an *in vitro* study. This supported the view that these bacilli are phenotypically resistant to the antibiotics tested which were rifampicin, isoniazid, ethambutol and ciprofloxacin irrespective of the cell age of the all tested mycobacterial cultures (Hammond et al., 2015). The identification of lipid body positive mycobacteria indicates that the pathogen utilises an alternative carbon source for energy acquisition, an important feature to ensure survival of the pathogen during infection, in particular dormancy.

The presence of 'differentially culturable tubercle bacteria' (DCTB) in human sputum (Mukamolova et al., 2010) (Chengalroyen et al., 2016) further identifies another subpopulation of NRP cells that also challenge the diagnosis of *M. tuberculosis* infection. To stimulate resuscitation of these dormant bacilli, they require supplementation of the Resuscitation promoting factor (Rpf) proteins (Mukamolova et al., 2010) or relief of induced stress such as the reintroduction of K⁺ nutrient

(Ignatov et al., 2015) and oxygen (Iona et al., 2016). Rpf are peptidoglycan-hydrolysing proteins that were discovered in *Micrococcus luteus* (Mukamolova et al., 1998) and are potential regulators of persistence and reactivation. Rpf dependent cells have been reported in extrapulmonary samples (O'Connor et al., 2015), infected murine macrophages (Biketov et al., 2000) and a murine model of infection (Turapov et al., 2014, Hu et al., 2015b). These findings further explain the difficulty in eradicating the dormant DCTB that may persist in TB treated patients and cause a relapse.

1.6 EXPERIMENTAL SYSTEMS FOR GENERATION OF DORMANT MYCOBACTERIA

There are currently several well-characterised systems for generation of dormant mycobacteria (Figure 1-2) described below.

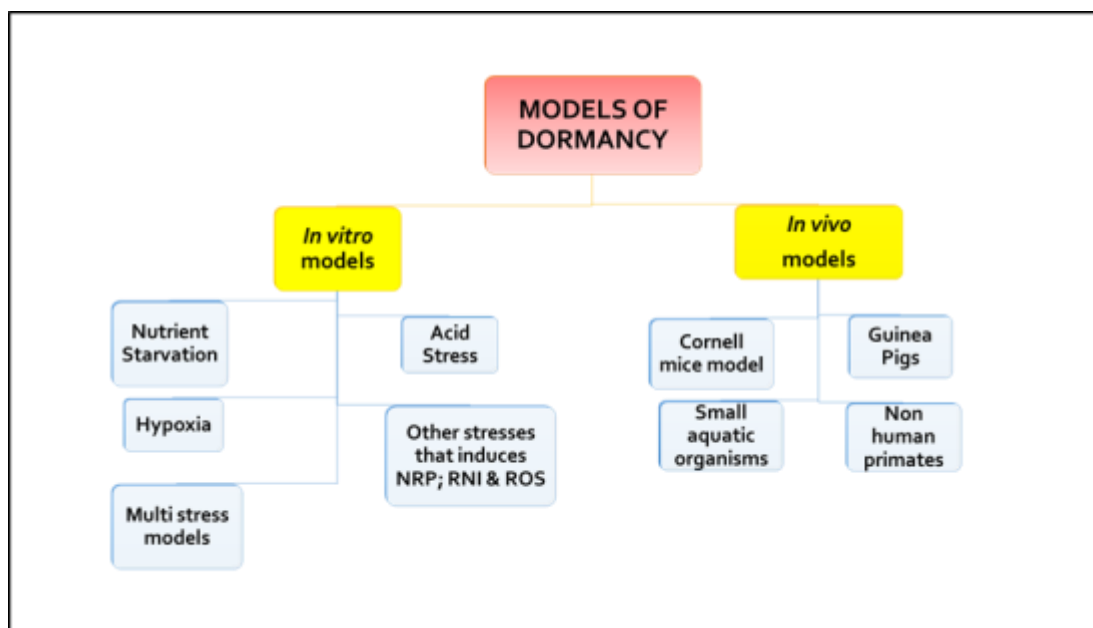


Figure 1-2: Models of dormancy or non-replicating persistence (NRP) in *M. tuberculosis*. NO- Nitric oxide

1.6.1 *In vitro* models

The *in vitro* model systems are designed to recapitulate the conditions faced by the pathogen *in vivo* (Sikri and Tyagi, 2013). However, the general problem in establishing *in vitro* models is generating NRP bacilli heterogeneity which different metabolic status (Ignatov et al., 2015).

1.6.1.1 Hypoxia model

The best-studied hypoxia model, Wayne's model, was based on the controlled agitation of tightly sealed liquid cultures exposed to limited headspace volumes of air (Wayne and Hayes, 1996). Wayne's hypoxia model involved the bacilli undergoing two stages of NRP. Exponential bacteria entering microaerophilic conditions where dissolved oxygen approaches 1% saturation (NRP-1 stage) and will start to slow their growth and this corresponds to termination of DNA synthesis and cell thickening. Next, bacilli gradually undergo anaerobiosis where dissolved oxygen drops below 0.06% saturation, termed NRP-2 stage. Importantly, these NRP mycobacteria will resume replication when oxygen is introduced (Wayne and Hayes, 1996).

In the Wayne model, the slow decline in oxygen allows *M. tuberculosis* to adapt to hypoxic conditions by shifting its metabolism and arresting growth (Wayne and Sohaskey, 2001, Boshoff and Barry, 2005). Some of the known genes induced in this model are involved in fatty acid metabolism; *tgs1* (encodes triacylglycerol synthase) and *icl* (encodes Isocitrate lyase), nitrate metabolism (*narK2* and *narX*), and alternative electron transport pathways (*fdxA*). This underlying genetic reprogramming is controlled by the dormancy survival regulon which is under a transcription factor, DosR that regulates approximately 50 proteins (Boon and Dick, 2002, Park et al., 2003, Voskuil et al., 2004). The expression of DosR regulated genes suggests a compensatory mechanism for respiration through an anaerobic electron transport system (Boshoff and Barry, 2005). The role of DosR during dormancy will be discussed in a separate section.

During adaptation to decreasing oxygen levels, mycobacteria also exhibit an orchestrated respiratory slowdown that involves a reduced but sustainable pool of ATP, maintenance of proton motive force and a shift in the NAD⁺/NADH ratio towards NADH to survive anaerobiosis (Rao et al., 2008). Due to the reduced availability of oxygen, nitrate is utilised as an alternative electron acceptor. Reduction of nitrate to nitrite provides energy for the NRP bacilli, thus inducing nitrate respiration (Sohaskey, 2008). Moreover, the upregulation of *icl* in hypoxic bacilli indicates an alternative metabolic pathway where ICL is a key enzyme of the glyoxylate (Wayne and Sohaskey, 2001, McKinney et al., 2000) and the methylcitrate cycles (Gould et al., 2006). Mycobacteria will utilise host fatty acids and cholesterol (Russell et al., 2010)

which are catabolised to acetyl-CoA and propionyl-CoA respectively. For energy acquisition, acetyl-CoA enters the glyoxylate cycle, an alternative pathway used to surpass the beta oxidation steps in tricarboxylic acid cycle (Pai et al., 2014) as means to avoid any carbon loss (Rhee et al., 2011). Acetyl-CoA is then converted to isocitrate. Malate synthase (MS) is another important enzyme in the glyoxylate cycle. ICL reversibly cleaves the isocitrate to glyoxylate and succinate, while MS will convert glyoxylate into malate by adding an acetyl group. Meanwhile, propionyl-CoA is incorporated into the methylisocitrate pathway to regenerate pyruvate and succinate, which can enter glyoxylate cycle (Lorenz and Fink, 2002, Munoz-Elias et al., 2006). These compounds influence the biosynthesis of the lipid macromolecules such as PDIM, TAGs and mycolic acid (Lee et al., 2013). TAGs will be incorporated as cell structural components or for storage, shown as lipid body positive bacilli. Subsequently, the most active and highly upregulated *tgs1* (*rv3130c*) that encodes TAG synthase, further supports that the main storage molecule for fatty acids is TAGs in *in vitro* NRP conditions, macrophage infection and human tuberculous sputum (Daniel et al., 2004, Daniel et al., 2011, Garton et al., 2008). A deletion of *tgs1* in *M. tuberculosis* eliminates the accumulation of TAGs demonstrated in *in vitro* NRP models including hypoxia (Daniel et al., 2004, Deb et al., 2009) suggesting the importance of TAGs for survival of NRP bacilli. The fatty acid metabolism of *M. tuberculosis* also shares an overlapping transcriptional response signature to that found in NRP bacilli induced by redox stress and hypoxia (Rodríguez et al., 2014), indicating a common phenomenon in stressed *M. tuberculosis* cells. In addition, the Wayne's hypoxia bacilli were shown to develop tolerance to isoniazid and rifampin and sensitivity to metronidazole, a pro-drug effective for anaerobic cells (Wayne and Sramek, 1994), and to nitroimidazole drugs (Wayne, 1996, Wayne and Sramek, 1994). Other hypoxic models such as rapid anaerobic dormancy (RAD) model used rapid depletion of oxygen to mimic NRP-2 conditions which is anaerobiosis. Similarly, *dosR* (Leistikow et al., 2010) and *lsr2* (a global transcriptional regulator) deletion mutants (Bartek et al., 2014) displayed impaired survival and developed a differential culturability phenotype indicating the role of these genes for adaptation to the rapidly declining oxygen tension.

The defined hypoxia model is another model that generates constant 0.2% oxygen tension in culture flasks. The survival of only 1% bacteria after a week of incubation in this model further supports that gradual adaptation to oxygen limitation is essential for the generation of NRP bacilli (Rustad et al., 2008). Transcriptomic analysis of *M. tuberculosis* grown in the model revealed that DosR was only required for the initial adaptation to hypoxia. For maintenance of dormancy, a second response termed as enduring hypoxia response (EHR) was induced resulting in the expression of ~230 genes (Rustad et al., 2008). The relevance of EHR in overall bacterial adaptation to hypoxic conditions and demonstration of NRP bacilli are yet to be determined.

1.6.1.2 Nutrient Starvation

Another system for generation of NRP is nutrient deprivation which includes maintenance of mycobacteria in phosphate buffer saline (PBS) where *M. tuberculosis* can survive under this condition for two years (Nyka, 1974). Transcriptome (Betts et al., 2002) and proteome analyses (Albrethsen et al., 2013) of starved *M. tuberculosis* revealed that these cells undergo a global down-regulation of expression of genes encoding proteins involved in carbohydrate/ energy metabolism, respiration machinery, cell division and transcription. *DosR* regulation is not involved during starvation. Instead, this global stringent response is mediated by RelA (Primm et al., 2000) and CarD (Stallings et al., 2009) which synthesises and degrades hyperphosphorylated guanine nucleotides (p)ppGpp that destabilise the RNA polymerase (RNAP) open complex, inhibiting transcription of stable RNAs. As a result, DNA replication and other cellular processes are inhibited (Magnusson et al., 2005, Ojha et al., 2000). In addition, a drastic decrease in respiration rate over the first 96 hours that results in the reduction of ATP levels was also reported (Loebel et al., 1933). Nutrient starved bacilli also developed antibiotic tolerance to isoniazid, rifampicin (Betts et al., 2002, Gengenbacher et al., 2010) and fluoroquinolones (Sarathy et al., 2013). Unlike Wayne's culture, starved *M. tuberculosis* bacilli are resistant to metronidazole indicating bacilli were not in an anaerobic state (Betts et al., 2002). The decreased intracellular accumulation of the tested antibiotics was proposed to be a result of the altered cellular permeability and not be influenced by efflux pumps or transporter proteins (Xie et al., 2005, Sarathy et al., 2013). Prolonged starved

M. tuberculosis bacilli have exhibited cell wall remodelling in lung lesions and reduced acid-fastness analogous to *M. tuberculosis* grown in distilled water or PBS (Nyka, 1974). The changes in morphology were also evident in saline shock- starved *M. smegmatis* cells where it was proposed mycobacteria undergo starvation-induced differentiation (Wu et al., 2016). Although the morphological change observed in *M. smegmatis* has not been explored in *M. tuberculosis*, the association with NRP remains to be elucidated.

In summary, the models mentioned above were demonstrated to generate NRP cells by contrary conditions- carbon depletion in oxygen-rich environment versus oxygen starvation in a nutrient-rich medium where both physiological and metabolic forms overlap and are identified as core features of dormancy.

1.6.1.3 Multiple- stress model

The multi-stress model includes exposure of *M. tuberculosis* to combined stresses such as low oxygen (5%), high CO₂ (10%), low nutrient (10% Dubos medium) and acidic pH (5.0). It was developed by Deb and colleagues (Deb et al., 2009). The transcriptional response in this model was similar to the starvation and hypoxia model. Genes involved in the biosynthesis of wax esters and TAG were also significantly upregulated (Deb et al., 2009), similarly observed in hypoxia-induced bacilli (Shi et al., 2010). Deletion of *tgs1* reduced the ability to accumulate TAG and exhibit tolerance to rifampicin and Isoniazid supporting a link between antibiotic susceptibility and TAG accumulation (Deb et al., 2009). However, generating reproducibility in data could present an issue as it involves manipulating different conditions in one setting and timely monitoring is required which can be laborious.

1.6.1.4 Acid stress model

Acidity is thought to be a major stress encountered by *M. tuberculosis* within granulomatous lesions (necrotic tissue, pH 6.5 and active lesion pH 5.5 or lower) and in the phagolysosomes of activated macrophages with pH 4.5 and lower (pH varies according to immunological state of activation) (Piccaro et al., 2013, Schaible et al., 1998, Sturgill-Koszycki et al., 1994). Incubation of *M. tuberculosis* in Sauton's medium subjected to gradual acidification (pH 8.5 to pH 5.5) for 60 days resulted in the accumulation of dark ovoid cells which could not produce colonies on solid media, i.e.

dormant cells. Oxygen was still enriched during the experiment indicating that the cultures were not undergoing any gradual oxygen depletion (Shleeva et al., 2011). Recently, it was shown that WhiB₃, a putative transcriptional regulator was required to resist acidic pH stress at pH4.0. In addition, WhiB₃ is also a regulator of redox homeostasis that influences the expression of virulence factors for phagosomal maturation and intraphagosomal survival, implying an overlapping regulatory network involved during adaptation to acidic pH in *M. tuberculosis* (Mehta et al., 2016). Reproducibility of acid stress models are known to be impeded by culture conditions used such as bacterial density and medium composition, reviewed in Vandal, 2009 (#78). As a result, the interpretation of the survival of *M. tuberculosis* deletion strains in different acid stress models were varied affecting the actual function of the tested genes.

1.6.1.5 The role of Nitric Oxide in induction of NRP

To date, there are no documented *in vitro* systems of NRP that model oxidative and nitrosative stresses. However, the effects of high concentration of NO with RNI *in vitro* induced a similar oxidative stress response that inhibits *M. tuberculosis* respiration and results in growth arrest (Voskuil et al., 2003). Subsequently, the lower concentration of NO 'signals' the significant upregulation of hypoxia-induced DosR regulon (Voskuil et al., 2003) that result in the reduction of respiration and replication for a long-term survival during dormancy (Voskuil et al., 2003). The significant upregulation of *narK2*, a nitrate transporter and member of DosR regulon during exposure to NO (Voskuil et al., 2003), hypoxia (Sohaskey and Wayne, 2003) and IFN γ -activated macrophages from NOS₂-expressing mice, allows the transport of nitrate into the cell and nitrite out of the cell. Nitrate, along with nitrite (NO₂⁻), is an auto-oxidation product of NO, which is the product of iNOS (Lundberg et al., 2004). The nitrate reduction activity is to induce redox homeostasis and energy production for anaerobic respiration (Sohaskey and Wayne, 2003, Wayne and Hayes, 1998, Cunningham-Bussel et al., 2013). Tan and colleagues have shown that the switch to nitrate respiration was also essential for the survival of *M. tuberculosis* during exposure to acid stress and nitrosative stress (Tan et al., 2010), conditions that are also proposed to exist during macrophage infection and dormancy. In other words, NO acts as a terminal electron

acceptor for *M. tuberculosis* to adopt dormancy (Voskuil et al., 2003). At the same time, it was proposed that NO act as a chemoattractant and regulates the development of giant cells (fusion of macrophages) and epithelioid cells for organisation of granuloma (Choi et al., 2002, Silva Miranda et al., 2012)

1.6.2 *In vivo* models

This section will describe an overview of some of the experimental animal models used to demonstrate the generation of dormant bacilli by inducing latent infection or granuloma formation. The challenges in interpreting such experiments *in vivo* are the lack of understanding of the host-pathogen interaction involved and association to human TB infection. Infected non-human primates (NHP) does cause TB infection resembling human and develop hypoxic TB granuloma (Peña and Ho, 2015, Mehra et al., 2015). However, use of NHP requires a higher cost of maintenance and comes with public ethical pressures. Hence it was advocated to be used only to the final stages of preclinical stages of vaccine or drug development trials (Kaufmann, 2003).

1.6.2.1 Cornell mice model

The drug-induced Cornell model developed in the 1950s was the first *in vivo* evidence of dormant bacilli (McCune et al., 1966). The highly infected mice were treated with isoniazid and pyrazinamide for 12 weeks that resulted in unculturable *M. tuberculosis*. After 90 days post termination of treatment, TB was reactivated and isolated bacilli were sensitive to isoniazid (McCune et al., 1966). However, the model failed to induce LTBI artificially and will only generate dormant bacilli upon antibiotic treatment (Gupta and Katoch, 2005). Its variant models were later used to study the immunological status of reactivation or rate of spontaneous reactivation after antimicrobial treatment (Scanga et al., 1999).

1.6.2.2 'Low-inoculum' infection

Using mice for infection experiments is cost manageable and offers genetic heterogeneity of a murine population (Kramnik and Beamer, 2016). One drawback in using mice is the inability to replicate necrotising cavities of granuloma (Flynn, 2006), therefore challenging in isolating NRP bacilli. A 'low-inoculum' infection has been used as a model of persistence for *M. tuberculosis* studies (Bartek et al., 2009,

Woolhiser et al., 2009). Infection resulting an initial instillation of 30-100 colony forming units (CFUs) in lungs per mouse led to an adequate adaptive immune response that led to chronic infection (Flynn and Chan, 2001) demonstrated by a high bacterial burden and pathology in lungs. The infected mice did not present any clinical signs and persisted for more than a year mimicking latent infection (Flynn, 2006). During this period, dormant bacilli were isolated but the eventual death of mice indicated reactivation of infection (Orme, 1988). The use of NO synthase inhibitor, aminoguanidine in this model demonstrated that RNI also play a major role in preventing reactivation of TB (Flynn et al., 1998). The lungs of infected guinea pigs were shown to have a similar pathology with granulomas, as infected humans (Basaraba et al., 2006). Isolation of antibiotic tolerant cells surrounding the necrotic area of the granuloma lesion suggest generation of dormant bacilli during infection (Lenaerts et al., 2007). Hence, the guinea pig can be modelled for generation of NRP bacilli. However, there is no evidence showing that guinea pigs are able to maintain a persistent bacilliary population and a latent infection (Flynn, 2006). There is a requirement to understand further the interaction of these persister cells with the host during this stage of infection.

1.6.2.3 Hollow fibre assay

The hollow fibre (HF) assay (Gazi et al., 2016) has been used to mimic *M. tuberculosis* persistence (Karakousis et al., 2004). Mycobacterial cells encapsulated within the semi diffusible HFs were subcutaneously implanted in mice generated dormant bacilli and had increased resistance to rifampicin compared to isoniazid (Karakousis et al., 2004). Hypoxia and NO may have a role in intrafiber bacillary growth containment shown by significant induction of *dosR* and *DosR* regulon genes (Karakousis et al., 2004). A hypoxia-specific marker, pimonidazole that binds to thiol-containing peptides stained the peri fibre tissues in a dose-dependent manner (Klinkenberg et al., 2008), further validates the hypoxic condition of the model.

1.7 MYCOBACTERIAL FACTORS INVOLVED DURING NON- REPLICATING PERSISTENCE

1.7.1 Transcriptional regulators (TRs)

The complex life cycle of *M. tuberculosis* that involves dormancy and resuscitation is achieved by encoding 190 regulator proteins that include 11 two-component signal transduction systems (TCSSs), six serine-threonine protein kinases, and 13 alternative sigma (σ) factors. It implies that transcription regulation is important for *M. tuberculosis* pathogenesis (Cole et al., 1998, (Tekaiia et al., 1999). The TCSSs identified in *M. tuberculosis* are PhoP-PhoR, RegX₃-SenX₃, DosR-DosS/DosT, Rv0600c-Rv0601-ctcrA, narL-Rv0845, TcrX-TcrY, MprA-MprB, PrrA-PrrB, TrcR-TrcS, PdtaR-PdtaS, MtrA-MtrB, and KdpD-KdpE (Bretl et al., 2011).

DosR-DosS/ DosT is a well-characterised TCSS system that is formed by one response regulator (DosR, Rv3133c) and activated under inducing conditions by transfer of the phosphosignal by either DosS (Rv3132c) or DosT (Rv2027c) sensor histidine kinases (Kumar et al., 2007, Roberts et al., 2004). DosR means "dormancy survival regulator" termed after DosR was shown to play an important role for survival of *M. bovis* BCG during long-term hypoxia (Boon and Dick, 2002). Hypoxia (Wayne and Hayes, 1996, Rustad et al., 2008), presence of low concentration of NO (Voskuil et al., 2003) and carbon monoxide, CO₂ (Kumar et al., 2008) have shown to increase expression of all 48 genes (known as the DosR regulon). Hence the O₂, NO, and CO are modulatory ligands of these kinases, making them indispensable for induction of DosR regulon (Roberts et al., 2004, Kumar et al., 2007). DosR regulon also governs the metabolic shift from aerobic to anaerobic in *M. tuberculosis* to ensure the survival of the bacilli during hypoxia and reverts to active replication upon reaeration (Leistikow et al., 2010) (Rustad et al., 2009, Wayne and Sohaskey, 2001). Many of the DosR regulon genes are conserved hypothetical proteins (CHP) with, as yet, still unknown products and functions.

It was proposed that DosR is also crucial for persistence in lungs (Boon and Dick, 2012), however, its involvement in virulence is still unclear with contrasting outcomes. A *dosR* deleted strain does not exhibit reduced virulence in both in C57Bl/6 mice, probably as the mice have not developed any lesions (Rustad et al., 2008) and in

C3HeB/FeJ mice, even though the mice develop hypoxic lesions (Gautam et al., 2015a). In severe combined immunodeficient mice, the mutant strain was hypervirulent probably due to the derepression of DosR genes (Parish et al., 2003a). Malhotra and colleagues have observed a significant decrease in gross lesions in infected organs and a reduction of 3-Log_{10} bacterial burden of *dosR* mutant in the spleen compared with wild-type guinea pigs (Malhotra et al., 2004). A recent macaque infection with *dosR* mutant exhibited severe growth attenuation. Bronchoalveolar lavage samples revealed highly elevated CCR5+ T cells in lungs (Mehra et al., 2015). The author also proposed that DosR is capable of inhibiting recruitment of a highly proliferative Th1-type response during early infection enabling *M. tuberculosis* to persist in lungs (Mehra et al., 2015).

Mechanistic links between DosR and other "master regulators," such as WhiB3 and the PhoPR two-component regulatory system suggest a wider stress-associated regulatory network linking between hypoxia and redox adaptation (DosR-WhiB3) and between hypoxia and cell wall lipid biosynthesis (WhiB3-PhoP) (Galagan et al., 2013, Asensio et al., 2006). A recent study demonstrated a novel redox-responsive TR of the cyclic AMP receptor (CRP)/ fumarate nitrate reduction regulator (FNR) superfamily, Rv1675c (Cmr) that regulates the expression of a subset genes of the DosR regulon (Smith et al., 2017). The biological role of Cmr in *M. tuberculosis* during stress responses and dormancy were further investigated described in Chapter 5.

1.7.2 Non-coding RNA (ncRNA)

Since the first experimental confirmation of nine non-coding small RNA (sRNAs) in mycobacteria published in 2009 (Arnvig and Young, 2009), there has been major interest in identifying more functional and regulatory roles of a diversity of sRNAs. Small RNAs are frequently implicated in adaptive responses to environmental changes, such as temperature, pH and metabolism of energy, lipids, and metabolites (Haning et al., 2014) (Arnvig et al., 2014) and are therefore expected to play regulatory roles in the pathogenesis of *M. tuberculosis*.

Further RNA- sequencing identified ~2000 sRNA candidates in *M. tuberculosis* (Pellin et al., 2012) and subsequent microarray analysis further confirmed 258 sRNAs

including intergenic sRNAs² and 152 antisense RNA³ (Miotto et al., 2012). The abundance of the sRNA was reported during oxidative stress (Arnvig and Young, 2009), stationary phase (Arnvig et al., 2011), starvation (Arnvig et al., 2011) and in 'unculturable' *M. tuberculosis* grown in K⁺-deficient Sauton medium for two weeks (Ignatov et al., 2015). For example, ncRv13661 (MTS2833) was significantly upregulated in these models indicating its potential role during dormancy (Arnvig et al., 2011, Ignatov et al., 2015). Furthermore, ncRv11733 recently assigned as 'DrrS' for DosR Regulated sRNA where the core promoter was activated by *dosR*, and that expression was highly induced by NO treatment (Moore et al., 2017). Additionally, another promising biomarker of infection, ncRv12659 was also identified to be abundant in dormant *M. tuberculosis* cells (Ignatov et al., 2015). It was demonstrated that the 5' end of sRNA was highly upregulated by 50-fold during starvation and 6-fold during murine infection which further raised the mechanism of sRNA processing but importantly its role during NRP (Houghton et al., 2013). The recent identification of ncRv12659 that is transcribed on the plus strand that overlaps *rv2660c* locus during PBS starvation have further disputed the high upregulation signals contributed by both *rv2660c* and *rv2661c*. Both of these annotated genes have been reported to be significantly expressed *in vitro* NRP models (Betts et al., 2002, Voskuil et al., 2004) (Rustad et al., 2008) (Salina et al., 2009, Soto-Ramirez et al., 2017), stress response (Schnappinger et al., 2003) and *in vivo* (Aagaard et al., 2011, Gautam et al., 2015b). The investigation on the biological role of these genes during *M. tuberculosis* infection are described in Chapter 3 and 4.

² Intergenic sRNAs, which are short transcripts (~50–300 nucleotides) that act on distantly encoded targets (Storz et al., 2011)

³ Antisense RNAs (asRNAs) are small, untranslated RNA that pair to target mRNAs at specific regions of complementarity to control their biological function by regulating gene expression at the post-transcriptional level (Saber et al., 2016)

1.8 AIMS AND SPECIFIC OBJECTIVES

The overall aim of this study is to investigate the functional role of selected genes that have been implicated in *M. tuberculosis* adaptation in response to stress and dormancy. A set of overlapping genes, *rv2660c*, *rv2661c* and *rv2662* that encode conserved hypothetical proteins, were associated with persistence and virulence through transcriptomic studies performed in various *in vitro* and *in vivo* models of dormancy. The expression of these genes was significantly upregulated in *M. tuberculosis* nutrient-starved cells. Furthermore, the identification of an overlapping ncRv12659 and significant upregulation *rv2662* during starvation conditions, as mentioned earlier through RNA sequencing, further challenged the existence of both *rv2660c* and *rv2661c*.

Rv1675 (Cmr) has recently been characterised as a redox-responsive transcriptional regulator of DosR regulon, indicative of an important role for entry and maintenance of dormancy. Nitric oxide is the major signalling molecule for inhibition of Cmr DNA binding causing derepression of DosR regulon. As much as the molecular characterisation of Cmr is slowly understood, the biological importance of Cmr to *M. tuberculosis* is starting to unravel. Cmr is not essential for growth and macrophage infection; however, it is essential for virulence. Unfortunately, the failure to complement mutant phenotype during murine infection revealed an initial evidence of the complexity of the regulation.

The specific objectives of this study are as follows;

- ✓ To determine essentiality of Rv2660c and Rv2661c in *M. tuberculosis* by generating deletion and over-expressing strains and characterising phenotypes of these strains during growth *in vitro*
- ✓ To investigate survival of deletion and over-expressing strains of *rv2660c* and *rv2661c* under various *in vitro* stress conditions, and during macrophage and mice infection
- ✓ To determine expression profiles of *rv2660c*, *rv2661*, *rv2662* and ncRv12659 in various *in vitro* stress experiments by quantitative RT-PCR (qRT-PCR)
- ✓ To investigate the role of Cmr in nitrosative and oxidative stresses.

CHAPTER 2

General Materials and Methods

CHAPTER 2 GENERAL METHODS AND MATERIALS

2.1 REAGENTS AND GROWTH MEDIA

2.1.1 Reagents and chemicals

Reagents and chemicals used in the study were from Sigma-Aldrich® or Fisher Scientific unless stated. Only molecular grade reagents, chemicals and water, H₂O (Gibco) were used for nucleic acid manipulations.

2.1.2 Growth media and supplements

Middlebrook 7H9 broth (Difco, Becton Dickinson) was prepared by dissolving 4.7g 7H9 powder in 900mL Nanopure water containing 5 ml of glycerol and autoclaved at 121°C for 15 minutes. The broth was further supplemented with 10% (v/v) Albumin dextrose complex (ADC) and 0.05% (w/v) Tween 80 (designated as supplemented 7H9) for cultivation of *M. tuberculosis* strains.

Middlebrook 7H10 agar (Difco, Becton Dickinson) was prepared by adding 19 g 7H10 powder and 5mL glycerol to 900mL Nanopure water and autoclaved at 121°C for 15 minutes. 10% (v/v) ADC was added to agar prior to use (designated as 7H10).

Sauton's medium included the following chemicals (per 1L): 500 mg KH₂PO₄, 500 mg MgSO₄·7H₂O, 5mg Ferric Ammonium Citrate, 4g L-Asparagine, 2g Citric Acid, 10mL Glycerol and 100µL of 1% (w/v) ZnSO₄. pH was adjusted to 7.4 by adding 10M NaOH before autoclaving at 121°C for 15 minutes.

Lysogenic Broth (LB) was a mixture of 10g tryptone (Difco, Becton Dickinson), 5g yeast extract (Difco, Becton Dickinson) and 5g sodium chloride in 1 litre distilled water. Lysogenic Agar (LA) was prepared with an additional 15g of agar to the mixture. Antibiotics were added when required.

Roswell Park Memorial Institute (RPMI) 1640 medium with L-glutamine and sodium bicarbonate (Sigma-Aldrich®) was supplemented with 10% (v/v) heat inactivated Foetal Bovine Serum, 100 units Penicillin and 0.1mg Streptomycin/mL for maintenance of cell lines.

Albumin Dextrose Catalase (ADC) was prepared by dissolving 50g Bovine Serum Albumin, 20g glucose and 8.5g sodium chloride in 1 litre of Nanopure water and filter sterilized using a 0.2 μ M filter unit (VWR).

Tween 80 stock solution was prepared by mixing 5g Tween 80 in Nanopure water making up to a final volume of 50 ml with a final concentration of 10% (w/v). The solution was sterilised by filtration through a 0.2 μ m filter unit and aliquoted prior storage at 4°C.

2.2 BACTERIAL STRAINS

All cultures were incubated at 37°C shaking unless otherwise stated.

Escherichia coli DH5 α competent cells (Bioline) was used as a host strain for cloning and plasmid propagation and were grown in either LB or LA medium. Liquid cultures were incubated shaking at 200rpm. Media were supplemented either with antimicrobials; 50 μ g mL⁻¹ Kanamycin for plasmids p2NIL and pMV261 or 100 μ g mL⁻¹ Ampicillin for pGoal19.

M. tuberculosis H37Rv was used as a parenteral strain (refer Table 2-1) to construct deletion mutants and over-expressing strains. *M. tuberculosis* strains were cultivated in supplemented 7H9 with or without antibiotics or Sauton's broth at 37°C with shaking at 100rpm in either universal tubes, 125ml and 250mL Erlenmeyer flasks or Roller bottles. Flasks and tubes were sealed with a micropore tape, double bagged and incubated with shaking (unless stated otherwise) at 100 rpm. One litre roller bottles holding up to 200mL culture were incubated rolling at 2 rpm. 7H10 agar (antibiotics added when required) plates were also sealed with a tape (when required), double bagged and incubated at 37°C.

For over-expressing strains, culture was supplemented with 50 μ g mL⁻¹ Kanamycin. An empty plasmid strain was used as a control in over-expression studies.

All manipulations involving *M. tuberculosis* cultures were performed in a microbiological safety cabinet (Talaat et al., 1998) Class II in Category 3 (C3) containment laboratory in accordance with the approved Code of Practice.

All strains used during the study are listed in Table 2-1.

<i>Bacterial strains</i>	Designated in thesis as:	Descriptions	Source
<i>M. tuberculosis</i> H37Rv (Chapter 3 and 4)	Wild-type	wild-type laboratory strain	Dr Valerie Mizrahi, University of the Witwatersrand, Johannesburg, South Africa
<i>M. tuberculosis</i> H37Rv (Chapter 5)	Wild-type	wild-type laboratory strain	(Smith et al., 2017)
<i>M. tuberculosis</i> H37Rv $\Delta rv266oc$	$\Delta rv266oc$	In-frame unmarked deletion strain of <i>rv266oc</i> and 3'end of <i>ncRv12659</i>	Dr. Galina Mukamolova UoL
<i>M. tuberculosis</i> H37Rv $\Delta rv2661c:rv266oc$	$\Delta rv2661c:rv266oc$	In-frame unmarked deletion strain of both <i>rv2661c</i> and <i>rv266oc</i> corresponding to 5'end of <i>rv2662</i> and 3'end of <i>ncRv12659</i>	Dr. Galina Mukamolova UoL
<i>M. tuberculosis</i> Δcmr	Δcmr	In-frame unmarked deletion strain of <i>cmr</i> (<i>rv1675c</i>)	(Smith et al., 2017)
<i>M. tuberculosis</i> <i>cmr</i> complement	Δcmr_{com}	<i>M. tuberculosis</i> $\Delta cmr/cm r$	(Smith et al., 2017)
<i>M. tuberculosis</i> H37Rv:: pMV261	<i>M. tuberculosis</i> pMV261	Strain harbouring empty plasmid pMV261	(Stover et al., 1991)

<i>M. tuberculosis</i> pMV261::rv2661c	<i>M. tuberculosis</i> pMV261::rv2661c	Strain harbouring a pMV261::rv2661c plasmid	Dr. Galina Mukamolova UoL
<i>M. tuberculosis</i> pMV261::rv2660c	<i>M. tuberculosis</i> pMV261::rv2660c	Strain harbouring a pMV261::rv2660c plasmid	Dr. Galina Mukamolova UoL
<i>M. tuberculosis</i> pMV261::rv2661c+rv2660c	<i>M. tuberculosis</i> pMV261::rv2661c+rv2660c	Strain harbouring a pMV261::rv2661c+rv2660c plasmid	Dr. Galina Mukamolova UoL
<i>M. tuberculosis</i> pMV261::rv1675c	<i>M. tuberculosis</i> pMV261::cmr	Strain harbouring a pMV261::cmr plasmid	Dr Sarah Glenn & Khalid Khan, UoL
<i>M. tuberculosis</i> pMV261::rv1675c C2A	<i>M. tuberculosis</i> pMV261:: cmr _{C2A}	Strain harbouring a mutated version of pMV261::cmr (C36A+C131A) plasmid	Dr Sarah Glenn & Khalid Khan, UoL
Plasmids	Designated as:	Descriptions	Source
p2NIL	p2NIL	Suicide gene delivery vector, Kanamycin ^R	(Parish and Stoker, 2000b)
pGOAL19	pGOAL19	hygR pAg ₈₅ - lacZ sacB Pacl cassette, Ampicillin ^R	(Parish and Stoker, 2000b)
pMV261	pMV261	<i>E. coli</i> -mycobacteria shuttle vector with <i>hsp60</i> promoter; Kanamycin ^R	(Stover et al., 1991)
pET28a	pET28a	Expression vector with <i>N</i> -terminal hexahistidine affinity tag	Novagen

pΔrv266oc	pΔrv266oc	Suicide plasmid for in-frame deletion of <i>rv266oc</i>	Dr. Galina Mukamolova UoL
pΔrv2661c	pΔrv2661c	Suicide plasmid for in-frame deletion of <i>rv2661c</i>	Dr. Galina Mukamolova UoL
pΔrv2661c:rv266oc	pΔrv2661c:rv266oc	Suicide plasmid for in-frame deletion of <i>rv2661c</i> and <i>rv266oc</i>	Dr. Galina Mukamolova UoL
pGS2103	pGS2103	pET28a derivative for expression of <i>cmr</i> ; Kan ^R	Dr. Laura Smith, University of Sheffield
pGS2475	pGS2475	pET28a derivative for expression <i>cmr_C36A/C131A</i> ; Kan ^R	Dr. Laura Smith, University of Sheffield

Table 2-1- *M. tuberculosis* bacterial strains and plasmids used in the study (mentioned in Chapter 3, 4 and 5).

R- denotes resistance

2.3 PREPARATION OF BACTERIAL STOCKS FOR *IN VITRO* EXPERIMENTS AND INFECTION

2.3.1 Starter culture

Starter culture of mycobacterial strains were performed by scraping frozen culture stock and inoculating into 5mL supplemented 7H9 into duplicate universal tubes. When grown to mid-exponential phase (OD_{580nm} 0.5- 0.7), the starter cultures were expanded in larger volume for use in experiments.

2.3.2 Preparation of frozen stocks of mycobacterial strains

For general laboratory stocks, frozen bacterial stocks were prepared by mixing 200 μ L of sterile 70% (v/v) glycerol and 800 μ L of mid-exponential culture grown in supplemented 7H9 (OD_{580nm} 0.5- 0.7) in 1.5mL cryogenic tubes and kept in $-80^{\circ}C$.

For macrophage infection experiments, frozen stocks of mycobacterial strains were prepared by expanding the starter culture in triplicates of 10mL supplemented 7H9 and grown to mid-exponential phase of OD_{580nm} of 0.5-0.7. Cultures were then centrifuged at 2500 x g for 15 minutes and pellets were resuspended twice in 10mL of sterile PBS. Frozen stocks are maintained as 1mL aliquots in RPMI 1640 medium and kept at $-80^{\circ}C$.

For the murine infection experiment, the frozen stocks of mycobacterial strains were prepared similarly from mid- exponential phase cultures but pellets were instead washed three times in 10% (v/v) glycerol. At the final stage, the bacterial pellet was resuspended in 1mL of 10% (v/v) glycerol and 100 μ L aliquots were frozen and stored at $-80^{\circ}C$ for up to 6 months.

2.4 OPTICAL DENSITY MEASUREMENTS

The optical density of *M. tuberculosis* culture was measured at 580nm (OD_{580nm}) using a Jenway Spectrophotometer. Culture (900 μ L) were transferred into 1.5mL cuvettes and carefully sealed with autoclave tape and parafilm. The sealed cuvettes were swabbed with 70% (v/v) ethanol before taking it out of the MSC for measurement. The 7H9 medium was used to blank prior to actual measurements. Cultures with OD_{580nm} greater than 1 were ten-fold diluted for correct reading.

2.5 COLONY FORMING UNIT COUNTS

Colony forming unit (CFU) counts were performed according to Miles and Misra method (Miles et al., 1938). Bacterial inoculum was ten-fold diluted in supplemented 7H9 and 10 μ L of each dilution were dropped in triplicate on duplicate 7H10 plates. Colonies were enumerated in all six replicates and CFU count per millilitres (CFUmL⁻¹) were calculated as below:

$$\text{Equation 2-1: } CFUmL^{-1} = \textit{Average colony counts} \times 100 \times \textit{Dilution Factor}$$

2.6 GENERAL IN VITRO STRESS ASSAYS

Viability of deletion and/or over-expressing strains were assessed by carrying out CFU counts. Where applied, percentage survival of each strain was calculated by dividing CFUs after each treatment by CFUs at time 0 hour (T₀), then multiplied by 100.

In addition, expression of target genes will be analysed from RNA isolated from exponential growth (untreated) and treated *M. tuberculosis* cells. Exponentially growing *M. tuberculosis* cells (T₀) were used for standardization of the gene expression throughout the experiment and reference as the optimal condition for growth. In each experiment, a standardized 9mL culture was used to isolate RNA obtained during both exponential growth and treated samples at pre- determined time points.

2.6.1 Oxidative stress

Bacteria were grown to mid-exponential phase (OD_{580nm} of 0.5-0.7) in 250 mL Erlenmeyer flasks containing 50 mL of supplemented 7H9 broth. Individual culture tubes (aliquoted as 5mL) were treated with 35% (v/v) hydrogen peroxide, H₂O₂ (Acros Organics) with a final concentration of 25mM (or otherwise stated) and incubated without shaking. Control cultures without H₂O₂ treatment were set up and designated as untreated cultures. Each experiment was performed in triplicate. CFU counts were determined at 4 and 24 hours.

2.6.2 Nitrosative stress

Fifty mL of late exponentially growing (OD_{580nm} of 0.8-1.0) starter culture in 250mL Erlenmeyer flasks were initially diluted to an OD_{580nm} 0.1 and aliquoted as 5mL in universal tubes. Individual culture in supplemented 7H9 were treated with a final concentration of 100 μ M nitric oxide (NO) donor, 6-methoxy-5-nitropyrimidin-4-yl

pyrrolidine-1-carbodithioate, further designated as NO 069 (Ryabova et al., 2004, Ryabova et al., 2005) designated as NO donor 069. Control tubes without treatment of NO donor were set up and incubated at 37°C without shaking. Each experiment was performed in triplicate.

2.6.3 Microdilution Resazurin Assay

A stock solution of Resazurin sodium salt (Sigma Aldrich) was prepared at 1% (wt/vol) in distilled water sterilized by filtration, and stored at 4 °C for up to 6 months.

Preparation NO donor, 6-methoxy-5-pyrimidin-4-yl pyrrolidine-1-carbodithiate (further designated as NO donor 069) for MIC determination were prepared fresh in C3 suite to ensure time of transportation to actual assay performed was minimal. A final concentration of 30mgmL⁻¹ of NO donor was prepared in 100µL DMSO. The mixture was further diluted 1 in 100 in supplemented 7H9 with 0.005% w/v Resazurin (assigned as supplemented 7H9-R) and was used as the working stock. A two-fold serial dilution of the working stock ranging from 0.1 to 12.8 µgmL⁻¹ (for Chapter 4) and 0 to 4µgmL⁻¹ of NO donor 069 (for Chapter 5) were prepared using the same medium. For each concentration, 100 µL were loaded in triplicate wells of clear, flat-bottomed 96-well microtitre plates (Corning).

For preparation of bacterial inoculum, a late exponential stage culture (OD_{580nm} of 0.8-1.0) was diluted to an OD_{580nm} 0.1 on the day of experiment. An approximate inoculum of ~5 X 10⁴ CFU (equivalent to 100µL of OD_{580nm} 0.1 suspension) were added to each well. Control wells representing supplemented 7H9-R with bacteria were also set up.

Plates were sealed with Petri seal adhesive sealing film (Sigma) and double bagged prior incubation at 37°C without shaking. A colour change in media from blue to pink was monitored from first week of incubation using an inverted mirror. Minimum inhibitory concentration (MIC) was determined as the lowest concentration of the compound that inhibited mycobacterial growth, with growth indicated by a visual colour change from blue to pink.

2.7 HEAT INACTIVATION OF MYCOBACTERIA FOR PCR

The pellet from 100µL culture was resuspended in same volume of H₂O and heat inactivated at 100°C for 30 minutes. When required, the boiled cultures (when cooled)

were ribolysed (Fastprep) at 6.5m/s for 15 seconds. Cellular debris was removed by centrifugation at 12,000 Xg for 15 minutes and supernatant used for polymerase chain reaction (PCR).

2.8 DEOXYRIBONUCLEIC ACID (DNA) MANIPULATIONS

2.8.1 Polymerase chain reaction (PCR)

Primers were designed using Primer-Blast software (Ye et al., 2012) and oligonucleotides were synthesized by Sigma-Aldrich. All primers used for generation and confirmation of *M. tuberculosis* strains are shown in Appendix 2-1.

Amplification of DNA fragments required for cloning utilized a High Fidelity Platinum® Taq DNA Polymerase (Invitrogen) using *M. tuberculosis* gDNA⁴ as the template. A 50µL reaction mixture contained 1X High Fidelity PCR Buffer, 2mM MgSO₄, 0.2mM of dNTP, 0.2µM forward and reverse primers, 10 ng template DNA and 0.2µL (1 unit) of Platinum® Taq DNA Polymerase. Cycling was performed using a Biorad thermocycler as follows: 94°C for 2 minutes for initial denaturation; 30 cycles of denaturation at 94°C for 15 seconds, 55°C (adjusted to melting temperature of primer) for 30 seconds, and extension for 68°C for 1 min/kb.

Culture PCR was performed using GoTaq® DNA polymerase (Promega) in 10µL reaction with 1X Green GoTaq® Reaction Buffer, 0.2mM dNTP, 0.5µM forward and reverse primers, 0.25 µL (1.25U) polymerase, 10ng DNA template from heat-inactivated culture and H₂O. Amplification cycle was as follows: 95°C for 2 minutes for initial denaturation; 30 cycles of denaturation at 95°C for 30 seconds, 55°C (adjusted to melting temperature of primer) for 30 seconds, and extension for 72°C for 1 min/kb. A final extension of 72°C for 5 minutes was set to complete the run. PCR products were analysed using agarose gel electrophoresis.

⁴ *M. tuberculosis* gDNA used for molecular work were obtained from BEI Resources, NIAID, NIH: Genomic DNA from *Mycobacterium tuberculosis*, Strain H37Rv, NR-48669 or lab stock

2.8.2 Agarose gel electrophoresis

DNA fragments were separated using 1% (w/v) agarose gels in TAE buffer (40mM Tris base, 20mM Acetic acid, 1mM EDTA); 0.1mgmL⁻¹ of ethidium bromide was added to allow visualization of the DNA with UV transillumination with a gel doc transilluminator. 1μL of 6X DNA loading buffer (GeneRuler™) was added to 5μL of the PCR mixture, and this was run along with 6μL DNA Ladder (GeneRuler™). Gels were run at 90 volts for 1 hour.

2.8.3 DNA and plasmid purification

Amplicons were purified directly from PCR using a Qiaquick® PCR Purification kit (Qiagen) or excised from agarose gel slices using a Qiaquick® Gel Extraction kit (Qiagen) as per manufacturer's protocols.

Plasmids were isolated from 5mL *E. coli* culture using a Gene Elute Plasmid Mini kit (Sigma), while a Qiagen® Plasmid Midi kit was used for purification of low copy plasmids from 50mL of overnight culture as per manufacturer's protocol.

DNA samples were eluted with 50μL of DNase/ RNase free water. DNA concentration was determined by Nanodrop before sending plasmids for sequencing to GATC Biotech.

2.8.4 Restriction enzyme digestion

Diagnostic restriction digestion of DNA was carried out in a 10μL reaction, while digestion of cloning vectors was performed in a 50μL reaction using buffers and enzymes from New England Biolabs (NEB). Reactions contained 1μl of each enzyme, 1 X Cutsmart Buffer and 500ng of DNA and incubated at 37°C for 1 hour. 6x Loading buffer was added before running a gel as described above.

2.8.5 Ligation

Ligation of linearised vector and insert DNA was performed using T₄ DNA ligase (Promega) as per manufacturer's protocol. A 10 μ L ligation mixture contained 100ng of purified vector, 100ng of purified insert DNA, 1 μ L of ligase 10X buffer with 1 μ L T₄ DNA ligase were incubated overnight at room temperature. The ligation mixture was used for transformation of *E. coli* DH5 α .

2.8.6 Transformation

The ligated plasmids (2-5 μ L) were added to 50 μ L of α - Select chemically competent cells (Bioline). The mixture was incubated on ice for 30 minutes and heat-shocked in 42 $^{\circ}$ C water bath for 45 seconds followed by incubation on ice for 2 minutes. After mixing with 900 μ L of preheated LB supplemented with 25mM MgSO₄, the mixture was incubated for 1hour at 37 $^{\circ}$ C with shaking at 200 rpm. The transformation mixture was spread on LB plates with required antibiotics for selection of transformants and incubated overnight.

2.8.7 Electroporation

Electrocompetent mycobacteria were prepared as previously described by Rindi and colleagues (Rindi et al., 2002). Briefly, 150mL of late logarithmic phase cultures (OD_{580nm} 1.0- 1.5) grown in roller bottles were washed thrice with 10% (v/v) glycerol (filter sterilized) by centrifugation at 3500 Xg for 15 minutes. Finally, the pellet was suspended in 1.4mL of 10% (v/v) glycerol. For electroporation, 400 μ L of competent cells were mixed with 500ng of replicating plasmid DNA or 5-10 μ g of suicide plasmids, incubated for 5 minutes at room temperature and transferred to a 2mm electrode-gap electroporation cuvettes (Eppendorf, UK). The cuvette was transferred to electroporation chamber of Bio-Rad Gene Pulser for a single pulse at 2500V, 25 μ F and 1000 Ω . The mixture was transferred to 3mL of supplemented 7H9 and incubated overnight at 37 $^{\circ}$ C with shaking. A negative control without plasmid DNA was also set up. After overnight incubation, the mixture was spread on antibiotics-supplemented 7H10 plates using different volumes; 2, 20 and 200 μ L of electroporated cells.

2.9 ISOLATION OF GENOMIC DNA FROM *M. TUBERCULOSIS* STRAINS

Genomic DNA was isolated by mechanical lysis as described by Belisle and Sonenberg (Belisle and Sonnenberg, 1998). Pellets of 10mL late exponential growing culture (OD_{580nm} 1-1.5) were resuspended in 20mL of breaking buffer [50mM TRIS-HCl pH= 8.0 (Fisher Scientific), 10mM EDTA (Sigma), 100mM NaCl (Ambion)] with a final concentration of $200\mu\text{g mL}^{-1}$ RNase (Qiagen) and centrifuged at 2500 Xg for 15 minutes. The bacterial suspension in 0.5mL breaking buffer was ribolysed (Fastprep) at 6.5ms^{-1} for 10 seconds. Once tubes were cooled, lysates were treated with 0.1 volume of 10% (v/v) SDS (Fisher Scientific) and $10\mu\text{L}$ of 10mg mL^{-1} Proteinase K to remove contaminants and incubated at 55°C for the first 3 hours and then following a second addition of both reagents, tubes were incubated for a further 1 hour. An equal volume of Phenol: Chloroform: Isoamyl alcohol 25:24:1 v/v/v was then added to remove contaminating proteins and manually mixed by inverting the tubes for 200 times. After centrifuging for 15 minutes at 12,000 Xg, the upper aqueous phase was transferred to a sterile eppendorf tube and taken out of C3 facility. For DNA precipitation, 0.1 volume of 3M sodium acetate (Sigma) and 1 volume of isopropanol were added before incubating at -20°C overnight. DNA pellets were obtained by centrifuging at 12,000 Xg for 30 minutes at 4°C and washed twice with ice cold 70% (v/v) ethanol and once with 100% ethanol. Air-dried pellets were resuspended in $200\mu\text{L}$ Tris-EDTA (10 mM Tris-HCl, 1 mM disodium EDTA, pH 8.0. buffer, Sigma). Concentration and purity of gDNA were assessed by Nanodrop and diagnostic digestions were analysed in 0.8% (w/v) agarose gel respectively.

2.10 RIBONUCLEI ACID (RNA) MANIPULATIONS

2.10.1 Preparation of Guanidine Thiocyanate (GTC) solution

Guanidine thiocyanate (GTC) solution was prepared by mixing the following reagents in a graduated 1000mL duran bottle.

590.8g Guanidine thiocyanate (Fisher Scientific)

5.0g N-lauroyl sarcosine

25mL 1M sodium citrate (pH 7.0)

5mL Tween-80

The solution was incubated without shaking at 37°C with some added distilled H₂O to dissolve overnight. The solution was adjusted to 1000mL by adding more distilled H₂O. Prior to use, 7mL β-mercaptoethanol was added to the solution. The bottle was stored covered in an aluminium foil and kept away from heat and light.

2.10.2 RNA extraction from *M. tuberculosis*

This is a method adapted from previous work (Waddell et al., 2004). A 9mL culture (unless otherwise stated) was mixed with 36mL GTC solution in 50mL centrifuge tube and centrifuged at 2500 X g for 30 minutes. Bacterial pellets were then resuspended in 10mL GTC solution and further centrifuged for 20 minutes. The remaining GTC solution was discarded and the pellets were resuspended in 1mL Trizol® reagent (Ambion) and disrupted using a FastPrep at 6.5ms⁻¹ for 45 seconds. Addition of 200µL chloroform to cell lysates allowed a partition of aqueous and phenolic phases after centrifuging at 9,600 Xg, 4°C for 15 minutes. The clear upper aqueous phase containing RNA was carefully re-extracted with an equal volume of chloroform. Following addition of the aqueous phase to a fresh tube, 0.8 volume of isopropanol was added. For RNA precipitation, the sample was incubated overnight at -20°C. After centrifugation at 9,600 Xg at 4°C for 15 minutes, the resulting RNA pellets were washed first with 1mL of ice-cold 70% (v/v) Ethanol and centrifuged at 9,600 Xg for 2 minutes. Next, the second wash was followed by adding 200µL of ice-cold 95% (v/v) Ethanol then centrifuged at 9,600 Xg for another 2 minutes at 4°C. The supernatant was discarded and the remaining RNA pellet was air dried by leaving the tube opened in a MSC Class II. The pellet was resuspended in 50µL DNase/ RNase free H₂O.

2.10.3 RNA cleanup and purification

To eliminate contaminating gDNA, a commercial TURBO DNA-free kit (Ambion) was used according to the manufacturer's protocol. Briefly, 0.1 volume 10X Turbo-DNase buffer and 1µL TURBO DNase were added to the samples and incubated at 37°C for 20 minutes. Next, 0.1 volume of DNase Inactivation Reagent was added and incubated at room temperature for 5 minutes. Supernatant containing DNase- free RNA samples were obtained after centrifugation at 10,000 Xg for 15 minutes. Concentration and purity of the RNA samples were assessed by Nanodrop.

When necessary, RNA was further purified by using an RNase Easy minikit (Qiagen) where Turbo-DNase treated samples were transferred to a gDNA eliminator spin column and processed according to the manufacturer's protocol. Samples were eluted from RNase Easy columns using 40µL of DNase/ RNase free H₂O and assessed for concentration and purity using Nanodrop.

2.10.4 Measuring RNA concentration

Purified RNA samples (1.5µL) were used to estimate RNA concentration by Nanodrop with an absorbance at 260nm. H₂O was used a blank for all samples. Concentration of RNA was expressed as ng/µL. All RNA samples were stored in -80°C.

2.10.5 Reverse transcription

First strand complimentary DNA (cDNA) was synthesized using Superscript™ II Reverse Transcriptase (Invitrogen) according to manufacturer's insert protocol using a gene specific reverse primer mix in 20µL reaction. Briefly, an initial 12µL reaction was prepared with gene specific reverse primer (GSP), dNTP and RNA samples and incubated at 65°C for 5 minutes to allow denaturation of secondary structure of RNA. Next, addition of 4µL of 5X First strand buffer and 2µL 0.1M DTT with 1µL of RNaseOUT™ (Invitrogen, when required) enhanced annealing of primers at 42°C for 2 minutes. Reverse transcription was initiated by adding 1µL of Superscript™ II RT. The reaction was proceeded in a thermocycler (Techne) programmed as follow; 42°C for 2 minutes and inactivation of reaction at 70°C for 15 minutes.

2.10.6 Quantitative Real Time PCR (qpcr)

An Absolute qPCR SYBR Green Mix (Thermo Scientific, 2008) was used according to the manufacturer's protocol. A 25µL reaction mix in 0.1mL strip tube (Qiagen) consisted of 1X Absolute qPCR SYBR Green Mix, 70nM GSP forward and reverse primer, 1µL template cDNA and 8µL H₂O. Each run included *M. tuberculosis* gDNA standards, cDNA samples and control samples (No-RT and NTC samples). These control samples were set up in parallel to the test samples to validate specificity of the assay. A duplicate reaction similar as above without addition of reverse transcriptase (designated as No-RT samples) was performed to detect the presence of contaminating gDNA. A no template control (NTC) contained all reaction components

except cDNA test samples (replaced with H₂O) to monitor presence of primer dimers or contamination from PCR components.

All samples were loaded in triplicate except the standard samples. All GSP primers used in the study are tabulated in Appendix 2.

The assay was performed in Corbett Rotor-Gene 6000 real-time thermocycler using the following cycling conditions: 95°C for 15 minutes to activate *Taq* DNA polymerase, followed by 40 cycles of 95°C for 15 seconds, annealing at 72°C for 20 seconds and extension step for 84°C for 20 seconds (Cheah et al., 2010).

A melting curve program was also set up by ramping 55°C to 99°C at 0.1°C per 5 seconds. A melting curve charts the 'melting' of double stranded (ds) to single stranded DNA. The melting temperature (T_m) is indicated by a reduction in fluorescence indicating SYBR Green dye dissociated from dsDNA. This is better illustrated using a negative derivation with a $-\Delta F/\Delta T$ (change in fluorescence/ change in temperature) plotted against temperature. A sharp peak for the target amplicon will be shown corresponding to the associated T_m , with a standard deviation of 0.5°C will be accepted. Melt curve analysis was performed to determine the specificity of the assay as it detects the presence of non-specific products such as primer-dimers. Representative melt curves generated from each experiment are found in Appendix 7. The cDNA samples were later stored at -20°C.

2.10.7 Analysis of qRT-PCR

4.1.1.1.1 Genomic DNA contamination

An important test for the quality of the RNA sample is to determine if it contains a significant amount of genomic DNA contamination. For each qPCR run, the experimental samples with their parallel no RT samples were loaded as triplicates to determine level of gDNA contamination. It was estimated by dividing the amplicon copy numbers in no-RT sample by test sample. A 10% threshold value obtained for each test sample will be analysed further for normalisation to *16S* gene (Garton et al., 2008).

4.1.1.1.2 Standard curve

A dilution series of known *M. tuberculosis* gDNA concentration were used to generate a standard curve to determine initial starting amount of target template and to assess reaction efficiency, sensitivity and reproducibility. A 1 in 2 dilution of 100ng/μL *M. tuberculosis* gDNA in H₂O with final concentration of 1X 10⁷ copies as the 1st standard sample was used for further dilutions. Using the information below,

- A- Avogadro's number, 6.022×10²³ molecules per mole,
- B- One mole per basepair (bp) weighs 650 grams(g)
- C- The number of molecules of *M. tuberculosis* gDNA template i.e. 4,411,529 bp (Cole, 1998)

The *M. tuberculosis* genome copy numbers are approximately 2.1 X10⁷ copies that was calculated using the following formula:

$$\text{Equation 2-2: } \quad \text{Number of copies} = \frac{\text{Amount of DNA (ng)} \times 6.022 \times 10^{23}}{\text{Length (basepair)} \times 1 \times 10^9 \times 650}$$

A total of eight *M. tuberculosis* gDNA standards ranging from 1X 10⁷ to 1X 10³ copies were used. After each run, both standard and melting curves were generated using Rotor Gene 1.7 software. A standard curve exhibits a threshold cycle, C_T in y-axis plotted against the concentration of each standards on the x-axis and is used to derive parameters such as correlation efficiency (R²), slope (M) and reaction efficiency. C_T is used to calculate the initial cDNA copy numbers as the value is inversely related to the starting amount of the target transcripts. Thus, the quantity of mRNA in each reaction was generated from the cDNA copy number with reference to the aforementioned standard curve (Forrellad et al., 2013)

Assay performance lies primarily on a good PCR amplification efficiency, ideally 100% indicating a perfect cDNA doubling after each cycle during exponential amplification. In practice, PCR efficiency between 90- 110% corresponding to a slope of between -3.58 and -3.10 is acceptable, using equation:

$$\text{Equation 2-3 } \quad \text{PCR Efficiency} = 10^{(-1/\text{slope})-1}$$

In addition, an ideal correlation coefficient of 1 correlates linearity of the standard curve. This reflected a linear dynamic range of the reaction where the highest to the lowest quantifiable copy number of template DNA fits in the standard curve. It is also a measure of replicate reproducibility (Bustin et al., 2009, Life Technologies, 2012). Analyses of assay performance for each experiment are compiled in Appendix 6.

4.1.1.1.3 Gene expression analysis

Quantitative results for cDNA copies in test samples were assayed in triplicate and were normalised to the chosen reference gene (16S) to obtain relative expression (RE) value. The aim of this was to compensate inter- (sample to sample) and intra- (run to run) assay variations (Pfaffl, 2001 #404). Where applicable, to determine the expression of low abundance genes, the copy numbers of the experimental cDNA samples were compared to the copy numbers of no-RT samples and was statistically determined. A significant difference was considered as an expression provided that it was not obscured with gross gDNA contamination.

A relative expression (RE) value was then calculated by dividing the target gene copy numbers in test samples by mean of 16S cDNA copy numbers. The normalised value for each target gene can then be compared for each treatment. The RE induction ratio (fold- change) was determined by dividing the RE value of target genes after treatment (different exposure time) by RE value during exponential growth or before treatment.

2.11 STATISTICAL ANALYSIS

All relevant statistical analysis was performed and plotted using Graph Pad Prism software (Prism Version 7). Statistical analyses were performed using Student t-test or one-way ANOVA using the Prism software.

Statistical analyses for infection experiments were done using nonparametric tests including the Mann-Whitney rank sum test or the Kruskal-Wallis test. All of these tests pool the data and rank the values. The statistic calculates the probability that the observed ranking occurred by chance.

P-values less than or equal to 0.05 were considered statistically significant.

CHAPTER 3

Initial investigations on determining the essentiality of *rv2660c* and *rv2661c* in *Mycobacterium tuberculosis*

CHAPTER 3 Initial investigations on determining the essentiality of *rv266oc* and *rv2661c* in *Mycobacterium tuberculosis*

3.1 INTRODUCTION

Rv266oc and Rv2661c are conserved hypothetical proteins (HPs) with only 12% identity at the protein level. The nucleotide sequences from *M. tuberculosis* H37Rv strain alignment showed no homology with genes of other bacterial species. These genes are highly restricted to pathogenic mycobacteria with similar conservation patterns (> 99% identity) seen in *M. bovis* BCG (annotated as mb2678c for *M. tuberculosis rv266oc* and mb2679c for *M. tuberculosis rv2661c*), *M. bovis* and MTBC strains such as *M. africanum* and *M. caprae*. Both HPs are encoded in minus strand; *rv2661c* spanning 390bp in positions 2981187 to 2981576 of the genome and adjacent *rv266oc* located 2980963 to 2981190 covering 228bp (Lew et al., 2011). Within the operon, *rv2662* is encoded on plus strand (Lew et al., 2011). This genomic organisation is seen in both *M. tuberculosis* H37Rv and *M. bovis* BCG (Lew et al., 2011) and suggest that function of these HPs is related to each other. Furthermore, a recent identification of nutrient-induced non-coding RNA, ncRv12659 that overlapped *rv266oc* locus highlighted the complexity of the genomic organisation (Houghton et al., 2013), illustrated in Figure 3-1.

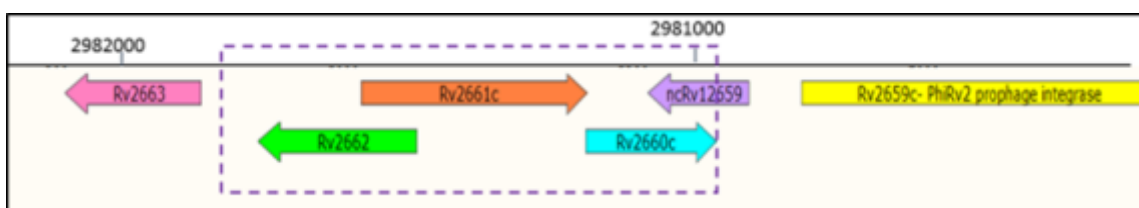


Figure 3-1: Schematic representation of the *rv266oc* and *rv2661c* genomic region in *M. tuberculosis*. Rv266oc and Rv2661c are located on Rv266oc- Rv2661c operon where the N-terminal region of Rv266oc extends to include part of the Rv2661c sequence and in the sense orientation. *rv2662c* overlaps by 86bp with *rv2661c* in an antisense orientation, while ncRv12659 overlaps with *rv266oc* sequences by 114bp (Lew et al., 2011).

Previous published transcriptomic profiling of *M. tuberculosis* in various models of TB infection including models of NRP (Table 3-1) has highlighted the role of these

annotated genes to the adaptation of *M. tuberculosis* during dormancy and virulence. An initial microarray study by Betts and colleagues identified a massive upregulation of *rv2660c* (280 fold), *rv2661c* (27- fold), *rv2662* (34- fold) from extracts of 96 hours nutrient starved *M. tuberculosis* cells in PBS (Betts et al., 2002). Furthermore, these genes were significantly upregulated during the transition of *M. tuberculosis* cells to 'non-culturability' state in a stationary phase that involved growing culture in a supplemented 7H9 medium for 62 days (Salina et al., 2009). These genes were also expressed in other *in vitro* NRP conditions such as in Wayne's hypoxia model (Voskuil et al., 2004), enduring hypoxia response (Rustad et al., 2008) and exposure to hydrogen peroxide (Schnappinger et al., 2003). In a similar study by Schnappinger and colleagues, they identified these three genes in the intraphagosomal *M. tuberculosis* transcriptome of IFN- γ activated bone marrow-derived murine macrophages at 24 and 48 hours of infection (Schnappinger et al., 2003). Recently, an *in vitro* fatty acid environment generated by growing *M. tuberculosis* in dextrose medium induced significant upregulation of *rv2660c* during exponential phase as opposed to different NRP stages (Soto-Ramirez et al., 2017). It was proposed that fatty acid, which is one of the lipid compounds involved in persistence might be the main stress determinants for expression of *rv2660c* (Soto-Ramirez et al., 2017).

Further *in vivo* global expression profiling by microarray identified expression of *rv2660c* in the human-like caseous lungs of C3HEB/FeJ mice during later stages of infection, which is at 20, 30 and 80 days post-infection (Gautam et al., 2015b). Expression of *rv2660c* and *rv2661* was also upregulated in lungs of BALB/c mice at 14, 21 and 28 days after exposure (Talaat et al., 2004). These findings corroborated with Aagaard and colleagues' study (Aagaard et al., 2011) that demonstrated a stable induction of *rv2660c* in lungs of *M. tuberculosis*-infected CB6F1 mice at 3 and 6 weeks of infection, analysed by quantitative RT-PCR. Hence proposing Rv2660c as a latency-associated antigen (Aagaard et al., 2011). The expression of *rv2660c* and *rv2661c* after 21 days of infection suggest its involvement in also controlling dissemination in lungs corresponding to activation of acquired immune responses in BALB/C mice (Orme et al., 1993, Dunn and North, 1996). In particular, Rv2661c was also identified in a chronically infected guinea pig after 90 days of infection (Kruh et al., 2010).

Collectively, the data suggest that *rv2660c* and *rv2661c* are important for *M. tuberculosis* to adapt and survive during NRP and infection.

A genomic scale screening study using a transposon insertion site-mapping method (TraSH) has identified Rv2661c as essential for *M. tuberculosis* survival in macrophage during host CD4 mediated tryptophan starvation (Zhang et al., 2013). Briefly, a library of *M. tuberculosis* transposon mutants were used to infect wild-type and CD4-deficient (MHC class-II-deficient, MHCII^{-/-}) mice. The mutants with *in vivo* growth defects in MHCII^{-/-} mice but growth in wild-type mice were identified as the 58 genes that are responsible for surviving the CD4 T-cell responses, termed as *M. tuberculosis* CD4 counteractome. A similar approach was used to identify genes required for *M. tuberculosis* survival during CD4 mediated tryptophan starvation by using a library of conditional mutants generated by growth on solid 7H10 medium (to induce tryptophan starvation) and compare with the counteractome signature. There were 12 genes including *rv2661c* and other genes responsible during tryptophan biosynthesis; *trpB*, *trpD* and *trpE*, (Lin et al., 2009). Host Indoleamine 2,3-dioxygenase-1 (IDO-1), activated by CD4 cells via IFN- γ signaling is the first rate-limiting enzyme of tryptophan metabolism (Zelante et al., 2009). The host immune-mediated response degrades intracellular tryptophan (Zhang et al., 2013). The authors inhibited bacterial tryptophan synthesis with an halogenated anthranilate (a tryptophan metabolite) analogue, 2-amino-6-fluoro- benzoic acid (6-FABA). This compound inhibited *M. tuberculosis* growth *in vivo*, thus a potential anti-infective agent (Zhang et al., 2013). *In vitro* assay has shown that 6-FABA was active against *M. tuberculosis* at an MIC of 5 μ M (Zhang et al., 2013). Since Rv2661c was implicated to be involved during tryptophan biosynthesis, we hypothesised that the *rv2661c* deletion strain would have higher sensitivity to 6-FABA, resulting in decreased MIC values compared with wild-type *M. tuberculosis*.

In contrast to Rv2661c, Rv2660c has been receiving focus in vaccine development. A multistage vaccine that combines classical preventive target antigens (antigens secreted in an early infection) and highly expressed key latency associated antigen was developed to improve the efficacy of current bacillus Calmette- Guerin (BCG) vaccine. The vaccine, H56: IC31 combines Ag85B (Rv1886c) and ESAT-6 (Rv3875) with Rv2660c was demonstrated as a post-exposure vaccination for *M. tuberculosis*-

infected individuals (Luabeya et al., 2015) and has entered clinical Phase 2 trial. The adjuvant IC₃₁ (Intercell) was selected as it promoted a strong Th1 response for control of infection and demonstrated to have an excellent safety profile in the first TB clinical trial (van Dissel et al., 2010). Performance of H56 vaccine with the other two different adjuvants; CAF₀₄ and CAF₀₅ also exhibited higher IFN- γ responses which demonstrated the efficacy of H56 in improving disease outcomes (Billeskov et al., 2016). A high-level Rv2660c T-cell response was elicited in BCG-immunized cynomolgus macaques (Lin et al., 2012). As a result, a delayed and reduced infection with *M. tuberculosis* was observed and prevented anti-TNF triggered reactivation of latent infection (Lin et al., 2012). However, boosting of this vaccine elicited a low level of Rv2660c T-cell responses in two different African groups of LTBI (Govender et al., 2010), LTBI Chinese patients (He et al., 2015) and became transient in the active TB infected patients (Luabeya et al., 2015). Immunisation with a recently developed DNA vaccine, p846 that combines Rv2660c with Rv3615c and Mtb 10.4 resulted in a 15-fold decrease in bacterial load after immunisation and the immunised mice exhibited fewer lesions in lungs (Kong et al., 2014), further highlighting the potential use of Rv2660c in post exposure TB vaccine.

In the past, microarray analysis has been the primary technology for gene expression analysis and has had some limitations such as cross hybridisation and the inability to identify novel transcripts. With the advances of high throughput genome sequencing, it was identified that transcription of *rv2660c* was actually from an antisense orientation in *M. tuberculosis* starved cells (Uplekar et al., 2013). The ncRv12659 that is convergent and overlaps with the *rv2660c* locus was massively upregulated at 24 hours of starvation and in murine infection (Houghton et al., 2013). Furthermore, the Rv2660c peptide was not detected during starvation using highly sensitive targeted mass spectrometry (Houghton et al., 2013, Albrethsen et al., 2013). In other study, a 14-kDa recombinant Rv2660c in *M. bovis* BCG over-expressing strain of Rv2660c were detected which were grown in acidic pH5.3 and later detected using Rv2660c monoclonal antibodies (Yihao et al., 2015) which further questioned the existence Rv2660c and upregulation of both *rv2660c* and *rv2661c* in models of NRP.

To address these questions, a panel of in-frame deletion mutants and over-expressing strains of *rv2660c* and *rv2661c* in *M. tuberculosis* were generated by Dr Galina

Mukamolova and subsequently confirmed in this study . The genetic recombination methods commonly used for generating deletion and over-expressing strains in mycobacteria are briefly mentioned below. Importantly, deleting *rv2660c* and *rv2661c* also resulted in partial deletion of respective *ncRv12659* and *rv2662*. Therefore, phenotypic changes observed in the deletion mutant can be attributed to several genes and non-coding RNA in this genomic region. This contribution could be further validated by complementation studies. In addition, this chapter also describes the initial investigations in determining the phenotypic characteristics of these deletion and over-expressing strains during growth in standard laboratory media.

Genes	Nutrient Starvation (Betts et al., 2002)	Wayne's Hypoxia Model (Voskuil et al., 2004)	Enduring Hypoxia Response (Rustad et al., 2008)	Stationary Phase (Salina et al., 2009)	5mM H ₂ O ₂ (Voskuil et al., 2011, Schnappinger et al., 2003)	48 hours of IFN-Activated macrophages (Schnappinger et al., 2003, Schnappinger et al., 2006)	CB6F1 mice -20 weeks infection (Aagaard et al., 2011)
<i>rv2660c</i>	282.24	9.1	2.96	19.7	3.84	3.4	860
<i>rv2661c</i>	26.77	-	2.8	-	1.07	2.5	n/a
<i>rv2662</i>	34.23	5.6	3.35	12.9	0.87	2.4	n/a

Table 3-1: Expression of *rv2660c*, *rv2661c* and *rv2662* in various *in vitro* NRP and stress models analysed by microarray. The major housekeeping gene, 16S *r*RNA was used as an internal control for the normalisation of mRNA levels in all the studies mentioned above except sigma factor gene *Sig A* for the oxidative stress assay (Schnappinger et al., 2003). Data presents mean induction ratios calculated compared from RNA of culture grown to mid-exponential phase in supplemented 7Hg.

3.1.1 Construction of genetic deletions in *M. tuberculosis* H37Rv

Genetic manipulation tools for mycobacteria have been developed for the last 15 years and have remained invaluable to understand the biology and pathogenesis of mycobacteria. They involve a construction of targeted genetic deletions to demonstrate gene essentiality, determine gene function and generate attenuated strains for vaccine research and drug development. Some previous genetic manipulation systems include the use of non-replicating (Husson et al., 1990, Parish and Stoker, 2000b) and replicating plasmids (Pashley et al., 2003), and long linear DNA fragments up to 40kbp (Balasubramanian et al., 1996). Gene replacement and deletion can be performed using suicide plasmids and homologous recombination approaches (Parish and Stoker, 2000a, Parish and Stoker, 2000b) or by using mycobacteriophage-mediated delivery (Bardarov et al., 2002). The system developed by Parish and Stoker (Parish and Stoker, 2000b) using pNIL/ pGOAL plasmids has been widely used for generation of unmarked mycobacterial mutants in *M. tuberculosis* (Chauhan et al., 2006, Cholo et al., 2006, Pang et al., 2007, Parish et al., 2003b, Saikolappan et al., 2012, Curry et al., 2005). In this study, the delivery vector is constructed by in-frame fusion of upstream and downstream regions of the target gene in a pNIL plasmid (p2NIL series), thus generating the genetic region missing the entire target gene. The marker cassette containing *lacZ*, *sacB* and *hyg* gene is introduced to enable screening for single and double crossover clones as illustrated in Figure 3-2 creating the delivery vector. Single crossover strains containing the plasmid can grow on kanamycin, produce blue coloured colonies on X-gal containing agar and are resistant to hygromycin. On the other hand, sucrose inhibits growth of single crossover strains due to the presence of *the sacB* gene in the plasmid. Cultivation of single crossover bacteria without selection pressure (antibiotics) results in the loss of the plasmid due to second homologous recombination. These double crossover strains have either a wild-type genome or a deletion of the target gene (Parish and Stoker, 2000b) which are sensitive to antibiotics and resistant to sucrose. Application of PCR, Southern hybridisation or whole genome sequencing can be used for confirmation of gene deletion.

An *in vitro* generated specialised transducing phage has also been used for generation of deletion mutants (Bardarov et al., 2002, Raman et al., 2001, Sirakova et al., 2001, Kandasamy and Narayanan, 2014). It involves an *E. coli* cosmid vector containing the allelic exchange substrates (AES) and cloning the recombinant cosmid into a conditionally replicating (temperature sensitive) shuttle phasmid. Further transfection of the mycobacteria at the permissive temperature of 30°C generated high-titre transducing phage. The transduction to mycobacterial host generates recombinants and was selected at 37°C as phages could not be replicated at this temperature (Bardarov et al., 2002, Bardarov, 1997). A more recent improvement to this system involves a single-step strategy for AES by using temperature-sensitive shuttle phasmid that only injects its DNA and does not propagate in the infected mycobacterial cell at 37°C (Jain et al., 2014). An unmarked double (leucine and pantothenate) auxotroph of *M. tuberculosis* H37Rv which displayed less virulence in mouse studies was constructed using this system (Jain et al., 2014).

Use of conditionally replicating temperature-sensitive phasmid as a delivery vector has improved reproducibility of allelic exchange in the slow-growing mycobacteria, allowing generation of >10⁶ different *M. tuberculosis* transposon (Tn) mutants (Pelicic et al., 1997). Insertional mutants were positively selected where the system was a combined *sacB* gene and a mycobacterial thermosensitive origin of replication and then efficiently counter-selected on sucrose at 39°C (Pelicic et al., 1997).

Generation of Tn-mutant libraries for large-scale phenotypic screening including genes required for pathogen adaptation to host was performed by using signature-tagged mutagenesis (Camacho et al., 1999). Mobile elements were inserted randomly that the chromosome became saturated with insertions. Identification of essential genes by this strategy was possible as it relied on the fact that such genes are devoid of insertions (Wei and Rubin, 2008). Transposons Tn5367 and Tn5368 containing insertion sequence IS1096 (Cirillo et al., 1991) were shown to mutagenise *M. bovis* BCG giving rise to a set of auxotrophic mutants (McAdam, 1995) and in several strains of *M. tuberculosis* (Bardarov, 1997, Pelicic et al., 1997). However, detection of very rare allelic exchange events was hindered by low transformation efficiencies and high frequencies of illegitimate recombination, where no more than 100 mutants per experiment have only been obtained (McAdam, 1995). Identification of genes that

were not disrupted among the large pool of insertion mutants were improved by sequencing Tn-chromosome junctions known as deep sequencing of Tn insertion (TnSeq) libraries (Gawronski et al., 2009, Hutchison et al., 1999). It was widely used in dissecting essential genes in particular metabolic pathways (Griffin et al., 2011) and mechanisms of pathogenesis (Zhang et al., 2012, Joshi et al., 2006) in *M. tuberculosis*. These essential genes identified in studies as mentioned above were broadly consistent with a TraSH study mapped by DNA microarray (Sasseti et al., 2003). Recently, sequencing of Himar1 library led to the identification of 7 sRNAs in *M. tuberculosis* found to be essential for growth *in vitro*, six of which occurred in 5'UTRs that likely represent processed transcripts (DeJesus et al., 2017).

The essentiality of a gene depends on the requirement and metabolic state of the pathogen throughout infection period. Hence, conditional gene knockdowns were generated to provide an additional advantage of modulating expression or repression at a particular defined phase of infection (Seeliger et al., 2012). Inducible systems are commonly used to silence genes via direct transcriptional control or expressing anti-sense mRNA and to overexpress proteins for biochemical and structural studies (Savary et al., 2011). These systems will be further described in the next section which covers strategies for gene over-expression. For gene silencing, a straightforward method involved replacing the native promoter of a target gene with a tightly regulated promoter whose activity can be controlled experimentally. The theophylline-inducible artificial riboswitch has emerged as an alternative system to exclude the use of exogenous regulator proteins and was competent to control gene expression during macrophage infection (Seeliger et al., 2012, Van Vlack and Seeliger, 2015). All regulatory elements were encoded within the 5'UTR of the mRNA, directly upstream of the target gene (Seeliger et al., 2012, Van Vlack and Seeliger, 2015). Its limitation included low-frequency homologous recombination in mycobacteria and retention of a residual, truncated gene copy (Van Vlack and Seeliger, 2015). Gene silencing by antisense inhibition has been performed in *M. tuberculosis* by generating constructs where target gene was placed in antisense orientation under an inducible promoter. The antisense sequences that hybridise to mRNA will repress the expression of the target gene upon induction and prevent translation (Parish and Stoker, 1997, Kaur et al., 2009).

The bacterial type II CRISPR-Cas9 (Clustered Regularly Interspaced Short Palindromic Repeats) -associated only protein-9 nuclease (Cas9) from *Streptococcus pyogenes* has emerged as a recent gene silencing tool that promises a robust, manageable and scalable platform for regulated gene silencing (Cong et al., 2013, Deltcheva et al., 2011). CRISPRi system involved the co-expression of DNA endonuclease-deficient Cas9 (dCas9) (Qi et al., 2013) and the small guide RNA specific to a target sequence, resulting in the DNA recognition complex that interfered with the transcription of corresponding DNA sequence (Jinek et al., 2012). CRISPRi system was shown to be competent in suppressing expression of multiple target genes in mycobacteria (Choudhary et al., 2015). Another group demonstrated that dCas9 protein derived from the CRISPRi locus of *Streptococcus thermophilus* (dCas9_{Stth1}) produced the most robust and consistent gene silencing in *Renilla* luciferase reporter assay with minimal proteotoxicity (Rock et al., 2017). Although it induced minimal upstream polar effect, CRISPRi system holds promising perspective for more *M. tuberculosis* drug discovery (Rock et al., 2017)

3.1.2 Construction of over-expressing strains in *M. tuberculosis*

As mentioned earlier, gene over-expression is another approach for the analysis of gene function (Ehrt and Schnappinger, 2006). Several plasmid-based mycobacterium vectors or mycobacteriophage- derived vectors have been successfully used for gene over-expression in both fast and slow-growing mycobacterium strains. The origin of replication identified in the *Mycobacterium fortuitum* plasmid pAL5000 (Ainsa et al., 1996, Picardeau et al., 2000) was widely explored and quickly became a foundation for the development of *Escherichia coli*-mycobacterium shuttle vectors such as pMV261 (Stover et al., 1991), pLA71 (Le Dantec et al., 2001), pMIP12 (Le Dantec et al., 2001, Lim et al., 1995) and PJK series (Kanno et al., 2016). The primary goal of plasmid development was to generate a stable recombinant BCG vaccine. These shuttle vectors were either maintained and replicated extrachromosomally in mycobacteria or integrated into the genome where gene expression in these plasmids was driven by mycobacterial promoters (Bastos et al., 2009). The heat shock protein promoters (P_{hsp60} from *M. bovis* BCG and P_{hsp70} from *M. tuberculosis*), the IS900 ORF promoter (PAN from *M. paratuberculosis*) and the mutated β -lactamase promoter (P_{BlaF*} from *M.*

fortuitum) are common ones, as reviewed by Bastos and colleagues (Bastos et al., 2009). These extrachromosomal plasmids generate high copy numbers in mycobacteria and have been shown to result *in vitro* and *in vivo* instability of recombinant vaccines caused by the unpredictable gene expression levels or protein toxicity (Joseph et al., 2006, Matsuo and Yasutomi, 2011). Moreover, the integrative vectors derived from temperate mycobacteriophages, such as L517 (Lee et al., 1991) or Ms6 (Dos Vultos et al., 2006) are characterised by the generation of low copy number. It has been reported that the vectors affected heterologous gene expression or interfere infection experiments in mycobacteria (Mo et al., 2007, Yi et al., 2007). Hence, gene expression could be experimentally controlled through the use of inducible systems. In particular, the dosing control afforded by inducible regulation can help reduce the harmful effects of over-expression of toxic proteins (Van Vlack and Seeliger, 2015). The acetamide-inducible promoters controlled by two positive regulators, AmiC and AmiD and a negative regulator, AmiA were used for development of the first inducible promoter system. The system can be induced by the addition of short aliphatic amides, acetamide or butyramide to the growth medium (Mahenthalingam et al., 1993). It was proven invaluable for generation of conditional mutant and protein over-expression. (Parish and Stoker, 1997, Parish et al., 1997, Brown and Parish, 2006). Other inducible systems include pNIT plasmids which carry the isovaleronitrile-inducible promoter (Pandey et al., 2009), pMY696 which has a pristinamycin-inducible promoter (Forti et al., 2009) and tetracycline repressor based (TetR) systems controlled by addition of tetracycline (Blokpoel et al., 2005, Ehrt et al., 2005).

Any systems have limitations, and an ideal inducible promoter system should meet the following criteria: (i) under repressing conditions, expression should be completely silent, (ii) provide significant level of over-expression (i.e. >1000- fold) that can be controlled in a dose-responsive manner, (iii) no interference to gene's native regulation under inducing conditions and (iv) rapid gene induction and protein depletion during *in vitro* growth and NRP and also during infection of host cells and animals (Schnappinger and Ehrt, 2014).

The aim of this study was to investigate the essentiality of *rv2660c* and *rv2661c* in *M. tuberculosis* during *in vitro* growth and during tryptophan starvation. The following objectives were carried out:

- Generation of three in-frame deletion mutants: an *rv2660c* single deletion mutant, an *rv2661c* single deletion mutant and an *rv2661c -rv2660c* double deletion mutant Parish and Stoker method (Parish and Stoker, 2000b)
- Generation of three over-expression strains pMV261::*rv2660c*, pMV261::*rv2661c* and pMV261::*rv2661c-rv2660c* over-expressing strains
- Initial characterisation of deletion mutants and over-expressing strains during *in vitro* growth using standard liquid and solid laboratory media
- Establishing the minimum inhibitory concentration of 2-amino-6-fluoro-benzoic acid (6-FABA) for the deletion mutants and wild-type of *M. tuberculosis*

3.2 METHODS

3.2.1 Bacterial strains

A list of deletion and over-expressing strains used in the study is found in Table 2-1. The *E. coli* DH5 α competent cells (Genotype: F- *deoR endA1 recA1 relA1 gyrA96 hsdR17(rk -, mk +) supE44 thi-1 phoA Δ (lacZYA argF)U169 Φ 80lacZ Δ M15 λ* , Bioline) was used in cloning.

3.2.2 Generation of single and double deletion of *rv2661c* and *rv2660c* strains in *M. tuberculosis*

Deletion delivery vectors designated further in thesis as p Δ *rv2660c*, p Δ *rv2661c* and p Δ *rv2661c:rv2660c* (Appendix 3) were constructed by Dr Galina Mukamolova (UoL) using homologous recombination method (Parish and Stoker, 2000b) shown in Figure 3-2 to generate respective deletion strains; Δ *rv2660c*, Δ *rv2661c* and Δ *rv2661c:rv2660c*. Two separate flanking regions upstream (FR2) and downstream (FR1) of the gene were amplified from *M. tuberculosis* H37Rv genomic DNA using respective primers described in Appendix 1. These primers were designed to introduce *HindIII* and *BamHI* restriction sites to FR2 while with amplified FR1, both *BamHI* and *NotI* sites introduced. The assigned DNA fragments used for construction of p Δ *rv2660c* were 2660FR2 and 2660FR1, for p Δ *rv2661c* (2661FR2 and 2661FR1) and p Δ *rv2661c:rv2660c* (2660FR1 and 2661FR2), illustrated in Figure 3-3. Both amplified fragments were individually cloned to *E. coli* pGEM[®]-T Easy vector (Promega) creating pGemT::FR1 and pGemT::FR2 plasmids using *E. coli* DH5 α . White colonies grown on LA plates with 50 μ g mL⁻¹ Ampicillin, 80 μ g mL⁻¹ X-gal and 100mM IPTG were selected for plasmid preps. Isolated constructs were sequenced to ensure no mutations created during PCR.

Confirmed DNA fragments were subsequently subcloned into p2NIL vector with the indicated restriction enzyme sites. Gel purified FR2 excised from pGemT::FR2 using *BamHI* and *HindIII* enzymes was ligated to similar digested purified p2NIL (creating p2NIL::FR2). The ligation mixture was transformed into *E. coli* DH5 α and transformants were checked for correct insert by performing diagnostic digestions. Subsequently, purified FR1 was then ligated to *BamHI*-*NotI* digested p2NIL::FR2 and resultant *E. coli* transformants were selected on kanamycin. A number of digestions

were employed to confirm both inserts in p2NIL plasmid. Next, the *PacI* cassette was excised from pGoal19 and then cloned into the single *PacI* site of the p2NIL derivative generating respective p Δ *rv2661c* (16438bp), p Δ *rv2660c* (16586bp) and p Δ *rv2661c:rv2660c* (16199bp) constructs.

These final suicide delivery plasmids (10 μ g) were electroporated into *M. tuberculosis* H37Rv. Following overnight incubation, the electroporated cultures were spread on supplemented 7H10 with Kanamycin and X-gal. After 6 weeks of incubation, the blue colonies were selected and were confirmed by PCR as single crossover clones. To stimulate double crossover, the blue colonies were inoculated into supplemented 7H9 without kanamycin and grown until late exponential stage. Cultures were then plated on supplemented 7H10 with 2% (v/v) sucrose, 80 μ g mL⁻¹ X-gal and 50 μ g mL⁻¹ kanamycin. After 4 weeks of incubation, white sucrose resistant colonies were then streaked on two separate plates, one containing sucrose and X-Gal; other supplemented without kanamycin. White kanamycin-sensitive colonies were screened by PCR using test or gene-specific primers.

Each of the generated deletion mutants will yield as follows; The resultant Δ *rv2660c* strain has a 213bp deletion of *rv2660c* sequence corresponding to deletion of overlapping 114bp at 3'end of *ncRv12659* sequence. The *Rv2661c* sequence was unaffected by deletion of *rv2660c*. As a result, only 9bp at 5'end and 6bp at 3'end of *Rv2660c* with introduced *BamHI* restriction site remained.

The Δ *rv2661c* strain has a 363bp deletion of *Rv2661c* sequence corresponding to deletion of overlapping 86bp at 5'end of *Rv2662* sequence. Only 9bp at 5'-end and 19bp at 3'end of *rv2661c* joined by *BamHI* restriction site followed by 187bp of *Rv2662* sequence remained in the strain.

Subsequently, a deletion of both gene sequences will result in partial deletions of both *Rv2662* and *ncRv12659* generating Δ *rv2661c:rv2660c* strain. A remaining 9bp at 5'end of *Rv2661c* and 6bp at 3'end of *Rv2660c* sequence with 58bp at 5'end *ncRv12659* and 187bp at 3'end of *Rv2662* sequence were maintained in this strain.

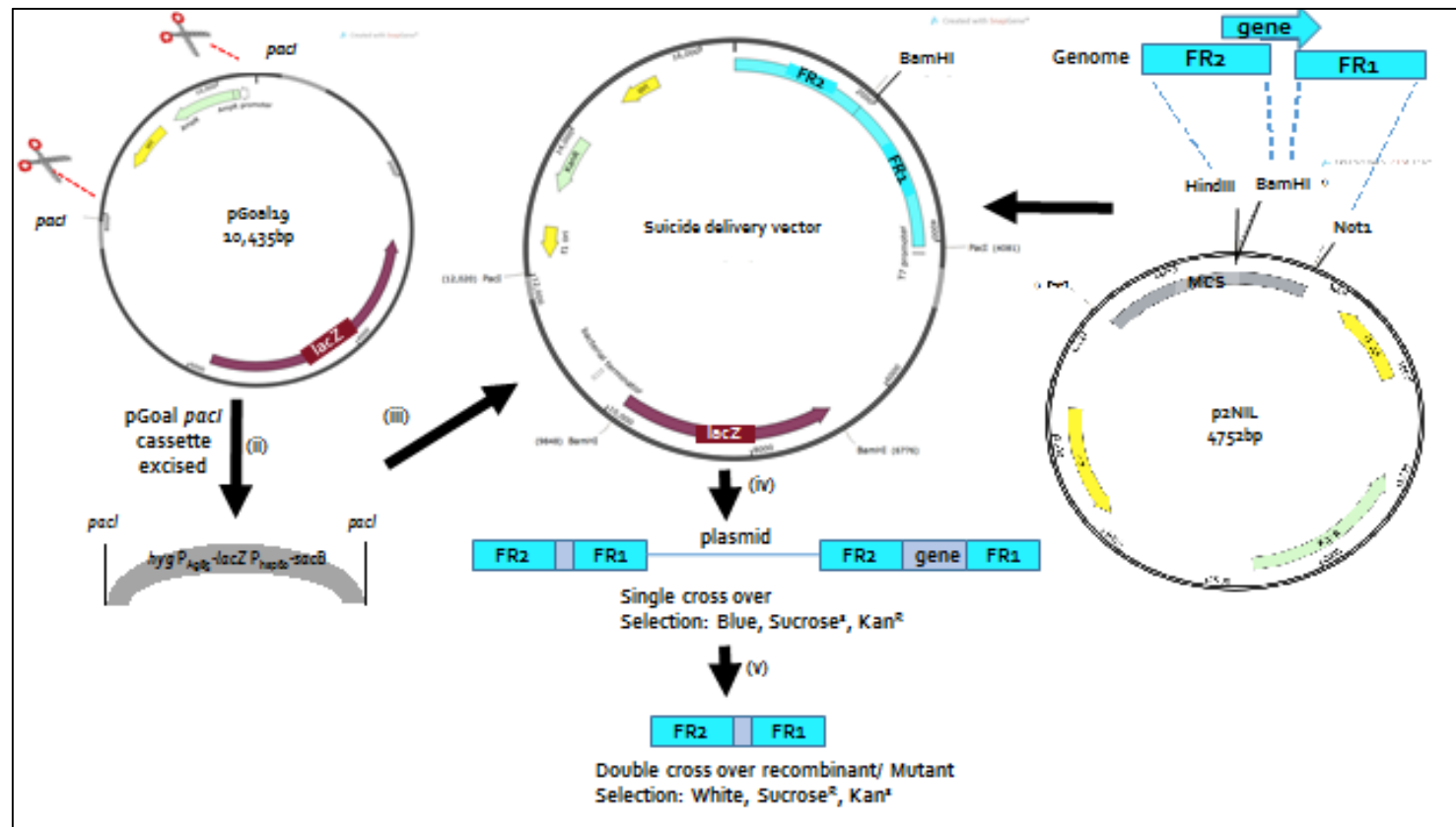


Figure 3-2: Strategy for generation of deletion mutants in *M. tuberculosis* using homologous recombination approach.

Procedure were adapted from Parish and Stover (Parish and Stoker, 2000b) and were carried out as follows: (i) Two separate amplified flanking regions, FR1 and FR2 for target gene were cloned into p2NIL (ii) A marker gene cassette with two *Pacl* restriction sites were excised from pGoal19 (iii) The *Pacl* cassette cloned into the p2NIL/deleted gene creating the final deletion delivery vector. The purified deletion construct was electroporated into *M. tuberculosis* H37Rv to generate final deletion strain (iv) Single cross over event (v) Double cross over colonies containing mutant allele selected based on growth of white colonies on media without kanamycin

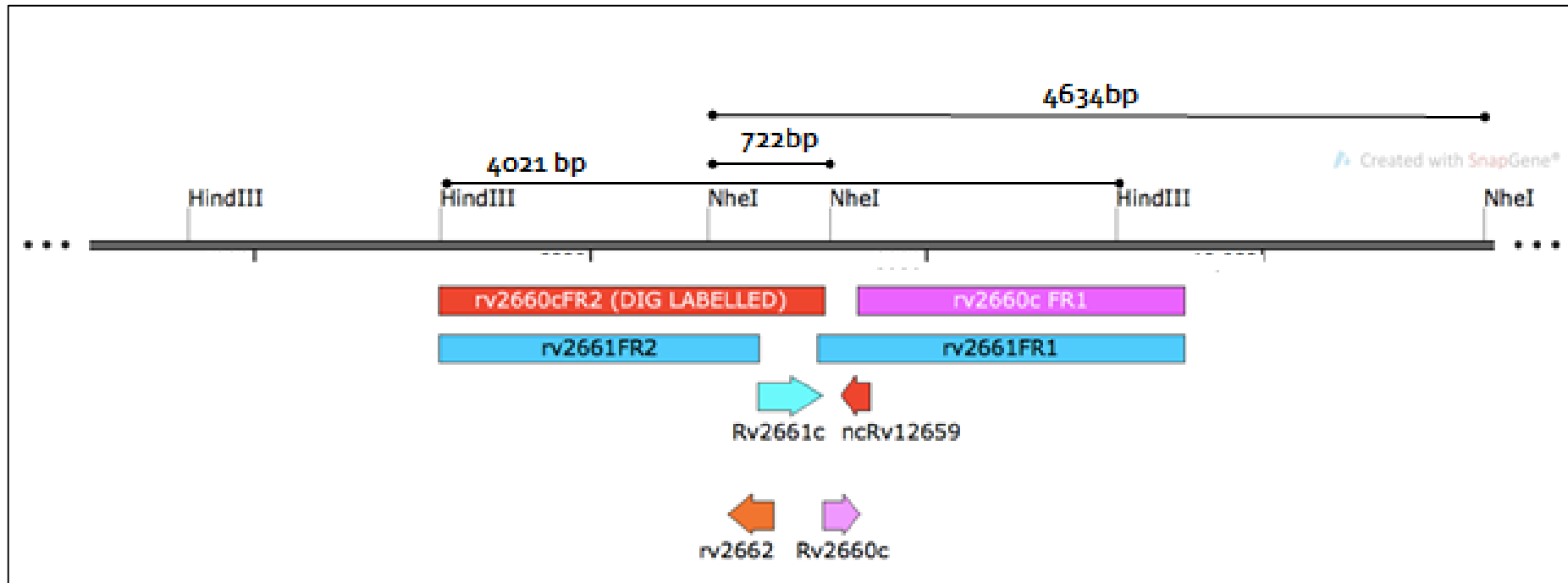


Figure 3-3: Physical map of *rv2661c-rv2660c* region with positions of flanking region and primers used for construction of deletion strains.

Physical map of the *Rv2661c-Rv2660c* region (position and orientation in genome represented as block arrows, shown in scale) depicting positions of flanking regions (shown as rectangular blocks) used for generation of deletion strains and primers (highlighted in purple fonts) to confirm deletion. For southern blotting, *rv2660cFR2* (2292bp) were DIG-labelled and used to hybridize *HindIII* and *NheI* digested fragments of wild-type and deletion strains

3.2.3 Southern Blot Hybridisation

The gene disruption by double crossover was further analysed by Southern hybridization, illustrated in Figure 3-4. Genomic DNA (2µg) of wild-type and three deletion strains was isolated and individually digested with restriction enzymes; *NheI* and *HindIII*, with overnight incubation at 37°C. The samples of digested gDNA were separated on a 0.8% w/v agarose gel for 80 volts for 3 hours and ran along with 6µL DNA Digoxigenin-labelled Ladder V11. Serial 15 minute washings were performed at room temperature and rinsing of gel in between washings proceeded as follows; depurination of DNA fragments using 0.25N HCl with two washes; denaturation with mixture of 0.5M NaOH and 1.5M NaCl with two washes and one wash for neutralisation step using mixture of 0.5M Tris-HCl (pH 7) and 3M NaCl for extended 30 minutes. Southern blotting was carried out in 20X SSC (3M NaCl, 300mM Sodium citrate- pH7) using a positivity charged nylon membrane (Supply et al., 2013). After an overnight DNA transfer from gel to membrane, the membrane was carefully lifted and immersed in 2X SSC for 10 minutes. DNA was cross-linked to the membrane using UV Straterlinker 2400 (Invitrogen) applying automated program twice. DNA-probe labelling, hybridization and detection were performed using the DIG high prime DNA labelling and detection starter kit 1 (Supply et al., 2013). Briefly, 3µg purified DNA fragment of 266oFR2 (2292bp) were denatured at 95°C for 10minutes prior incorporation of DIG-11-dUTP by Klenow polymerase using DIG high prime resulting DIG- labelled 266oFR2 as hybridisation probe. Hybridisation was performed by immersing the membrane in denatured DIG-labelled probe and preheated DIG Easy Hub solution at 65°C overnight with gentle agitation. Post hybridisation washes involved stringent washes twice in 2x SSC with 0.1% w/v SDS for 5 minutes and 0.5X SSC with 0.1% SDS for 15 minutes at 65°C. For detection of hybridisation signals, the membrane was washed in 1X Maleic acid buffer, pH7.5 (0.1M Maleic acid, 0.15M NaCl with 0.3% (v/v) Tween-20 and blocked in similar buffer without Tween-20 for 30 minutes. The membrane was transferred in anti-DIG antibody (diluted 1:5000 in blocking solution) conjugated to alkaline- phosphatase for another 30 minutes and followed by subsequent washing in 1X Maleic acid with 0.3% (v/v) Tween-20 twice for 15 minutes. The colour reaction was performed with nitro blue tetrazolium salt and 5-

bromo-4-chloro-3-indolyl phosphate, NBT/BCIP solution (diluted 1:50 in detection buffer) in the dark for 16 hours until appearance of bands was observed and reaction was stopped by washing membrane in H₂O.

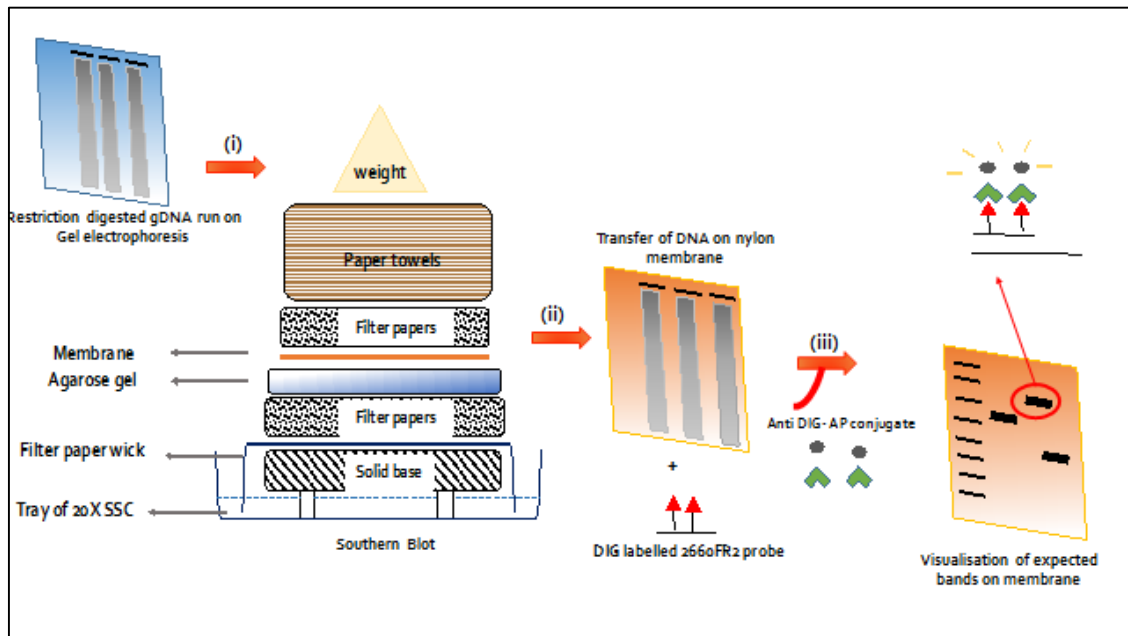


Figure 3-4: Overview of Southern Blot hybridisation.

(i) Genomic DNA seen as smears on agarose gel were layered according to the figure with positive charged nylon membrane on top to allow transfer of DNA fragments (ii) After overnight transfer, incubation of DNA on membrane with DIG labelled DNA probe resulted in complementary sequence binding (iii) Addition of anti- DIG antibody conjugated with alkaline phosphatase and substrate NBT/BCIP allowed colorimetric detection of the hybridised DIG probe to restriction DNA fragment to generate purple precipitate visualised on the membrane.

3.2.4 Generation of single and double over-expressing strains of *rv2661c* and *rv2660c* strains in *M. tuberculosis*

For over-expression of *rv2660c* and *rv2661c*, the full-length coding sequences of *rv2660c* and *rv2661c* were amplified by Dr Galina Mukamolova (UoL) using corresponding primers 2660pMVF/2660pMVR, 2661pMVF/2661pMVR and 2661pMVF/2660pMVR. Amplified genes were cloned in *Bam*HI-*Eco*RI sites of pMV261 plasmid and confirmed by sequencing. Plasmid maps of each construct are shown in Appendix 4.

Each recombinant plasmid (500ng) was then electroporated into *M. tuberculosis* and transformants were selected on 7H10 agar containing 50µg mL⁻¹ Kanamycin. The identity of all strains was confirmed by colony PCR using pMV261 specific primers pMV261F and pMV261R. The PCR amplification cycling conditions used are described in section 2.5.1 except that a higher annealing temperature of 63°C.

3.2.5 qRT-PCR

Total RNA (300ng) extracted from mid-exponential growing cultures of over-expressing strains was reverse transcribed and cDNA copies generated from each run were normalised to 16S cDNA copies. Assay performance for the two independent qRT-PCR runs were initially analysed and parameters such as gDNA contamination, correlation coefficient, PCR efficiency were all within acceptable range (Appendix 6). Melting curve analysis of test samples revealed single sharp peaks aligned with all standard *M. tuberculosis* gDNA samples, indicating specific amplicons were obtained (Appendix 7).

3.2.6 *In Vitro* growth analysis

Starter *M. tuberculosis* cultures in mid-exponential phase were diluted to an OD_{580nm} 0.01 in 10mL of supplemented 7H9 medium or Sauton's broth. Growth was monitored for 14 days by measuring OD at 580nm. Growth curves were generated and growth parameters, growth rate (k) and doubling time (D_T), analysed using the exponential growth tab from Prism 7.0 (Graphpad) software. The software computes D_T as ln(2)/K, where ln stands for natural logarithm. Data were represented as mean with 95% confidence level as recommended by the software.

3.2.7 Determination of MIC using 2-amino-6- fluorobenzoic acid (6-FABA)

A stock solution for 100mM 2-amino-6- fluorobenzoic acid (6-FABA) was prepared fresh by dissolving 15.5 mg 6-FABA (Sigma) in 1mL DMSO and kept at -20°C. On the day of experiment, 1mM 6-FABA in supplemented 7Hg-R was prepared and diluted accordingly to obtain final concentration of 1, 2, 5, 10 and 20µM 6-FABA. A detailed procedure of using a microdilution Resazurin assay can be found in Section 2.6.3. Mid-exponential stage cultures (OD_{580nm} of 0.5-0.7) diluted to an OD_{580nm} 0.1 were used to inoculate to each tested concentration. Plates were incubated at 37°C and MIC was determined after 1 week of incubation.

3.3 RESULTS

3.3.1 Confirmation of *rv2661c* and *rv2660c* deletion strains in *M. tuberculosis* H37Rv

Earlier, individual FR1 and FR2 (illustrated in Figure 3-2) were assembled in p2NIL with marker genes excised from pGoalL resulting in the following suicide vectors; p Δ *rv2661c*, p Δ *rv2660c* and p Δ *rv2661c:rv2660c*. Electroporation of individual recombinant plasmids into *M. tuberculosis* H37Rv led to DCO colonies.

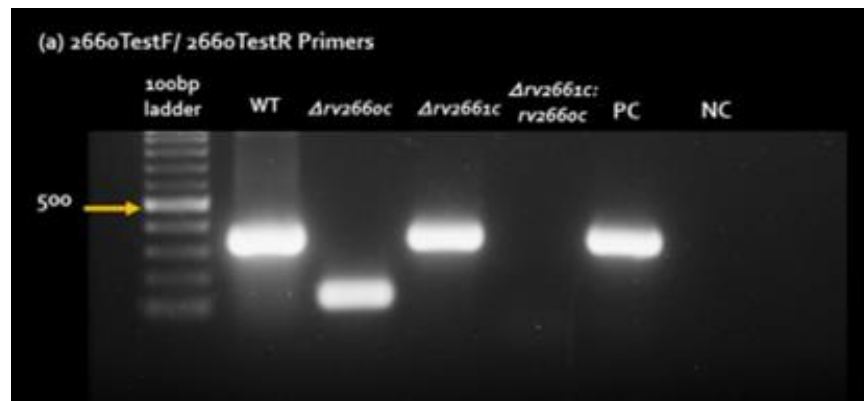
Mutant clone 6 of Δ *rv2661c*, clone 12 of Δ *rv2660c* and clone 3 of Δ *rv2661c:rv2660c* were further subjected to diagnostic culture PCR and Southern hybridization (this study) prior to phenotypic characterisation. Two sets of test primers and two sets of gene-specific primers were used to confirm deletions of the respective genes. Expected amplicon sizes in both wild-type and deletion mutants using these primer pairs are tabulated in Table 3-2. Using test primer pair 2660TestF/ 2660TestR, an ~140bp amplicon was produced from Δ *rv2660c* compared with both wild-type and Δ *rv2661c* that have both yielded ~350bp size band illustrated in Figure 3-5a. For confirmation of *rv2661c* deletion (Figure 3-5b), a band of 420bp (Lane 1) was observed from Δ *rv2661c* and a much smaller 180bp amplicon was yielded from Δ *rv2661c:rv2660c* (Lane 2). Furthermore, when gene specific primer for *rv2660c* sequences (RT2660F and RT2660R) were used to amplify Δ *rv2660c* and Δ *rv2661c:rv2660c* sequences, no product was generated and this was expected as the *rv2660c* genomic region was deleted. However, ~180bp band was observed with Δ *rv2661c* (gel not shown).

Southern blot hybridization was performed using the confirmed clones to support findings of culture PCR. DIG-labelled flanking region 2660cFR2 (2291bp) was hybridised with *NheI* and *HindIII* digested gDNA isolated from deletion strains. The resultant band size was compared to the wild-type *M. tuberculosis*. As shown in Figure 3-6, these bands were visualised as purple precipitate after overnight incubation with anti-DIG antibodies. It demonstrated successful hybridisation of gDNA from each deletion strain to labelled DNA probe. The expected sizes of each hybridised DNA fragment is shown in Table 3-3. As *NheI* is the only enzyme that digested *rv2660c* genomic region (illustrated in Figure 3-3), a clear wide distinct size difference was

observed between wild-type and $\Delta rv266oc$ strain which yielded $\sim 718bp$ and $\sim 4400bp$ respectively. The $\Delta rv2661c$ strain yielded the smallest band size of $\sim 360bp$ shown in Figure 3-6a.

A faint band of $\sim 4000bp$ was observed from $\Delta rv2661c:rv266oc$ digested with *NheI* (Figure 3-6b). Digest with *HindIII* yielded $\sim 3400bp$ band size which confirmed deletion of both sequences in $\Delta rv2661c:rv266oc$.

(a)



(b)

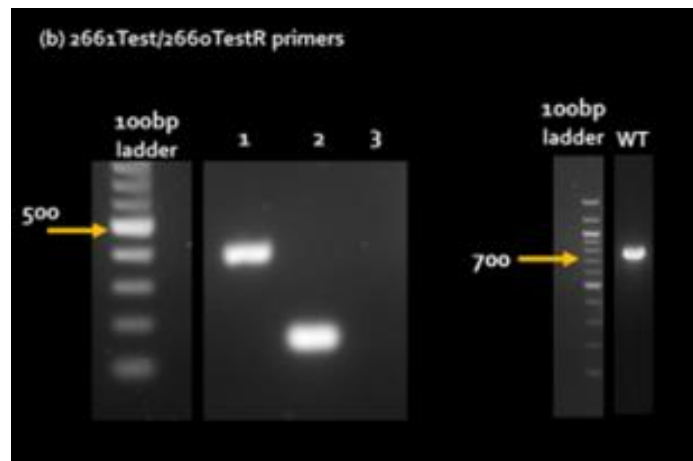


Figure 3-5: Gel analysis showing PCR products of wildtype and deletion strain genomic DNA using test primers. Primer sets used were (a) 2660TestF and 2660TestR primers. PC- *M. tuberculosis* gDNA; NC-Control with water, (b) 2661Test and 2660TestR; Lane1- $\Delta rv2661c$, Lane 2- $\Delta rv2661c:rv2660c$, Lane 3- Negative control. Right gel -wildtype strain. DNA ladder; Generuler 100bp ladder

Test & Gene-specific Primers	Expected size (base pairs, bp)			
	Wild-type	$\Delta rv2660c$	$\Delta rv2661c$	$\Delta rv2661c:rv2660c$
2660TestF + 2660TestR	349	142	349	no product
2661TestF+ 2660TestR	776	569	420	183
‡RT2660F + RT2660R	182	no product	182	no product
‡RT2661F1 +RT2661R1	80	80	no product	no product

Table 3-2: Expected sizes for each PCR products using respective test and ‡gene specific primers

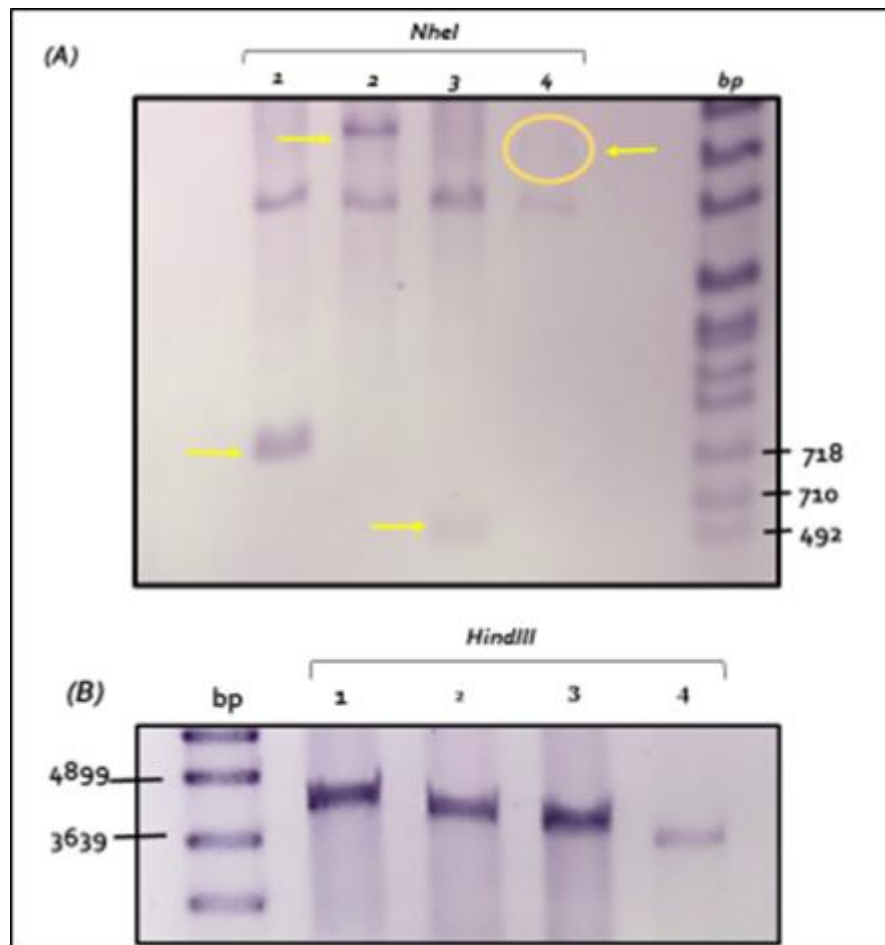


Figure 3-6: Southern blot of digested wild-type and deletion strain genomic DNA. (A) *NheI* and (B) *HindIII* restriction enzymes were used for digestion of gDNA and hybridised to a DIG-labelled 266oFR2 DNA fragment. DNA Molecular weight DIG labelled Ladder VII, Roche (0.081- 8.57Kbp) were used as DNA ladder

Lane position on blot	Strains	Restriction Enzymes with expected gDNA band sizes (bp)	
		<i>HindIII</i>	<i>NheI</i>
1	Wild-type	4021	722
2	$\Delta rv266oc$	3814	4406
3	$\Delta rv2661c$	3667	368
4	$\Delta rv2661c:rv266oc$	3428	4020

Table 3-3: Expected band sizes of *HindIII* and *NheI* digested wildtype and deletion strains hybridised with DIG-labelled 266oFR2 DNA fragment

3.3.2 Confirmation of the over-expressing strains of *rv2661c* and *rv2660c* in *M. tuberculosis* H37Rv

In this study, we have confirmed over-expression of both *rv2661c* and *rv2660c* by performing culture PCR of the *M. tuberculosis* transformants and analysing the target gene expression in each strain using qRT-PCR.

Initially, the coding sequences of respective annotated genes were cloned downstream of the *hsp60* promoter in pMV261 generating recombinant plasmids; pMV261::*rv2661c* (4870bp) and pMV261::*rv2660c* (4705bp). Another plasmid construct, pMV261::*rv2661c+rv2660c* (5094bp) harbouring both *rv2661c* and *rv2660c* sequences was also electroporated into *M. tuberculosis* H37Rv (Appendix 4). A control strain of *M. tuberculosis* harbouring the empty plasmid of pMV261 (4488bp) was also generated and yielded a band size corresponding with an expected size (255bp; lane 1, illustrated in Figure 3-7). The culture PCR using pMV261 primer pairs yielded larger bands of expected size for over-expressing strains compared to the control strain as additional coding sequences were cloned. *M. tuberculosis* pMV261::*rv2660c* yielded a band corresponding with the expected size (480bp; lane 2) while *M. tuberculosis* pMV261::*rv2661c* yielded a larger band size (645bp; lane 5). *M. tuberculosis* pMV261::*rv2661c+rv2660c* yielded a faint band (869bp; lane 3), thus confirming insertion of both coding sequences.

Relative expression (RE) ratio was analysed to demonstrate the magnitude of over-expression of *rv2661c* and *rv2660c* in respective over-expressing strains, shown in Table 3-4. Expression of *rv2660c* were massively induced in *M. tuberculosis* pMV261::*rv2660c* with 453 ± 12 - fold and *M. tuberculosis* pMV261::*rv2661c+rv2660c* with 620 ± 380 - fold compared to expression of the control strain. As expected, there was no enhancement of expression of *Rv2660c* in *M. tuberculosis* pMV261::*rv2661c* as *rv2660c* sequences were absent in this strain. This was similarly observed for *rv2661c* expression in *M. tuberculosis* pMV261::*rv2660c*. Indeed, there was also a massive expression of *rv661c* in *M. tuberculosis* pMV261::*rv2661c* with 783 ± 398 - fold and a 538 ± 216 -fold in *M. tuberculosis* pMV261::*rv2661c+rv2660c* compared to expression in control strain. As a control, expression of *ncRv12659* was investigated and it was found that it was not detected in any over-expressing strains, indicating specificity of

RT12659 primers in amplifying only ncRv12659. These data confirmed the over-expression of these annotated genes in respective strains.

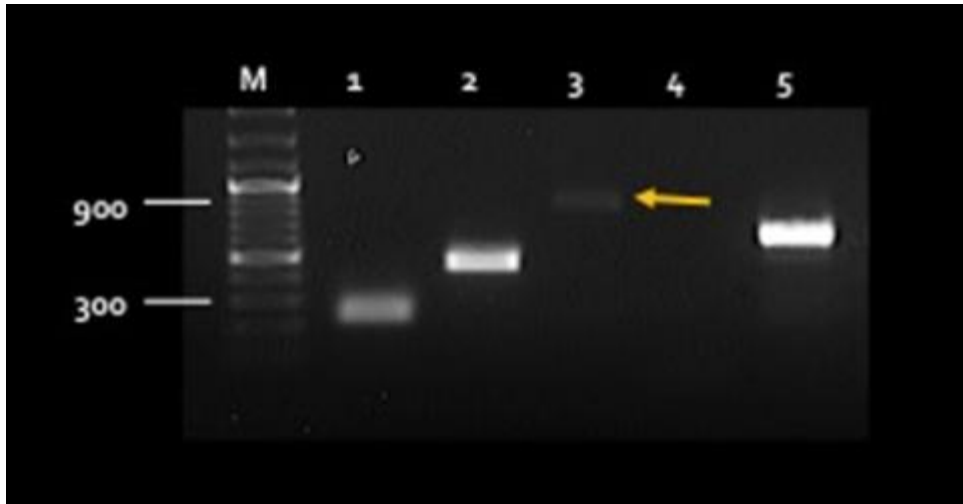


Figure 3-7: Gel analysis showing PCR products of control (empty plasmid) and over-expressing strains using pMV261 primers. Lane 1: *M. tuberculosis* pMV261, Lane 2: *M. tuberculosis* pMV261::rv266oc, Lane 3: *M. tuberculosis* pMV261::rv2661c+rv266oc, Lane 4: Negative control, H₂O, Lane 5: *M. tuberculosis* pMV261::rv2661c, M: GeneRuler™

Strains	Genes	Expression normalised to 16s (n=3)		Relative Expression Ratio \pm SD
		Mean	Standard Deviation	
pMV261	<i>rv2660c</i>	6.85×10^{-5}	6.74×10^{-5}	NA
	<i>rv2661c</i>	3.73×10^{-4}	6.0×10^{-4}	
	ncRv12659	1.68×10^{-3}	2.21×10^{-3}	
<i>M. tuberculosis</i> pMV261:: <i>rv2660c</i>	<i>rv2660c</i>	6.04×10^{-2}	4.18×10^{-2}	453 ± 13
	<i>rv2661c</i>	1.47×10^{-4}	2.32×10^{-4}	0.7 ± 1.1
	ncRv12659	5.34×10^{-4}	7.13×10^{-4}	0.3 ± 0.3
<i>M. tuberculosis</i> pMV261:: <i>rv2661c</i>	<i>rv2660c</i>	7.14×10^{-5}	5.72×10^{-5}	1.2 ± 1.0
	<i>rv2661c</i>	2.40×10^{-1}	1.30×10^{-1}	783 ± 398
	ncRv12659	1.68×10^{-3}	9.36×10^{-4}	1.2 ± 0.6
<i>M. tuberculosis</i> pMV261:: <i>rv2661c</i> + <i>rv2660c</i>	<i>rv2660c</i>	3.57×10^{-2}	1.05×10^{-2}	620 ± 390
	<i>rv2661c</i>	1.58×10^{-1}	5.54×10^{-2}	583 ± 216
	ncRv12659	7.19×10^{-4}	6.54×10^{-4}	0.5 ± 0.4

Table 3-4: Relative expression of *rv2660c* and *rv2661c* in control and respective over-expressing strains. Relative expression values were obtained by normalising target cDNA copy numbers to 16S and then calculating the fold difference of expression in the strain in question compared with the strain containing pMV261. Data represent mean \pm standard deviation from three biological replicates

3.3.3 *In vitro* growth of *rv266oc* and *rv2661c* deletion strains in standard culture medium

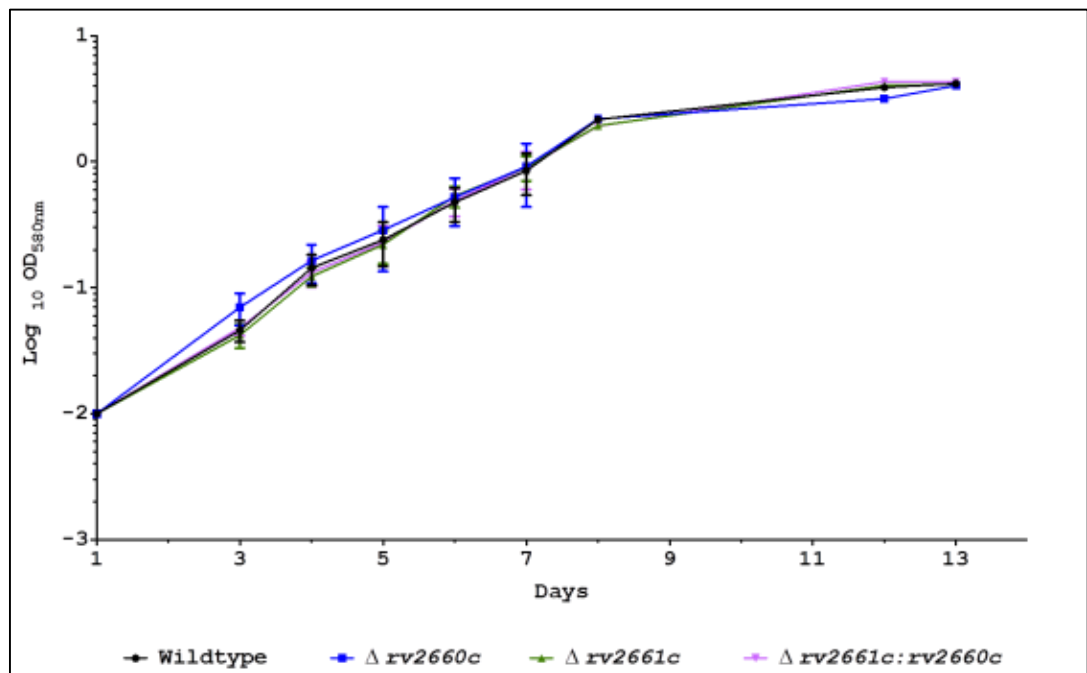
To understand the physiological role of Rv266oc and Rv2661c in *M. tuberculosis*, we first examined the growth characteristics of the wild-type *M. tuberculosis* and respective mutants cultured *in vitro*. Equal numbers of the deletion strains; $\Delta rv2661c$, $\Delta rv266oc$ and $\Delta rv2661c: rv266oc$ (3×10^6 CFU mL⁻¹ average starting inoculum) were grown in two different liquid media; supplemented 7H9 and Sautons' medium (pH 7.5) shown in Figure 3-8. Growth parameters growth rate and doubling time for each strain grown in both media are tabulated in Table 3-5.

Wild-type and deletion strains did not exhibit any difference in growth kinetics over 13 days' growth in supplemented 7H9, reaching an approximate maximum OD of 4.0 ($p=0.99$, One-Way Anova). When grown on supplemented 7H10 agar plates, colonies appeared wrinkled and ruffled showing no differences in colony morphology between wild-type and deletion strains. As shown in Figure 3-9, images were taken at day 12, and none of the deletion strains exhibited any colony growth defects illustrated in each serial dilutions of the culture.

Next, growth of deletion mutants in Sauton's medium was compared and this also exhibited no difference in growth kinetics throughout the experiment ($p=0.98$) shown in Figure 3-8b. Bacterial clumping was evident in Sauton's medium at day 3 thus cultures were subjected to gentle pipetting for cell dispersion to avoid massive variations in OD measurements. The maximum OD reached was at day 13, wildtype (2.43 ± 0.15), $\Delta rv266oc$ (2.52 ± 0.33), $\Delta rv2661c$ (2.33 ± 0.29) and $\Delta rv2661c: rv266oc$ (2.5 ± 0.27) indicative of a much slower growth rate and doubling time compared to growth in supplemented 7H9 (Table 3-5).

Overall these data suggest that single and double deletion of *rv266oc* and *rv2661c* have no effect on growth of *M. tuberculosis in vitro*. The partial deletions of *rv2662* and *ncRv12659* in respective deletion strains also suggested their non- essentiality during *M. tuberculosis* growth.

(a) Supplemented 7H9 medium



(b) Sauton's medium

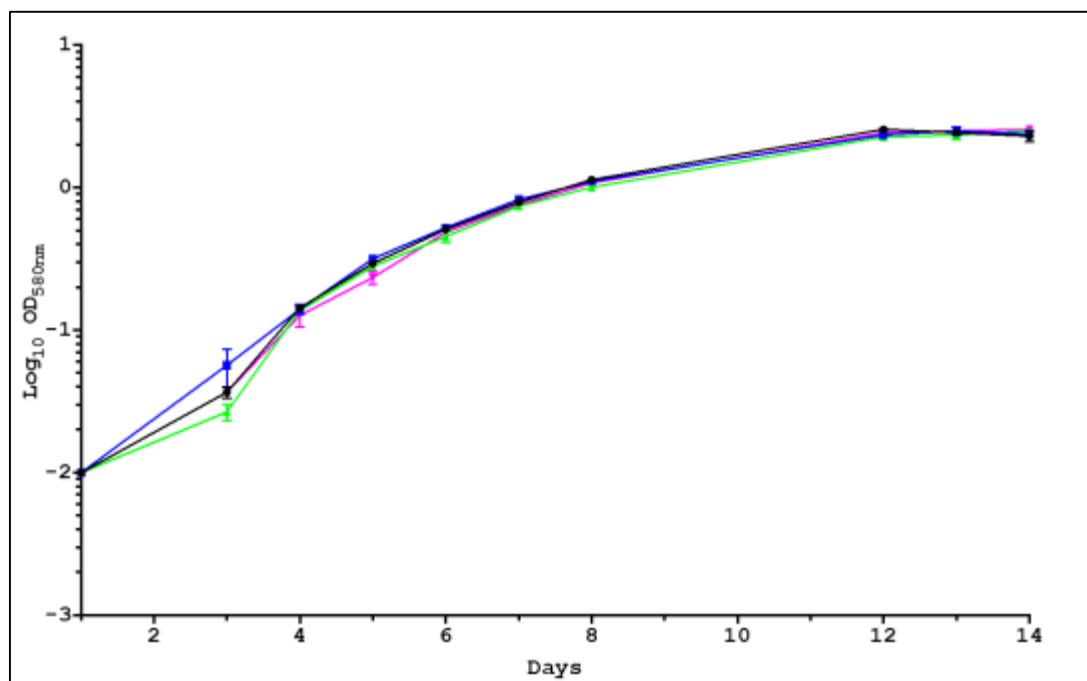


Figure 3-8: Growth curve *M. tuberculosis* deletion strains of *rv2660c* and *rv2661c*. Optical density measurements at 580nm, $\text{OD}_{580\text{nm}}$ was determined when grown in (a) Supplemented 7H9 with 10%ADC and 0.05% Tween-80 and (b) Sauton's (pH7.5). Data represent mean $\text{OD}_{580\text{nm}} \pm$ standard error of mean from 3 independent experiments performed in triplicates

Strains	Growth parameter values with confidence level, CI %			
	Growth rate/ hours ⁻¹		Doubling time (hours)	
	Supplemented 7H9	Sauton's	Supplemented 7H9	Sauton's
Wildtype	0.019 (CI 0.019-0.02)	0.0277 (CI 0.027-0.028)	25 (CI 24.4-25.7)	36 (CI 35-37)
$\Delta rv266oc$	0.019 (CI 0.018-0.02)	0.0279 (CI 0.0272-0.0286)	24.8 (CI 24.3-25.5)	36 (CI 34-38)
$\Delta rv2661c$	0.019 (CI 0.018-0.02)	0.0273 (CI 0.0269-0.0277)	25.4 (CI 25-25.8)	36 (CI 35-38)
$\Delta rv2661c::rv266oc$	0.019 (CI 0.018-0.02)	0.0273 (CI 0.0266-0.0279)	25.4 (CI 24.9-26.1)	36 (CI 35-38)

Table 3-5: Growth parameters of wildtype and deletion strains of *rv266oc* and *rv2661c* grown in standard culture media. Data of growth rate and doubling time are expressed as mean (95% Confidence level; Lower limit- Upper limit) generated by Prism software.

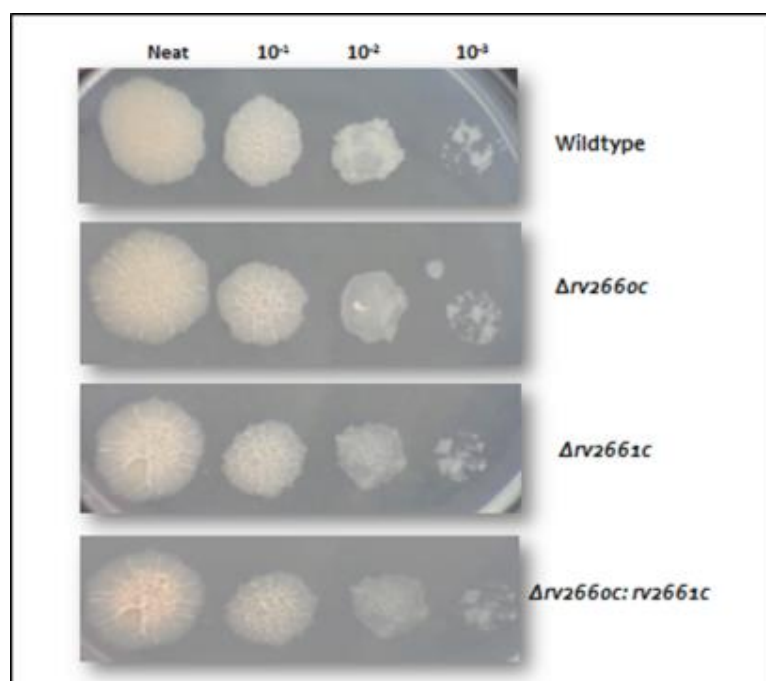


Figure 3-9: Colony morphology of *M. tuberculosis* wild-type and deletion strains *rv266oc* and *rv2661c*. Mycobacterial cultures were ten-fold serially diluted and spotted for each dilution (from left to right; Neat, 1:10, 1:100 and 1:1000) on supplemented 7H10 plate.

3.3.4 *In vitro* growth of over-expressing strains of *rv266oc* and *rv2661c* in standard culture medium

The constitutive over-expression of *rv2661c* and *rv266oc* in *M. tuberculosis* had no significant difference in growth kinetics compared to control strain when grown in supplemented 7H9 supplemented with kanamycin (personal communication, Dr. Mukamolova). When over-expressing strains were grown on supplemented 7H10 with kanamycin, the gross colony morphology of the over-expressing strains exhibited no observable differences compared to control strain, as shown in Figure 3-10. Colonies were recovered after three weeks of incubation. Colony surfaces were smooth and appeared flat. Rate of colony growth was also comparable with each serial dilution made for each strain. This suggested that over-expressing *rv2661c* and *rv266oc* has no toxicity effect during *in vitro* growth of *M. tuberculosis*.

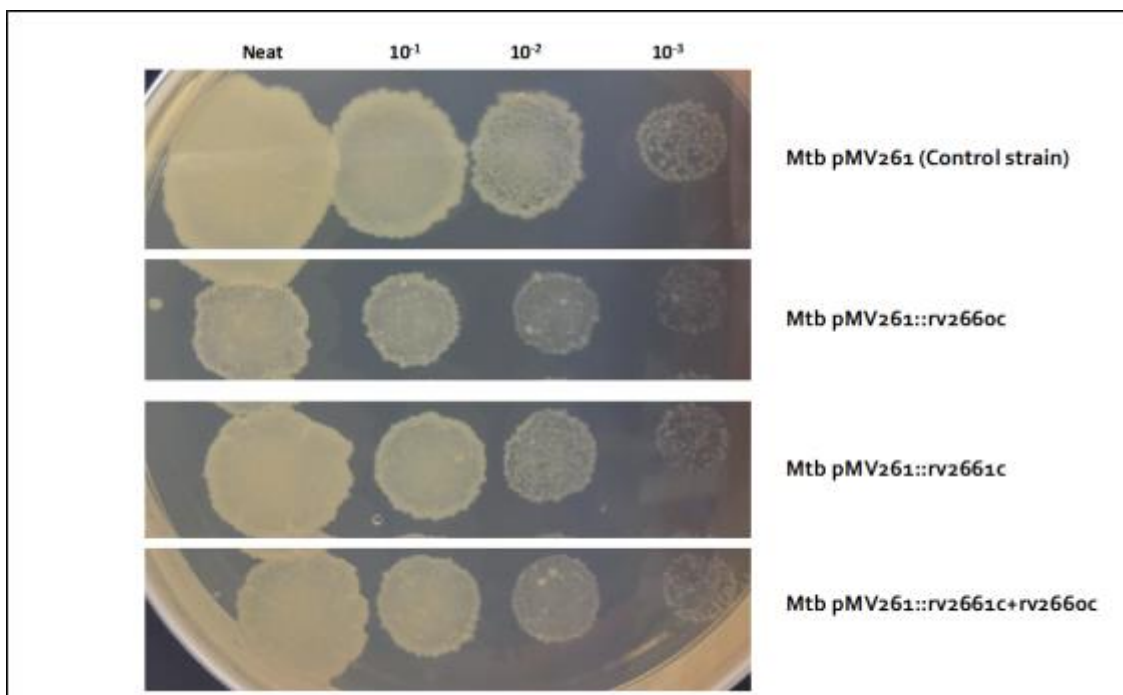


Figure 3-10: Colony morphology of over-expressing strains *rv266oc* and *rv2661c* in *M. tuberculosis*. Mycobacterial cultures were ten-fold serially diluted and spotted for each dilution (from left to right; Neat, 1:10, 1:100 and 1:1000) on supplemented 7H10 with 50µg mL⁻¹ Kanamycin. Images were taken after 4 weeks of incubation.

3.3.5 Sensitivity of *rv2660c* and *rv2661* deletion mutants to 6-FABA compound

Three independent experiments were performed where mycobacterial strains were grown in supplemented 7H9 in the absence of tryptophan with varying final concentration of 6-FABA ranging from 1 to 20 μ M. After one week of incubation, a colour change of resazurin was observed. The MIC of 6-FABA for wild-type and tested deletion strains were identical (5 μ M). The data demonstrated that all strains are equally sensitive to 6-FABA compound indicating neither *rv660c*, *rv2661c*, *rv2662* and *ncRv12659* were not specifically involved in tryptophan biosynthesis.

3.4 DISCUSSIONS

3.4.1 Successful generation of deletion and over-expressing strains of *rv266oc* and *rv2661c* in *M. tuberculosis*

The first evidence for gene essentiality arose from the failure to delete the targeted gene (Wei and Rubin, 2008). However, the successful generation of unmarked in-frame single and double *rv266oc* and *rv2661c* deletion mutants allowed us to conclude that these genes are not essential for *M. tuberculosis* growth. In-frame single deletion mutants were generated to avoid disrupting the overlap of 4bp between both genes. Furthermore, the system successfully generated a double deletion mutant and importantly aimed to reduce polar effects of downstream genes (Parish and Stoker, 2000b). It is vital to ensure defined mutations due to the complexity of the *rv2661c-rv266oc* genomic region. The efficacy of this system was particularly reflected in some studies involving generation of mutants of combined gene deletions of two regulatory component system such as *mprA-mprB* (Pang et al., 2007) and *senX3-regX3* (Parish et al., 2003b), and *ceoA-ceoB* for potassium uptake (Cholo et al., 2006). In addition, the generation of double deletion *fbpA* (encode Antigen 85 complex) and *sapM* (encode for acid phosphatase) further revealed another outcome of the system such as the discovery of a potential anti-TB vaccine (Saikolappan et al., 2012).

Deletion of *rv266oc* and *rv2661c* has also resulted in partial deletion of the 3' end of *ncRv12659* that overlaps with the *Rv266oc* sequence, and the 5' end of *Rv2662* which overlaps with the sequence of *Rv2661c*. These were ascertained by sequencing the mutated genomic regions, followed by confirmation of PCR products with test and gene specific reverse primers. In addition, Southern blotting of *NheI* and *HindIII* digested genomic DNA of deletion strains that hybridised with DIG-labelled DNA fragment of 266oFR2 further confirmed the target gene deletions. *NheI* was selected as it is the only enzyme that cleaved the *rv2661c-rv266oc* genomic region, while an additional *HindIII* blot served as supporting data.

Gene over-expression was often sought when gene deletion was not possible or compensated by other genes with similar annotated function. For example, over-expression of *Lsr2*, a global transcriptional regulator of *M. tuberculosis* using pMV261 plasmid was used to demonstrate its protective role during oxidative stress (Colangeli

et al., 2009) as the gene was not able to be deleted in *M. tuberculosis* (Colangeli et al., 2007). Over-expression of a universal stress protein provides information about its function as over-expression increases its effect on other universal stress proteins. Some examples are over-expression of Rv1996 that resulted in increased isoniazid susceptibility (Hu et al., 2015a) or over-expression of Rv2623 that arrested the growth of both *M. smegmatis* and *M. tuberculosis* (Drumm et al., 2009), while over-expressing its neighbouring *rv2624* increased the survival of the strain during hypoxia and macrophage infection (Jia et al., 2016).

In this study, we have also successfully overexpressed *rv2660c* and *rv2661c* using an extrachromosomal *E. coli*- mycobacterial plasmid vector, pMV261 vector (Stover et al., 1991). The purpose of creating these over-expressing strains was to increase the phenotypic effect in the *M. tuberculosis* strains. PCR analysis of the over-expressing strains confirmed that respective plasmids: pMV216:*rv2660c*, pMV216:*rv2661c* and pMV216:*rv2661c+rv2660c* were still intact, and demonstrated that additional coding sequences of individual genes were inserted. The expression of these genes that have been placed under the control of a heat shock protein promoter, P_{hsp60} resulted in high level of expression (Stover et al., 1993, Hickey et al., 1996) during exponential growth phase. When both genes are simultaneously overexpressed, the comparable massive expression suggest that these genes were co-transcribed from the same promoter.

3.4.2 Deletion and over-expression of *rv2660c* and *rv2661c* in *M. tuberculosis* did not affect growth *in vitro*

All assayed strains (deletions and over-expressing strains) demonstrated comparable growth with the wild-type or control strain. These findings suggest that these genes are not essential for *in vitro* growth. The absence of growth defects from over-expressing strains indicated that over-expressing these genes has not triggered any abnormal activity, or caused any pathway modulation which could cause toxicity effects (Moriya, 2015). Our findings also support previous studies that have listed *rv2661c* and *rv2660c* to be non-essential. These studies involved using growing libraries of transposon mutants on supplemented 7H10 medium identified using TraSH (Sasseti et al., 2003) and also genome-wide transposon mutagenesis using highly parallel Illumina sequencing (Griffin et al., 2011).

However, the over-expression of ncRv12659 in *M. tuberculosis* H37Rv caused a detectable growth impairment in standard medium and resulted in a significant upregulation of more than 50 genes, in particular PhiRv2 prophage genes; *rv2659c* and *rv2658c* (Houghton et al., 2013). Another gene, *desA3* was shown to be highly downregulated (7-fold). In another parallel analysis, they investigated the expression of *desA3* in PhiRv 2-negative strain, N0072 and *M. bovis* BCG with and without the over-expressing ncRv12659 construct and did not demonstrate any pronounced reduction in *desA3* expression in any strain. Their finding suggests that ncRv12659 was unlikely to influence the physiological growth of the over-expressing strain in *M. tuberculosis* H37Rv but rather the PhiRv2 genes. However, the mechanism and functional role of these genes remained to be determined (Houghton et al., 2013).

3.4.3 Deletion of *rv2660c* and *rv2661c* do not affect sensitivity of *M. tuberculosis* to 6-FABA

Halogenated anthranilates such as 6-FABA are known potential anti-infective compounds for *Pseudomonas aeruginosa* (Lesic et al., 2007). These anthranilic acid (AA) analogues were shown to inhibit 4-hydroxy-2-alkylquinoxalines (HAQs) synthesis by competing with AA for the active site of PqsA, responsible for HAQ biosynthesis. AA, a primary precursor of HAQ is responsible for activation of a LysR-type transcriptional regulator, MvfR which is involved in one of the quorum sensing regulatory pathways in *P. aeruginosa* (Santos et al., 2012, Lesic et al., 2007). In addition, these compounds could perturb tryptophan production by competing with AA for TrpD, the initial enzyme in the tryptophan biosynthesis which utilises AA as a substrate. An introduction of exogenous tryptophan would rescue growth of bacteria when grown in 6-FABA. (Lesic et al., 2007).

Similarly, in *M. tuberculosis*, it was proposed that these halogenated anthranilates were bactericidal and affect tryptophan biosynthesis. Both 6-FABA and 5-FABA were active against wild-type *M. tuberculosis* with an MIC of 5 µM as compared to *M. smegmatis* (MIC of 65 µM). Moreover, the introduction of 6-FABA to *M. tuberculosis* deletion strains of *trpE* and *trpD* resulted in a pronounced reduction of CFU counts by $\sim 1 \times 10^6$ fold compared to the untreated inoculum (Zhang et al., 2013), further speculating other inhibitory effects in the tryptophan biosynthesis pathway.

Since *Rv2661c* was implicated to be involved during tryptophan biosynthesis (Zhang et al., 2013), we have employed similar approach by assessing the sensitivity of deletion strains of *rv2661c* and *rv2660c* to 6-FABA by microdilution resazurin assay. However, none of the tested deletion strains showed any difference in sensitivity to the compound. We conclude that *rv2660c*, *rv2661c*, *rv2662* and *ncRv12659* have no direct role during tryptophan biosynthesis pathway and hence, unlikely to contribute during tryptophan starvation.

3.5 CONCLUSIONS

The studies in this chapter are as follows:

- ✓ The ability to generate deletion and over-expressing strains of *rv2660c* and *rv2661c* in *M. tuberculosis* and the demonstration of no growth impairment indicated that these genes are non-essential for *M. tuberculosis*. The partial deletion of the overlapping gene, *rv2662* and 3' end of non-coding RNA, ncRv12659 on the plus strand also suggest its lack of importance in the aforementioned growth condition.
- ✓ Genes located in the *rv2661-rv2660c* locus, including ncRv12659 have no direct role in tryptophan biosynthesis.

CHAPTER 4
Investigating the role of
rv2660c* and *rv2661c
in *Mycobacterium tuberculosis*
during infection

CHAPTER 4 Investigating the role of *rv2660c* and *rv2661c* in *Mycobacterium tuberculosis* during infection

4.1 INTRODUCTION

The successful generation of deletion and over-expressing strains of *rv2660c* and *rv2661c* (including partial deletions of *rv2662* and *ncRv12659*) in *M. tuberculosis* established the non-essentiality of these genes for growth *in vitro*. This chapter further describes phenotypic characterisation of the mutants and over-expressing strains when exposed to individual stresses thought to mimic intracellular conditions in activated macrophages (MacMicking et al., 1997a) and during NRP (Wayne and Sohaskey, 2001). The two most common *in vitro* NRP models used in the investigation were nutrient starvation (Betts et al., 2002) and Wayne's hypoxia model (Wayne, 1996, Wayne and Hayes, 1996) where these annotated genes and *ncRv12659* were significantly induced (Houghton et al., 2013, Cortes et al., 2013, Voskuil et al., 2004). In line with their upregulation in other stress conditions (Schnappinger et al., 2003, Schnappinger et al., 2006), the survival of these strains under oxidative and nitrosative stresses *in vitro* as well as during macrophage infection, were also investigated. The experiments aimed to clarify the biological importance of the significant upregulation of the annotated genes and *ncRv12659* during adaptation to dormancy and stress responses.

Expression of *rv2660c* and *rv2661c* was previously detected in *M. tuberculosis* from infected lungs of BALB/c (Talaat et al., 2004, Aagaard et al., 2011) and C3HEB/FeJ mice (Harper et al., 2011, Gautam et al., 2015b), suggesting a potential role for these genes during infection. Hence, *in vivo* murine infection experiments were employed to get insights into the survival of the double deletion mutant during actual mycobacterial infection.

Previous transcriptomic data that have been published on the upregulation of these annotated genes were based on microarray analysis. Since the publication of the first whole genome sequencing data for *M. tuberculosis* (Cole et al., 1998), whole genome microarrays have been employed in mycobacterial research. Microarray involves hybridisation of fluorescently labelled cDNA produced from mRNA with an array of probes (DNA fragments or oligonucleotides) immobilised on a solid surface. The

technology was used to analyse the transcriptomics of the pathogen's response to an anti-TB drug, isoniazid (Wilson et al., 1999) or understanding the adaptive responses of *M. tuberculosis* by transcriptional profiling wild-type and mutant strains in established *in vitro* models such as macrophage infection, starvation in PBS and hypoxia (Betts et al., 2002, Rustad et al., 2008, Rohde et al., 2012, Deb et al., 2009). Over the years, the technology was still preferred due to lower cost, less labour and feasibility of high throughput analysis.

Nevertheless, advances in RNA sequencing (RNA-Seq) technologies provide an opportunity to extend these studies. The benefits of RNA-Seq outweigh microarray, such as relatively low background signal, highly reproducibility and accuracy in quantifying RNA expression and identification of the precise location of transcriptional boundaries up to single base resolution (Wang et al., 2009). RNA-Seq provides more transcriptomic insights through dynamic transcript coverage, resulting in discovery of novel ncRNA involved in post-transcriptional regulation, which contribute to the mycobacterial responses to varying physiological conditions (Arnvig et al., 2011, Arnvig and Young, 2012, Pellin et al., 2012). A current example related to this study is the identification of highly upregulated ncRv12659, transcribed opposite *rv2660c* locus (Houghton et al., 2013). In addition, the discovery of leaderless transcripts using a combination of genome TSS mapping and protein abundance analysis have revealed the physiological contribution of these transcripts during *M. tuberculosis* starvation (Cortes et al., 2013).

These technologies have limitations in their application for cDNA or RNA quantitation. While both microarray and RNA-Seq involve the whole genome transcriptome, qRT-PCR is often used for comparable analysis to quantify specific cDNA target copies. It is a standard practice to confirm results of microarray analysis by quantitative RT-PCR. qRT-PCR is used to detect gene expression through amplification of complementary DNA (cDNA) transcripts from mRNA by reverse transcriptase, followed by PCR and quantification using DNA-intercalating fluorescent dyes or fluorescent probes (Bustin et al., 2005). The previous authors have also employed qRT-PCR in parallel to the RNA-Seq data and found only the 5' end amplicon of ncRv12659 that was induced by 50-fold during starvation and not the 3' end of ncRv12659 (corresponding to *rv2660c* sequences) (Houghton et al., 2013).

Taken into the account the information gathered from the published studies and results obtained from the survival of the mutant strains during starvation, the reassessment of the expression of *rv266oc* and *ncRv12659* using qRT-PCR was necessary. Together, it will also provide a comprehensive expression analysis of the other two genes; *rv2661c* and *rv2662* during nutrient starvation but also in several *in vitro* conditions.

The aim of this study was to further establish the role of annotated genes and non-coding element located in the *rv2661c-rv266oc* locus during infection. The objectives were;

- To investigate survival of deletion and/ or over-expressing strains of *rv266oc* and *rv2661c* during nutrient starvation, Wayne's hypoxia model and under oxidative and nitrosative stresses
- To investigate intracellular growth and replication of double deletion mutant in resting and IFN γ activated macrophages
- To investigate intracellular growth and replication of double deletion mutant during mouse infection.
- To optimise protocols for evaluation of low level expression genes
- To analyse levels of expression of *rv266oc*, *rv2661c*, *rv2662* and *ncRv12659* during starvation, oxidative and acidic stress conditions and compare these with previously published data

4.2 MATERIALS AND METHODS

4.2.1 *In vitro* non-replicating persistence models and stress experiments

4.2.1.1.1 Nutrient Starvation

The assay was performed according to Betts et al. (Betts et al., 2002). Starter cultures of mycobacterial strains were grown to late-exponential phase (OD_{580nm} 0.8-0.9) in supplemented Middlebrook 7H9 medium without shaking and then diluted 1:100 into a roller bottle in 100 ml of supplemented 7H9 with 0.0025% (v/v) Tween-80. Once growth had reached mid-exponential phase (OD_{580nm} 0.5-0.7), the 100mL bacterial suspensions were transferred to 50mL centrifuge tubes and centrifuged at 2400X g for 15 minutes. Cell pellets were washed twice in sterile phosphate buffer saline (PBS) before final resuspension in the same buffer. Addition of sterile methylene blue (Sigma) at a final concentration of $1.5 \mu\text{g mL}^{-1}$ cultures in PBS allowed a visual indication of oxygen depletion over starvation period. Control tubes with PBS and methylene blue without bacterial culture were also set up. Cultures were incubated at 37°C without shaking. CFU counts were determined from 5mL aliquots of culture at 1, 2, 3 and 6 weeks of incubation. RNA was isolated from two independent experiments and performed in triplicate at 0 (T_0), 24 and 96 hours.

4.2.1.1.2 Oxidative stress

For assessment of viability, oxidative stress experiment can be referred in Section 2.6.1. Final concentrations of 10mM and 25mM H_2O_2 were used to evaluate resistance of deletion mutants and wild-type strain to oxidative stress. CFU counts were determined at 0, 4 and 24 hours post treatment from culture performed in triplicate. For RNA extraction, culture conditions and time points were used as adapted from the work of Schnappinger and colleagues (Schnappinger et al., 2003). Exponentially growing cultures of *M. tuberculosis* H37Rv (OD_{580nm} 0.5-0.7) were diluted 1:100 in 125mL Erlenmeyer flasks containing 25mL supplemented 7H9 and allowed to grow to early-log phase, OD_{580nm} 0.3-0.4. Individual 10mL aliquots with required final concentration of H_2O_2 ; 5mM and 25mM were set up. After 40 minutes and 4 hours of incubation without shaking, 9mL of culture were processed for RNA isolation and the

remaining 1 mL was used for CFU counts to monitor any loss of viability post treatment.

4.2.1.1.3 Wayne's Hypoxia Model

The assay was conducted as described by Wayne and Hayes (Wayne, 1996). Starter cultures were grown to mid-exponential phase (OD_{580nm} 0.5-0.7) and diluted 100-fold in 50mL supplemented 7H9 using 250mL Erlenmeyer flasks (Corning). When OD_{580nm} reached 0.4, mycobacterial strains were further diluted 100-fold in supplemented 7H9 medium containing $1.5 \mu\text{g mL}^{-1}$ of methylene blue. Individual 12.7mL diluted culture were aliquoted in a sterile screw-capped round bottom polypropylene tube (15 X 152mm) (BD Biosciences) containing a 8mm Teflon coated magnetic stir bar (Fisher Brand™). Control tubes with methylene blue without bacterial strains were also set up. All test tubes were tightly sealed with a PVC insulation tape (19mm x 33mm, Sivitek) and double bagged before incubation. All tubes were placed in transparent 2 litre polypropylene beakers and positioned on a multi stirring magnetic stirrer (Stuart, SB 161-3). Stirring speed was set at mark '3' to generate slowly stirring cultures. Tubes were incubated for 12 weeks. At each designated time point, OD measurements were taken followed by CFU counting. After sampling, tubes were carefully disposed. Experiments were performed using three biological replicates.

4.2.2 Thin Layer Chromatography (TLC) of phthiocerol dimycocerosate (PDIM) analysis

Semi-quantitative analysis of PDIMs was done as previously described (Besra, 1998, Dobson et al., 1985).

M. tuberculosis H37Rv and $\Delta rv2661c: rv2660c$ in 100 ml supplemented 7H9 were grown to mid exponential phase and later aliquoted as 20mL culture in 50mL centrifuge tubes. Cells were harvested by centrifugation at 3500X g for 20 minutes, followed by washing with sterile PBS. Bacterial pellets were heat inactivated at 85°C for 2 hours before removing from the C3 containment laboratory.

The next procedure in the experiment was performed by Malgorzata Wegrzyn and Dr Natalie Garton (UoL). Bacterial pellets were resuspended in 2mL 10:1 (v/v) Methanol: 0.3% (w/v) aqueous NaCl to which the same volume of petroleum-ether (boiling point

40- 60°C) was added. After 15 minutes of vigorous mixing, the samples were centrifuged at 700X g for 10 minutes to allow phase separation where the upper (petroleum-ether) phase containing non- polar lipid extracts was removed. Addition of another 2mL petroleum ether allowed final extraction from the lower methanolic phase and dried under stream of nitrogen at 35°C. Lipid samples were resuspended in 250µl chloroform prior to TLC analysis.

Aluminium-backed silica TLC plates pre-coated with fluorescent indicator F254 (Macherey Nagel™) with dimension of 6.6 x 6.6cm (this is used for two- dimensional TLC analysis. Using a syringe with borosilicate glass barrel (Hamilton Microliter™), 1µL of the lipid extract was spotted at the origin of the plate. For detection of PDIMs, plates were run three times in petroleum ether (60- 80°C) /ethyl acetate (98:2, v/v) in first dimension, followed by petroleum ether (60- 80°C): acetone (98: 2, v/v) once in the second dimension. The position of menaquinone was initially marked using a handheld UV lamp and the plate was subsequently developed after spraying the plate with 5% (w/v) molybdophosphoric acid in ethanol, followed by heating the plate with a heat gun.

4.2.3 Macrophage infection and microscopy

4.2.3.1.1 General methods

Recovery of macrophage cell lines from liquid nitrogen- Eukaryotic cell batches frozen down in liquid nitrogen (main stock) were carefully retrieved and quickly thawed under warm running tap water. To avoid contamination from water, vial was thoroughly wiped with 70% (v/v) Ethanol and then centrifuged at 100 Xg for 5 minutes to remove storage medium. The cell pellet was resuspended in 10mL of pre-warmed supplemented RPMI-1640 containing 10% (v/v) heat-inactivated FBS, 100 units Penicillin and 0.1mg Streptomycin (hereafter as supplemented RPMI). Cell suspensions were then transferred to 75cm² vented culture flasks (Corning) and allowed to proliferate to 1 X10⁶ cells prior subculturing. All cell lines were incubated of at 37°C in a humidified atmosphere of 5%CO₂

Preparation of working frozen stock- Culture grown from main stock was split into two 75cm² vented flasks and grown to 70-80% confluency. Cells were transferred into

50mL centrifuge tubes and centrifuged at 200 Xg for 5 minutes. Cell pellets were resuspended in pre-warmed 'freezing' medium (8mL supplemented RPMI, 1mL FBS and 1mL sterile dimethyl sulphoxide, DMSO). Aliquots of 1mL in screw top cryovial tubes (with rubber sealing O rings in the lid to prevent liquid nitrogen entry) were initially frozen overnight in -80°C freezer before final storage at -150°C.

Maintenance- Cells were resuscitated from -150°C and thawed according to the 'Recovery of macrophage cell line' protocol stated above. Both J774.1 and THP-1 cell lines were maintained in 10mL supplemented RPMI in vented 75cm² flasks. Cells were passaged twice a week by splitting using a 1/5 dilution and transferred for incubation.

Trypan Blue Viability Test- A 20µL mixture made from equal volume of 0.4% Trypan Blue solution (Sigma) and cells were prepared. Ten (10) µL of the mixture were spotted on a haemocytometer. Cells were counted cells in four 1x 1mm squares of chamber under 20X magnification. Two separate counts were kept: one as total cells and also a non-viable cell count (seen as blue cells). Each square of the haemocytometer, with a cover-slip in place, represented a total volume of 0.1 mm³ or 10⁻⁴ cm³ which was equivalent to approximately 10⁴ cells mL⁻¹. Hence, the total number of cells and the viability of cells were determined as follow:

$$\begin{aligned} \text{Total cells} &= \text{Average counts of cells} \times \text{Dilution Factor (2)} \\ &\times \text{Original volume of culture in flasks} \times 10^4 \end{aligned}$$

$$\text{Viability of cells (\%)} = \frac{\text{Total Viable Cells (unstained)}}{\text{Total cells (stained and unstained)}} \times 100$$

Preparation of cell lines prior infection- Cells (20mL) were cultivated in a vented 225cm² tissue culture flask and centrifuged at 200X g for 5 minutes using 50mL centrifuge tube. Pellets were washed twice with RPMI-1640 before adjusting to the required density in RPMI -1640 with 10% v/v FBS (designated further as RPMI-I) and seeded in 24-well tissue culture plates (Corning).

Preparation of bacterial strains for infection- On the day of infection, frozen *M. tuberculosis* stocks were thawed. The medium was replaced with pre-warmed RPMI-1640 and subjected to centrifugation at 12,000X g for 20 minutes. The bacterial

suspensions were carefully syringed using a 23G blunt end needle (Harvard Apparatus Limited) inserted into a 2mL Luer lock syringe (Fisher Scientific, TWT-450-010S). Syringing was performed thrice to ensure single cell suspensions and used for infection of cell monolayers at various multiplicities of infection (Jones-López et al., 2013).

Preparation of macrophage lysates for CFU assay- Infected macrophages were initially washed in pre-warmed sterile PBS thrice and lysed with sterile cold PBS containing 0.25% v/v Triton X-100. The cells were incubated for 10 minutes at room temperature. Using a P1000 pipette and tip, adherent cells were carefully scraped and transferred into a screw capped 1.5mL Eppendorf tube. Lysates were further serially diluted for CFU assay. Plates were returned to incubator immediately for further incubation.

4.2.3.1.2 Murine J774.1 infection

At 24 h prior to infection, the pre-washed J774.1 cells in RPMI-I were initially checked for viability and found to be 85-90%. A total of 1×10^5 cells were seeded per well for proliferation and adherence to bottom of well overnight. Approximately 2×10^5 cells were used for infection.

J774.1 monolayers were infected with *M. tuberculosis* and $\Delta rv2661c:rv2660c$ using an MOI 10 and incubated for 3 hours. Repeated washings with pre-warmed PBS (three times) aimed to remove adherent extracellular bacilli. The medium was replaced with RPMI-I. Viability of intracellular mycobacteria was monitored post 3 (designated as time= 0 hour, T_0), 24, 48 and 96 hours of incubation and assessed by CFU counts.

4.2.3.1.3 Human Monocytic Leukemia Cell Line, THP-1 infection

THP-1 cells (laboratory stock, 2×10^5 cells mL^{-1}) in RPMI-I were initially supplemented with 100 ngmL^{-1} phorbol 12-myristate 13-acetate (PMA, Sigma-Aldrich). PMA, an inflammation inducer, was used to terminate cell proliferation (Tsuchiya et.al, 1982) and to differentiate adherent macrophages (Theus et al., 2004). Only actively growing THP-1 cells from low (4-6) passage cultures with viability of 98% and above were used for infection. The homogenous THP-1 cells (1mL) were seeded into 24-well tissue culture plates in triplicate and for microscopy, 0.5mL THP-1 cells was aliquoted into 4-chamber slide system (Chamber Slide™ System, Thermo Scientific™). Macrophage

differentiation was carried out for 72 hours and adherent cells were washed with RPMI-1640 medium twice to remove remaining PMA solution before cultivation in RPMI-I for an additional 72 hours.

IFN γ activation of THP-1 macrophages was performed by treating these cells with 15ngmL⁻¹ of human recombinant IFN γ (InVivoGen) for 24 hours in similar medium prior infection.

Resting and IFN γ activated THP-1 monolayers were infected with the required MOI and incubated for 3.5 hours (unless stated otherwise, also designated as T₀) at 37°C. To ensure inactivation of extracellular bacteria, infected cells were treated with amikacin at final concentration of 200ngmL⁻¹ for one hour followed by three washings with pre-warmed sterile PBS. Control wells containing RPMI medium without amikacin were also set up. Infected cells were maintained in RPMI-I for 8 days.

Viability of THP-1 cells was maintained by replacing medium every two days and cells were visually inspected for confluent growth using an inverted mirror. For assessment of viable intracellular bacilli, CFU counts of *M. tuberculosis* strains were determined 4.5 (designated as time= 0 hour, T₀), 24, 96 and 192 hours of infection.

Microscopy- Fluorescence microscopy was carried out to confirm the presence of intracellular bacilli during infection. A similar infection protocol was followed as above and performed in 4-well chamber slides. Infected monolayers were fixed using vapour from 23% (w/v) formaldehyde solution and stained with Auramine-O. On each chamber, 10% (v/v) glycerol was placed and a microscope slide was carefully mounted prior microscopy. Infected cells were examined with an inverted microscope (Nikon Eclipse Ti) under X100 objective oil immersion. The first image of *M. tuberculosis* - infected macrophages was taken under phase contrast and the second fluorescence image was detected using an Auramine filter (Chromas 31015 bespoke) with fluorescence imaging parameters (excitation 460 \pm 25nm; emission 550 \pm 25nm). Acquired images were optimised using NIS Elements image analysis software (Nikon).

4.2.4 Murine infection

Murine infection experiments were carried out in accordance with the Animals (Scientific Procedures) Act of 1986 and Home Office project licence. Experiments

were approved by the University of Leicester Research Ethics committee. The experiments were performed by Dr Galina Mukamolova and Dr Sarah Glen (UoL). For infection, 100 μ L frozen aliquots of *M. tuberculosis* H37Rv and $\Delta rv2661c:rv2660c$ were thawed and centrifuged at 12,000X g for 10 minutes. The supernatants were discarded and pellets were resuspended in PBS to generate a bacterial suspension with an approximate count of 2×10^6 CFU mL⁻¹. Eight to ten week-old female BALB/c mice (Charles River Laboratories, United Kingdom) were lightly anesthetized with 2.5% (v/v) isofluorane over oxygen at 1.6 to 1.8 liters min⁻¹ and infected intranasally with 50 μ L of the inoculum. Bacterial loads of each strain were assessed in respective lung, spleen and liver from five infected mice at each time point; 24 hours post-infection, 1, 2, 4 and 6 weeks of infection. Organ tissues were homogenized in 5mL sterile PBS with beads of diameter 6.35mm or 1/4inch using Fast Prep at 6.0 ms⁻¹ for 30 seconds. Homogenates were serially diluted for CFU assay to assess bacterial loads.

4.3 RESULTS

4.3.1 Phenotypic characterisation of *rv266oc* and *rv2661c* deletion and over-expressing strains of *M. tuberculosis* H37Rv during *in vitro* non-replicating persistence and under stress exposure

4.3.1.1.1 Nutrient starvation

A mean starting inoculum of $1.27 \times 10^8 \pm 2.4 \times 10^7$ CFU mL⁻¹ of wild-type and deletion strains in 5 mL sterile PBS were used for the experiment. After one week of incubation, CFU counts for all tested strains increased by 2-fold with a mean $2.2 \times 10^8 \pm 9.5 \times 10^6$ CFU mL⁻¹. With further incubation, there was no considerable net decrease in CFU counts of tested strains; the CFU counts maintained in the range of $(1.8- 2.5) \times 10^8$ CFU mL⁻¹ until week 6 (Figure 4-1) The plateau in CFU counts suggested cells were still viable despite nutrient limitation for 6 weeks.

To note, there was a 1.5-fold difference in CFU counts between wild-type and $\Delta rv2661c:rv266oc$ at 6 weeks, but the difference was not statistically significant ($p=0.39$). There was no colour change of Methylene blue supporting the notion that viable cells had reduced respiratory activity throughout starvation (Loebel et al., 1933, Betts et al., 2002). Cell aggregation was observed at 3 weeks, probably due to the absence of Tween-80 but dispersed readily upon careful pipetting.

These findings suggest that the single or double deletion of *rv266oc* and *rv2661c* including the partial deletion of *rv2662* and *ncRv12659* had no influence on survival of *M. tuberculosis* during prolonged incubation in PBS.

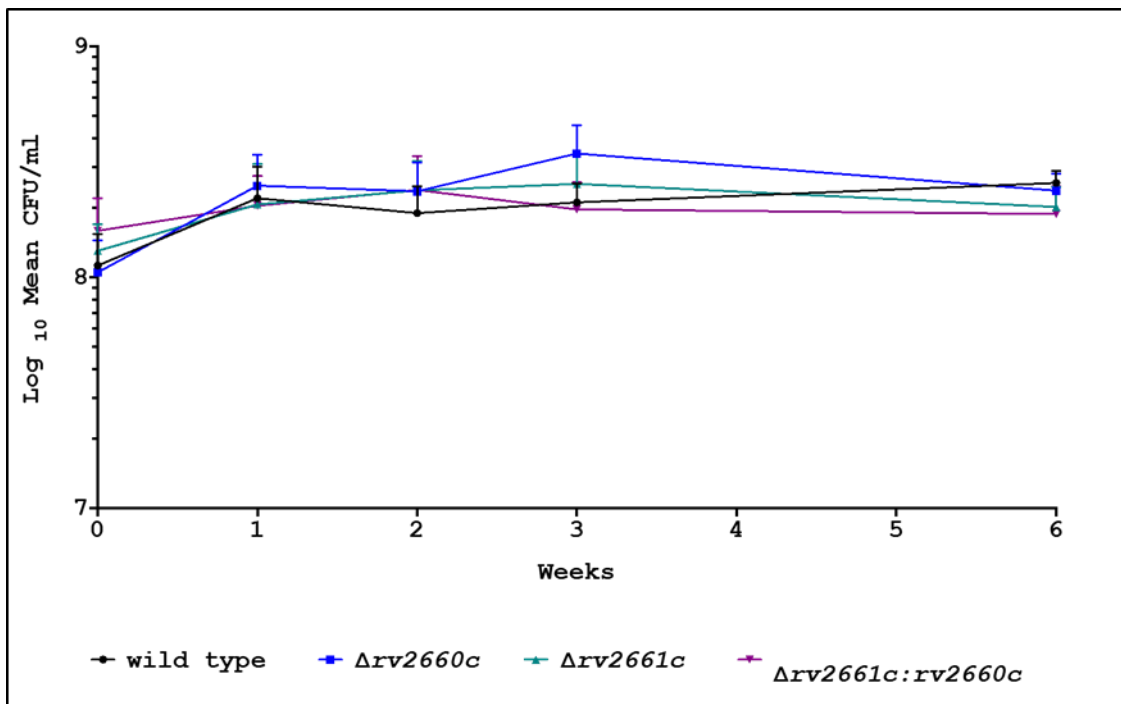


Figure 4-1: Survival of *rv2660c* and *rv2661c* deletion strains of *M. tuberculosis* H37Rv during nutrient starvation. Tested strains were *M. tuberculosis* H37Rv (black line), *M. tuberculosis* $\Delta rv2660c$ (blue line), *M. tuberculosis* $\Delta rv2661c$ (green line) and *M. tuberculosis* $\Delta rv2661c:rv2660c$ (purple line). Data represent mean CFU mL⁻¹ ± SEM from two independent experiments performed in triplicates presented in Log₁₀ scale graph.

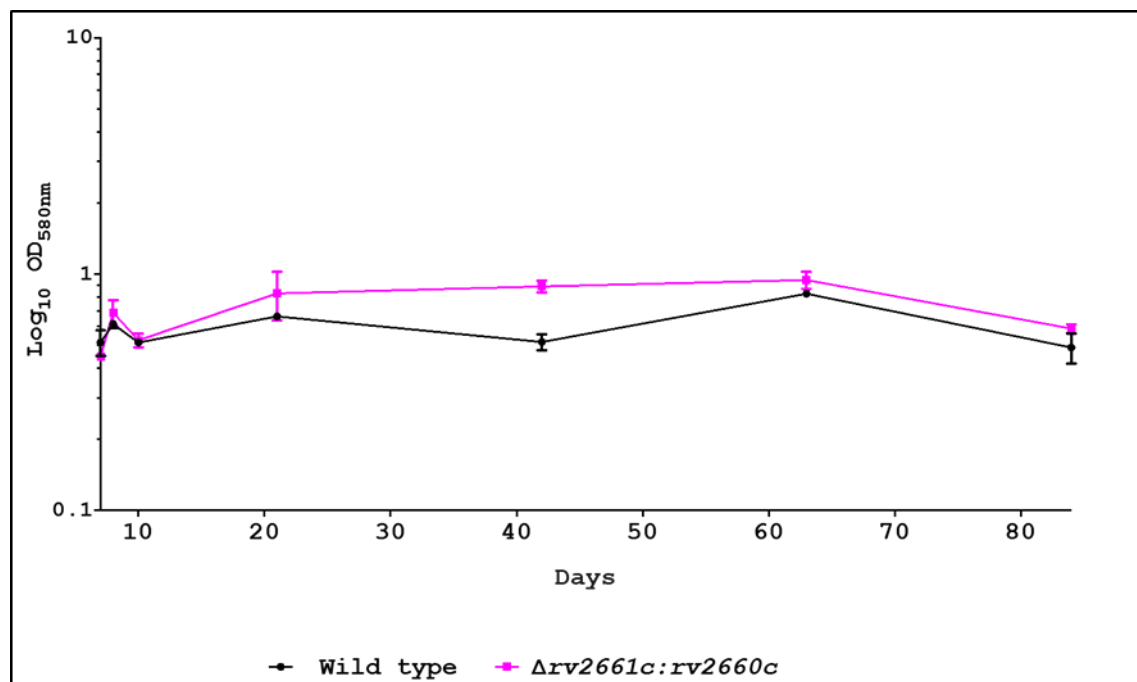
4.3.1.1.2 Wayne's model

A starter inoculum of 1.2×10^6 CFU mL⁻¹ (*M. tuberculosis*) and 2×10^6 CFU mL⁻¹ ($\Delta rv2661c:rv2660c$) were used. OD and CFU counts were obtained to assess growth and survival of tested strains. Both strains grew exponentially reaching a mean maximum OD 0.65 ± 0.04 (Figure 4-2A) at day 8 corresponding to mean $(9.83 \pm 1.17) \times 10^7$ CFU mL⁻¹ (Figure 4-2B). With further incubation, growth rate started to decline exhibiting no net increase in OD_{580nm}. Importantly, the CFU counts for these strains remained comparable with no significant net decrease until the final week of the experiment, where at week 12, CFU counts of $\Delta rv2661c:rv2660c$ were $(7.0 \times 10^6 \pm 5.57 \times 10^5)$ CFU mL⁻¹ showing no statistical differences in counts compared to wild-type strain, $(1.67 \times 10^7 \pm 6.67 \times 10^5)$ CFU mL⁻¹ ($p=0.10$). Both observations were shown to be consistent where cells began to cease replication from day 8 and gradually adapting to the

lower oxygen saturation environment (Wayne, 1996, Wayne and Hayes, 1996). Corresponding to this, discolouration of methylene blue in cultures from week 3 indicated oxygen depletion indicative of the NRP stage 2 and metabolism shut down (Wayne, 1996).

The presence of pellicles in all replicates was observed from week 6 onwards (Figure 4-3B). Samples were carefully pipetted from the middle section of the bacterial suspensions to avoid sampling pellicles and cell deposits or sediments settling at the bottom of the tubes. Since there was no significance difference in growth and viability of $\Delta rv2661:rv2660c$ compared to the wild-type strain, the data suggest that *rv2660c*, *rv2661c*, *rv2662* and *ncRv12659* were not required for the survival of *M. tuberculosis* at any stage of Wayne's NRP model.

A)



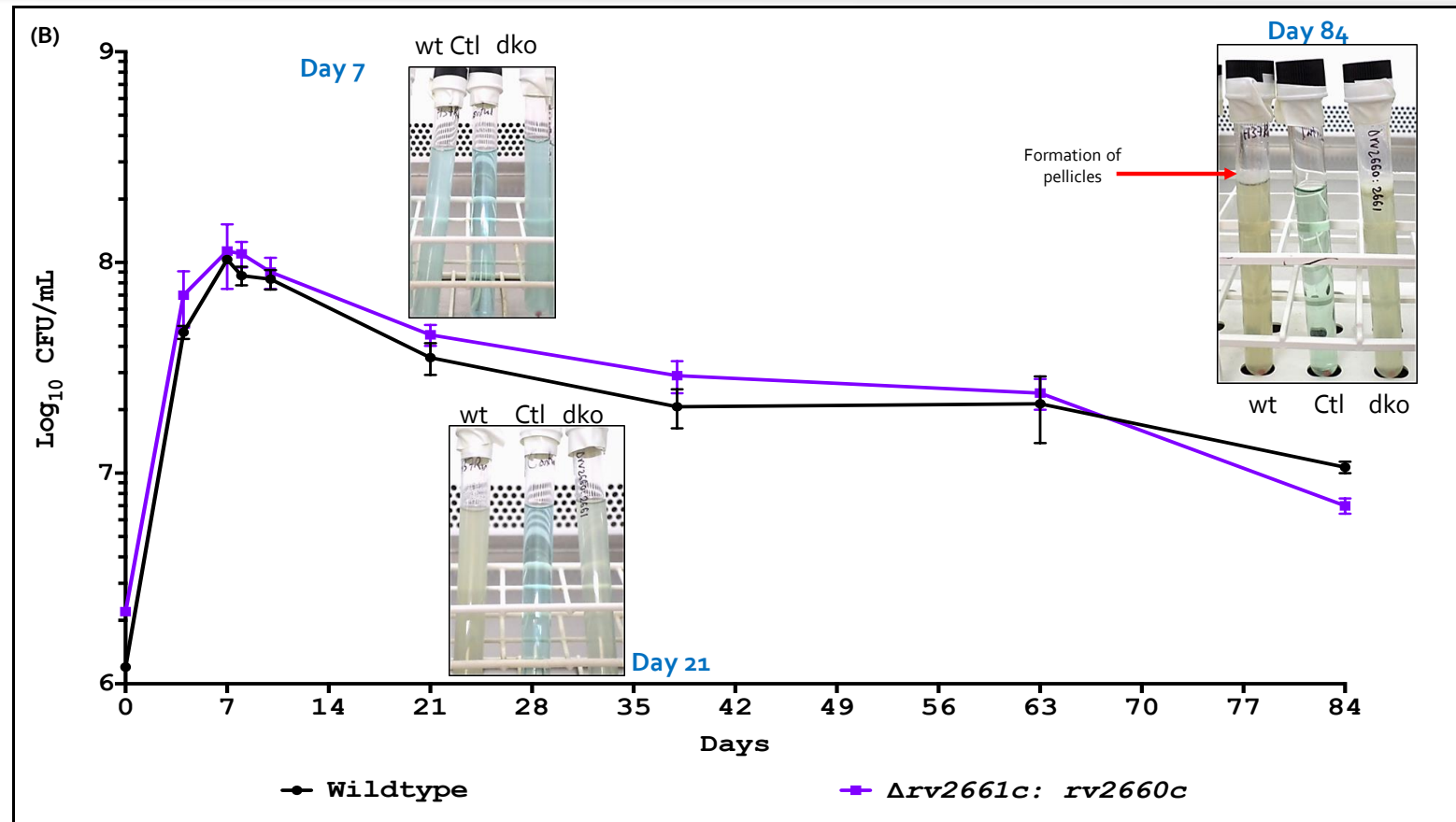


Figure 4-2: Growth and survival of *M. tuberculosis* wild-type and $\Delta rv2661c:rv2660c$ in Wayne's Hypoxia Model.(A) Optical density (OD_{580nm}) and (B) Viability counts were assessed for both *M. tuberculosis* ,wt (black line) and $\Delta rv2661c:rv2660c$,dko (purple line).Images represent strains compared to Control tube (Ctl, medium with methylene blue only) at day 7 (Exponential stage), day 21 (early NRP₂, methylene blue decolorized) and day 84 (Late NRP₂, pellicles circled In red seen as early as week 6). Data represent mean CFU mL⁻¹ ± SEM performed in triplicates presented in Log₁₀ scale graph

4.3.1.1.3 Oxidative stress responses

The experiment was initiated by growing wild-type and deletion strains; $\Delta rv266oc$, $\Delta rv2661c$ and $\Delta rv2661c:rv266oc$ (mean inoculum of 2.88×10^7 CFU mL⁻¹) in supplemented 7H9 with a final concentration of 10mM hydrogen peroxide (H₂O₂). However even after 24 hours of exposure, CFU counts of all strains were doubled indicating resistance to the effects of 10mM H₂O₂ (data not shown).

Using a higher concentration of 25mM H₂O₂, a mean inoculum of mycobacterial strains of $(2.0 \times 10^8 \pm 1.65 \times 10^7)$ CFU mL⁻¹ were exposed for 2 hours and a 97% reduction in survival of all strains was observed (Figure 4-3A). The results were consistent in two independent experiments. With 4 hours of exposure, the survival of all strains declined further, to $2.47 \pm 2.32\%$ (wild-type), $1.11 \pm 0.54\%$ ($\Delta rv266oc$), $0.55 \pm 0.18\%$ ($\Delta rv2661c$) and $0.63 \pm 0.34\%$ ($\Delta rv2661c:rv266oc$) with no statistical difference between strains ($p=0.51$). Ultimately after 24 hours of exposure, no colonies were recovered indicating that the concentration of H₂O₂ was detrimental for all strains (LOD= 66 CFU mL⁻¹).

The survival of over-expressing strains of $rv266oc$ and $rv2661c$ was also investigated using a similar concentration of H₂O₂. After 4 hours of exposure, pMV261:: $rv2661c$ ($5.98 \pm 2.79\%$) and pMV261:: $rv2661c+rv266oc$ ($7.58 \pm 4.80\%$) have showed enhanced survival compared to control strain ($0.64 \pm 0.61\%$) (Figure 4-3B). However, there was no statistical difference in percentage survival between tested strains ($p=0.22$). The survival of pMV261:: $rv266oc$ could not be assessed because of the large variation in values obtained from three independent experiments (% survival: 19.09%; 41.7% and 1.29%).

The experiments demonstrated that deletion and over-expression of $rv2661c$ and $rv266oc$ have no significant effect on the survival of *M. tuberculosis* during oxidative stress.

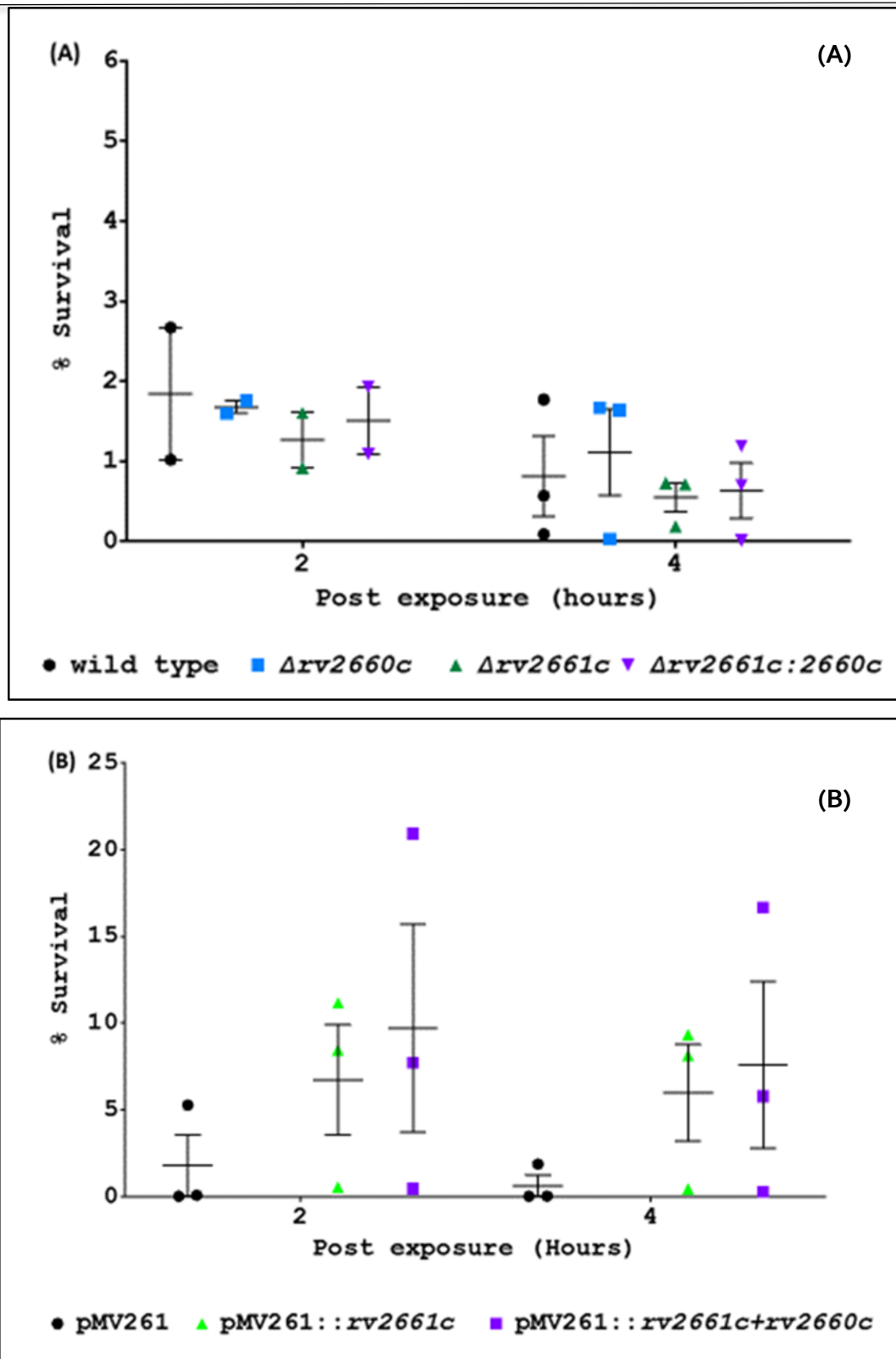


Figure 4-3: Effect of oxidative stress on the survival of both deletion and over-expressing of *rv2660c* and *rv2661c*. Survival of (A) deletion and (B) over-expressing strains in supplemented 7Hg with final concentration of 25mM H₂O₂. Data represent Mean \pm SEM from three independent experiments performed in triplicates [two experiments for 2 hours time point shown in (A)]

4.3.1.1.4 Nitrosative stress

The nitric oxide (NO) donor, 6-methoxy-5-pyrimidin-4-yl pyrrolidine-1-carbodithiate (further designated in the thesis as NO donor o6g) was chosen as it was shown to release NO spontaneously and under enzymatic catalysis conditions (Ryabova et al., 2004, Ryabova et al., 2005). According to the published results, it produced the greatest amount of nitrite anion and released disulphides (Ryabova et al., 2005) that aided NO liberation. Survival of *M. bovis* BCG was significantly reduced after 24-hour exposure demonstrating bactericidal properties of this NO donor (Sanyi, 2016).

Initially, the minimum inhibitory concentration (MIC) of the compound for both panels of deletion ($\Delta rv266oc$, $\Delta rv2661c$ and $\Delta rv2661c:rv266oc$) and over-expressing strains (*M. tuberculosis* pMV261::rv266oc, pMV261::rv2661c and pMV261::rv2661c+rv266oc) were determined using a resazurin microdilution assay (section 2.6.3 for protocol). Three independent experiments were performed for each panel of strains. All deletion mutants were inoculated at $(2.05 \times 10^5 \pm 4.84 \times 10^4)$ CFU per well, and the plates were examined after 2 weeks of incubation. The MIC for all deletion strains and wild-type strains were $0.8 \mu\text{g mL}^{-1}$. For over-expression strains and the control strain, a mean inoculum of $(6.951 \pm 4.84) \times 10^4$ CFU was used. The MIC was determined to be $6.4 \mu\text{g mL}^{-1}$. The results demonstrated that deletion and constitutive over-expression of both and either gene did not affect the sensitivity of *M. tuberculosis* to the NO donor o6g.

Next, the bactericidal effect of NO donor on deletion and over-expressing strains was investigated. A mean inoculum of $(1.95 \times 10^7 \pm 4.61 \times 10^6)$ CFU mL⁻¹ of mycobacterial strains was grown in supplemented 7H9 with a final concentration of 100 μM NO donor o6g. The concentration of the NO donor used for deletion strains was ~100 fold and for overexpressing strains was ~16- fold from the determined MIC. The variability of all strains was unaffected after 4 hours of exposure. It was only following further incubation to 20 hours that CFU counts started to decline. For the deletion strains, their survival was comparable to the wild-type strain (Figure 4-4A). There was also no statistical difference between strains ($p=0.71$).

At 24 hours of exposure, the survival of over-expressing strains was further reduced by more than 1 - log₁₀ fold compared to 4 hours exposure (Figure 4-4B). However, survival

of *M. tuberculosis* pMV261::rv266oc (7.05 ± 6.82), *M. tuberculosis* pMV261::rv2661c ($0.78 \pm 0.79\%$), *M. tuberculosis* pMV261::rv2661c+rv266oc ($0.48 \pm 0.48\%$) and control strain ($3.78 \pm 1.95\%$) exhibited no statistical difference between strains ($p=0.44$).

Collectively, our data demonstrated that the deletion and over-expression of *rv2661c* and *rv266oc* did not impair the survival for *M. tuberculosis* during 24 hours of exposure to the NO donor.

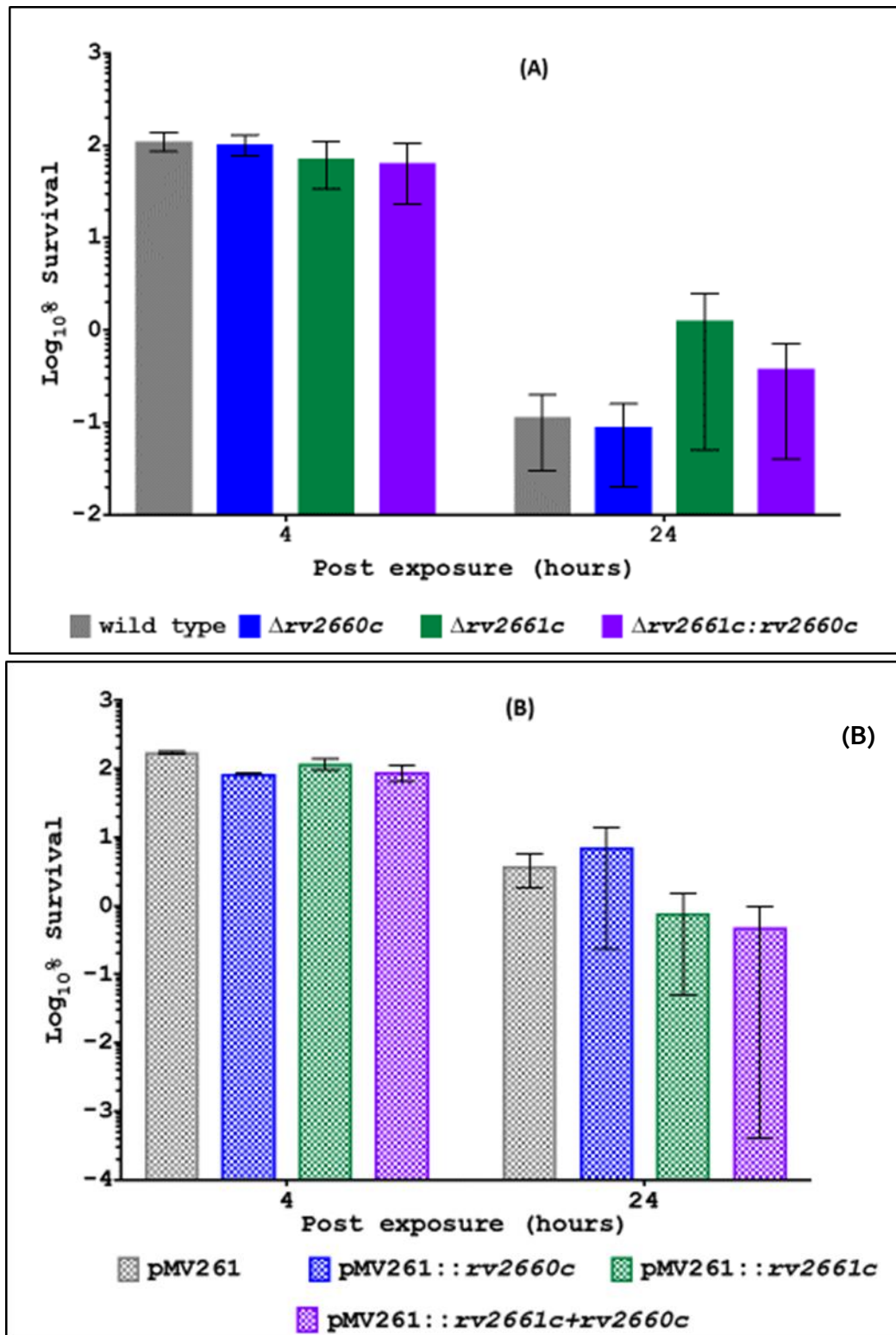


Figure 4-4: Effect of nitrosative stress on the survival of both (A) deletion and (B) over-expressing of *rv2660c* and *rv2661c*. Survival of mycobacterial strains grown in supplemented 7H9 with final concentration of 100 μ M 6-methoxy-5-pyrimidin-4-yl pyrrolidine-1-carbodithiate shown in Log₁₀ scale graph. Data represent Mean \pm SEM from two independent experiments.

4.3.2 Intracellular replication and survival of *rv2661c* and *rv2660c* deletion strains in macrophages

4.3.2.1.1 Murine J774.1 macrophages

The murine J774.1 cell line was infected with an MOI of 10 using a mean inoculum of 1.88×10^6 CFU mL^{-1} (*M. tuberculosis* wildtype) and 1.22×10^6 CFU mL^{-1} ($\Delta rv2661c:rv2660c$). Control wells with macrophages only were included for visual comparison of macrophage detachment during the time course of the experiment. After 4 hours of infection (T_0), CFU recovered from the infected cell culture wells were reduced to 18958 ± 6418 CFU mL^{-1} (*M. tuberculosis* wildtype) and 27000 ± 5880 CFU mL^{-1} ($\Delta rv2661c:rv2660c$) showing no significant difference in uptake ($p=0.19$) shown in Figure 4-5. To take into account the variations between the inoculum of tested strains, the counts obtained at T_0 were expressed as a percentage of respective inocula for analysis of uptake efficiency. Hence, uptake of both strains was less than 2%.

The intracellular bacterial load of both strains began to increase after 24 hours of infection and slowly increased until the end of the infection period. Importantly, there was no significant difference in CFU counts of $\Delta rv2661c:rv2660c$ and wild-type strain (24h: $p=0.40$, 48h: $p=0.70$, 96h: $p>0.99$) throughout the experiment.

The comparable intracellular replication of the double mutant strain and wild-type consistent in both experiments indicated that neither of the annotated genes nor *ncRv12659* are important for *M. tuberculosis* to survive and persist in murine macrophage infection.

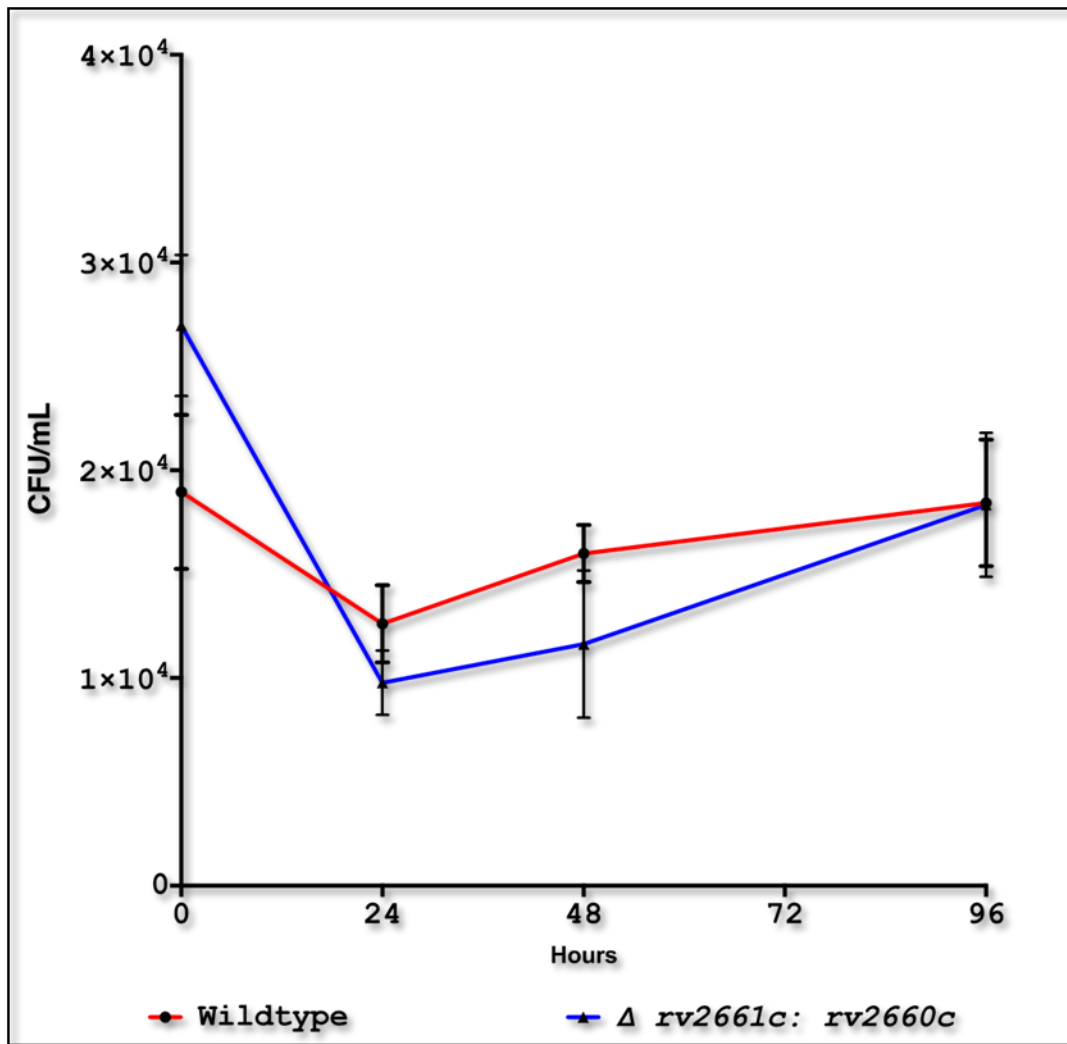


Figure 4-5: Intracellular replication in naïve J774.1 macrophages. Two strains: *M. tuberculosis* (red line) and $\Delta rv2661c:rv2660c$ (blue line) were infected using MOI 10 for 4 hours (shown as Time 0). Infection proceeded for 5 days and viability of intracellular bacilli was monitored with at each time point. Graph shown is a representative of the two independent experiments. Data represent average \pm SEM from three technical samples.

4.3.2.1.2 Human THP-1 macrophage cell lines

To compare intracellular replication of the tested strains during J774.1 infection, human THP-1 macrophages were used. Two validation experiments were carried out to establish a protocol for THP-1 infection model that included an application of Amikacin to kill extracellular bacilli and MOI optimisation.

Optimisation studies- With Amikacin treatment, three different conditions including a control were set up. Using MOI 1 for infection, the co-cultures were incubated for 3 hours. The infected monolayers were then washed with pre-warmed PBS for three times and subjected to three separate conditions: These conditions were (1) untreated infected cells were maintained in supplemented RPMI; (2) infected cells were treated with $200 \mu\text{g mL}^{-1}$ Amikacin for an additional one hour, washed three times with PBS and maintained in fresh supplemented RPMI; (3) Infected cells were maintained in supplemented RPMI with $20 \mu\text{g mL}^{-1}$ Amikacin throughout the experiment.

A mean inoculum of $2.25 \times 10^5 \text{ CFU mL}^{-1}$ was used to infect PMA-differentiated THP-1 cells. The bacterial load for cells treated with higher concentration of Amikacin have gradually increased up to ~6-fold at 72 hours and further increased to a final ($5.67 \times 10^5 \pm 7.95 \times 10^4$) CFU mL^{-1} at 7 days. These findings suggest an effective step in reducing extracellular bacilli that resulted in a robust replication of the strain when a low bacterial load was used to infect the macrophages. In contrast, bacterial counts in untreated cells increased only by 2.2- fold at 72 hours and then the CFU counts declined. When the lower concentration of Amikacin was maintained throughout the experiment, a decrease in viable counts were also observed which indicated more bacterial killing.

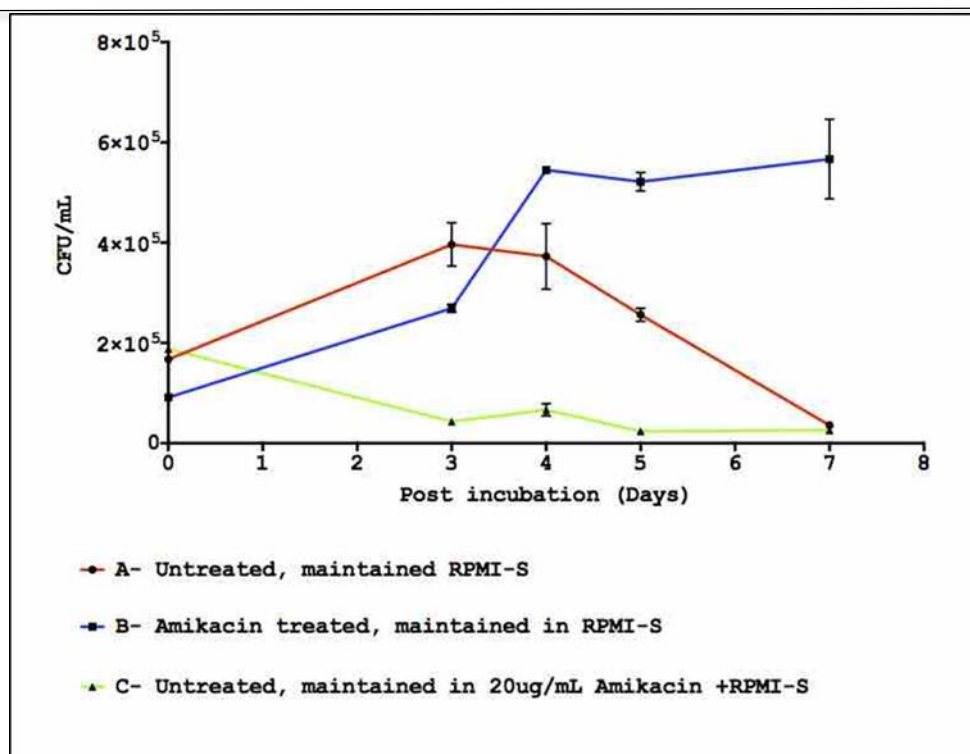


Figure 4-6: Effect of Amikacin on intracellular replication of *M. tuberculosis* H37Rv during resting THP-1 macrophage infection. Human THP-1 were seeded at 2×10^5 cells/ well and differentiated to adherent macrophages with RPMI + 10% Foetal Bovine Serum (FBS) (RPMI-S) containing 100 ng mL^{-1} phorbol 12-myristate 13-acetate (PMA) for 48 hours. RPMI-S containing PMA were replaced with RPMI-S only and equilibrated for 24 hours, 37°C , 5% CO_2 . Adherent THP-1 macrophages were infected using MOI 1 for 3 hours. Infected monolayers were washed with pre-warmed PBS three times and subjected to three separate conditions: (A) Untreated monolayers maintained in RPMI-S (black line), (B) Infected monolayers treated with RPMI-S with final concentration of $200 \mu\text{g mL}^{-1}$ Amikacin incubated for an additional one hour and maintained in RPMI-S (red line) (C) Infected monolayers maintained in RPMI-S with final concentration of $20 \mu\text{g mL}^{-1}$ Amikacin (Purple line). On alternate days, the infected monolayers were replaced with respective medium. Intracellular bacilli were obtained by lysing monolayers with cold PBS containing 0.2% (v/v) Triton X-100 at different time points. Lysates were serially 10-fold diluted and plated on supplemented 7H10 plates. CFUs were enumerated after 2-3 weeks of 37°C incubation. Data represent average \pm SEM from three biological replicates.

A second validation experiment involved application of different MOIs; 1, 2, 5 and 10. With lower MOIs (1 and 2), there were comparable net increase in replication until 4 days of infection. Subsequently to infection with MOI of 5, the replication of the mycobacteria was only observed after 3 days of infection indicating a delayed onset of

replication. In contrast, infection with MOI of 10 resulted in no net growth relative to the decline in intracellular CFU counts.

Therefore, a THP-1 infection protocol with lower MOIs for 4 hours, including treatment of the infected co-cultures with $200\mu\text{g mL}^{-1}$ Amikacin for 1 hour, was established.

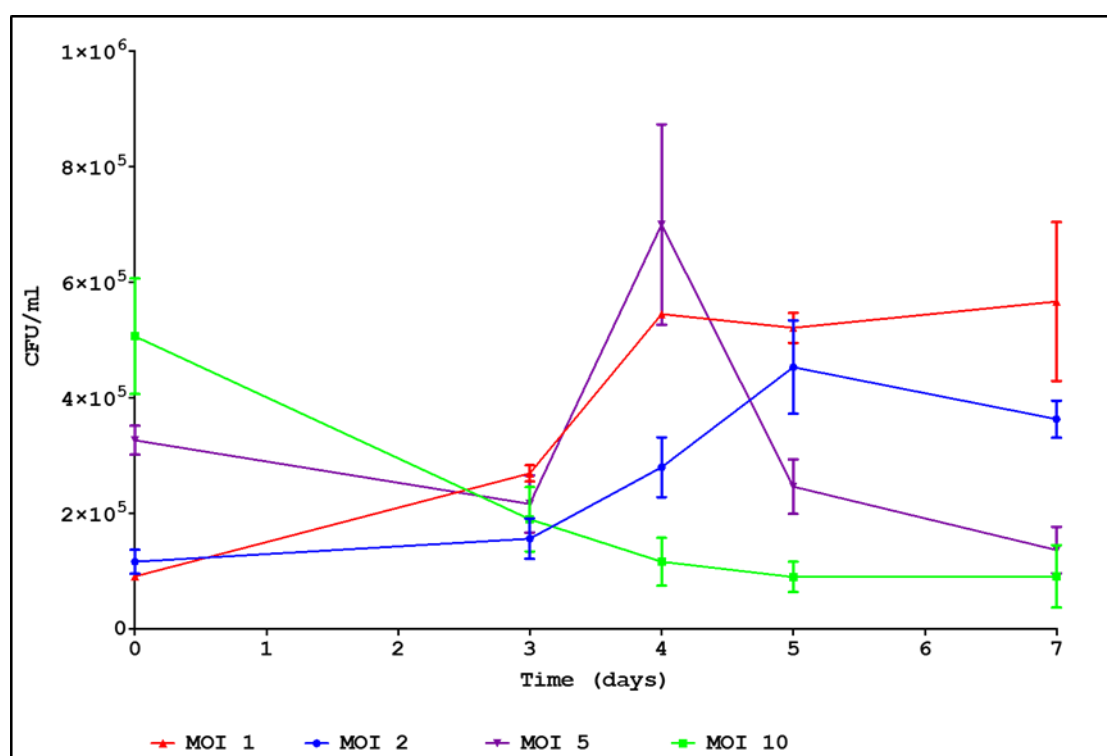


Figure 4-7: Intracellular growth of *M. tuberculosis* H37Rv infected with different MOIs in resting THP-1 macrophage infection. Human THP-1 were seeded at 2×10^5 cells/ well and differentiated to adherent macrophages with RPMI + 10% Foetal Bovine Serum (FBS) (RPMI-S) containing 100ng mL^{-1} phorbol 12-myristate 13-acetate (PMA) for 48 hours. Medium containing PMA were replaced with RPMI-S only and equilibrated for 24 hours, 37°C , 5% CO_2 . Adherent THP-1 macrophages were infected with *M. tuberculosis* H37Rv using MOI 1 (Red line), MOI 2 (Blue line), MOI 5 (Purple line) and MOI 10 (Green line) for 3 hours. Infected monolayers were washed with pre-warmed PBS three times and subjected to Amikacin treatment (RPMI-S with final concentration of $200\mu\text{g mL}^{-1}$ Amikacin) for one hour and maintained in RPMI-S. Intracellular bacilli were obtained by lysing monolayers with cold PBS containing 0.2% (v/v) Triton X-100 at different time points. Lysates were serially 10-fold diluted and plated on supplemented 7H10 plates. CFUs were enumerated after 2-3 weeks of 37°C incubation. Data represent average \pm SEM from three biological replicates.

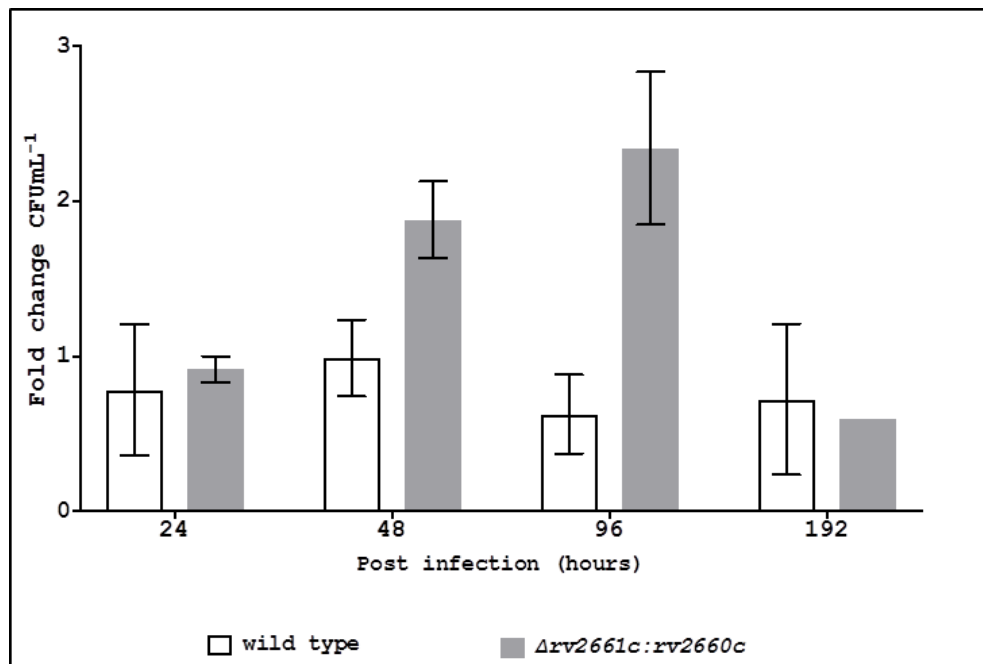
Macrophage infection studies (MOI 2)

Similar to the J774.1 infection experiment, $\Delta rv2661c:rv2660c$ and wild-type strain were used to infect resting THP-1 cells. CFU counts of each strain were expressed as fold change relative to counts after 3.5 hours of incubation, to also account for the variation in inoculum used for infection. The wild-type strain has showed an uptake efficiency of 22% and exhibited no net increase in replication over the 192 hours of infection (Figure 4-8A). In contrast, the $\Delta rv2661c:rv2660c$ strain has showed at least a 2-fold increase at 48 and 96 hours of infection compared to T_0 . Importantly, there was no statistical difference in CFU counts between both strains at 48 hours ($p=0.126$) and 96 hours ($p=0.97$).

Next, the $\Delta rv2661c:rv2660c$ strain was used to infect IFN γ -activated THP-1 cells. We reasoned that infecting IFN γ -activated macrophages with mycobacterial strains would stimulate their bactericidal effect (Kimball et al., 1995), and may result in a larger magnitude of difference in replication. After an overnight incubation of the THP-1 cells with 15 ngmL⁻¹ IFN γ , the results obtained for both bacterial strains were comparable to the infection in resting macrophages (shown in Figure 4-8B) indicating that the concentration of IFN γ was insufficient to activate the macrophages. The differences observed between both strains at 48 hours ($p=0.27$) and 96 hours ($p=0.08$) was not statistically significant.

Collectively, both experiments demonstrate that *rv2660c*, *rv2661c*, *rv2662* and *ncRv12659* are not required by *M. tuberculosis* to replicate and survive in THP-1 macrophages.

(A)



(B)

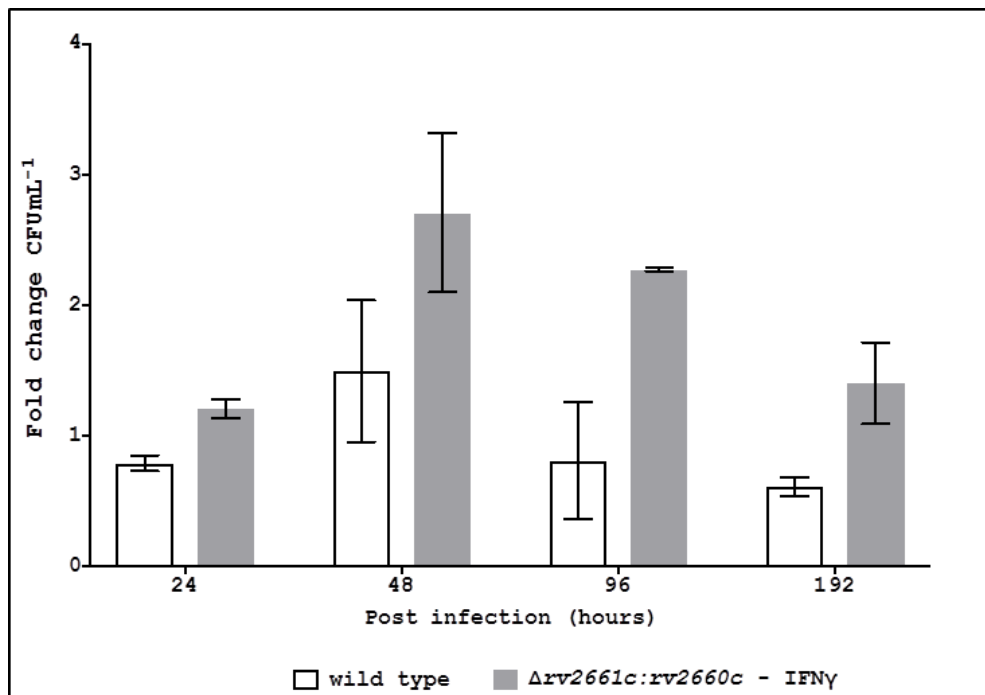


Figure 4-8: Intracellular replication in THP-1 macrophages using MOI 2. Two strains: *M. tuberculosis* (clear bar) and $\Delta rv2661c:rv2660c$ (grey bar) were used to infect in (A) resting cells for 3.5 hours and (B) IFN γ - activated cells for 4 hours. Infection proceeded for 8 days and the viability of the intracellular bacilli was monitored at each time point. Fold change was determined using each CFU count at each time point relative to T₀. Data represent average \pm SEM from two independent experiments performed in triplicate.

Macrophage infection studies (MOI 0.5)- Naïve THP-1 cells were infected with mean counts of $(8.4 \pm 1.48 \times 10^4)$ CFU mL⁻¹ for *M. tuberculosis* wild type and $(7.35 \pm 2.33 \times 10^4)$ CFU mL⁻¹ for $\Delta rv2661c:rv2660c$.

After 24 hours of infection, CFU counts of $\Delta rv2661c:rv2660c$ were significantly reduced to 3800 ± 265 CFU mL⁻¹ ($p=0.02$) and further reduced to 2400 ± 361 CFU mL⁻¹ at 48 hours ($p=0.025$) compared to wild-type (Figure 4-9). It is also worth noting that growth of mutant was slower than wild-type strain on 7H10 agar at both time points suggesting potential damage of mutant cells. Interestingly, the double mutant strain was able to persist and began proliferating with CFU counts comparable to wild-type strain until the end of the experiment. Internalisation of the both mycobacterial strains in THP-1 cells was confirmed by fluorescence microscopy (Figure 4-10).

The data should only be regarded as preliminary as it was only from one experiment and more replicates are required. However, the data indicates a transient attenuation of the double mutant strain at 24 and 48 hours of infection suggesting a possible role of the annotated genes and ncRv12659 during the early stage of infection.

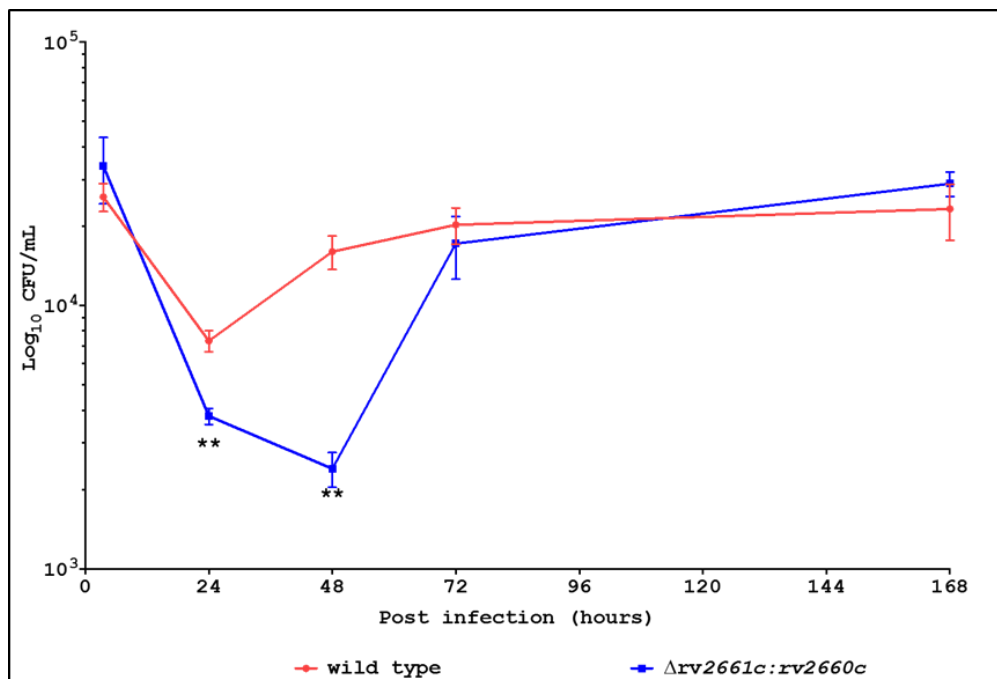


Figure 4-9: Intracellular replication in THP-1 macrophages using MOI 0.5. Two strains: *M. tuberculosis* wild type (red line) and $\Delta rv2661c:rv2660c$ (blue line) were used to infect using MOI 0.5 in resting cells for 4 hours. Infection proceeded for 7 days and the viability of intracellular bacilli was monitored at each time point. Data represent average \pm SEM three biological replicates * $p < 0.05$, ** $p < 0.01$ analysed by Mann-Whitney Test.

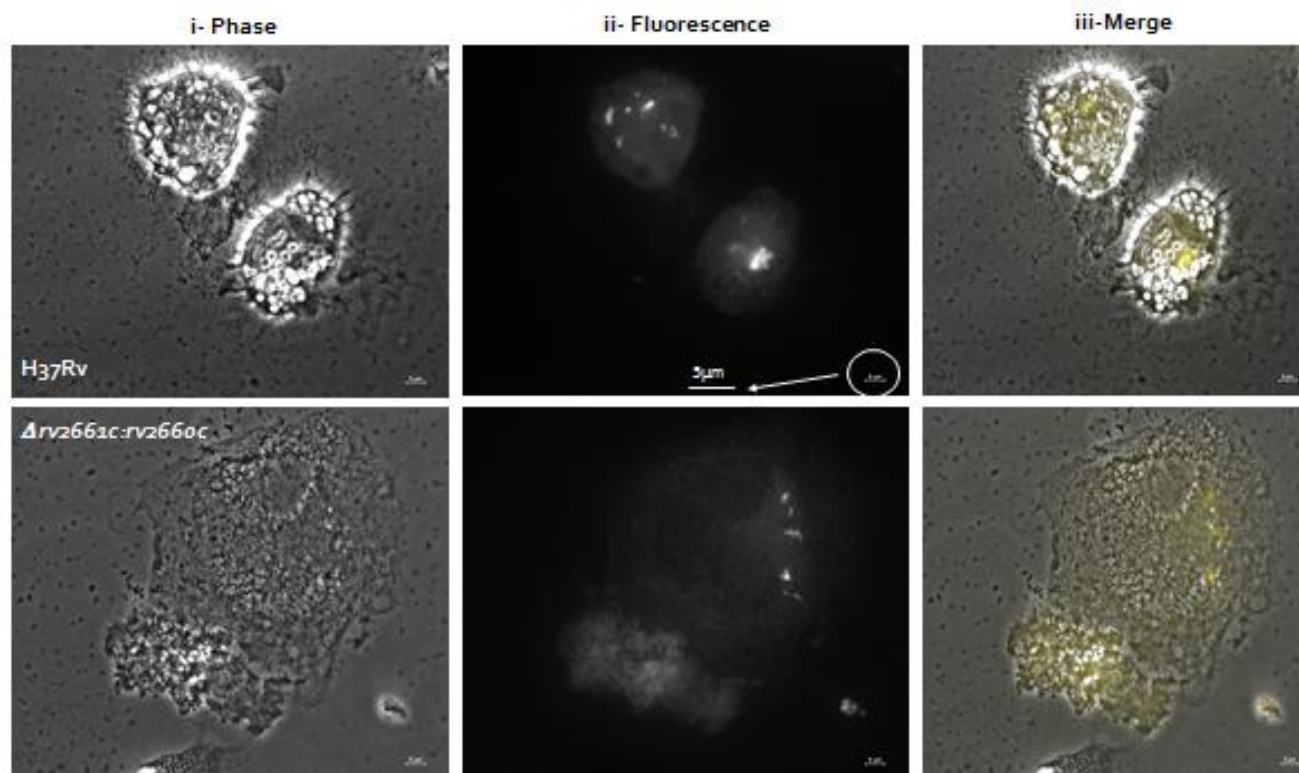


Figure 4-10: Microscopy images of internalised mycobacterial strains in resting THP-1 cells. Representative images from the 48 hour time point are presented and cells were examined using an inverted microscope (Nikon Eclipse Ti) under X100 objective oil immersion. Three different images were acquired to capture as follows; (i) Phase contrast image- THP-1 macrophages, (ii) Fluorescence image - Auramine- O stained mycobacterial strains (Top row-wild-type strain, Bottom row- *M. tuberculosis* $\Delta rv2661c:rv2660c$) and (iii) A merged image of internalised fluorescence *M. tuberculosis* strains in THP-1 cells. Acquired images were optimised using Nikon NIS Elements image analysis software. Scale bar= 5µM (shown in bottom left corner in each image).

4.3.3 Replication of *rv2661c* and *rv2660c* deletion strains in BALB/c mice

Infected mice were culled at various time points over 6 weeks for determination of viable bacilli in affected organs, however results of only day 28 of infection could only be taken into account, as the experiment was hampered with technical complications. BALB/c mice were infected intranasally with wild-type *M. tuberculosis* and $\Delta rv2661c:rv2660c$ with a mean dose of $5.03 \times 10^4 \pm 0.04$ CFU and $7 \times 10^4 \pm 2.3$ CFU respectively. At day 28, the bacterial loads in lungs of both $\Delta rv2661c:rv2660c$ (6.49 Log_{10} CFU) and wild-type strain (6.52 Log_{10} CFU) were comparable, as illustrated in Figure 4-11. In the spleen, $\Delta rv2661c:rv2660c$ was detectable with only 96 ± 76 CFU compared to wild-type, $1.25 \times 10^3 \pm 0.06$ CFU ($p > 0.99$). In the liver, there was no statistical difference in bacterial load between $\Delta rv2661c:rv2660c$ (853 ± 739 CFU) compared to wild-type strain, 293 ± 189 CFU ($p = 0.11$). These findings indicated that the double deletion strain was still replicating and causing disease in mice. In addition, there was absence of PDIMs in both deletion and wild-type strain that have no further effect on replication of both strains *in vivo* (shown in Figure 4-12). Hence, the comparable bacterial load between both strains suggest that the deletion of *rv2660c*, *rv2661c*, *rv2662* and ncRv12659 from *M. tuberculosis* did not result in attenuation of the pathogen replication at 28 days of infection.

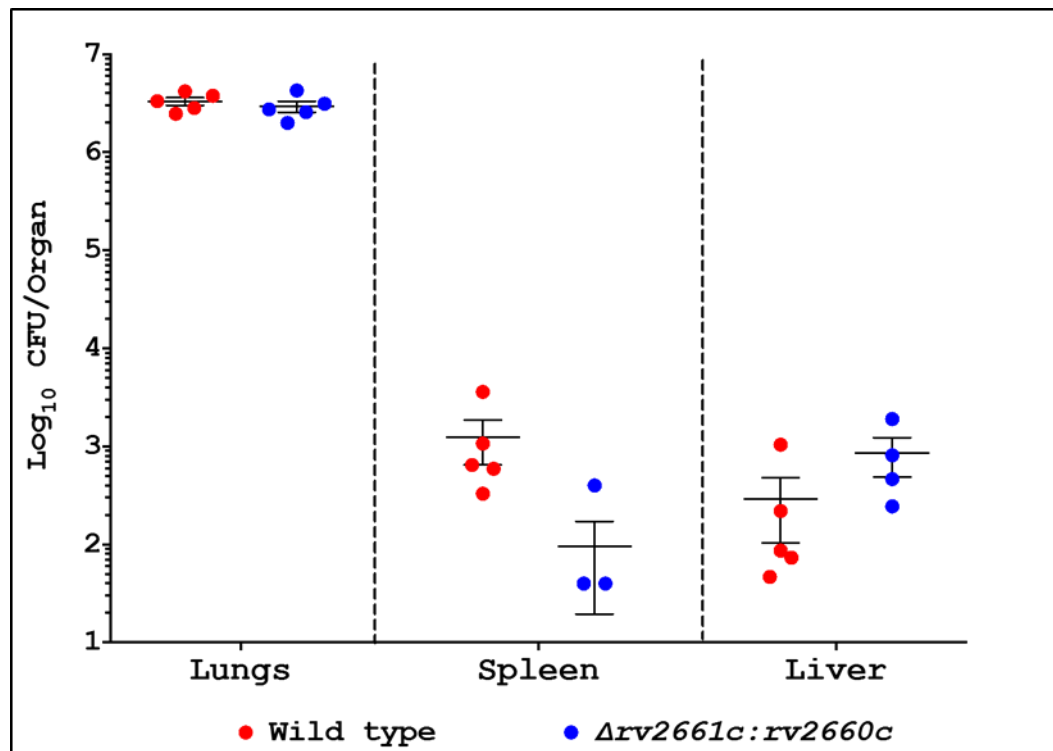


Figure 4-11: Intracellular growth of *M. tuberculosis* wild-type and $\Delta rv2661c:rv2660c$ deletion strain during BALB/c mice infection. Mice were infected with wildtype strain (Red dot) and $\Delta rv2661c:rv2660c$ (Blue dot). CFU counts at 28 days of infection from five replicates (organs from individual mice); Lung (Left), spleen (Middlebrook et al., 1947) and liver (Right) were recovered. Data represent mean \pm SEM of five replicates.

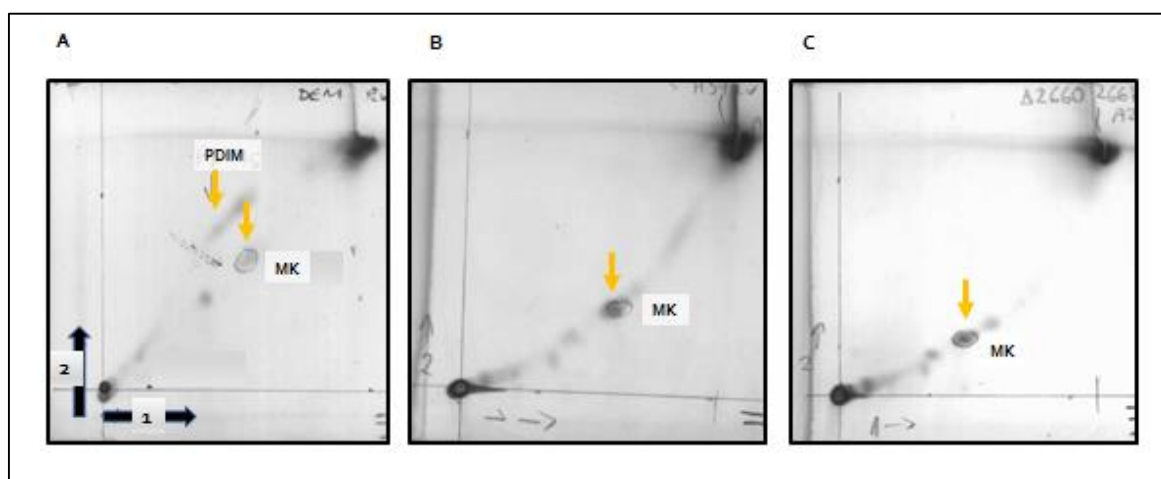


Figure 4-12: Phthiocerol dimycocerosate (PDIM) analysis using thin layer chromatography (TLC). Images represent (A) An example of elongated PDIM spot seen above menaquinone (MK) (Besra, 1998). PDIM was not detected in both (B) *M. tuberculosis* H37Rv and (C) *M. tuberculosis* $\Delta rv2661c:rv2660c$ strain.

4.3.4 Gene Expression Profiling of *rv2660c*, *rv2661c*, *rv2662* and ncRv12659 by qRT-PCR

The expression of each target transcript was investigated in three different *in vitro* conditions; nutrient starvation, oxidative stress and acidic pH stress. The mean target copy numbers and relative gene expression (RE) value for the transcripts in each assay are compiled in Appendix 8.

Firstly, the relative expression of *rv2660c*, *rv2661c*, *rv2662* and ncRv12659 during exponential growth in *M. tuberculosis* was comparably low within a RE value range of less than 10^{-4} in most assays. The relative abundance of each transcript to 16S only yielded $0.006 \pm 0.003\%$ for *rv2660c*, $0.005 \pm 0.004\%$ for *rv2661c*, $0.002 \pm 0.001\%$ for *rv2662* and $0.04 \pm 0.02\%$ for ncRv12659. The low abundance of the transcripts suggests the lack of importance of these annotated genes and ncRNA in response to *M. tuberculosis* growth *in vitro*.

During stress conditions, the expression of each target transcript was analysed as a RE ratio and compiled in Table 4-1. During nutrient starvation, expression of the annotated genes; *rv2660c*, *rv2661c* and *rv2662* was not detected in two independent experiments. There were no statistical differences between the copy numbers of the cDNA samples when compared to the copy numbers of the no-RT samples from RT2661c and RT2662 primer run. In addition, the melting curves derived from RT2660 primer run indicated the presence of non-specific amplicons shown in Appendix 7, Figure 18. The starved induced samples demonstrated two peaks corresponding to T_m $80.8 \pm 0.2^\circ\text{C}$ (higher peak) and actual target T_m $88.8 \pm 0.2^\circ\text{C}$ (subtle peak). The findings were consistently observed in two independent experiments from the starvation experiment and not from the other two stressed- induced cells (oxidative and acidic pH). The findings could only suggest an absence of *rv2660c* mRNA transcripts in starved cells or optimisation of the qPCR run is required. Nevertheless, an approximate 9.0 \pm 5.5-fold marked increase of ncRv12659 expression at 24 hours of starvation ($\text{RE} = 3.63 \times 10^{-3} \pm 1.04$) and 9.8 \pm 6.4-fold at 96 hours compared to baseline level value of $(3.99 \pm 1.28) \times 10^{-4}$ were obtained. Although the degree of upregulation of ncRv12659 expression was much lower than the 50-fold detected by Houghton and

colleagues (Houghton et al., 2013); this analysis confirms the upregulation of the non-coding RNA during adaptation of *M. tuberculosis* to nutrient shift down but not the genes of interest.

Exposure to 5mM H₂O₂ for 40 minutes resulted in the downregulation of *rv2662c* by 3-fold. In contrast, *rv2660c* and ncRv12659 were induced with the same level of expression of (2.3± 1.4)-fold and (2.3± 0.6)-fold respectively. Since only two biological samples were employed, further replicates are required to demonstrate, if indeed both transcripts respond to the similar level of oxidative stress thought to exist during intraphagosomal oxidative burst. When *M. tuberculosis* wild-type strain was exposed to 25mM H₂O₂ for 40 minutes, a different transcriptional response was observed. There was only a minimal increase in relative expression of *rv2661c* of (1.7± 1.5)-fold and *rv2662* of (3.1± 4.4)-fold. The *rv2661c* transcripts were still detected after further 4 hours of exposure. In addition, at this later time point of exposure, a low level of *rv2660c* of (2.4± 2.1)- fold compared to baseline expression level were detected. As a control, $\Delta rv2661c:rv2660c$ was also included in this experiment and as expected, no target transcripts were detected which confirmed the specificity of primers. Collectively, these transcripts were only expressed at a low level in response to H₂O₂ exposure that implies that the annotated genes and ncRNA might not have any contributory role during oxidative stress.

Finally, exposure of *M. tuberculosis* to acidic pH of 5.3 after 2 hours of incubation have only resulted in a minimal level of *rv2660c* with (1.7±2.1)-fold and *rv2662* with (1.4± 1.9)-fold induction expression, compared with exponential growth. Interestingly, ncRv12659 was also detected with (3.0± 4.3)-fold [RE= 0.01 ± (1.85 X10⁻³)] relative to baseline level value of (4.84±1.28) X 10⁻⁴. With further exposure of 4 hours, ncRv12659 was not detected, implying the target transcripts were only induced during initial exposure to acid stress. However, more replicates are required to confirm the true expression of the transcripts due to data variation.

Stress experiments	Time of exposure	Relative expression ratio normalised to 16S			
		<i>rv2660c</i>	<i>rv2661c</i>	<i>rv2662</i>	ncRv12659
Nutrient Starvation	24 hours	Not expressed	Not expressed	Not expressed	9.0± 5.5
	96 hours	Not expressed	Not expressed	Not expressed	9.8± 6.4
Oxidative stress- 5mM H ₂ O ₂	40 minutes	2.3± 1.4	Not expressed	Not expressed	2.3± 0.6
Oxidative stress- 25mM H ₂ O ₂	40 minutes	Not expressed	1.7± 1.5	3.1± 4.4	-
	4 hours	2.4± 2.1	1.1± 1.0	Not expressed	-
Acidic pH 5.3	2 hours	1.7± 2.1	-	1.4± 1.9	3.0± 4.3
	4 hours	Not expressed	-	Not expressed	Not expressed

Table 4-1: Compilation of relative expression induction ratio of *rv2660c*, *rv2661c*, *rv2662* and ncRv12659 transcripts in *M. tuberculosis* compared to exponential growth. Gene expression was analysed in conditions of PBS starvation, oxidative and acidic stress. Values represent Mean± SD. Values less than 1 will be denoted as not expressed.

4.4 DISCUSSIONS

4.4.1 The *rv2661c* and *rv2660c* genomic region does not influence *M. tuberculosis* survival in PBS

The study by Loebel and colleagues (Loebel et al., 1933) investigated the effects of nutrient limitation that resulted in a gradual shutdown of respiration to minimal levels. The bacilli remained viable and resumed growth once returned to enriched medium (Gengenbacher and Kaufmann, 2012). The constant CFU counts of all tested strains in our study suggest that they are in a viable NRP state, although parameters such as antibiotic tolerance or metabolic status were not investigated. The unchanged colour of Methylene blue in these culture supports the hypothesis that cells had low respiratory rate (Loebel et al., 1933, Betts et al., 2002).

There were two other observations noted in these experiments. Firstly, initial incubation in PBS demonstrated a 2-fold increase in CFU counts at one week of incubation, reasoned probably from inadequate washings in PBS (probably needed more than 3 times) prior incubation might provide residual nutrient left in culture. Hence, the cells have doubled overnight, shown in the 1 week time point. Secondly, cell clumping was quite prominent, but well-dispersed when disturbed. However, cell clumping was thought as a survival mechanism during starvation where viable cells adhere to surrounding dying cells to obtain nutrients (Smeulders et al., 1999). Since there was no great variation in CFU counts between experiments, clumping was not thought to be significant.

Importantly, single or double deletions of *Rv2660c* and *Rv2661c*, that also involved partial deletions of *Rv2662* and *ncRv12659*, did not affect the ability of *M. tuberculosis* to survive. The observed phenotypic characteristics of these mutants during starvation were further supported by our expression data, with high ~9- fold upregulation *ncRv12659*. The difference in our value to the 50- fold in Houghton's study (Houghton et al., 2013) could be due to the different dynamic range of techniques employed in each RNA quantification, different *M. tuberculosis* strains, volume of culture used for extraction and data analysis. However, despite of the high transcriptional response of *ncRv12659* in starvation, the ncRNA has no biological importance for the pathogen to survive during long-term starvation.

Transcripts	TSS-RNA Sequencing ^a -(Houghton et al., 2013); ^b (Cortes et al., 2013)	Microarray (Betts et al., 2002)	qRT-PCR (This study)
<i>rv2660c</i>	X ^a	√	X
<i>rv2661c</i>	NA	√	X
<i>rv2662</i>	√ ^b	√	X
ncRv12659	√ ^a	NA	√

Table 4-2: Comparison of *rv2660c*, *rv2661c*, *rv2662* and ncRv12659 transcripts detected between published studies and the current study. √- expressed; X- Not expressed; NA- Not Analysed. ^a and ^b are references for RNA sequencing assay performed.

On the other hand, we have finally demonstrated that *rv2660c* and *rv2661c* were not upregulated during starvation which contradicted previous microarray data (Betts et al., 2002) (Table 4-2). It could be due to related biases introduced during cross hybridisation, where even a limited stretch of sequence complementarity was sufficient to promote hybridisation between two unrelated sequences. Hence, the probe would continue to generate a level of false signal masking the actual signal which could be lower or even undetectable (Draghici et al., 2006, Zhao et al., 2014). The overlapping 117bp of *rv2661c* and *rv2662* provided a window of chance for such event to occur. In addition, transcription of a non-coding RNA could contribute to the signal (Houghton et al., 2013). The lack of statistical difference between the experimental and no-RT samples across six biological replicates indicated that *rv2662* was not expressed. However, further optimisation of qRT-PCR protocol or more replicates are required to validate this finding, as *rv2662* was previously shown to be massively upregulated by 141-fold by RNA-Seq during starvation (Cortes et al., 2013). Our findings presented a similar profile to *rv2557* and *rv2558* that encode HPs were highly upregulated during starvation (Betts et al., 2002). The single and double deletion mutants did not affect the survival of *M. tuberculosis* under *in vitro* starvation and in replication in mouse model (Gordhan et al., 2006). SigF, an alternative RNA

polymerase sigma factor induced during starvation and other *in vitro* stress conditions, was also not required for *M. tuberculosis* survival during 28-days of starvation (Williams et al., 2007). These observations strengthen the notion that upregulation of a gene in certain conditions, does not mean that it is essential for survival in these conditions.

4.4.2 The *rv2661c* and *rv2660c* genomic region does not influence *M. tuberculosis* survival during hypoxia

Under this model, the exponential growth of *M. tuberculosis* began to adapt to gradual oxygen shift down, beginning from microaerophilic NRP Stage 1. This appears to be critical to hypoxic survival in anaerobic phase (NRP Stage 2) (Wayne and Hayes, 1996). Similar to nutrient starved bacilli, bacteria subjected to hypoxia display features such as persistence without multiplication, increased lipid content, reduced metabolism and increased tolerance to drugs, except for anaerobic bacilli that demonstrate metronidazole sensitivity (Wayne and Sramek, 1994, Wayne, 1996, Rodríguez et al., 2014).

The experiment was set up using time points similarly used by Voskuil and colleagues for microarray profiling of *M. tuberculosis* using Wayne's model (Voskuil et al., 2004). They had used day 4 to represent arrest in growth for *M. tuberculosis*, day 6 and 8 for microaerophilic phase, day 10 and 20 to represent mid-anaerobic NRP stage 2, while day 30 and 80 represented the late stage of NRP. Their OD measurement data could graphically show if our experiment exhibited a three-stage OD pattern similar to other published results (Voskuil et al., 2004, Wayne and Hayes, 1996). In this experiment, *M. tuberculosis* strains grew exponentially to day 7 and subsequently entered anaerobiosis as indicated by discolouration of Methylene blue at 21 days. It was apparent that the microaerophilic phase would be between 10-21 days, but the exact timing of this was not evident due to lack of time points. The NRP stage 1 phase should be presented by steady state increase of OD, prior to a plateau in OD measurements on entering NRP stage 2 (Wayne, 1996).

Formation of pellicles from 6 weeks was considered as a biofilm-like structure similarly observed by Orme and colleagues at 28 days incubation in the same model

(Woolhiser et al., 2007). Forming pellicles was suggested as one of the aerobe's strategies. An aerotactic response would result in migration to the air-liquid interface for increased accessibility to oxygen (Yamamoto et al., 2011). The presence of mycobacterial pili might have a role in surface attachment and cell adhesion that leads to biofilm formation (Saiyur Ramsugit, 2014). It was shown that mycobacterial pellicles had abundant virulence factors such as trehalose dimycolate (cord factor) (Ojha et al., 2008, Kulka et al., 2012) and were observed to form on the caseum of the granuloma, thus they do have implications for *M. tuberculosis* pathogenesis during infection (Canetti, 1955). However, little is known about the optimal environmental conditions for the formation of pellicles in mycobacteria.

The deletion of *rv2661c* and *rv2660c* did not influence survival of *M. tuberculosis* during hypoxia, despite the marked up-regulation of expression of these genes documented in several studies (Rustad et al., 2008, Voskuil et al., 2004). Some examples of genes showing similar profiles, are genes encoding Mycobactins or *M. tuberculosis* siderophores, *mbtB* and *mbtI*, that were highly induced during the NRP₁ stage. However, deletion of these genes did not influence loss of viability during the first 28 days of NRP (Schreuder and Parish, 2014). *Rv2745c* (*clgR*), encoding a transcriptional regulator that controls expression of *clp*, was induced under a variety of stresses including hypoxia but was not essential for mycobacterial survival during hypoxia (McGillivray et al., 2015).

Overall, our data suggest that the deletion of the locus encoding *rv2660c*, *rv2661c*, *rv2662* and ncRv12659 did not influence growth or survival of *M. tuberculosis* under microaerophilic and hypoxic conditions, nor, affect the pathogen's ability to produce pellicles.

4.4.3 Deletion and over-expressing *rv2661c* and *rv2660c* did not affect the ability of *M. tuberculosis* to survive during oxidative and nitrosative stress

To elucidate the initial role of *rv2661c* and *rv2660c* in both stress conditions, we have investigated the survival of deletion and over-expressing strains in H₂O₂ (oxidative stress agent) and a NO donor, 6-methoxy-5-pyrimidin-4-yl pyrrolidine-1-carbodithiate (NO donor o6g).

An initial attempt to determine the phenotype characteristic of the deletion strains was done when exposed to 10mM H₂O₂. The concentration of H₂O₂ was not lethal enough to cause any bactericidal effect to the strains and was proposed to exert DNA damage only (Voskuil et al., 2011). In contrast, another study using H37Rv strain demonstrated a drop of 2.55-Log₁₀ in CFU counts after 24 hours of exposure indicating the difference in experimental conditions such as the volume of culture used might result in different observations (Hu and Coates, 2009).

Exposure to 25mM H₂O₂ showed comparable bactericidal effects on all tested strains after 2 hours of exposure, suggesting that the deletion of genes did not impair *M. tuberculosis* survival under oxidative stress. This was supported by the over-expression studies. However, due to the data variability obtained for the over-expressing strains, more replicates are required to provide the precise estimate of the treatment effect on the survival of these strains (Biau et al., 2008). A similar observation was also identified during nitrosative stress.

There were few technical challenges encountered that might explain variations in the CFU counts. Firstly, growth characteristics of the studied strains and the nature of the redox stress experiments required a prolonged incubation. The induced stresses have caused a delay in mycobacterial growth, hence a minimum of two independent experiments were performed. The oxidative stress experiment took two months to complete with the deletion strains while over-expressing strains took an additional 1-2 weeks. The nitrosative experiment took 3- 3.5 months to complete as colonies took more than 1- 2 months to recover. We postulated the remaining NO donor present in a 10µL bacterial drop for CFU assay continued the bacteriostatic effect resulting in a further delay in recovery. It is usually the most dilute culture in which colonies appeared first. It was shown that effects from low to moderate concentrations of RNI resulted in more than three weeks of incubation for strain recovery (Firmani and Riley, 2002). Secondly, changes in temperature and humidity in C3 Facility may have affected bacterial recovery. It was suggested that changes in temperature affected the solubility of oxygen, as cold temperature would caused an increase in dissolved oxygen concentration (Averill and Eldredge, 2012). When cells are exposed to high extracellular oxygen concentrations, oxygen diffuses through the membranes and gains electrons from various redox enzymes to produce partially reduced oxygen

species, such as superoxide and H₂O₂ (Imlay, 2008, Imlay, 2013) inducing oxidative stress. The event would affect the performance of an NO donor as the half-life of NO is also dependent on oxygen tension (Ignarro, 1989). Hence, to address additional stress variables, most experiments were performed in another facility with well controlled temperature and humidity. Lastly, the fluctuating humidity of incubators resulted in occasional 'heavy' condensation of plates and bags. Changing relative humidity was shown to affect the morphological colony characteristics and cell elasticity (Nikiyan et al., 2010). An increased humidity could also exert a positive effect on water absorption leading to a formation of a water monolayer on bacterial cells (Peccia et al., 2001). Although there was no concrete evidence of the effects of high humidity to delay growth in this experiment, the changing physiological characteristics of the strains could contribute an additional stress that affected colony recovery.

In this study, the expression of the target genes was also investigated in two different final concentrations of H₂O₂ (5mM and 25mM) in supplemented 7Hg to induce oxidative stress in *M. tuberculosis* cells. The 5mM H₂O₂ was selected as it was shown to stimulate strongly transcriptional oxidative stress response genes (Voskuil et al., 2011). It overlapped with genes expressed in response to infection of activated macrophages (Schnappinger et al., 2003). Hence, the concentration is more likely to represent the ROI level encountered by *M. tuberculosis in vivo*. Microarray data from Schnappinger and colleagues (Schnappinger et al., 2003) have revealed induction of the target genes at 40 minutes which prompted this investigation. In this study, we found that at 5mM H₂O₂, only *rv2660c* and *ncRv12659* were expressed at a low level. Similarly, *rv2660c* and *rv2662* were also expressed in *M. tuberculosis* exposed at 25mM H₂O₂. However, a concentration of 25mM H₂O₂ might not exist during infection, and the relevance of the expression of these genes can be questioned. It was proposed that even lethal concentrations of H₂O₂ (50-100mM) could be present through accumulation of ROI from an oxidative burst effect from prolonged exposure of ROI at lower magnitude (Voskuil et al., 2011). It was shown that at lethal concentration of 50-100mM H₂O₂, there was a significant upregulation of some TRs such as *SigB* and *SigH*, genes responsible for iron- sulphur cluster repair and ROI damage, but none for DNA damage (Voskuil et al., 2011). We could not explain why the genes are induced at

higher ROI level. However, at this stage, we can only propose that expression of these genes was subtle and that this may not have caused any significant phenotypic effect at cellular level (as demonstrated in both deletion and over-expression studies).

4.4.4 Low transcriptional response of *rv2660c*, *rv2662* and *ncRv12659* in *M. tuberculosis* when exposed to acidic pH 5.3

Intraphagosomal pH might be one of the earliest environmental cues by which *M. tuberculosis* sets its survival strategy responses by reprogramming its translational processes (Rohde et al., 2007). The ability to resist and survive a range of acidic pH from pH 6.4 in resting macrophages, to acidic pH 4.5 upon IFN γ - activation (Schaible et al., 1998, MacMicking et al., 2003) promotes successful colonisation of *M. tuberculosis in vivo* (reviewed in (Ehrt and Schnappinger, 2009). This investigation was prompted to investigate if indeed, *rv2660c* was overexpressed in acid medium and to relate this to the recent findings from Yihao and colleagues. (Yihao et al., 2015). The challenges in carrying out this experiment was the lack of information on the actual culture conditions used in their study (Yihao et al., 2015). Hence, we designed our experiments using media employed by Piddington's group (Piddington et al., 2000) to extract RNA from *M. tuberculosis* grown in supplemented 7H9 adjusted to pH5.3 buffered with 100mM MES. The time point for exposure was selected based on a microarray study that has used similar medium pH to mimic intraphagosomal pH (Rohde et al., 2007).

We could only detect minimal relative expression of *rv2660c*, *rv2662* and *ncRv12659* during earlier acidic pH exposure. Due to data variations, the results should be considered preliminary and require more replicates. Similarly, the low response presented by these genes and ncRNA could not have any important role in protecting the pathogen in such conditions. Our experiment could also be improved by investigating expression at pH6.5 that represents a pH level within resting macrophages and to evaluate if the induction of *ncRv12659* is acid pH-dependent. However, the detected Rv2660c protein from culture supernatant in Yihao's study (Yihao et al., 2015) was questionable. Using a transmembrane Hidden Markov Model program (TMHMM Server, Version2.0) (Krogh et al., 2001, Sonnhammer et al., 1998) linked in Tuberculist (Lew et al., 2011), both HPs were predicted to lack

transmembrane helices. Another program, SignalP 4.1 server (Petersen et al., 2011) has predicted the absence of signal peptides in Rv2660c and Rv2661c suggesting a missing function as secretory proteins. Additional controls and confirmation of identified proteins by mass-spectrometry could further validate the predictions.

4.4.5 Macrophage infection

A series of macrophage infection experiments were performed to elucidate if any of these genes are involved during the early stage of infection. Resting/ Naïve macrophages were initially employed as these cells act as the first line of defence for rapid clearance of *M. tuberculosis* following IFN γ activation (Kaufmann, 2002). Hence, intracellular replication of mycobacterial strains in resting macrophages was initially investigated to mimic infection in a susceptible host.

4.4.5.1.1 Intracellular replication of double deletion strains of *rv2661c* and *rv2660c* in murine J774.1 cells

A high MOI of 10 (1: 10 CFU) was selected to infect cell lines with heavy bacterial loads to promote high uptake and initiate sufficient intracellular growth, however the wild-type strain failed to demonstrate a significant net increase in replication. Similar results were previously obtained in the laboratory (A.Sarbybaeva, 2015, Sanyi, 2016). There are many factors that can influence the replication of mycobacteria in macrophages, for example, extensive washings may result in detachment of infected monolayers. This experiment suggests that using an appropriate MOI for infection is critical. The high MOI used might have resulted in significant lysis of infected J774.1 macrophages (Butler et al., 2012, Iona et al., 2012) which would release intracellular bacilli into the medium. However, it is worth noting that infected monolayers were observed to be still attached to the bottom of the wells which implied that the cell lines remained viable throughout the experiment. Microscopic examination would provide a more reliable indication. In addition, the poor efficiency of uptake of 1-2% obtained for both strains suggested an altered J774.1 phenotype, probably a contribution of extended passaging of the cells (Hughes et al., 2007). However, since the double deletion strain exhibited a comparable lack of replication as wild-type

during J774.1 infection, it would be interesting to compare replication in another macrophage model of infection.

4.4.5.1.2 Establishing THP-1 macrophage infection model

THP-1 macrophages were chosen as a model as they resemble the biological properties of peripheral blood monocytes and human alveolar macrophages regarding bacterial uptake, survival and replication (Tsuchiya et al., 1980, Stokes and Doxsee, 1999, Theus et al., 2004). Hence, it would allow a much closer representation of the interaction of *M. tuberculosis* with human macrophages.

Several validation studies were performed in this study to ascertain the actual replication of intracellular bacilli and an adequate bacterial burden to enhance growth. The removal of unphagocytosed bacilli was necessary before analysing intracellular growth (Maurin and Raoult, 2001), thus the introduction of 200µg mL⁻¹ amikacin was probably efficient to inactivate remaining extracellular bacilli. The prolonged incubation of co-culture in a small concentration of amikacin might have resulted in intracellular amikacin activity developed through gradual uptake of the antibiotic by the eukaryotic cells (Tulkens, 1990, Maurin and Raoult, 2001). Hence, initial treatment with a higher concentration of Amikacin was an important step in our methodology.

Data from second validation experiment supported the notion that THP-1 macrophages were able to control mycobacterial net growth with low bacterial burden following infection with an MOI of 1-2. Similarly, as shown in the J774.1 macrophage experiment, a high MOI of 10 resulted in the massive decline of intracellular counts. In contrast to our findings, infection of macrophages derived from human monocytes (hMDMs) with *M. tuberculosis* at MOI 10 resulted in a robust increase in CFU counts while with MOI 1 demonstrated no significant proliferation of *M. tuberculosis* (Raffetseder et al., 2014). Another recent study also confirmed the significant increase of bacillary load in both hMDMs and THP-1 macrophages with MOI 10 after 24 hours infection (Mendoza-Coronel and Castanon-Arreola, 2016). The difference in our findings regarding the higher MOI may be explained in part by the difference in cell systems, the virulence of H37Rv strain and specific growth cell conditions. However, in our hands, treating infected macrophages with 200µg mL⁻¹

amikacin for 1 hour and using low MOI of 1-2 demonstrated a robust net bacterial proliferation in resting THP-1 cells.

4.4.5.1.3 Replication of double deletion strains of *rv2661c* and *rv2660c* during THP-1 macrophage infection

Using a lower bacterial load to infect THP-1 cells with the established protocol, a similar growth kinetics of both strains were observed in resting and IFN γ activated macrophages. The lack of robust replication of the wild-type strain in resting macrophages led us to question the efficiency of the strain to survive and persist in this system. A parallel analysis using other virulent *M. tuberculosis* strains such as clinical strains could provide a control and validate the former statement. The concentration of IFN γ was probably insufficient to promote antimicrobial activity in our infection system model, hence a higher concentration is proposed.

Another infection experiment with MOI 0.5 was carried out to closely mimic *in vivo* conditions where smaller numbers of *M. tuberculosis* usually establish an infection and allow an adequate viable population of macrophages to permit intracellular *M. tuberculosis* proliferation (Zhang et al., 1998). The transient attenuation of the mutant strain at 24 and 48 hours of infection in this experiment indicated that it is more sensitive to killing due to increased physiological stress and antimicrobial activities at these time points (Rohde et al., 2012). Unfortunately, in a repeated experiment, a technical issue was encountered that affected colony recovery at both time points. Only data at 72 hours and 7 days of infection were reproducible indicating that the double mutant strain was able to replicate in the extended infection period. As this result is considered preliminary, the previous results in J774.1 and THP-1 macrophage infection highlighted that the annotated genes and ncRv12659 have no important role to *M. tuberculosis* during macrophage infection.

4.4.6 Replication of double *rv2661c* and *rv2660c* mutant in mice

The murine infection data was only reliable at day 28 post-infection, however, the fact that replication of the $\Delta rv2661c:rv2660c$ strain was unaffected indicated that it was not essential for *M. tuberculosis* virulence during active TB infection. This finding was in line with Houghton's study where *rv2660c* was not detected during 31 days of murine infection (Houghton et al., 2013), a similar murine model used by Anderson and colleagues in the development of the H56 vaccine (Aagaard et al., 2011). In contrast, the latter group have detected consistent expression of *rv2660c* at 3 and 20 weeks of

infection (Aagaard et al., 2011). Another murine infection experiment would be required to obtain the full growth profile of the deletion strain *in vivo* and a parallel reassessment of *rv2660c* expression for confirmation of previous transcriptomics data. In addition, we have also established the absence of PDIMs in both deletion and wild-type strains, probably lost during serial passaging (Goren et al., 1974) and this lipid would have no further effect on replication of both strains *in vivo*.

4.5 CONCLUSIONS

The significant findings of this study are highlighted as follows:

- ✓ *rv2660c* and *rv2661c* which include *rv2662* and non-coding RNA, ncRv12659 were not required for survival of *M. tuberculosis* during adaptation to *in vitro* NRP, oxidative and nitrosative stresses
- ✓ In addition, these annotated genes and ncRv12659 are not required for *M. tuberculosis* intracellular survival during *in vitro* macrophage infection and murine infection
- ✓ Gene expression analysis revealed *rv2660c*, *rv2661c* and *rv2662* transcripts were not detected during starvation and were minimally induced during *in vitro* oxidative stress.
- ✓ ncRv12659 was highly upregulated only during starvation.

CHAPTER 5

Investigating the role of *rv1675c* (*cmr*) in
Mycobacterium tuberculosis
during *in vitro* stress conditions

CHAPTER 5 Investigating the role of *rv1657c* (*cmr*) in *Mycobacterium tuberculosis* during *in vitro* stress conditions

5.1 INTRODUCTION

Transcriptional regulators of the cyclic AMP receptor protein (CRP)/fumarate nitrate reduction regulator (FNR), CRP/FNR family are structurally related proteins consisting of approximately 230–250 amino acid residues and widely distributed in bacteria (Kolb et al., 1993). Typical transcription regulators have two conserved domains: a C-terminal DNA-binding domain with the Helix-turn-Helix (Gupta et al., 2016) motif which fits into the major groove of DNA and an N-terminal ligand-binding domain. The ligand-binding domain can recognise various small effector molecules such as 3',5'-cyclic adenosine monophosphate (cAMP), 2-oxoglutarate, NO and O₂ (Matsui et al., 2013), hence the specificity of ligand is usually determined experimentally.

The CRP, encoded by *rv3676*, (Stapleton et al., 2010, Kahramanoglou et al., 2014, Choudhary et al., 2014) and the cAMP macrophage regulator (Cmr), encoded by *rv1675c* (Smith et al., 2017, Ranganathan et al., 2015, Gazdik et al., 2009) are the best-characterised members of CRP/FNR family in *M. tuberculosis*. cAMP, an important signalling molecule, is generated from ATP by adenylate cyclases. Mycobacteria possess 17 adenylate cyclases and one of them Rv3676 is required for virulence (Agarwal et al., 2009). Unlike the *E. coli* homologue, CRP_{Mtb} showed a relatively weak interaction with cAMP, resulting in a small enhancement of DNA binding (Stapleton et al., 2010, Agarwal et al., 2009). CRP^{Mtb} regulates transcription of several genes involved in persistence and resuscitation of dormant mycobacteria, including *rpfA* (Rickman et al., 2005), *whiB1* (Stapleton et al., 2012, Agarwal et al., 2006) and *frdA* (Akhter et al., 2007).

The precise role of Cmr in virulence and regulation of gene expression remains unclear. Originally it was found that expression of four cAMP inducible genes *groEL2*, *rv1265*, *rv0532* and *mdh* (Gazdik et al., 2009) were dysregulated in the *cmr* deletion mutant. These genes were also induced during macrophage infection (Gazdik et al., 2009). However, the *cmr* deletion mutant had no growth defect during mouse bone marrow-derived macrophage infection (Smith et al., 2017). Interestingly, the *cmr*

deletion mutant strain had attenuated replication in lungs and spleens after 30 days of murine infection, but not in later stages after 70 days of infection (Smith et al., 2017). This attenuation could not be complemented by reintroduction of *the cmr* gene in the deletion mutant (Smith et al., 2017).

Several studies investigated Cmr binding to DNA. As mentioned above Cmr was required for regulation of expression of four genes. However, it had low DNA binding affinity to the DNA upstream regions of *groEL2*, *rv1265* and *mdh* as determined by electromobility shift assays (EMSA) (Gazdik et al., 2009). Moreover, Cmr did not require cAMP for activation of *groEL2* expression (Stapleton et al., 2012, Smith et al., 2017). A ChIP-Seq (chromatin immunoprecipitation- DNA sequencing) study by Ranganathan and colleagues has identified 368 Cmr binding sites across *M. bovis* BCG genome (Ranganathan et al., 2015). *M. tuberculosis* Cmr is 99% identical by 244 amino acid to Mb1702c in *M. bovis* BCG (Lew et al., 2011). The identified Cmr binding sites in *M. bovis* BCG were found clustered together within the chromosome suggesting cooperative binding of Cmr. They have also identified 26 closely spaced Cmr binding sites proximal to seven of the DosR regulon gene clusters. However, EMSA studies failed to demonstrate *in vitro* Cmr binding to individual sites and physical interactions between cAMP and Cmr (Ranganathan et al., 2015). A recent publication by Smith and colleagues (Smith et al., 2017) reported that Cmr did not bind cAMP as it lacks primary cAMP binding pocket (Reddy et al., 2009) and iron-sulphur clusters (Körner et al., 2003) found in other CRP family members. In fact, Cmr DNA binding was inhibited by nitrosation (treatment with a nitrosating agent, S-nitroglutathione) and to a lesser extent by oxidation of two conserved cysteine residues; Cys36 and Cys131 (Smith et al., 2017).

Recent studies have also established that Cmr regulates its own expression and binds to a 16-bp palindromic DNA sequence (Ranganathan et al., 2015) located between two *cmr* transcriptional start sites (TSS) (Smith et al., 2017) shown in Figure 5-1. Cmr binding in the *cmr-rv1676* intergenic region repressed transcription from the TSS₁ located 183bp upstream of *cmr* start codon, but Cmr binding activated transcription of divergent *rv1676* from the TSS₂ (located 82bp upstream of *cmr* start site) (Smith et al., 2017, El-Robh and Busby, 2002).

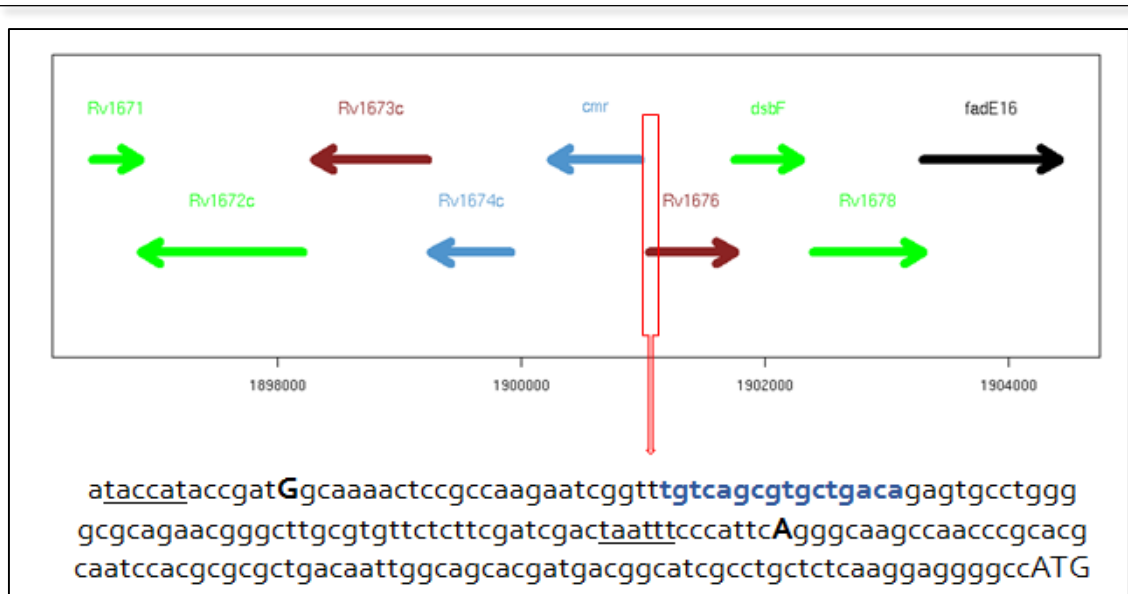


Figure 5-1: Genomic organisation of *rv1675c* (*cmr*) in *M. tuberculosis*. The DNA sequence covering the *cmr*-*rv1676* intergenic region shows the location of the two TSSs (bold upper case), potential -10 elements (underlined), Cmr- binding site (blue fonts) and Cmr start codon (ATG), adapted from (Smith et al., 2017).

Transcriptomic profiling of a *cmr* deletion mutant revealed significant upregulation of DosR regulon genes, suggesting that Cmr is a repressor of *dosR* transcription (Smith et al., 2017). The finding corroborated with the demonstration of Cmr binding to the upstream region of *dosR* (*rv3133c*) and *rv3134c* (Smith et al., 2017). The current working model for regulation of the DosR regulon in response to both nitrosative and oxidative stresses by Cmr is illustrated in Figure 5-2.

This chapter is focused on investigating the effect of *cmr* deletion and over-expression on *M. tuberculosis* survival under nitrosative and oxidative stresses. Further into the study, *cmr* expression under nitrosative stress was tested using quantitative RT-PCR. Finally, single nucleotide polymorphism (SNP) analysis of wild-type and Δ *cmr* mutant was performed to investigate possible reasons for the lack of complementation of Δ *cmr* phenotypes.

The following objectives of this study are as follows:

- To generate two *cmr* over-expression strains; *M. tuberculosis* pMV261::*cmr* and *M. tuberculosis* pMV261::*cmr*_{C2A} (*cmr* site-directed mutagenesis double mutant variant where both cysteine residues of Cmr were replaced with alanine)

- To investigate survival of deletion and over-expressing strains of *cmr* during oxidative and nitrosative stresses
- To analyse the expression of *cmr* in wild-type and complemented mutant strains during nitrosative stress

Part of the study was published in paper entitled "Cmr is a redox- responsive regulator of DosR that contributes to *M. tuberculosis* virulence" (Smith et al., 2017) attached in Appendix 10.

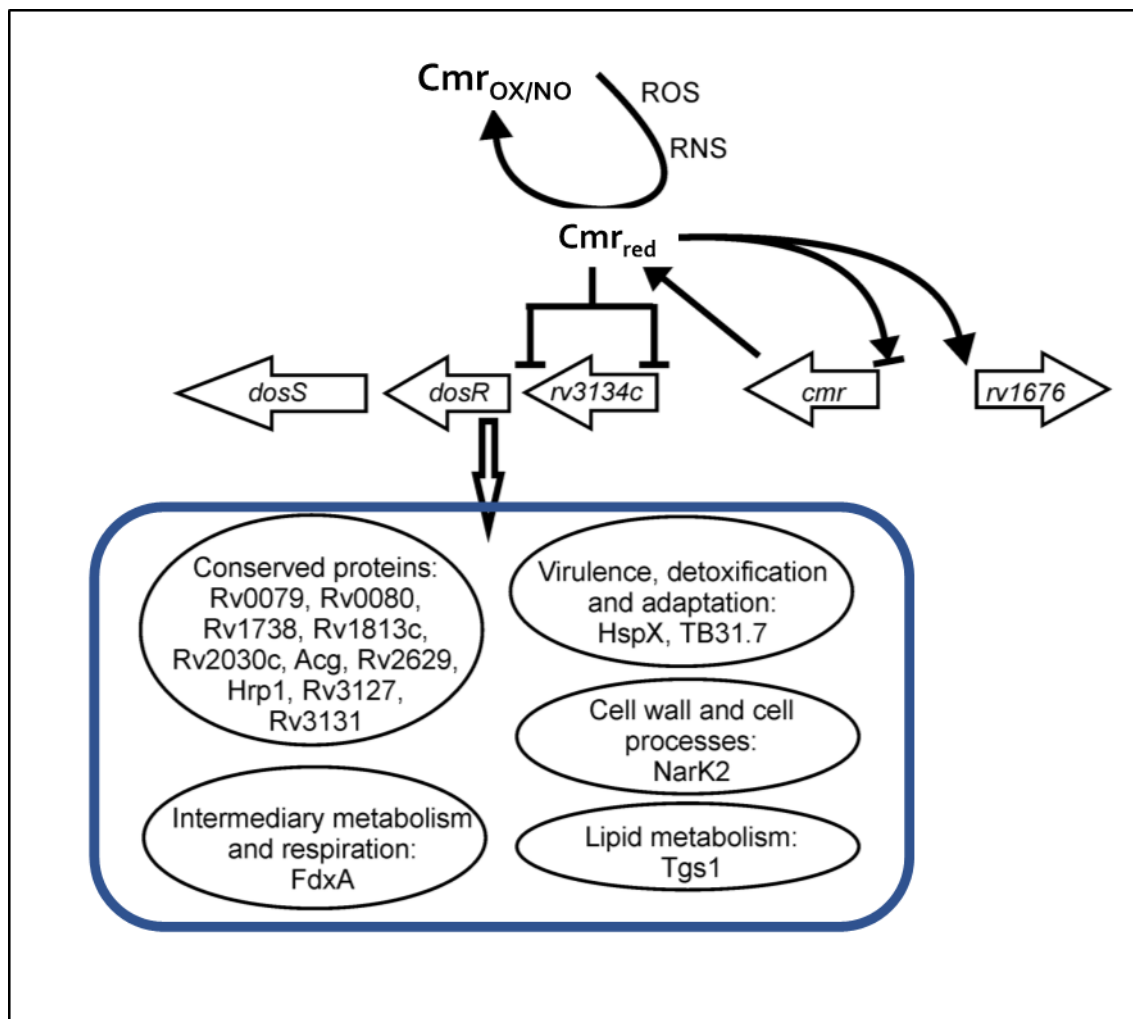


Figure 5-2: A proposed model for Cmr-mediated nitrosative and oxidative stress responses in regulation of the DosR regulon. Cmr in its reduced state (Cmr_{red}) will act as a dual regulator of its own expression, activates expression of divergent *rv1676* and also represses *DosR* expression. When exposed to nitrosative stress (and to a lesser extent with exposure to ROI) shown as $Cmr_{ox/NO}$, Cmr site-specific DNA-binding is inhibited. This results in de-repression of *dosR* and expression of a subset of *DosR* regulon (in the blue box). Adapted from (Smith et al., 2017).

5.2 MATERIALS AND METHODS

5.2.1 Bacterial strains

Details of strains used in this study are in Chapter 2. *M. tuberculosis* H37Rv wild-type strain, unmarked deletion strain of *cmr* (Δcmr) and *cmr* complemented strain (Δcmr_{Com}) were provided by Dr. Roger Buxton from NIMR and are described in a published paper (Smith et al., 2017).

5.2.2 Construction of over-expressing strains of *cmr* and *cmr* mutant variant

Plasmids pGS2103 (pET28a-*cmr*) and pGS2475 (pET28a-*cmr*_C36A/C131A) were provided by Dr. Laura Smith (University of Sheffield). The *cmr* variant encoding the double cysteine mutant was generated by site directed mutagenesis (SDM) using QuikChange II Site-Directed Mutagenesis Kit (Agilent Genomics). This resulted in the replacement of the both cysteine residues at position 36 and 131 with alanine (further abbreviated as C2A).

Amplification of the full coding sequence of *cmr* and *cmr*_{C2A} variant was performed using pGS2103 and pGS2475 as templates. DNA fragments were individually digested using *Bam*HI and *Eco*RI restriction enzymes and ligated to similarly digested pMV261 plasmid. As a result, the respective coding sequences were cloned downstream of the *hsp60* promoter to generate recombinant plasmids pMV261::*cmr* and pMV261::*cmr*_{C2A} respectively. These were constructed by Dr Sarah Glenn and Khalid Khan (UoL). The identity of the cloned genes was confirmed by sequencing. Plasmid maps of these constructs are shown in Appendix 4.

In this study, each recombinant plasmid (500ng) was then electroporated into *M. tuberculosis* H37Rv (exact background as used for the preparation of the Δcmr mutant), and transformants were selected on 7H10 agar containing 50 μ g mL⁻¹ Kanamycin to generate an empty plasmid control *Mtb* pMV261 and two *cmr* over-expressing strains *M. tuberculosis* pMV261::*cmr* and *M. tuberculosis* pMV261::*cmr*_{C2A} respectively. The identity of all strains was confirmed by colony PCR using pMV261 specific primers pMV261F and pMV261R. The PCR amplification cycling conditions used are described in Section 2.8.1 except with a higher annealing temperature of 55°C.

5.2.3 Combined cold and oxidative stress experiments

The cold shock exposure was performed prior to oxidative stress experiments.

Bacteria were grown to mid-exponential phase (OD_{580nm} of 0.5-0.7) in 250 mL Erlenmeyer flasks containing 50 mL of supplemented 7H9 broth. For each strain, 6 screw-capped tubes with 1.2 mL of culture were prepared. Three tubes were incubated at 4°C and the other three tubes - at 37°C without shaking for 16 hours. Survival patterns of each strain after cold shock were assessed by CFU counts. The pre-incubated cultures were treated with H_2O_2 (Acros Organics) to a final concentration of 25 mM for 4 hours followed by CFU count assays.

5.2.4 qRT-PCR

Details for RNA extraction and qRT-PCR are described in Chapter 2.

For confirmation of *cmr* expression in over-expressing strains, mid exponential phase (OD_{580} 0.5-0.7) cultures were used. To demonstrate the effect of nitrosative stress on expression of *cmr*, RNA was isolated from an early logarithmic phase (OD_{580nm} 0.15-0.2) of Δcmr , Δcmr_{com} and wild-type *M. tuberculosis* H37Rv cultures. For reverse transcription, 500 ng of total RNA was employed. qRT PCR was performed using gene specific primers: MYCO16s (for *16S*) and RT1675 (*cmr*). Primer sequences are in Appendix 2. Three technical replicates were performed for each experimental sample. Only samples with low genomic DNA contamination were analysed.

5.2.5 Whole genome sequencing

Genomic DNA of the wild-type strain and Δcmr was isolated as previously described in Chapter 2. Purified genomic DNA samples were sequenced using the Illumina HiSeq 2500 platform (Illumina, USA) at the GATC- Biotech (Constance, Germany). To generate high-quality data, a sliding window algorithm was applied to trim substring of low-quality read bases usually occurring at 3' end (Cox et al., 2010, Falgueras et al., 2010). The first and last base's quality scores that exceeded a specific threshold of 15 were removed. Sequencing data were collected in paired-end mode (from both ends of each fragment) with a read length of 125 bp. These short reads were aligned to the genome of *M. tuberculosis* H37Rv as a reference sequence (Genbank accession number NC_000962) using the Burrows-Wheeler Aligner Program (Li and Durbin, 2009) with default parameters for each sample. The depth of coverage (mean number of reads

covering each site over entire ~4.4MB genome) was 104.8X (*M. tuberculosis*) and 141.63X (Δcmr). The single nucleotide polymorphisms (SNP), insertions and deletions were identified using GATK's Unified Genotyper (McKenna et al., 2010, DePristo et al., 2011) and any false positive variants were filtered by GATK's Variant Filtration module. Detected variants were annotated in their gene context (such as amino acid and codon change and functional class of SNP) by snpEff (Cingolani, 2012). Synonymous mutations within coding sequence were not included in the final analysis which focused on mutations that were not likely to contribute difference in survival phenotype of both strains. This experiment contributed towards the publication shown in Appendix 10.

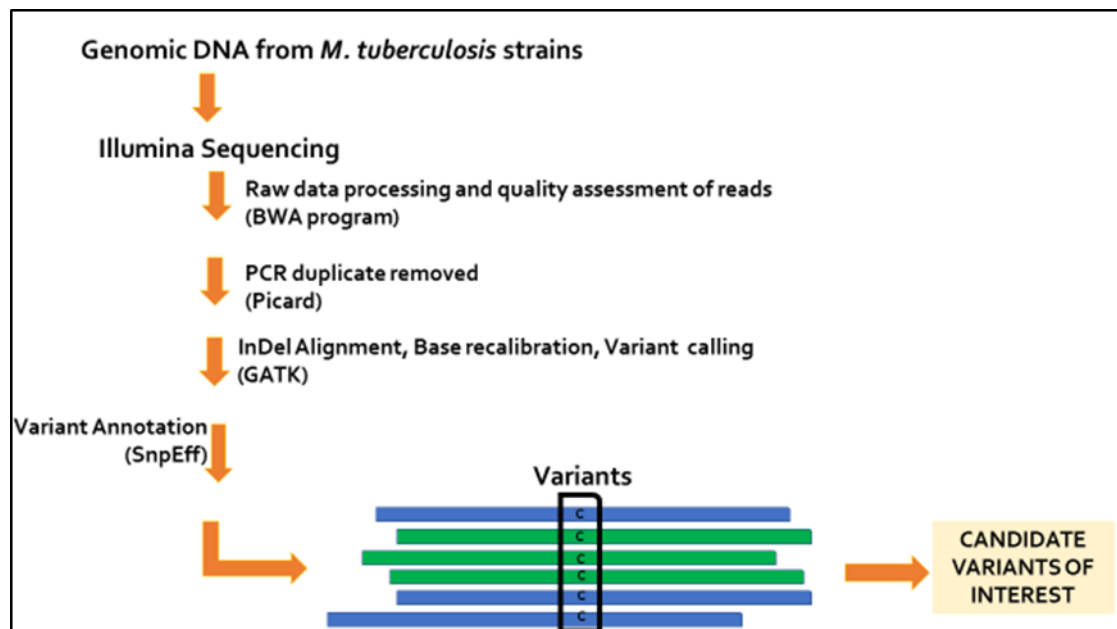


Figure 5-3: Whole genome sequencing (WGS) and workflow analysis. The Illumina platform was employed to sequence the ends of millions or billions of DNA fragments in parallel and performing read assembly for analysis. After sequencing and read mapping steps, PCR duplicates, realignment around Indels, base recalibration, Single nucleotide polymorphism (SNP) and variant calling including annotations are all WGS-specific computational analysis to extract variant information. Adapted from (Chaitankar et al., 2016).

5.3 RESULTS

5.3.1 Confirmation of the identity of the *cmr* over-expressing strains in *M. tuberculosis* H37Rv

Colony PCR of the control pMV261 strain of *M. tuberculosis* yielded a band of expected size (255bp; Lane 1) in Figure 5-4. Furthermore, colony PCR of *M. tuberculosis* pMV261::*cmr* and *M. tuberculosis* pMV261::*cmr*_{C2A} yielded similarly sized bands of the expected size (990bp; Lane 2 and Lane 3 respectively). The analysis confirmed the presence of the correct plasmids in respective strains.

The constitutive over-expression of *cmr* in respective strains was further assessed by qRT-PCR using *cmr* gene-specific primers. Assay performance information and melt curve analysis can be found in Appendices 6 and 7. All non- reverse transcribed control samples produced copy numbers less than 10% of the tests, indicative of low levels of gDNA contamination. Comparable levels of 16S rRNA expression were obtained for all tested strains ($p=0.8$) with a mean $(3.0 \pm 2.43) \times 10^8$ copies. The *cmr* copy numbers for each strain were normalised to 16S copy numbers to obtain relative expression (RE) values. The fold difference in expression was obtained by comparing RE value of each *cmr* over-expressing strain to the control strain as shown in Table 5-1.

Relative expression of *cmr* in empty plasmid strain was used as a baseline value. There was significant over-expression of *cmr* in *M. tuberculosis* pMV261::*cmr* with 620 ± 11 -fold and in *M. tuberculosis* pMV261::*cmr*_{C2A} with 471 ± 75 - fold higher expression relative to expression in the control strain. The qRT-PCR analysis further confirmed the constitutive over-expression of *cmr* and *cmr*_{C2A} in respective over-expressing *M. tuberculosis* strain.

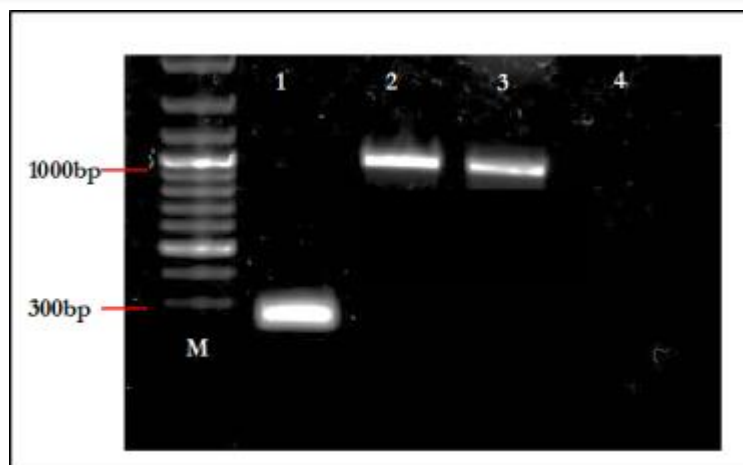


Figure 5-4: Gel analysis showing PCR products of control (empty plasmid) and *cmr* over-expressing strains using pMV261 primers. Lane 1: *M. tuberculosis* pMV261, Lane 2: *M. tuberculosis* pMV261::*cmr*, Lane 3: *M. tuberculosis* pMV261::*cmr*_{C2A}, Lane 4: Negative control, H₂O, M: GeneRuler™

Strains	cDNA copy numbers (n=3)		<i>Cmr</i> expression normalised to <i>16S</i> (n=3)	Fold difference
	<i>16s</i>	<i>cmr</i>		
<i>M. tuberculosis</i> pMV261	(5.23 ± 1.72) X 10 ⁸	1.04 X 10 ⁴ ± 8.93 X 10 ³	(1.92±1.23) X 10 ⁻⁵	-
<i>M. tuberculosis</i> pMV261:: <i>cmr</i>	(1.46 ± 2.15) X 10 ⁹	(5.88 ± 8.55) X 10 ⁶	0.012± 0.013	620± 11
<i>M. tuberculosis</i> pMV261:: <i>cmr</i> _{C2A}	1.33 X 10 ⁸ ± 8.69 X 10 ⁷	1.13 X 10 ⁶ ± 5.38 X 10 ⁵	0.009± 0.001	471± 75

Table 5-1: Relative expression of *cmr* in control and respective over-expressing strains. Relative expression values were obtained by normalising cDNA copy numbers to *16S*. Data represent mean ± standard deviation from three biological replicates.

5.3.2 *In vitro* growth of the *cmr* over-expressing strains

Colonies of the control strain grown on 7H10 agar with kanamycin were recovered after 3 weeks of incubation. However, the growth of both *cmr* and *cmr_{C2A}* over-expressing strains was delayed compared to the control strain. The delayed growth of over-expressing strains was also observed when grown in a supplemented 7H9 liquid medium. An image of the colonies grown on the same 7H10 plate at four weeks of incubation is shown in Figure 5-5. Over-expressing strains produced smaller colonies which could be seen in culture diluted to 1:1000 and 1:10000. However, there was no difference in colony morphology of these strains as surfaces were smooth and appeared flat. This experiment demonstrated that both over-expressing *cmr* and *cmr_{C2A}* slightly inhibited growth of *M. tuberculosis in vitro*.

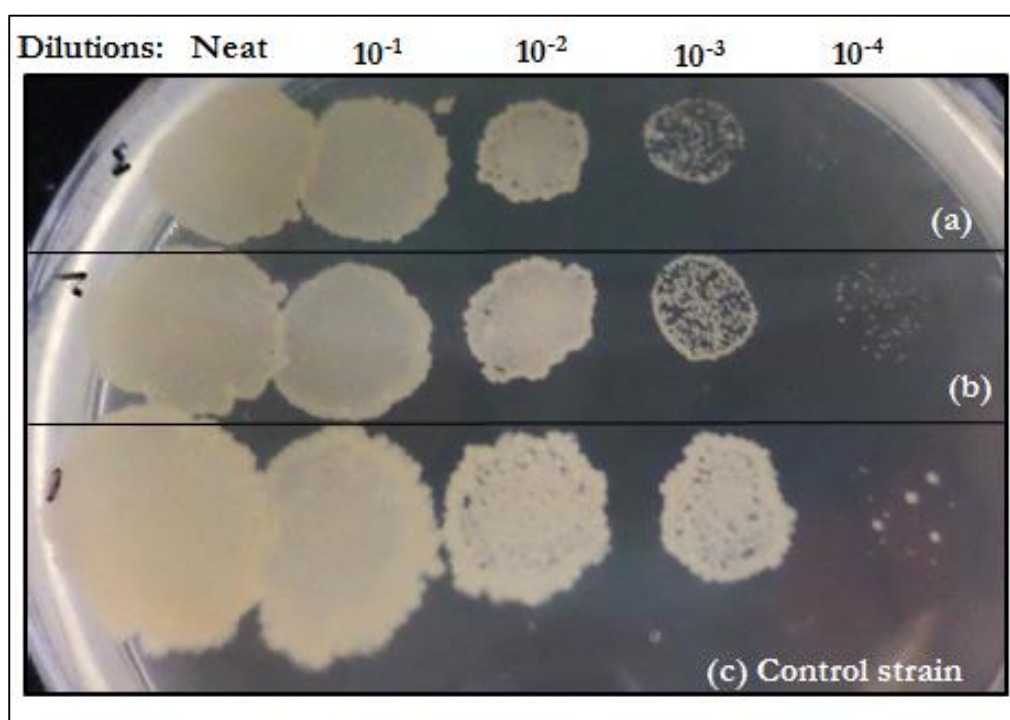


Figure 5-5: Colony morphology of over-expressing strain of *cmr* and its mutant variant in *M. tuberculosis*. Mycobacterial cultures: (a) *M. tuberculosis* pMV261::*cmr_{C2A}*, (b) *M. tuberculosis* pMV261::*cmr* and (c) Control (Empty plasmid) strains were ten-fold serially diluted and spotted for each dilution (from left to right; Neat, 1:10, 1:100, 1:1000 and 1:10000) on supplemented 7H10 with 50 µg mL⁻¹ Kanamycin. Image was taken after 4 weeks incubation.

5.3.3 Investigating the role of *cmr* in survival of *M. tuberculosis* in response to *in vitro* stress (Published in Smith et al., 2017)

5.3.3.1 Nitrosative stress

NO donor 6-methoxy-5-pyrimidin-4-yl pyrrolidine-1-carbodithiate was employed to induce nitrosative stress as detailed in Chapter 4. The MIC of each strain to the compound was determined. After 2 weeks of incubation, the MIC of wild-type and Δcmr were comparable ($1\text{-}2\mu\text{g mL}^{-1}$), however Δcmr_{Com} was more sensitive with a reduced MIC of $0.2\text{-}0.4\mu\text{g mL}^{-1}$. The difference in MIC provided initial evidence for potential dysregulation of *cmr* in this strain (Smith et al., 2017).

Exposure to $100\mu\text{M}$ NO donor for 4 hours did not signify any effect on the survival of wild-type ($133\pm 26.3\%$), Δcmr ($102.8\pm 18.5\%$) and Δcmr_{Com} ($65\pm 12.7\%$) strains. However, following a 20-hour exposure to the donor, there was a substantial decline of viable cells (Figure 5-6). Interestingly, Δcmr survived significantly better than the wild-type strain in both experiments (p values from both experiments; $p=0.02$ & $p=0.048$). The Δcmr also survived better than Δcmr_{Com} ($p<0.01$). The lack of complementation indicated hypersensitivity to NO and was further investigated by analysing the expression of *cmr*.

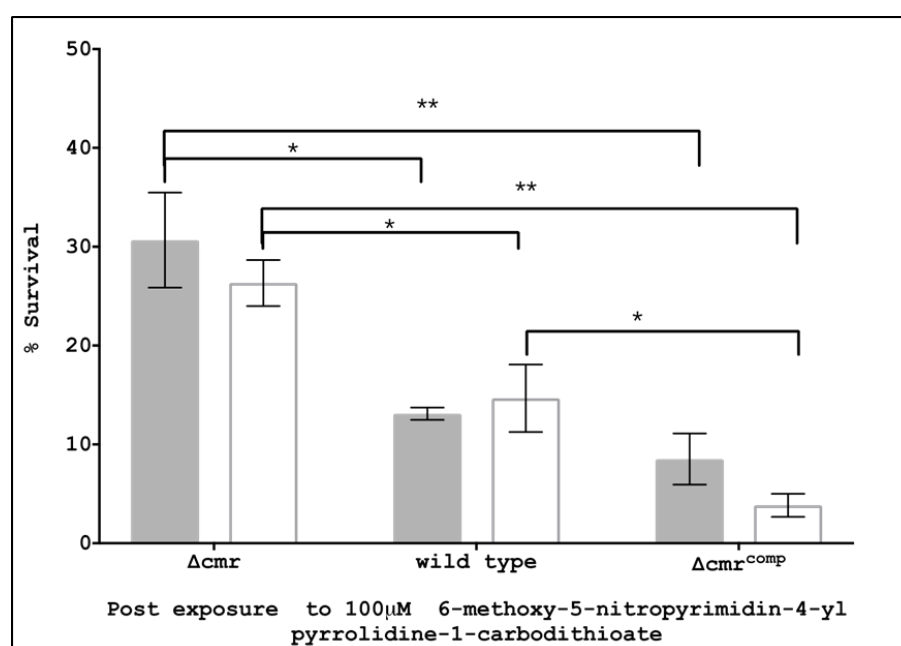


Figure 5-6: Effect of nitrosative stress on the survival of *cmr* mutant. Survival of mycobacterial strains grown in supplemented 7H₉ with 20 hours of exposure of a final

concentration of 100 μ M 6-methoxy-5-pyrimidin-4-yl pyrrolidine-1-carbodithiate. The results of two independent experiments (filled and unfilled bars) are shown. Data represent Mean % survival \pm SEM from three biological replicates. * $p < 0.05$, ** $p < 0.01$ analysed by t-test.

5.3.3.2 Expression of *cmr* in wild-type and *cmr* complemented mutant during growth and nitrosative stress

To further demonstrate if indeed *cmr* was dysregulated in the complemented strain, expression of *cmr* was analysed in Δcmr_{Com} using qRT-PCR and compared with expression in wild-type strain. As a control, *cmr* mutant was included, and the melt curve analysis demonstrated multiple melt peaks corresponding to non-specific amplification (Appendix 7, Figure 37) which was expected as the genomic region of *cmr* was deleted. As shown in Figure 5-7, during early exponential growth culture, expression of *cmr* was ~2.2- fold increased in Δcmr_{Com} relative to the wild-type strain (Smith et al., 2017). Exposure to 100 μ M NO donor for 40 minutes resulted in a minimal 1.5-fold change in *cmr* expression in Δcmr_{Com} [RE value: $(3.75 \pm 2.72) \times 10^{-4}$]. There was no significant difference in expression compared to untreated culture [RE value: $(2.51 \pm 2.91) \times 10^{-4}$] ($p = 0.43$). However, at this time point of nitrosative stress, *cmr* was not induced in wild-type strain. Therefore, the nitrosative stress had no significant effect on the expression of *cmr* in the Δcmr_{Com} strain compared with wild-type strain.

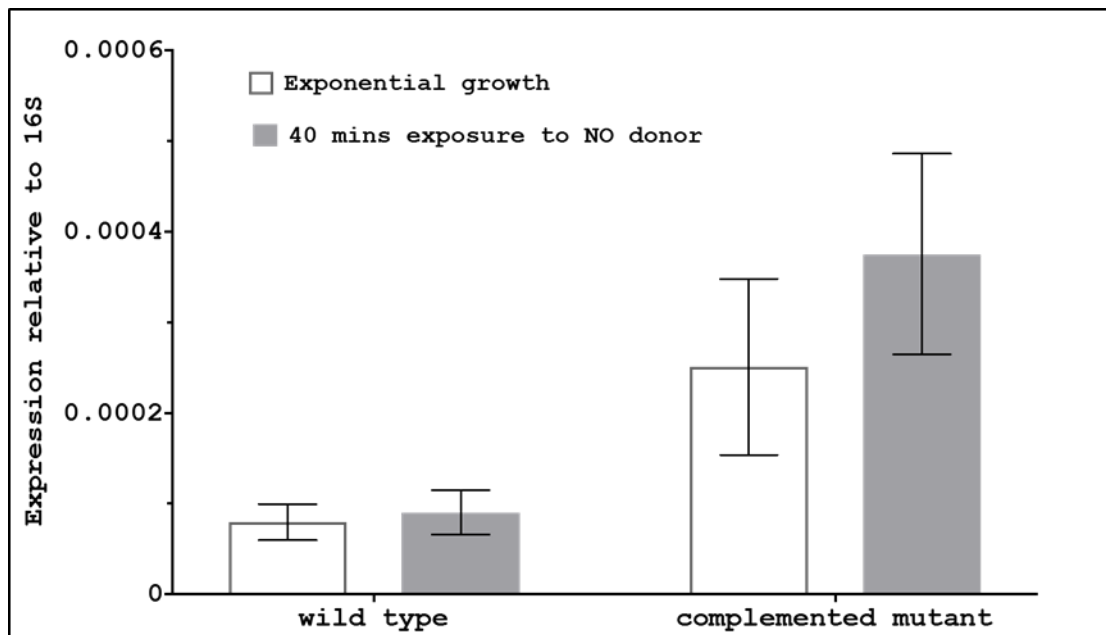


Figure 5-7: **Normalised expression of *cmr* during nitrosative stress.** Relative expression of *cmr* in both wild-type and *cmr* complemented mutant exposed to 100 μ M NO donor 6-methoxy-5-pyrimidin-4-yl pyrrolidine-1-carbodithiate for 40 minutes. Data represent mean \pm SEM from three independent experiments.

5.3.4 Oxidative Stress

Oxidation of Cmr had resulted in decreased DNA binding (Smith et al., 2017) suggesting that *cmr* could also have a potential role during oxidative stress. For these experiments, survival of both *cmr* mutant and over-expressing strains were investigated by exposure to 25mM H₂O₂.

Initial inocula of wild-type strain ($1.48 \times 10^8 \pm 3.6 \times 10^7$ CFU mL⁻¹) and Δcmr ($1.47 \times 10^8 \pm 5.51 \times 10^7$ CFU mL⁻¹) were exposed to H₂O₂ for 4 hours, resulting in a reduction of CFU counts by more than 90%. In the first experiment performed, Δcmr has instead exhibited a significant survival advantage compared to the wild-type strain after 4 (p<0.001) and 24 hours of exposure. At the later time point, no colonies of the wild-type strain were recovered. On repeating this experiment twice in December 2015, the Δcmr strain showed an opposite survival pattern, presenting a poor tendency to survive ($3.17 \pm 1.72\%$) with no statistical difference in survival compared to the wild-type strain ($8.38 \pm 5.22\%$, p=0.06). Further 20-hour exposure resulted in similar survival defect of Δcmr ($0.03 \pm 0.04\%$) compared to wild-type strain, $2.32 \pm 3.83\%$ (p=0.11), as

shown in Figure 5-8. The discrepancies in mutant phenotype were proposed to be due to the initial exposure of strains to the cold temperature of the laboratory prior oxidative stress experiment. However, the results obtained were variable and more experiments are required to conclude if *cmr* is required during oxidative stress.

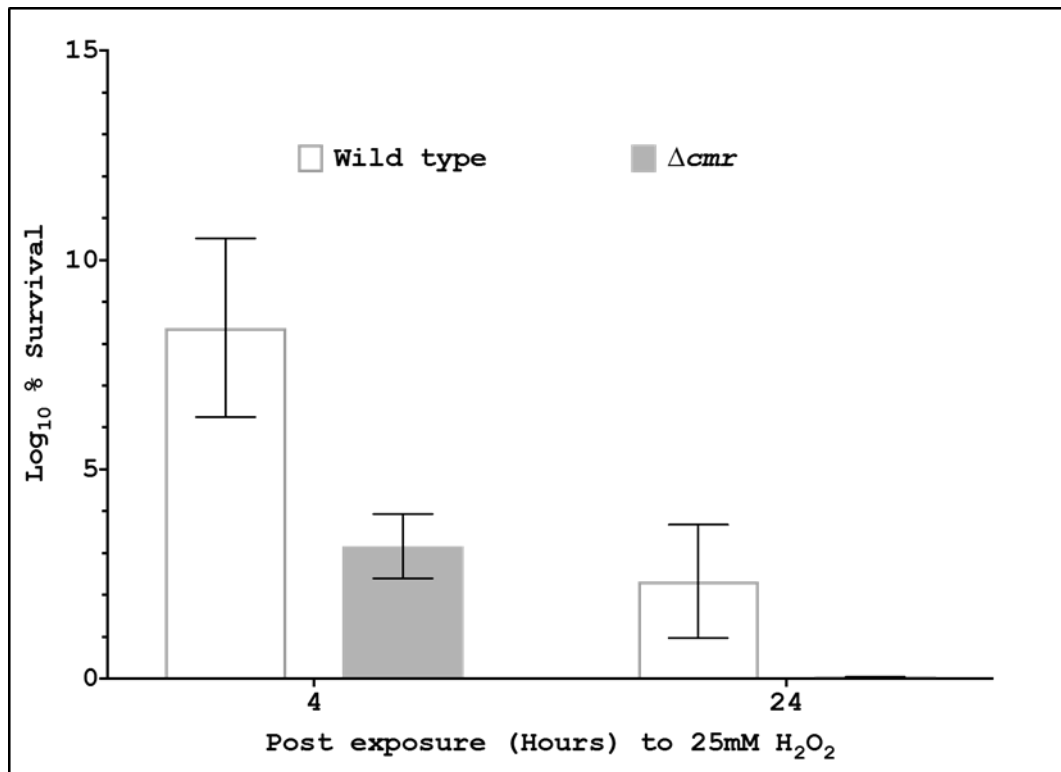


Figure 5-8: Effect of oxidative stress on the survival of *cmr* mutant. Both wild-type strain (unfilled bars) and *cmr* mutant (filled bar) were exposed to 25mM H₂O₂ for 4 and 24 hours. Data represent Mean % survival \pm SEM from two independent experiments performed in triplicates.

To investigate if cold temperature affected the sensitivity of tested strains to oxidative stress, the control and over-expressing strains were initially subjected to cold shock for 24 hours prior to oxidative stress. With an initial mean inoculum of $(3.01 \times 10^7 \pm 7.25 \times 10^6)$ CFU mL⁻¹, strains were incubated at both 4°C and 37°C (control culture). Based on two independent experiments, exposure to cold temperature for 24 hours did not affect the survival of the empty plasmid strain compared with over-expressing strains, as shown in Figure 5-9. To note, CFU counts of *M. tuberculosis* pMV261::*cmr* and *M. tuberculosis* pMV261::*cmr*_{C2A} were lower than the pre-cooled wild-type strain, and this was expected due to their delayed growth. Collectively,

these experiments demonstrated that exposure to cold temperature for 24 hours did not significantly affect the viability of the all tested strains.

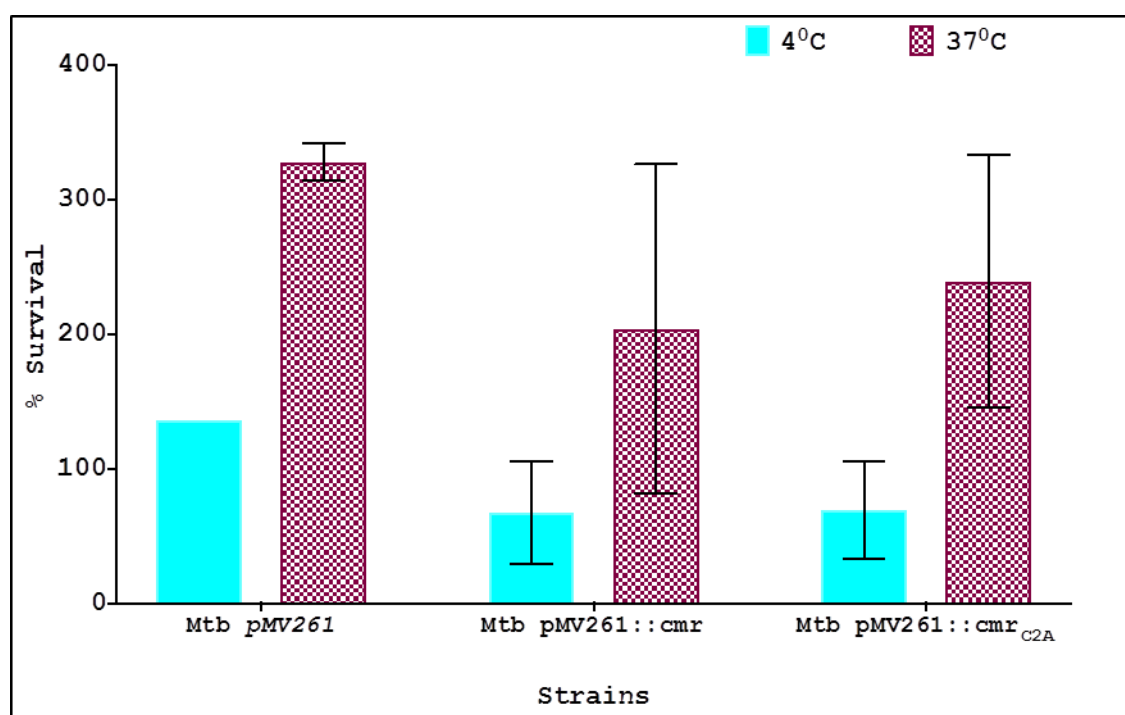


Figure 5-9: Effect of cold shock on the survival of *cmr* over-expressing strain. *M. tuberculosis* pMV261, *M. tuberculosis* pMV261::*cmr* and *M. tuberculosis* pMV261::*cmr*_{C2A} were exposed to cold stress at 4°C (blue bars) and also incubated at 37°C (red spotted bars) as control culture for 24 hours. Data represent mean \pm SEM from two independent experiments.

Next, the same pre-cooled strains were immediately treated with 25mM H₂O₂ and incubated for 4 hours. The observations from these experiments are as follows. Firstly, exposure to cold temperature did not increase the sensitivity of the control strain to oxidative stress ($p=0.29$), shown in Figure 5-10. Secondly, the viability of *cmr* over-expressing strain was comparable to the control strain (maintained at 37°C) with exposure to H₂O₂ ($p=0.63$) which further suggest *cmr* would have no protective role for the survival of *M. tuberculosis* when encountered to oxidative stress.

Interestingly, pre-cooling of *cmr* over-expressing strain prior to H₂O₂ exposure resulted in a significant survival advantage when compared to empty plasmid strain ($p=0.04$). This observation suggests that exposure to cold shock increases the survival tolerance of *cmr* over-expressing strain to H₂O₂ exposure.

In addition, *M. tuberculosis* pMV261:: *cmr*_{C2A} was included in this experiment to evaluate the effect of over-expressing an equivalent of a 'permanently reduced' form of *cmr* in the dual stress conditions. *M. tuberculosis* pMV261:: *cmr*_{C2A} demonstrated increased tolerance to H₂O₂ and survived better than the control plasmid strain (p=0.004). A similar tolerance pattern was also observed for the pre-cooled strain compared to *M. tuberculosis*:: pMV261 (p=0.002). These findings indicated that over-expressing *cmr*_{C2A} enhanced the survival of *M. tuberculosis* during oxidative stress and pre-exposure to cold temperature had no effect on its sensitivity to oxidative stress.

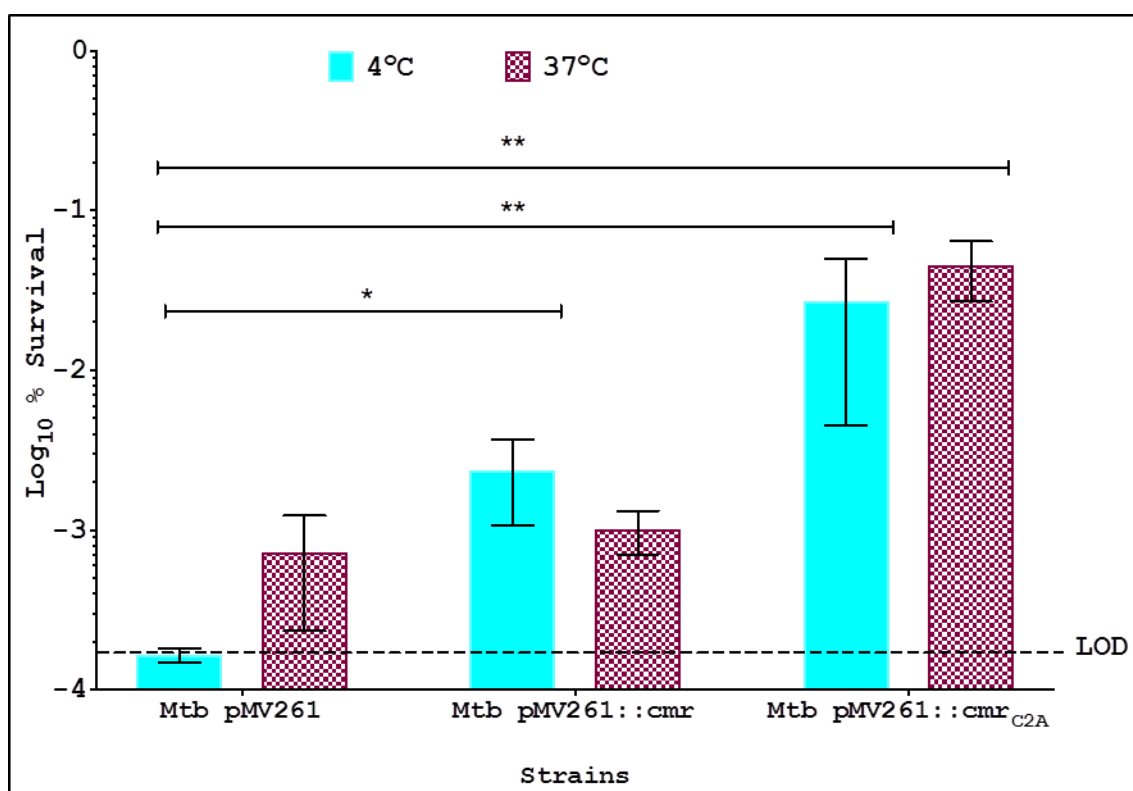


Figure 5-10: Effect of oxidative stress on the survival of pre-cooled *cmr* over-expressing strains. *M. tuberculosis* pMV261, *M. tuberculosis* pMV261::*cmr* and *M. tuberculosis* pMV261:: *cmr*_{C2A} were pre-cooled (incubated in 4°C, blue bars) and aliquoted as control (incubated in 37°C, red spotted bars) culture. After 24 hours of cold exposure, culture in supplemented 7Hg was treated with a final concentration of 25mM H₂O₂ and further incubated at 37°C for 4 hours. Data represent mean ±SEM from two independent experiment *p<0.05, **p<0.01 analysed by t-test. LOD denotes Limit of detection.

5-3-5 Whole genome sequencing of *M. tuberculosis* strains (Published in Smith et al., 2017)

To understand the lack of complementation in both murine infection and nitrosative stress experiments, WGS was performed to determine if there were any genomic variations in the wild-type and *cmr* mutant strain. In addition, the investigation was carried out to establish if the *cmr* mutant strain had SNPs that would impair its virulence.

Analysis of WGS revealed that both strains harboured only missense mutations relative to the reference *M. tuberculosis* H37Rv sequence (Genbank accession number NC_000962). The SNPs identified in the *cmr* mutant strain and H37Rv wild type used in this study compared with a reference H37Rv genome sequence are tabulated in Table 5-2. The parent strain had three SNPs resulting in E419K mutation of *PpsA* (*rv2931*), a component of phenolphthiocerol synthesis type 1 polyketide synthase involved in PDIM synthesis, R51G mutation of *ParD* (*rv1960*) antitoxin and T234I mutation of *rv2962* (uridine 5'-diphospho-glucuronosyltransferase). The corresponding genes are non-essential for growth *in vitro* (Griffin et al., 2011). Rv2931 is highly similar by 76.1% to *M. leprae* ML2357 (Tuberculist, 2017), however, has been shown to have five SNPs in *M. tuberculosis* strains (Lamichhane et al., 2003). The Rv1960 is part of toxin-antitoxin (TA) operon (*parDE1*) with Rv1959c, member of the ParDE family (Ramage et al., 2009) that has not been characterised yet (Tuberculist, 2017). Furthermore, *rv2962* was found to not be required in an aerosol model of murine infection (Hisert et al., 2004) and was proposed to be involved in the first glycosylation step of phenolphthiocerol which was not required for synthesis of PDIM (Kirksey et al., 2011).

There were four common gene deletions associated with transposases (*rv079*, *rv3184*, *rv3184* and *rv3326*) in both strains. The *rv079*, *rv3184* and *rv3184* genes encode putative transposases and were found to be deleted in some *M. tuberculosis* clinical isolates (Tsolaki et al., 2004). In addition to the intentional *cmr* deletion in the mutant, there were four SNPs in genes also known to be non-essential for growth *in vitro* (Griffin et al., 2011); *fadE6*: SNP resulting in P71L; *rv2323*: SNP, L202P; *rv3331*: SNP, P423T and *prpD*: SNP resulting in a R9P mutation. The latter gene, a possible methylcitrate dehydratase (Lew et al., 2011) has been noted to have a similar SNP in a

monoisolate clinical strain, *M. tuberculosis* BTBo4-172. These individual SNPs would unlikely to have any detrimental effect on Δcmr strain.

Another identified SNP in Δcmr is in *rv2984* (*ppk1*, ATP-polyphosphate phosphotransferase) which was found to be essential for growth *in vitro* in *M. smegmatis* (Sureka et al., 2007) but not in *M. tuberculosis* (Singh et al., 2013). A mutant of *ppk1* in *M. tuberculosis* also exhibited growth attenuation during macrophage and was transiently attenuated after 40 days infection in guinea pigs (Singh et al., 2013). Although it is implicated in virulence similarly to *cmr* (Singh et al., 2013, Smith et al., 2017), it is also unlikely that the SNP in *rv2984* contributed to the survival advantage of Δcmr in the earlier nitrosative stress experiment. Hence, the WGS results demonstrated that none of this particular polymorphisms could account for the inability to complement *cmr* mutant phenotype.

Strain	Gene	Comment	Reference
Mutant	<i>fadE6</i> , <i>rv0271</i>	SNP: P7L, the first residue in the domain acyl-CoA-dehydrogenase domain; nonessential for growth; pseudogene in <i>M. leprae</i>	(Lew et al., 2011, Griffin et al., 2011)
Mutant	<i>rv0796</i>	Deleted (14 bp remaining); transposase; deleted in clinical isolates	(Lamichhane et al., 2003)
Mutant	<i>rv1130</i> , <i>prpD</i>	SNP: R9P; the same SNP is found in <i>M. tuberculosis</i> BTB04-172 (monoisolate); R9H in <i>M. tuberculosis</i> TKK-01-0058 Erdman <i>prpDC</i> mutant is unable to grow on propionate; growth is severely impaired in non-activated murine bone marrow-derived macrophages; growth and persistence in the lung and spleen is comparable to wild-type; absent in <i>M. leprae</i>	(Lew et al., 2011, Munoz-Elias et al., 2006, Smith et al., 2017)
Mutant	<i>rv1675c</i> , <i>cmr</i>	Deleted (12 bp remaining)	(Smith et al., 2017)
Parent	<i>rv1960</i> , <i>parD1</i>	SNP: R51G; ParD antitoxin; nonessential for growth; absent in <i>M. leprae</i> ; SNPs were found in <i>M. tuberculosis</i> strains: M1V; A78P; G82A	(Kapopoulou et al., 2011, Lew et al., 2011, Smith et al., 2017)
Mutant	<i>rv2323</i> , <i>dhaH</i>	SNP: L202P; multiple SNPs in <i>M. tuberculosis</i> strains, R30H; V72I, A120T, H201Y, T213A; S222N; non-essential amidinotransferase; pseudogene in <i>M. leprae</i>	(Lew et al., 2011, Smith et al., 2017, Kapopoulou et al., 2011)
Parent	<i>rv2931</i> , <i>ppsA</i>	SNP: E419K; Phenolphthiocerol synthesis type-I polyketide synthase; nonessential for growth; present in <i>M. leprae</i> ; multiple SNPs in <i>M. tuberculosis</i> strains: G549S, A803T, V862I, R877H, H955P	(Lew et al., 2011, Lamichhane et al., 2003)
Parent	<i>rv2962</i>	SNP: T234I; other SNP in database H233Q; in <i>M. leprae</i> T234Q; non-essential uridine 5'-diphospho-glucuronosyltransferase	(Lew et al., 2011, Kapopoulou et al., 2011)

Mutant	<i>rv2984, ppk1</i>	SNP: Q476R in phospholipase domain; essential for <i>in vitro</i> growth; impaired stress survival; down-regulation results in impaired survival in macrophages	(Lew et al., 2011, Singh et al., 2013, Kapopoulou et al., 2011)
Mutant	<i>rv3184</i>	Deleted (12 bp remaining); transposase; deleted in clinical isolates	(Lew et al., 2011, Tsolaki et al., 2004, Kapopoulou et al., 2011)
Mutant	<i>rv3185</i>	Deleted (0 bp remaining); transposase; deleted in clinical isolates	(Lew et al., 2011, Tsolaki et al., 2004, Kapopoulou et al., 2011)
Mutant	<i>rv3326</i>	Deleted (8 bp remaining); transposase	(Lew et al., 2011)
Mutant	<i>rv3331, sugI</i>	SNP: P423T; other SNP in database P423L (most strains); non-essential sugar transporter; pseudogene in <i>M. leprae</i>	(Lew et al., 2011, Kapopoulou et al., 2011)

Table 5-2: Single nucleotide polymorphisms (SNP) identified in the *cmr* mutant strain and wild type H37Rv used in this study, compared with an *M. tuberculosis* H37Rv reference sequence (Genbank NC_000962) (Smith et al., 2017)

5.4 DISCUSSIONS

5.4.1 Cmr plays a significant role in the survival of *M. tuberculosis* during nitrosative stress

The impairment of Cmr binding from nitrosation of the two cysteine residues implicates that nitrosative stress affects Cmr regulation. The *cmr* mutant displayed a significant enhancement in survival compared to wild-type indicating a significant role of Cmr in protecting the pathogen during nitrosative stress. A similar increased survival to RNI was observed in an *M. tuberculosis* serine/threonine kinase *pknH* deletion strain, where it exhibited a 2-fold increase in survival compared with wild-type when exposed to acidified nitrite (Papavinasundaram et al., 2005). The *pknH* mutant generated higher bacterial load in lungs of infected mice, that suggested further that *M. tuberculosis* used the PknH kinase-mediated signalling mechanism as an indirect or direct approach to regulate growth *in vivo* as part of a survival strategy (Papavinasundaram et al., 2005). The similar survival pattern illustrates the complexity of regulatory pathways involved during nitrosative stress.

It is also possible that the increased survival of Δcmr could be an indirect consequence of derepression of the DosR regulon, which potentially acts as a compensatory mechanism to sense and respond to redox signals. The upregulation of a subset of the DosR regulon, genes such as *dosR*, *rv3131c*, *rv3134c*, *rv2623*, *tgs1*, *fdx4* and *hspX* in the *cmr* mutant strain is similar to a particularly virulent of *M. tuberculosis* lineage, W/Beijing (Reed et al., 2007, European Concerted Action on New Generation Genetic Markers and Techniques for the Epidemiology and Control of Tuberculosis, 2006). The global success of W/Beijing strains is associated with its enhanced pathogenicity, transmission, multidrug resistance traits and underlying over-expression of DosR regulon in standard growth conditions *in vitro* (Reed et al., 2007). In comparison, non-Beijing strains, such as those in Euro-American or Indo-Oceanic lineages (Fallow et al., 2010), *dosR* was minimally induced during *in vitro* growth conditions. In the laboratory strain of *M. tuberculosis* H37Rv (a member of the Euro-American *M. tuberculosis* lineage), DosR regulon genes are only induced when the strain is exposed *in vitro* to hypoxia, NO or carbon monoxide (Saini et al., 2004, Voskuil et al., 2003, Shiloh et al.,

2008). The over-expression of *dosR* in W/Beijing strains prior to encountering signalling molecules such as O₂ or NO were suggested to provide an advantage survival strategy to pre-condition the strain before facing host's immune defence mechanism (Fallow et al., 2010). This strategy was proposed in particular to prepare the pathogen before macrophage entry or during macrophage activation where lethal amounts of NO are produced (Fallow et al., 2010). This proposed advantage of W/Beijing strains of infection 'preparedness' may hold for Δcmr , since it shows enhanced survival to nitrosative stress. In addition, the downstream genes of *cmr* which are *rv1671* and *rv1672-rv1674c* (Region of Difference 150) were found to be deleted in six strains from East Asia clade of W/Beijing strains suggesting that these genes could modulate expression of *cmr* resulting in over-expression of DosR regulon (Tsolaki et al., 2004).

5.4.2 The lack of complementation was not caused by SNPs in either wild-type or *cmr* mutant strain.

The inability to complement the mutant phenotype in nitrosative stress (this study) and murine infection (Smith et al., 2017) was further addressed in this study. The potential polar effect on downstream genes *rv1674c-rv1672c* due to the *cmr* deletion was excluded, as microarray studies demonstrated that expression of these genes was unaffected in the mutant strain (Smith et al., 2017). The Δcmr_{com} however, had an increased sensitivity to the NO donor which explained its inability to survive compared to the two other tested strains. Furthermore, the slightly increased *cmr* expression in Δcmr_{com} during growth, and at 40 minutes exposure to the NO donor, relative to the wild-type strain further implicates dysregulation of Cmr. The findings in this experiment gave an initial indication that a precise amount of Cmr is required and that this has to be tightly controlled to ensure the survival of *M. tuberculosis* during nitrosative stress.

WGS has been shown to provide a rapid and comprehensive view of the genotype of *M. tuberculosis* for detection of genes that are associated with virulence. It further contributes to the understanding of evolutionary relationships and also defines transmission between individuals to investigate outbreaks with the combination of epidemiological data (Walker et al., 2013). In addition, WGS was shown to accurately

predict the drug susceptibility phenotype of an isolate within a clinically relevant time frame, as compared to traditional antibiotic susceptibility testing (Witney et al., 2016). Sequencing of the genome of Δcmr and the wild-type strain was employed in this study to detect polymorphisms that could have affected survival phenotype. The cmr_{com} strain was not included as it was earlier shown to be dysregulated. A similar strategy was also employed to investigate divergent growth phenotypes exhibited by Rv1248c, *hoas* (a thiamin diphosphate (ThDP)-dependent enzyme that functions in the TCA cycle) transposon and deletion mutant strains by WGS (Maksymiuk et al., 2015).

The majority of SNPs in the Δcmr strain were found in putative transposases for insertional sequence IS6110. IS6110 is a repetitive mobile genetic DNA element specific for *M. tuberculosis* complex strains that consists of 1358bp with 30bp inverted repeat ends which encode two open reading frames *orfA* and *orfB*. Production of functional transposase (to ensure their mobility in the genome) requires ribosomal frameshift between these two open reading frames (Thierry et al., 1990, Millán-Lou et al., 2013, Siguier et al., 2014). Based on the variable copy numbers and various genomic locations of IS6110 in the *M. tuberculosis* genome, a point mutation in the stated transposases would not have caused a deleterious effect on the mutant strain.

In silico analysis of individual genes with observed SNPs revealed that they would not have a direct cause for the increased resistance of the mutant to nitrosative stress. For example, the *ppk1* mutant in *M. tuberculosis* only demonstrated marginal growth *in vitro* with a difference of less than 0.5-Log₁₀ difference in CFU counts. It was also not required for oxidative, nitrosative (in acidified NANO₂ at 3 days) and acidic stress (Singh et al., 2013). The effect of this single amino acid change would be substantially less deleterious than the effect of gene deletions or insertions (Tsolaki et al., 2004). Ultimately, to be certain it will have to be experimentally confirmed by deletion studies using similar experimental stress conditions. In addition, it is possible that interactions between, or in concert with, each polymorphic gene could cause a phenotypic effect change (Stucki and Gagneux, 2013). However, this is beyond the capacity of the study to investigate these assumptions.

Hence, sequencing the genome of Δcmr did not reveal potential explanations for its phenotype. This strongly supports the notion that it was an imbalance of *cmr*

expression that modulated the Cmr regulation process, and that the observed mutant phenotypes resulted from the *cmr* deletion.

5.4.3 Phenotypic characterisation of *cmr* and *cmr* mutant variant (*cmr_{C2A}*) over-expressing strains in *M. tuberculosis*

In this study, we have also investigated the effects of over-expressing *cmr* to growth and survival of *M. tuberculosis* during oxidative stress. Initial *cmr* deletion studies in *M. tuberculosis* have confirmed that *cmr* is not essential for growth *in vitro* as mutation did not affect growth in Dubos medium (Smith et al., 2017) and minimal Sauton's medium (personal communication, Dr Sarah Glenn). However, the constitutive over-expression of *cmr* and its mutant variant, *cmr_{C2A}* in *M. tuberculosis* may have caused transcriptional dysregulation leading to delayed growth on standard laboratory medium.

It was earlier established in our study that over-expression of *cmr* did not affect viability of *M. tuberculosis* under oxidative stress. However, the enhanced survival of over-expressing strain of *cmr_{C2A}* during oxidative stress despite pre-exposure to cold temperature, further supports the view that Cmr regulation is a complex process. Regulation of Cmr might be further complicated by its capacity to respond oxidation and nitrosation of the two cysteine residues (Smith et al., 2017). The phenomenon could be similar to the redox activation of *E. coli* OxyR, a LysR-Type transcriptional regulator. It occurs via formation of an intramolecular disulphide bond between two conserved cysteine residues (Cys 199 and Cys 208) (Zheng et al., 1998, Lee et al., 2004). Kim and colleagues have shown that a single cysteine in OxyR can yield some transcriptionally active forms that have a distinct structure and which generated a different DNA binding affinity and cooperativity of response. These findings reflected the ability of OxyR to sense multiple redox signals and process individual signals into distinct and graded transcriptional responses (Kim et al., 2002). Hence the proposed functional capability of OxyR could be applicable to *cmr* as it is also a redox sensor that alters its binding affinity upon oxidative and nitrosative stress. Our study has also demonstrated that the vital fine tuning of *cmr* expression level was required to ensure survival fitness in the wake of changing environmental signals.

The possible role of Cmr during cold stress could be further explored with more replicates. Successful TB transmission (between expulsion from an infected patient and inhalation by a new host) results from a multitude of determinants (Jones-López et al., 2013). One relevant environmental stress which *M. tuberculosis* will experience on aerolisation and to which it will respond is cold stress (Manganelli et al., 1999). The effect of cold stress on the expression of genes or even sRNAs has not been extensively studied (Manganelli et al., 1999, Shires and Steyn, 2001). However, the fact that some of these genes or sRNAs was shown to be highly induced indicated that they are essential during *M. tuberculosis* life cycle. Sigma factors are known as the general stress responders, reviewed in (Sachdeva et al., 2010), where changes in σ factors in response to different stresses can shift the pathogen's expression profile. Cold temperature induces expression of *sigB*, *sigH*, and *sigI* while repressing transcription of *sigC*, *sigE*, *sigG* and *sigM* (Manganelli et al., 1999). σ^I was the most highly induced with a 3-fold increase during 2h of mild cold shock exposure (Manganelli et al., 1999). A major cold-shock inducible gene in *M. smegmatis*, *hlp*, a DNA histone-like gene was shown to be 5.7-fold increased in expression after temperature shift to 10°C (Shires and Steyn, 2001). Further experiments could be carried out to investigate the effects of cold temperature on *cmr* such as replicating similar experimental conditions with Δcmr or analysing the transcriptional response of known cold-responsive genes in wild-type, mutant or over-expressing strain.

In addition, our findings have also implied that cold temperature has no significant effect on the survival of plasmid control strain compared with *cmr* over-expressing strains, prior to oxidative stress. Hence, the importance of controlling or minimising other stresses that might affect survival of *M. tuberculosis* strains when performing a single *in vitro* stress experiments should be a consideration of future experiments. As a consequence, results could be misinterpreted, but coincidentally it has also revealed a possible stress determinants for Cmr regulation.

5-5 CONCLUSIONS

The specific findings of this study are as follows:

- ✓ Cmr has no significant role for survival of *M. tuberculosis* as the mutant survives better and the over-expressing strain was hypersensitive to NO. This is a negative correlation.
- ✓ Cmr has no protective role in the survival of *M. tuberculosis* during oxidative stress. Data from both *cmr* deletion and over-expressing strains were variable and more replicates could confirm these observations.
- ✓ Over-expressing *cmr* in *M. tuberculosis* caused delayed growth in standard laboratory medium.
- ✓ Over-expressing *cmr* enhanced the survival of *M. tuberculosis* as it preconditioned the pathogen during cold stress to further resist the assaults of oxidative stress.
- ✓ Survival fitness of *M. tuberculosis* depends on the fine tuning of *cmr* expression. This was based on observations of the study as follows
 - Over-expression of *cmr* failed to complement the mutant phenotype by exhibiting significant survival defect compared to the wild-type strain. The complemented strain was hypersensitive to the NO donor and exhibited enhanced *cmr* expression level compared to wild-type strain
 - Over-expression of *cmr* double mutant (*cmr_{C2A}*) variant resulted in a significant survival advantage during oxidative stress despite pre-exposure to cold temperature.

CHAPTER 6
Final conclusions
and
future perspectives

CHAPTER 6 Final conclusions and future perspectives

The success of *M. tuberculosis* as a highly adaptable human pathogen relies upon its ability to switch to dormancy and establish an infection, despite the assaults of the host's immune system and a hostile living microenvironment. The survival strategies employed by the pathogen depend on transcriptional reprogramming, metabolic alteration and development of phenotypic resistance to antimicrobial agents. Dormant mycobacteria are of particular interest, since they are believed to be associated with latent tuberculosis infection and persisting infections. However, the precise pathways and genes involved in the development of dormancy remained poorly understood.

The first global transcriptomic profiling of *M. tuberculosis* back in 2002 was considered as major breakthrough that provided knowledge on the regulatory pathways and physiological characteristics of NRP cells, in particular starved cells (Betts et al., 2002). *Rv2660c*, *rv2661c* and *rv2662*, all encoding hypothetical proteins with unknown function, were among the genes significantly upregulated in the starved cells (e.g. ~280-fold up-regulation of *rv2660c*). This significant upregulation stimulated significant interest of scientific community and even resulted in introduction of the 'latency' gene concept (Govender et al., 2010, Aagaard et al., 2011, Yihao et al., 2015). Several studies reported T-cell responses to Rv2660c peptides in samples from latently infected patients (Govender et al., 2010, He et al., 2015) and a new H56 vaccine, which includes Rv2660c showed a robust boosting effect in a cynomolgus macaque model of latent infection (Lin et al., 2012). It has been considered as a candidate post-TB exposure vaccine and progressed to Phase II clinical trial. However, a few *M. tuberculosis* proteome studies involving nutrient starvation (Albrethsen et al., 2013, Houghton et al., 2013) and in-depth proteome mapping analysis (Kelkar et al., 2011) have failed to detect the Rv2660c peptides. Application of RNA-Seq technology resulted in identification of novel non-coding RNA, ncRv12659, and challenged previously published data on high upregulation of *rv2660c* and *rv2661c* during starvation (Houghton et al., 2013).

Our study aimed to address the controversies regarding the *rv2660c-rv2661c* genomic region role in *M. tuberculosis* biology. Importantly, we have generated a panel of in-

frame deletion mutants and over-expressing strains of *rv2660c* and *rv2661c* and investigated the biological meaning of the upregulation of these annotated genes and ncRNA during adaptation to dormancy and stress responses. The deletion of *rv2660c* and *rv2661c* in *M. tuberculosis* has also resulted in partial inactivation of ncRv12659 and *rv2662* respectively. Detailed phenotypic investigations have confirmed that none of the genes were essential for growth *in vitro* or *in vivo*. Furthermore, the deletion of these genes did not impair survival of mycobacteria during nutrient (PBS starvation) or oxygen (Wayne model) depletion. We have also found that neither target genes, nor, ncRv12659, were advantageous for the survival of *M. tuberculosis* during exposure to oxidative and nitrosative stresses. The reassessed expression of these genes and ncRv12659 during PBS starvation using qRT-PCR was indeed in accordance with Houghton and colleagues' findings (Houghton et al., 2013). The high transcriptional response of ncRv12659 in *M. tuberculosis* was exclusively starvation-induced and not found in either oxidative or acidic pH stresses. The other annotated genes were also minimally induced, further supporting their lack of importance in the *M. tuberculosis* response to both of these stress conditions.

ncRv12659 originates within the PhiRv2 prophage and the ncRv12659 promoter is relatively repressed in the stable lysogen. It was suggested that during nutrient starvation, the derepression of ncRv12659 together with PhiRv2 genes such as *rv2659c* had initiated a switch to lytic production (Houghton et al., 2013). Our study has highlighted that ncRv12659 does not have any biological importance to the survival of *M. tuberculosis* during starvation. We propose that the ncRv12659 starvation response is for the benefit of the prophage, whereby it contributes to extending the phage genome half-life by possibly switching into a pseudolysogenic state. Pseudolysogeny is an unstable condition which frequently arises due to nutrient-limited conditions where the prophage genome fails to replicate (as in lytic production) or establishes as a non-integrated preprophage (Feiner et al., 2015). When nutrient becomes available, the PhiRv2 prophage is stimulated to complete lytic life cycle and exploit other bacterial cells for growth. This proposed model does support the findings of Houghton and colleagues, whereby over-expression of ncRv12659 resulted in the upregulation of more than 50 genes including PhiRv2 genes and caused a slight growth impairment of *M. tuberculosis* H37Rv in standard

laboratory medium (Houghton, 2015). The interaction between mycobacteria and PhiRv2 prophage in response to the significant transcriptional upregulation of ncRv12659 during nutrient starvation remains to be determined. Nevertheless, our study has opened up a new perspective towards one of the regulatory mechanisms of sRNA in maintaining dormancy through the control of PhiRv2 prophage lifecycle.

The lack of attenuation observed in the double deletion mutant in a murine infection model demonstrated that the genes of interest and ncRv12659 were not involved during active TB infection. Although the murine infection data were only limited to the 28 day timepoint and that a full growth profile of the double deletion mutant may be required, the results strongly suggest that these genes and ncRv12659 have no direct involvement bacterial survival in mice. The majority of the H56 vaccination data have shown that Rv2660c exhibited the lowest immunogenicity (Aagaard et al., 2011) (Luabeya et al., 2015). The success of H56 vaccine was probably through the beneficial fusion of the three antigens that stimulated a specific immune response that elicited sufficient protection to the host (Hoang et al., 2013, Dietrich et al., 2005, Aagaard et al., 2011). Nevertheless, as suggested previously, *rv2660c* may be expressed under specific environmental conditions (Houghton et al., 2013) but that would be an exhaustive search with the knowledge gathered in this study. *Rv2660c* was probably misannotated as a coding gene and its expression was mimicked by ncRv12659, but importantly, we have established that the *rv2660-2661c* region was not required for *M. tuberculosis* stress responses and dormancy. Current evidence supporting the role of these proteins in LTBI is also rather inconclusive. With this, we propose that Rv2660c, Rv2661c and Rv2662 should not be regarded as *M. tuberculosis* 'latency-associated' antigens.

The recent identification of Cmr (Rv1675c) as a redox sensor that controls expression of the DosR regulon opened as a novel regulatory mechanism for adaptation to growth in non-permissible conditions in *M. tuberculosis*. Cmr has several unique features that make it distinct for other mycobacterial TR. Cmr lacks an iron-sulfur cluster and senses redox radicals via a dithiol-disulphide switch of the two conserved cysteines. Cmr differs from *M. tuberculosis* Crp, another known member of CRP/FNR superfamily, where Cmr responds to NO as an effector molecule and not cAMP. *In vitro* studies confirmed that the high-affinity site-specific DNA binding is impaired by

nitrosative stress via nitrosation of the cysteine residues and is less affected by oxidation (Smith et al., 2017). To further understand the role of Cmr regulation, we have determined the phenotypic characteristics of a *cmr* mutant and over-expressing strains during oxidative and nitrosative stresses. Interestingly, the enhanced survival of the *cmr* mutant during nitrosative stress was proposed as to be an indirect consequence from the depression of DosR regulon which somehow pre-conditioned the mutant strain before facing further stresses (Smith et al., 2017). *Cmr* over-expression studies have further revealed the complexity of Cmr-mediated gene regulation. Both *cmr* and *cmr_{C2A}* over-expressing strains had impaired growth and produced smaller colonies on agar. Over-expression of *cmr* had no effect on the survival of *M. tuberculosis* during oxidative stress, however, pre-cooling the strains enhanced their tolerance to H₂O₂. Interestingly, the over-expression of *cmr* double mutant form (*cmr_{C2A}*) resulted in more pronounced improvement of survival during oxidative stress. The C2A mutation locked the Cmr into its reduced state and resulted in significantly impaired DNA binding (Smith et al., 2017). Therefore, it is plausible to suggest that the mutated form could directly or indirectly derepress the DosR regulon. How this mechanism influences the survival of the over-expressing *cmr_{C2A}* strain during oxidative stress requires further investigation. In fact, it would also be interesting to study the survival of over-expressing strains during nitrosative stress and in Wayne NRP model to further explore the hypothesis.

The reasons for the failed complementation of Cmr phenotype remain unclear. Whole genome sequencing analysis showed no major additional gene variations in both wild-type and *cmr* mutant suggesting that observed mutant phenotypes resulted from the *cmr* deletion. Expression of *cmr* is finely tuned and this tightly-controlled mode of regulation was presumably not restored in the complemented mutant.

This study has demonstrated that Cmr was responsible for the regulation of *M. tuberculosis* stress responses. We have also highlighted that the survival fitness of the pathogen depended on a precise level of *cmr* expression in response to NO signalling, which affects the expression of the DosR regulon. A comprehensive expression profile of Cmr-dependent genes and DosR regulon genes in the wild-type and the *cmr* mutant strains during nitrosative and the other two stress responses, will provide a better understanding on how Cmr mediates responses to ensure survival and

persistence of *M. tuberculosis*. Determining the molecular mechanism behind Cmr regulation will also progress our knowledge on how Cmr might contribute in maintaining *M. tuberculosis* redox balance, as it was thought that redox imbalance would trigger other mechanisms that caused the pathogen to switch to dormancy. Nevertheless, the novel Cmr- dependent pathway exploited by the pathogen is a potential target for drugs that could be effective against dormant *M. tuberculosis*.

Appendices

APPENDICES

Appendix 1. LIST OF PRIMERS USED FOR CONSTRUCTION AND CONFIRMATION OF DELETION AND OVER-EXPRESSING STRAINS

Primers	Sequences 5'→3'	Restriction sites	Application
266oFR2F	CTTGGAAAGCTTTGTCACACCAAGTGTTTCGACCAG	<i>HindIII</i>	Amplification of flanking region upstream of <i>rv266oc</i> sequence, 266oFR2
266oFR2R	CTGGTCGGATCCCGCTATCACGCTGTTGTCGCGTCC	<i>BamHI</i>	
266oFR1R	AGCGACTGCGGCCGCCGGCGGTCATGCGGCACCACC	<i>NotI</i>	Amplification of flanking region downstream of <i>rv266oc</i> sequence, 266oFR1
266oFR1F	TTGAACGGATCCCCTAGTGGGCCGGTGGGATACTG	<i>BamHI</i>	
2661FR1F	TCGGTGGGATCCGTGGACGCGACAACAGCGTGATAG	<i>BamHI</i>	‡Amplification of flanking regions of upstream and downstream of <i>rv2661c</i> sequence, 2661FR2 and 2661FR1
2661FR2R	GAGCCGGGATCCCCTCATCGCGACCTACGACCCCTG GAT	<i>BamHI</i>	
266opMVF	AGAGGATCCAGAATAGCGGGCGTTCGACCA	<i>BamHI</i>	Generation of <i>M. tuberculosis</i> pMV261:: <i>rv266oc</i>
266opMVR	GGAGAATTCTAGTGAAACTGGTTCAATCC	<i>EcoRI</i>	
2661pMVF	AGAGGATCCAATGAGGGCTCGCAGCGATGCT	<i>BamHI</i>	Generation of <i>M. tuberculosis</i> pMV261:: <i>rv2661c</i>
2661pMVR	GGAGAATTCTCACGCTGTTGTCGCGTCCAC	<i>EcoRI</i>	
C36A_F	GGATTGCGCGGGCCGTCGGTCGCGGAGGCTCG	-	Site directed mutagenesis C36A
C36A_R	CGAGCCTCCGCGACCGACGGCCCGCGCAATCC	-	
C131A_F	GACCCAAGCGACCGCCCTGTTCTGGACCGG	-	Site directed mutagenesis C131A
C131A_R	CCGGTCCAGGAACAGGGCGGTCGCTTGGGTC	-	

1675pMV261 F	AGAG GATCCA ATGGCAGATCGGTCCGGTGC	<i>Bam</i> HI	Generation of <i>M. tuberculosis</i> pMV261:: <i>cmr</i> and <i>M. tuberculosis</i> pMV261:: <i>cmr</i> _{C2A}
1675pMV261 R	TAG GAA TTCTCATTGAGCCCCGGGCGCG	<i>Eco</i> RI	
Test Primers	Sequences 5'→3'		Applications
2660TestF	GGACGCGACAACAGCGTGATAG		Confirmation of Δ rv266oc and Δ rv2661c:rv266oc
2660TestR	GACTACATCAGATGCCGCTTGCTT		Confirmation of Δ rv266oc, Δ rv2661c and Δ rv2661c:rv266oc
2661Test	GCGATACAGGCTGTGGCG		Confirmation of Δ rv2661c and Δ rv2661c:rv266oc
pMV261F	TGATCACCGCGGCCATGATGG		For confirmation of coding sequences cloned in pMV261
pMV261R	TCGCCCCGCCAGCGTAAGTA		

Table - 1: List of primers used for construction and confirmation of deletion and over-expressing strains in *M. tuberculosis*

‡Amplification of flanking region upstream of *rv2661c* sequence, 2661FR2, primer set (2660FR2F and 2661FR2R) were used. For amplification of flanking region downstream of *rv2661c* (2661FR1), primers 2661FR1F and 2660FR1R were employed. For generation of *M. tuberculosis* pMV261::*rv2661c+rv266oc*, primers 2661pMVf and 2660pMVR were used. Bold fonts are for restriction sites. The underlined bases define those changed to produce the alanine variation.

Appendix 2. **GENE SPECIFIC PRIMERS USED IN QRT-PCR**

Transcripts	Designation	Sequence 5'→3'	Amplicon size (bp)
<i>16S</i>	MYCO _{16SF}	GAAACTGGGTCTAATACCG	173
	MYCO _{16SR}	ATCTCAGTCCCAGTGTGG	
<i>rv2660c</i>	RT _{2660F}	GCTTGCAGCAACAGGCCAGG	182
	RT _{2660R}	AGTATCGCGCACCACGATTG	
<i>rv2661c</i>	RT _{2661F}	GAGGCCAGTCTGTGAAGTCC	100
	RT _{2661R}	GCCTGCGGATTATCAACGAG	
	‡RT _{2661F1}	CTGTGAAGTCCCGCACGTCTGAAT	80
	‡RT _{2661R1}	ATCAACGAGGGCACTGATGGATGA	
<i>rv2662</i>	RT _{2662F}	GAGCTTCTGGACCGATTC	227
	RT _{2662R}	TTCTCACCAGCGCAAACA	
ncRv12659	RT _{12659F}	CAGGTCAGACAGTATCCCA	147
	RT _{12659R}	GTTACGCAGCCCAGATTT	
<i>rv1675c</i> , <i>cmr</i>	RT _{1675F}	AATCCGTGTGCGACAATCCA	115
	RT _{1675R}	GTGACGATGTGTCGGCATTG	

Table - 2: List of gene specific primers used in qRT-PCR

‡used to confirmed deletion strain of *rv2661c* (Chapter 3)

Appendix 3. DELETION DELIVERY PLASMID VECTORS OF *rv2660c* AND *rv2661c* CONSTRUCTED USING FLEXIBLE CASSETTE METHOD (Parish and Stoker, 2000b)

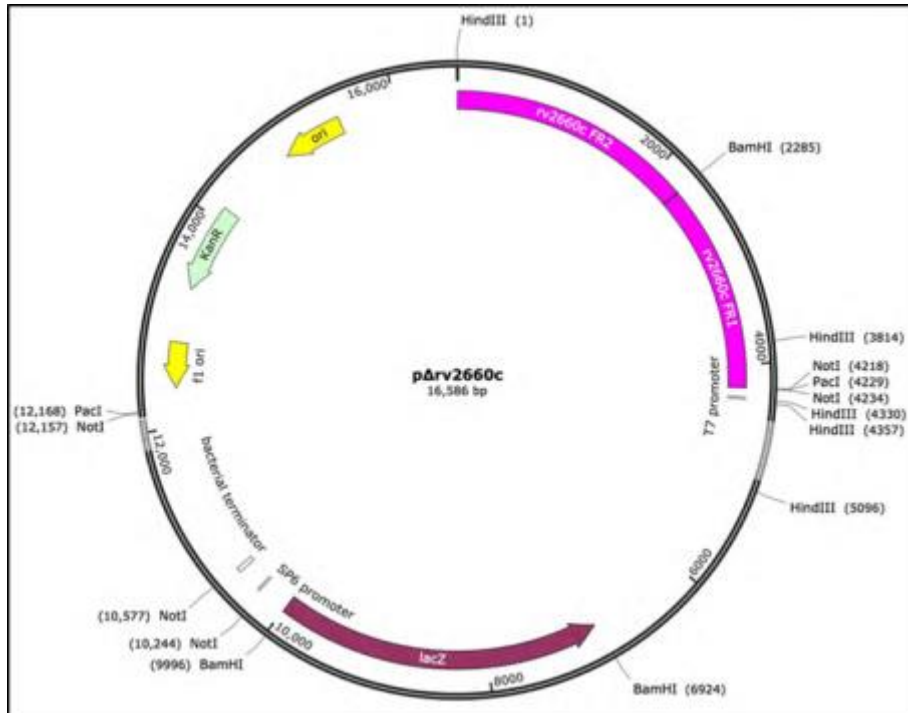


Figure- 1: Plasmid construct for $\Delta rv2660c$ deletion delivery vector, $p\Delta rv2660c$

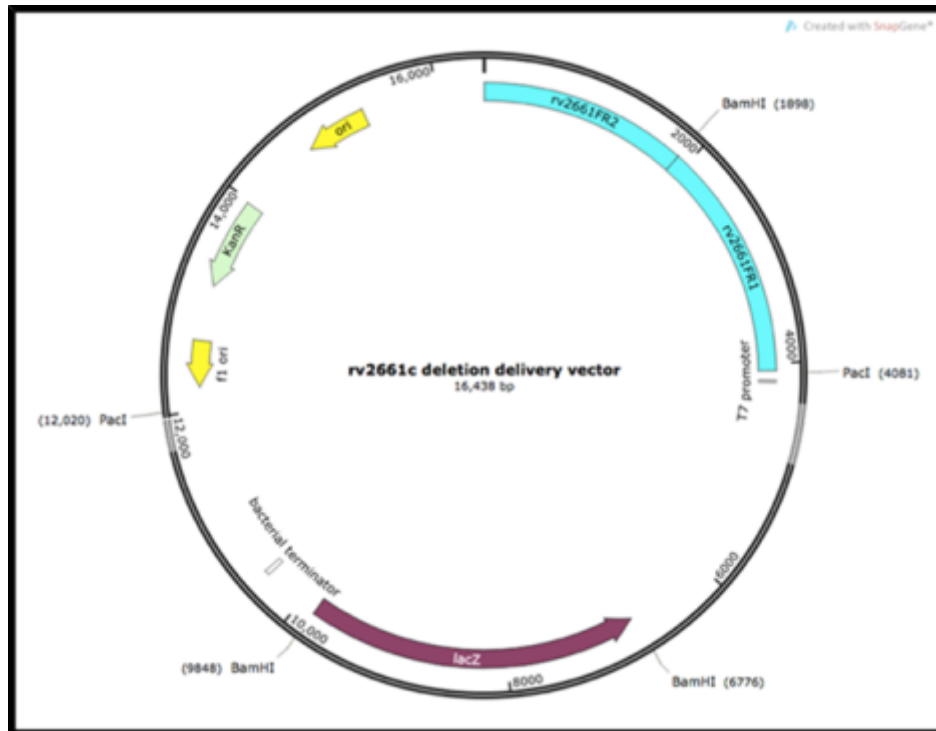


Figure- 2: Plasmid construct for $\Delta rv2661c$ deletion delivery vector, $p\Delta rv2661c$

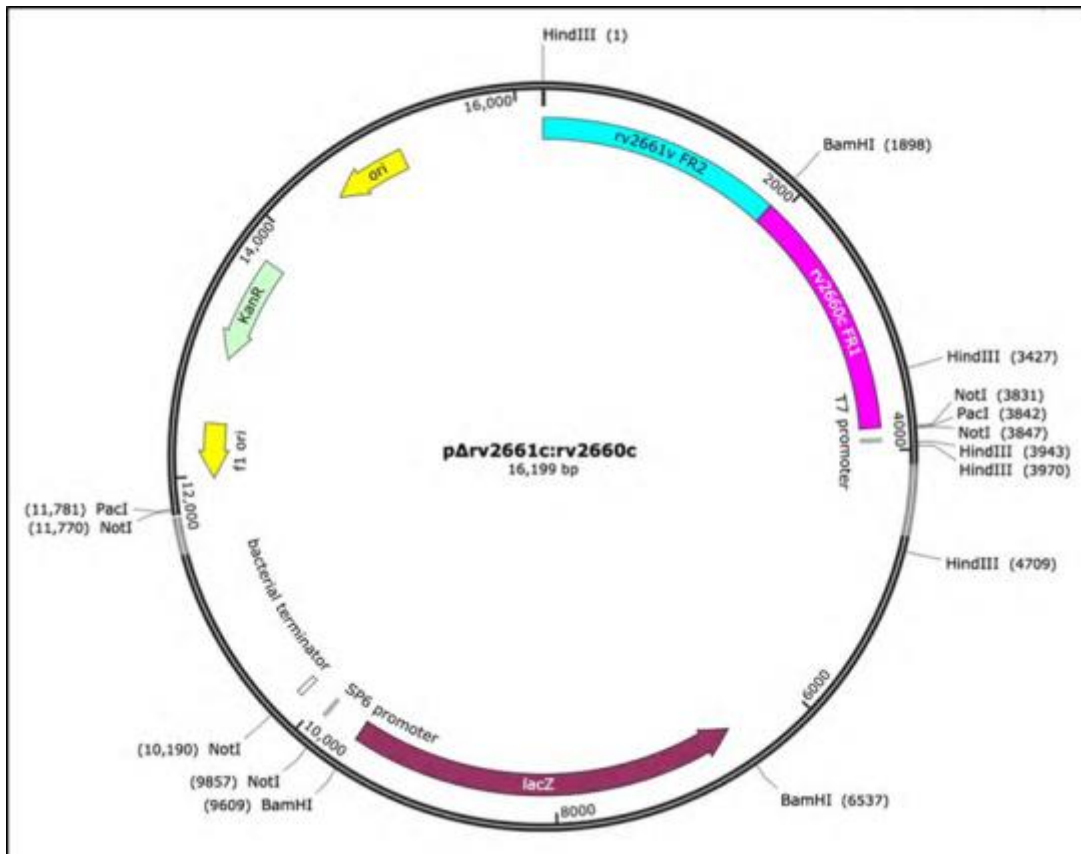


Figure- 3: Plasmid construct for $\Delta rv2661c:rv2660c$ delivery vector, $p\Delta rv2661c:rv2660c$ (16,199bp)

Appendix 4. PLASMID CONSTRUCTS USED FOR GENERATION OF OVER-EXPRESSING STRAINS

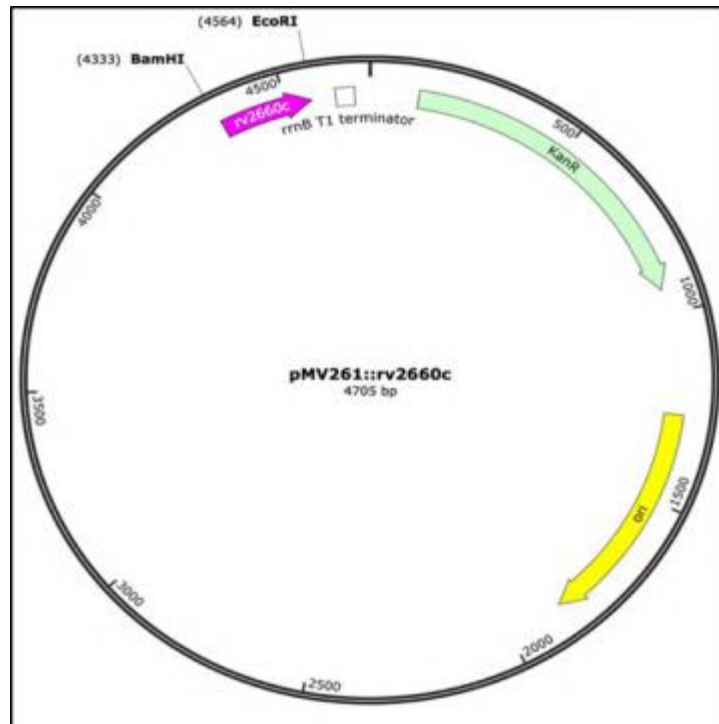


Figure- 4: Plasmid construct for pMV261::rv2660c

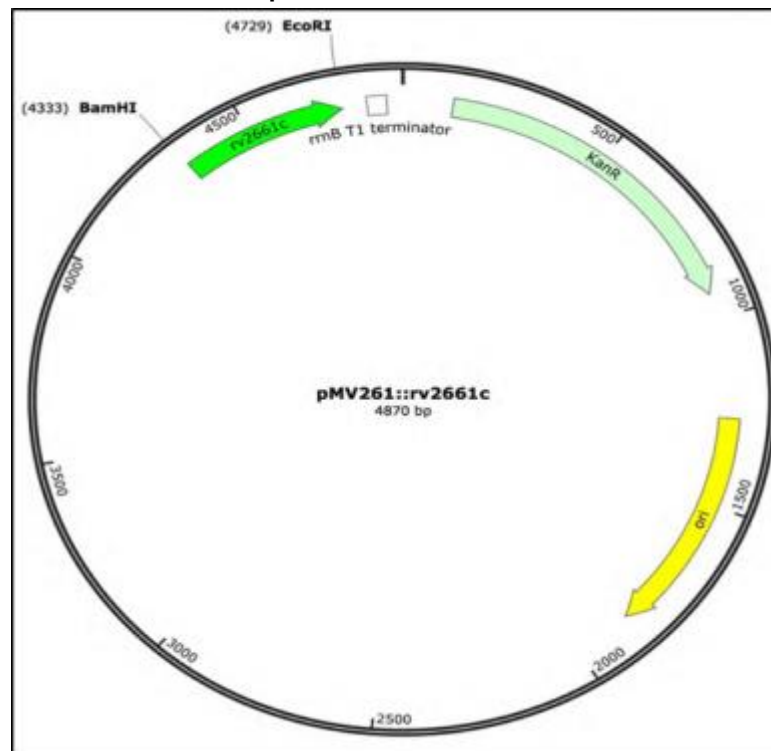


Figure- 5: Plasmid construct for pMV261::rv2661c

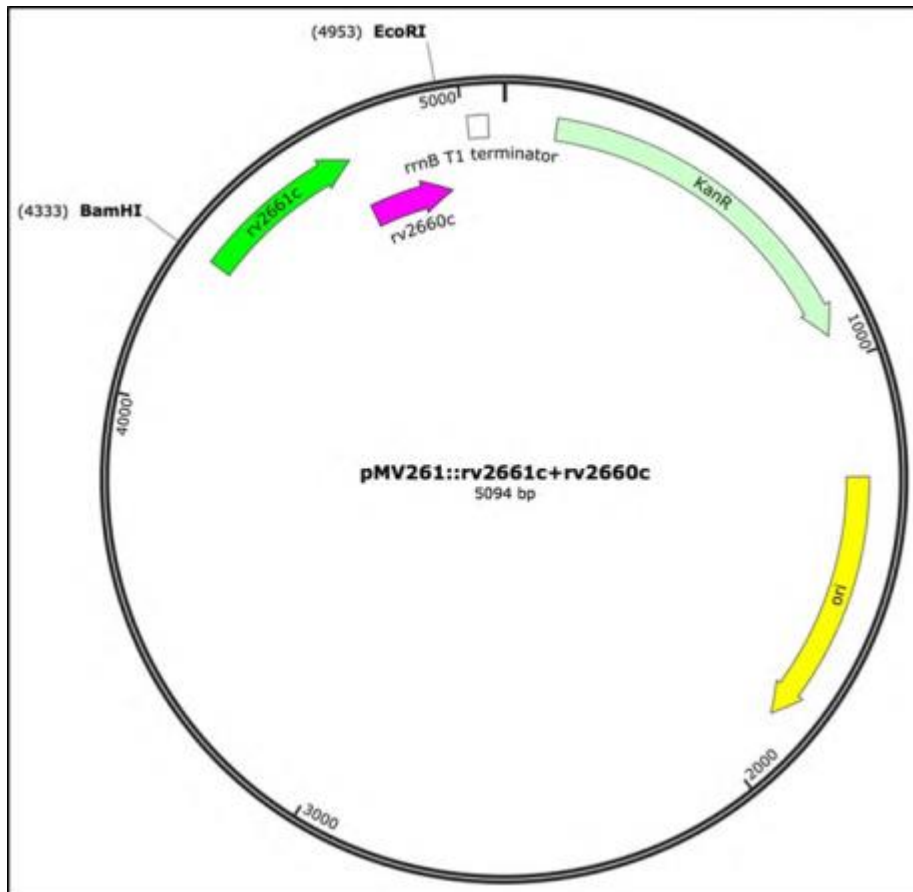


Figure- 6: Plasmid construct for pMV261::rv2661c+rv2660c

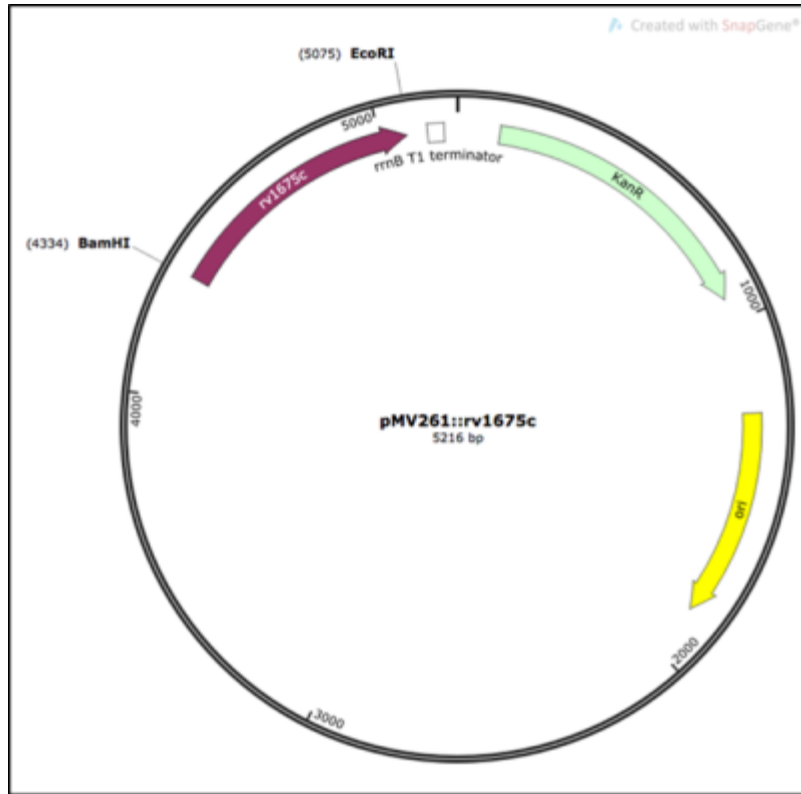


Figure- 7: Plasmid construct for pMV261::rv1675c / pMV261::cmr

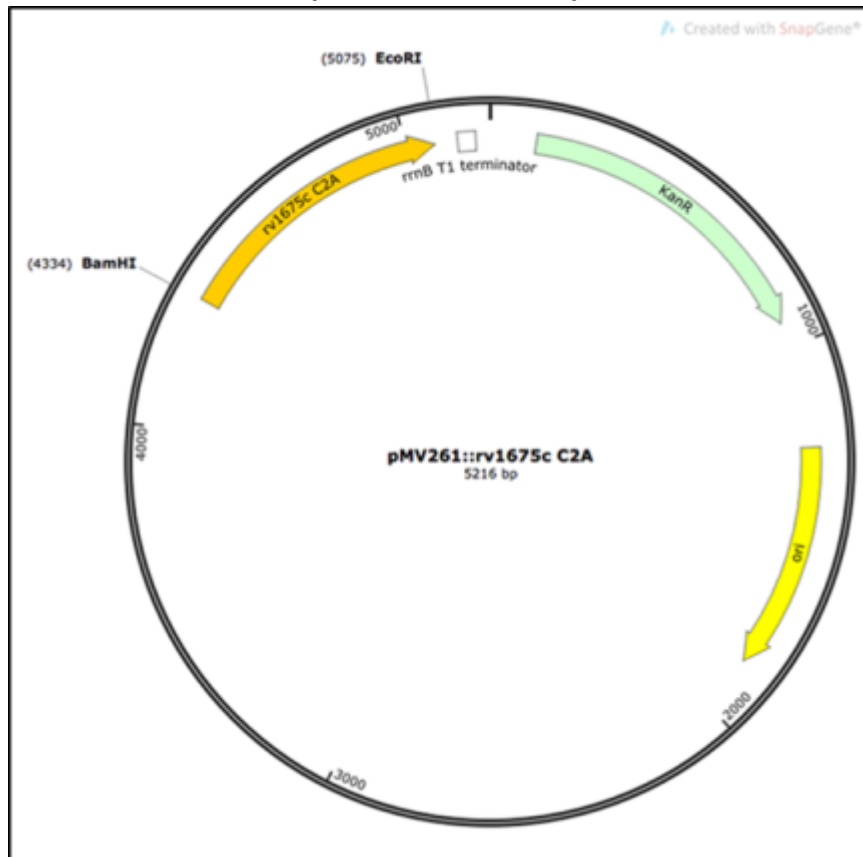


Figure- 8: Plasmid construct for pMV261::rv1675 C_{2A} / pMV261::cmr_{C2A}

Appendix 5. SEQUENCE MAP OF REGION AMPLIFIED USING GENE- SPECIFIC PRIMERS FOR *rv266oc* AND *ncRv12659*

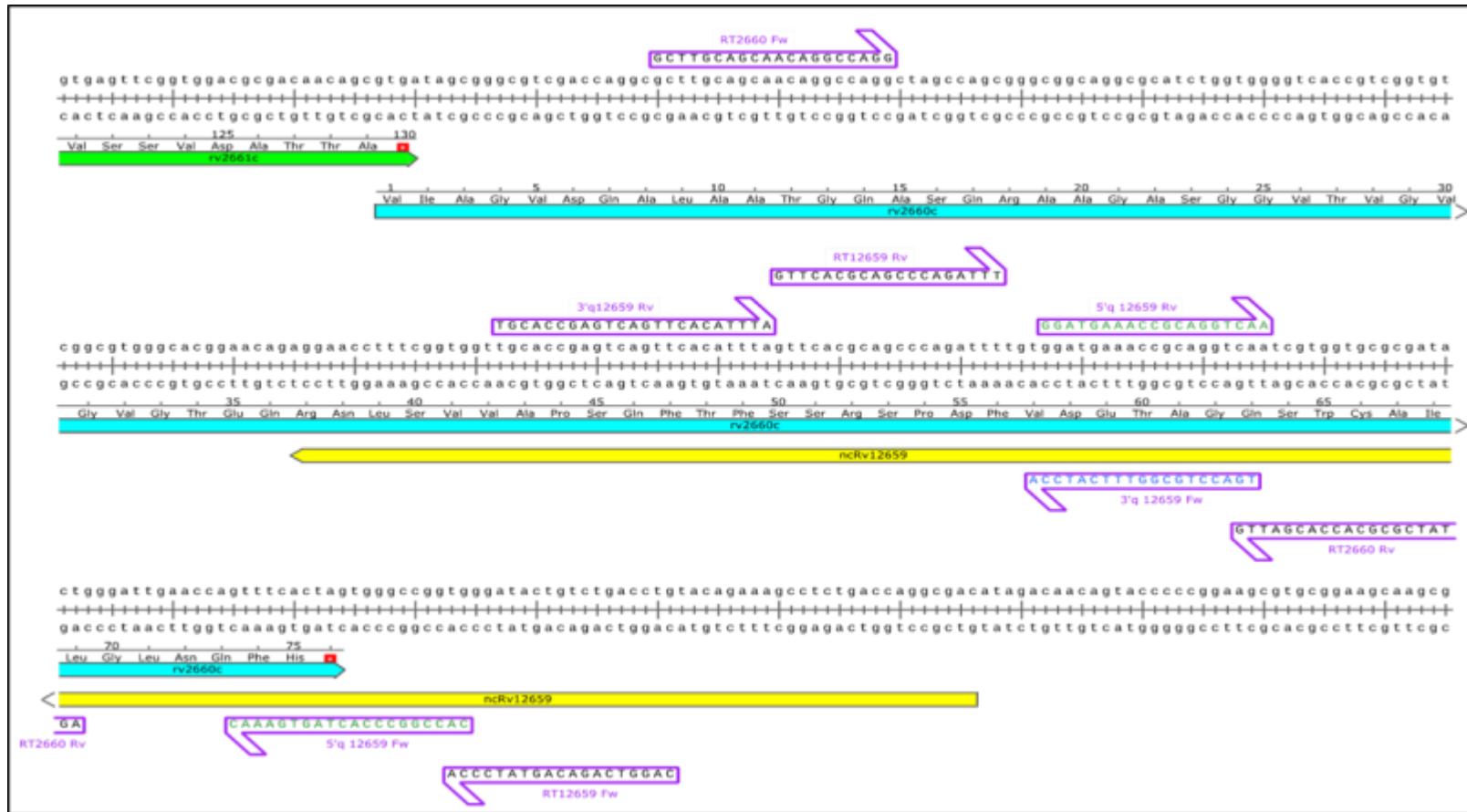


Figure- 9: Sequence map of region amplified with gene specific primers for *rv266oc* and *ncRv12659*. Primers (purple arrow) used in this study: RT2660 and RT12659 primer pair (Govender et al., 2010). Primers used in Houghton's study (Houghton et al., 2013) for amplifying 5' end and 3' end of *ncRv12659*; 5'q 12659Fw + 5'q 12659Rv (green) and 3'q 12659Fw + 3'q 12659Rv (blue). Image was generated using Snapgene®Viewer (V3.3.3)

Appendix 6. QRT-PCR ASSAY PERFORMANCE

The parameter values for assessing qRT-PCR assay performance are correlation efficient, R² (acceptable range 0.9 to 1) and PCR efficiency, shown as percentage values (acceptable range 90-110%). These were analysed from each individual qPCR assay (denoted as 1, 2 and 3).

Assay with specific primers	R ²		PCR efficiency (%)	
	1	2	1	2
MYCO 16s	0.96	0.98	100	90
RT2660	0.95	0.99	98	90
RT2661	0.96	0.98	100	98
RT12659	0.98	0.99	89	100

Table - 3: QRT-PCR assay performance for confirmation of over-expressing strains of rv2660c and rv2661c in *M. tuberculosis* (Chapter 3)

Assay	R ²		PCR efficiency (%)	
	1	2	1	2
MYCO 16s	0.94	0.97	98	97
RT2660	0.99	0.99	120	100
RT2661	0.97	0.99	94	66
RT12659	0.98	0.98	98	90

Table - 4: QRT-PCR assay performance for nutrient starvation experiment (Chapter 4)

Assay	R ²				PCR efficiency (%)			
	5mM H ₂ O ₂	25mM H ₂ O ₂			5mM H ₂ O ₂	25mM H ₂ O ₂		
	1	1	2	3	1	1	2	3
MYCO 16s	0.90	0.96	0.89	0.90	95	98	90	92
RT2660	0.92	0.90	0.93	0.83	90	90	87	90
RT2661	0.94	0.98	0.96	0.97	101	92	101	94
RT2662	0.99	0.99	0.99	0.88	89	94	99	90
RT12659	0.98	0.99	0.96	0.74	95	82	80	98

Table - 5: QRT-PCR assay performance for oxidative stress experiment (Chapter 4)

Assay	R ²		PCR efficiency (%)	
	1	2	1	2
MYCO 16s	0.99	0.97	90	97
RT2660	0.96	0.92	92	92
RT2661	0.99	0.99	120	96
RT2662	0.96	0.99	94	98
RT12659	0.98	0.98	98	98

Table - 6: QRT-PCR assay performance for acidic pH, pH5.3 (Chapter 4)

Assay with specific primers	R ²	PCR efficiency (%)
MYCO 16S rRNA	0.97	94
RT1675c	0.99	96

Table - 7: QRT-PCR assay performance for confirmation of over-expressing strains of *cmr* and *cmr*_{C2A} strains

All three biological replicates were loaded in one qPCR run

Assay	R ²			PCR efficiency (%)		
	1	2	3	1	2	3
16S rRNA	0.98	0.98	0.99	95	88	92
RT1675	0.99	0.97	0.97	99	105	100

Table - 8: QRT-PCR assay performance for nitrosative stress experiment

Appendix 7. MELTING CURVES

These are representative melting curves generated from each qPCR run in each experiment with respective primers. The single peak in each graph corresponded to the melting temperature, T_m of the generated amplicons.

a) CONFIRMATION OF OVER-EXPRESSING STRAINS OF *rv266oc* AND *rv2661c* IN *M. TUBERCULOSIS* (CHAPTER 3)

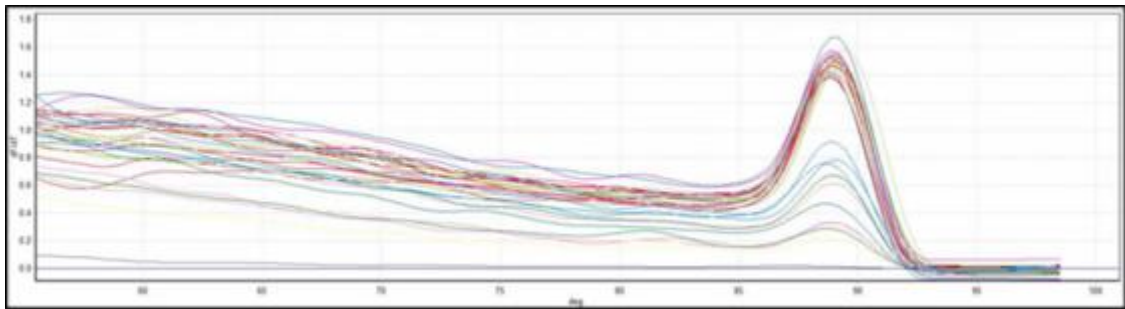


Figure- 10: Melting curves for *rv266oc* and *rv2661c* over-expressing and control strains including No-RT and gDNA standard samples using MYCO 16s primers
Lower peaks represent No-RT samples

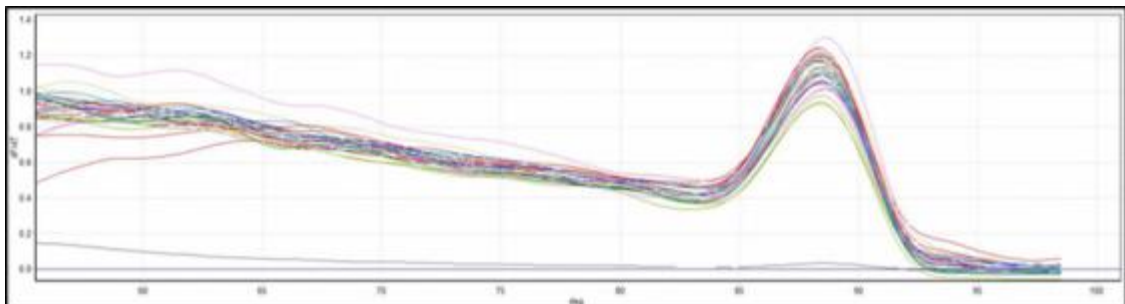


Figure- 11: Melting curves for *rv266oc* and *rv2661c* over-expressing and control strains including No-RT and gDNA standard samples using RT266o primers

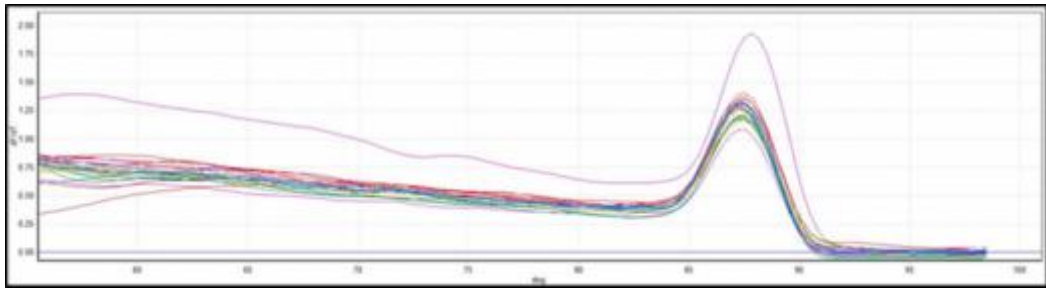


Figure- 12: Melting curves for *rv2660c* and *rv2661c* over-expressing and control strains including No-RT and gDNA standard samples using RT2661 primers

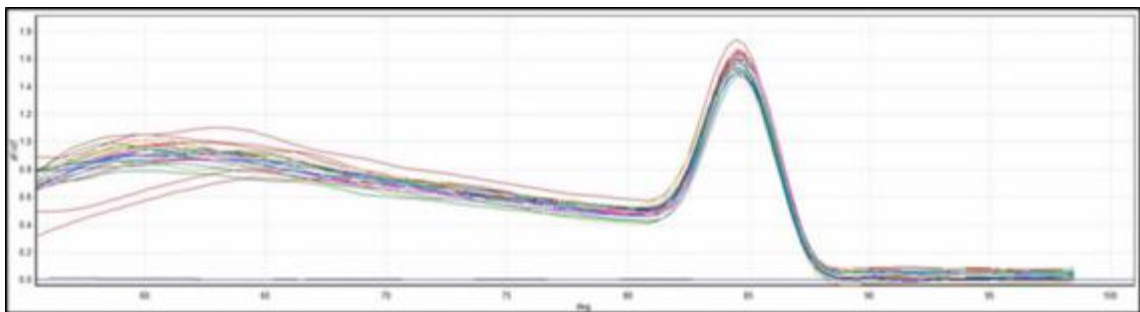


Figure- 13: Melting curves for *rv2660c* and *rv2661c* over-expressing and control strains including No-RT and gDNA standard samples using RT12659 primers

b) NUTRIENT STARVATION EXPERIMENT

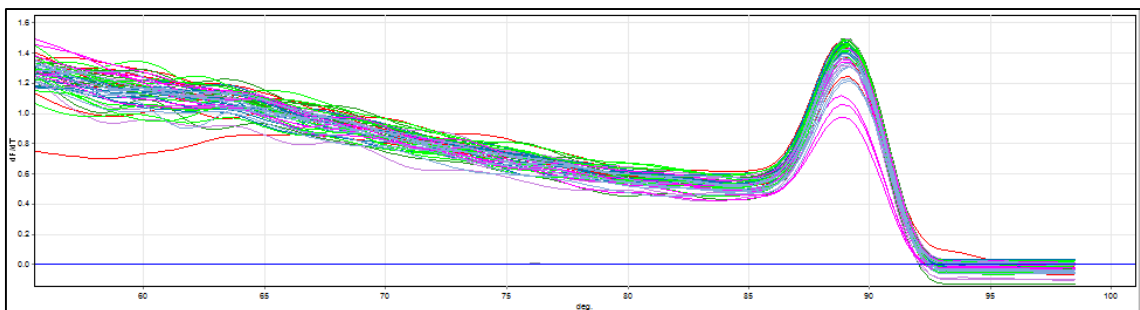


Figure- 14: Melting curves for *M. tuberculosis* wild-type strain including No-RT and gDNA standard samples using MYCO 16s primers from nutrient starvation experiment

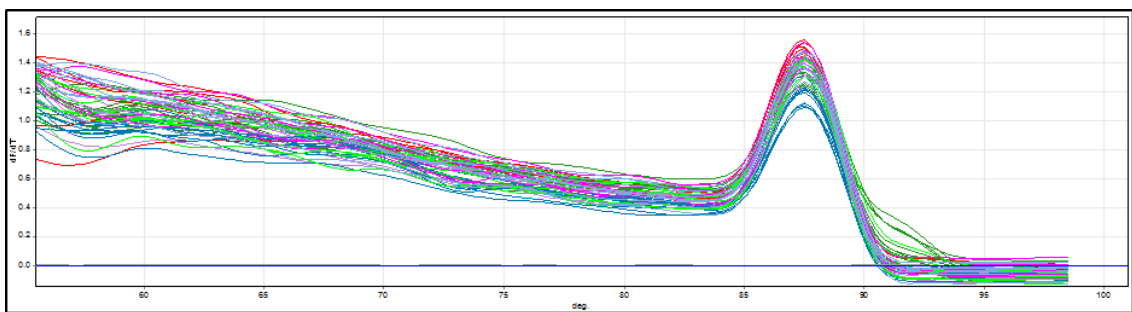


Figure- 15: Melting curves for *M. tuberculosis* wild-type strain including No-RT and gDNA standard samples using RT2661 primers from nutrient starvation experiment

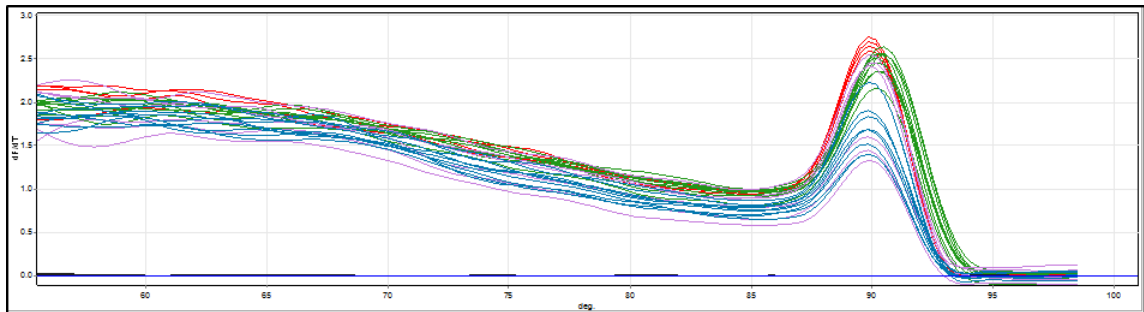


Figure- 16: Melting curves for *M. tuberculosis* wild-type strain including No-RT and gDNA standard samples using RT2662 primers from nutrient starvation experiment

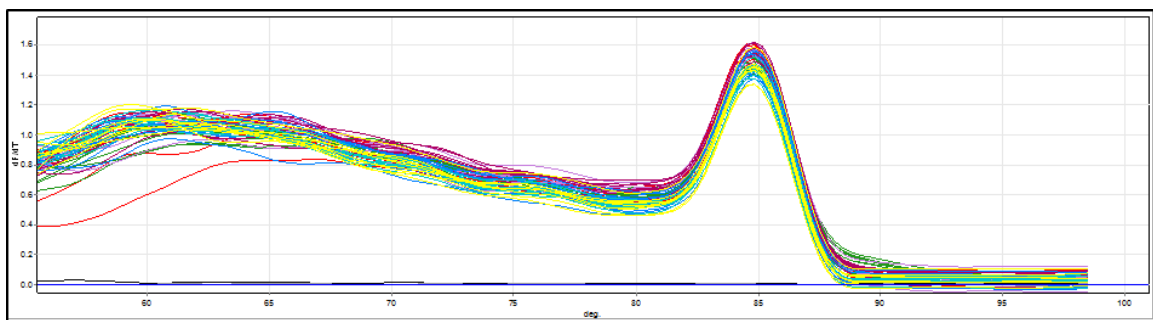
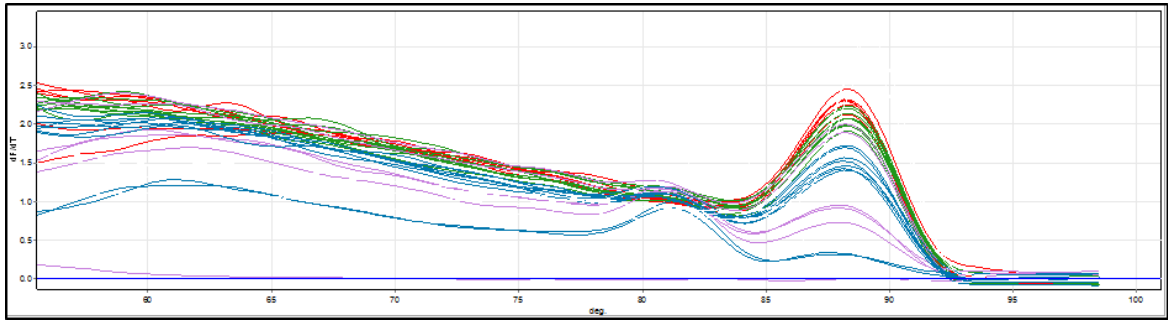


Figure- 17: Melting curves for *M. tuberculosis* wild-type strain including No-RT and gDNA standard samples using RT12659 primers from nutrient starvation experiment

1st qRT-PCR run



2nd qRT-PCR run

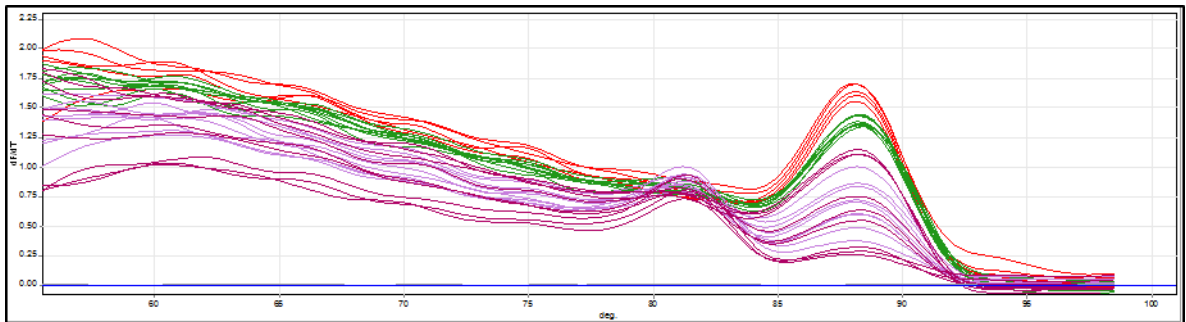


Figure- 18: Melting curves for *M. tuberculosis* wild-type strain and gDNA standard samples using RT266o primers

All *M. tuberculosis* gDNA standards and exponential growth samples demonstrated expected T_m of $88.8 \pm 0.2^\circ\text{C}$ (shown as red and green lines respectively) while negative control (in black) is represented by a straight line. *M. tuberculosis* starved cells sampled at 24 and 96 hours presented T_m at $80.8 \pm 0.2^\circ\text{C}$ compared with actual target T_m of $88.8 \pm 0.2^\circ\text{C}$. This figures are two independent PCR runs using cDNA from two separate experiments.

c) OXIDATIVE STRESS (5mM HYROGEN PEROXIDE) EXPERIMENTS

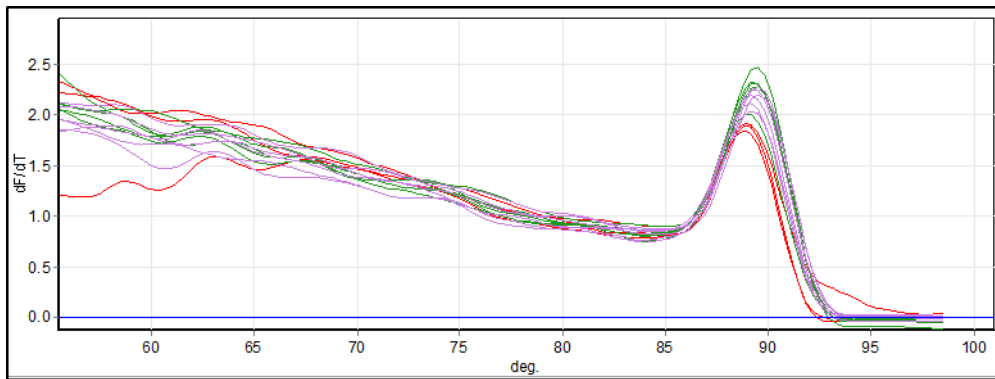


Figure- 19: Melting curves for *M. tuberculosis* wild-type strain including No-RT and gDNA standard samples using MYCO 16s primers from oxidative stress (5mM H₂O₂) experiment

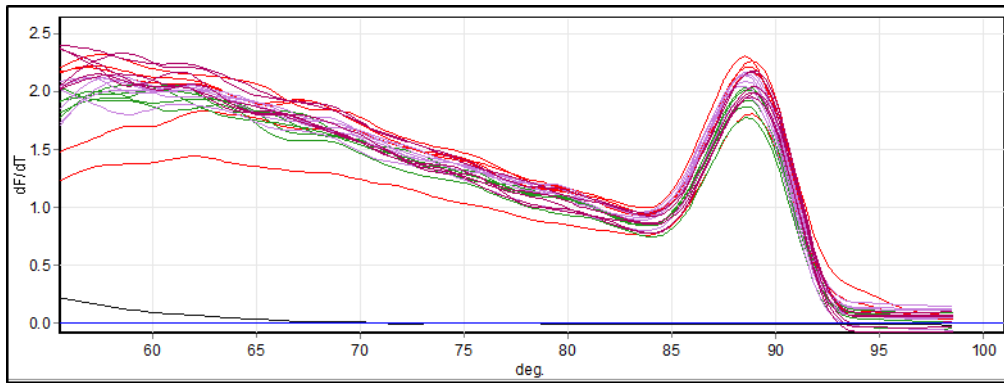


Figure- 20: Melting curves for *M. tuberculosis* wild-type strain including No-RT and gDNA standard samples using RT266o primers from oxidative stress (5mM H₂O₂) experiment

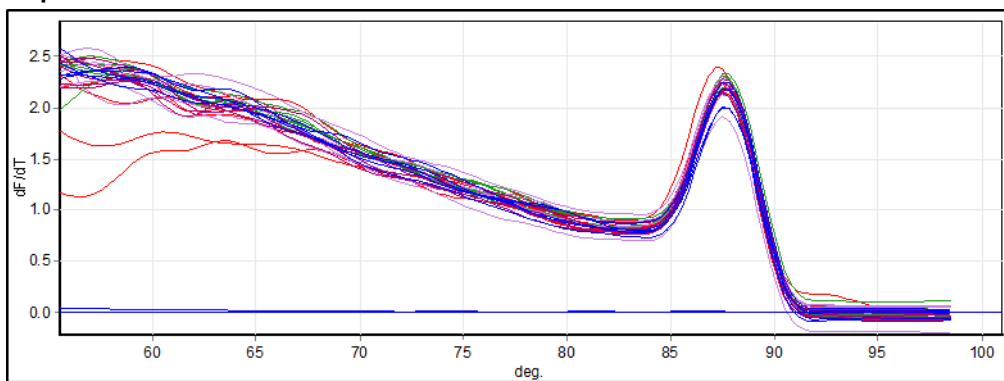


Figure- 21: Melting curves for *M. tuberculosis* wild-type strain including No-RT and gDNA standard samples using RT2661 primers from oxidative stress (5mM H₂O₂) experiment

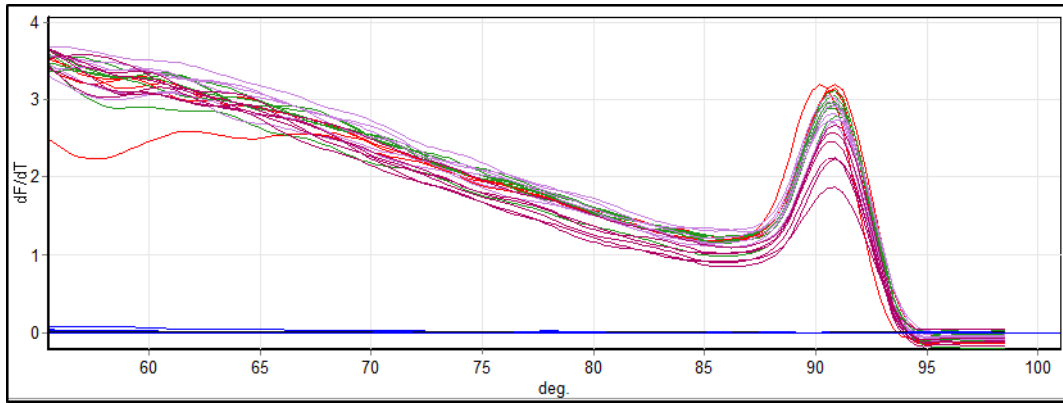


Figure- 22: Melting curves for *M. tuberculosis* wild-type strain including No-RT and gDNA standard samples using RT2662 primers from oxidative stress (5mM H₂O₂) experiment

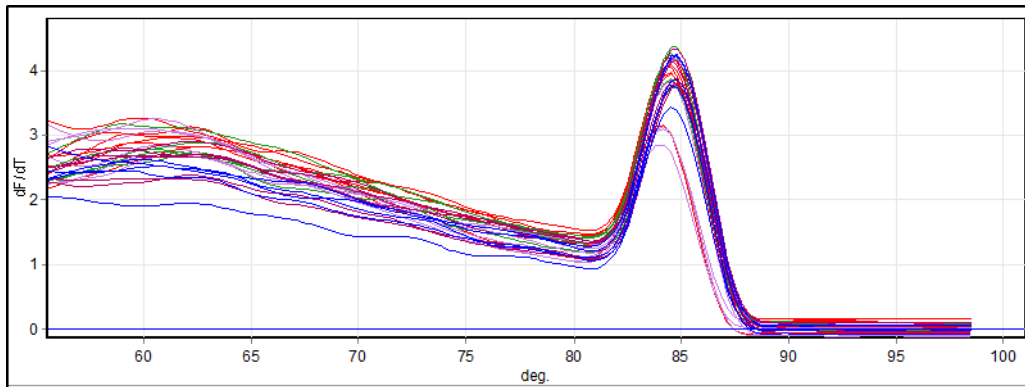


Figure- 23: Melting curves for *M. tuberculosis* wild-type strain including No-RT and gDNA standard samples using RT12659 primers from oxidative stress (5mM H₂O₂) experiment

d) OXIDATIVE STRESS (25mM HYROGEN PEROXIDE) EXPERIMENT

Samples presented in different colours as follow; gDNA standards (Red lines), *M. tuberculosis* H37Rv (Dark yellow), $\Delta rv2661c:rv2660c$ (Dark Green), *M. tuberculosis* H37Rv; No- RT samples (Light yellow), $\Delta rv2661c:rv2660c$; No- RT samples (Light green)

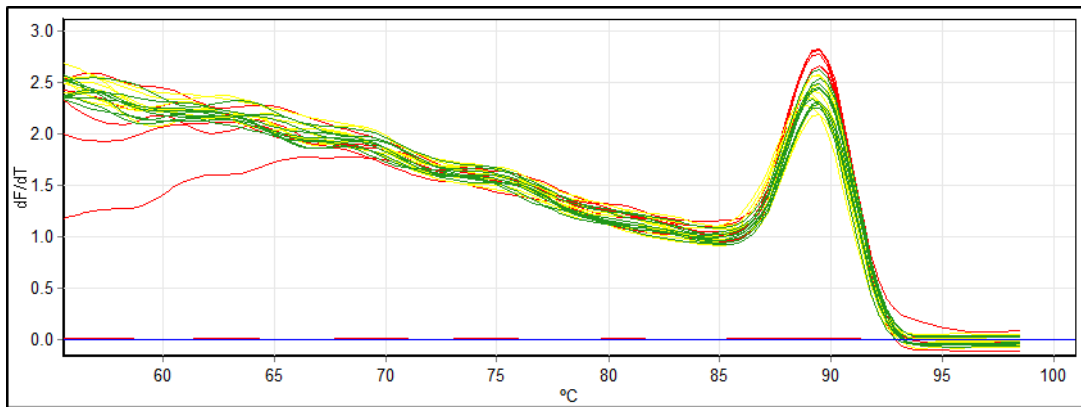


Figure- 24: Melting curves for *M. tuberculosis* wild-type and $\Delta rv2661c:rv2660c$ strain including No-RT and gDNA standard samples using MYCO 16S primers from oxidative stress (25mM H_2O_2) experiment

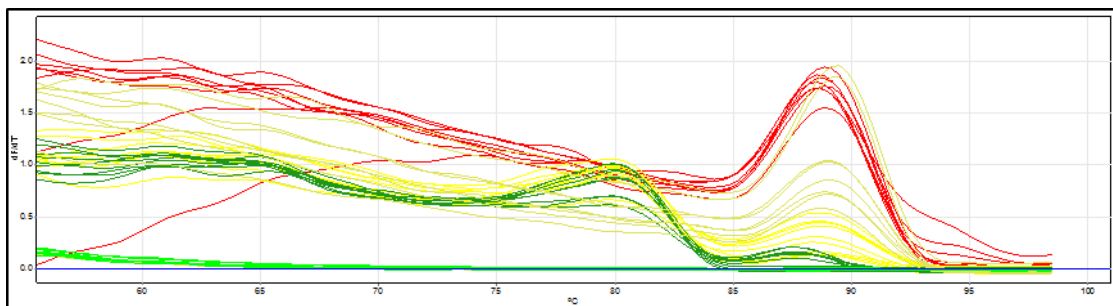


Figure- 25: Melting curves for *M. tuberculosis* wild-type and $\Delta rv2661c:rv2660c$ strain including No-RT and gDNA standard samples using RT2660 primers from oxidative stress (25mM H_2O_2) experiment

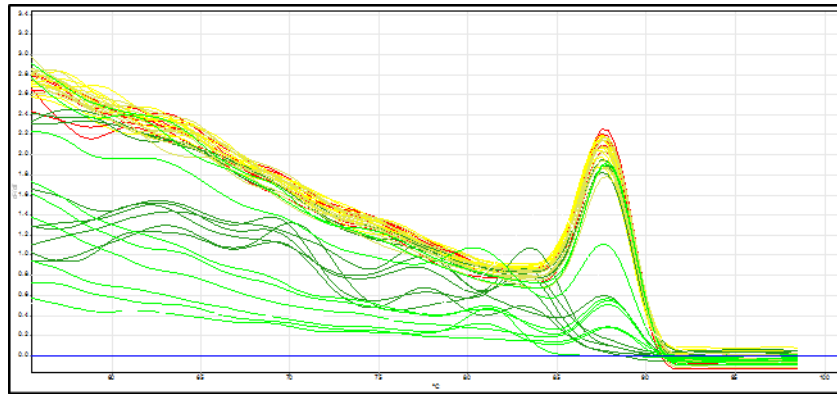


Figure- 26: Melting curves for *M. tuberculosis* wild-type and $\Delta rv2661c:rv2660c$ strain including No-RT and gDNA standard samples using RT2661 primers from oxidative stress (25mM H₂O₂) experiment

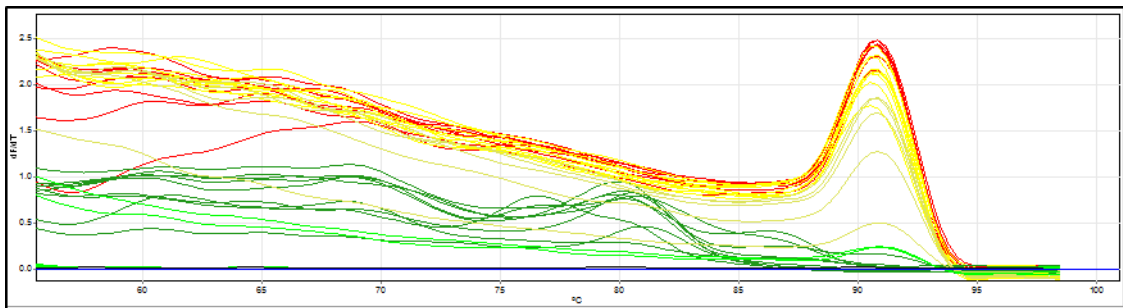


Figure- 27: Melting curves for *M. tuberculosis* wild-type and $\Delta rv2661c:rv2660c$ strain including No-RT and gDNA standard samples using RT2662 primers from oxidative stress (25mM H₂O₂) experiment

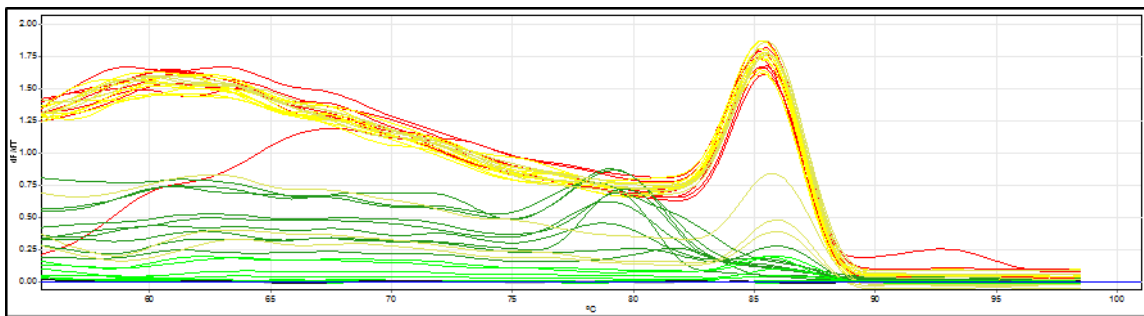


Figure- 28: Melting curves for *M. tuberculosis* wild-type and $\Delta rv2661c:rv2660c$ strain including No-RT and gDNA standard samples using RT12659 primers from oxidative stress (25mM H₂O₂) experiment

e) ACIDIC pH OF 5.3 EXPERIMENTS

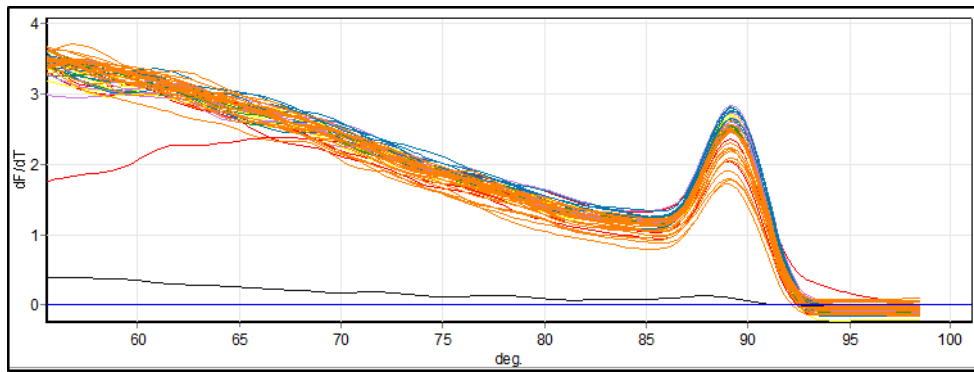


Figure- 29: Melting curves for *M. tuberculosis* wild-type strain including No-RT and gDNA standard samples using MYCO 16S primers from acid stress experiment

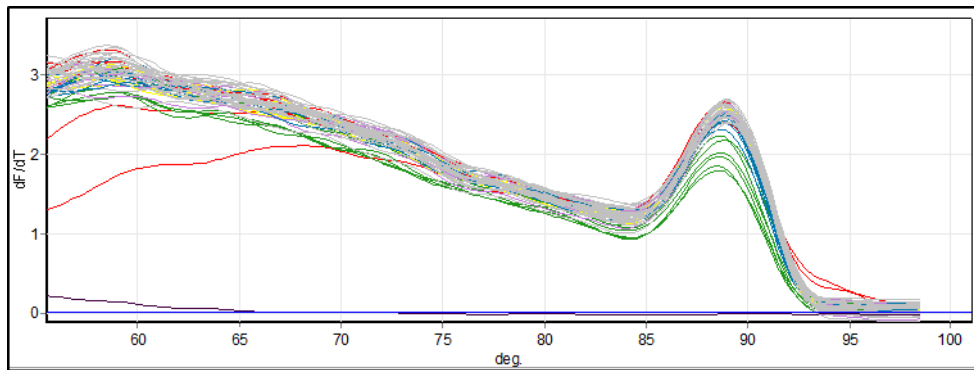


Figure- 30: Melting curves for *M. tuberculosis* wild-type strain including No-RT and gDNA standard samples using RT266o primers from acid stress experiment

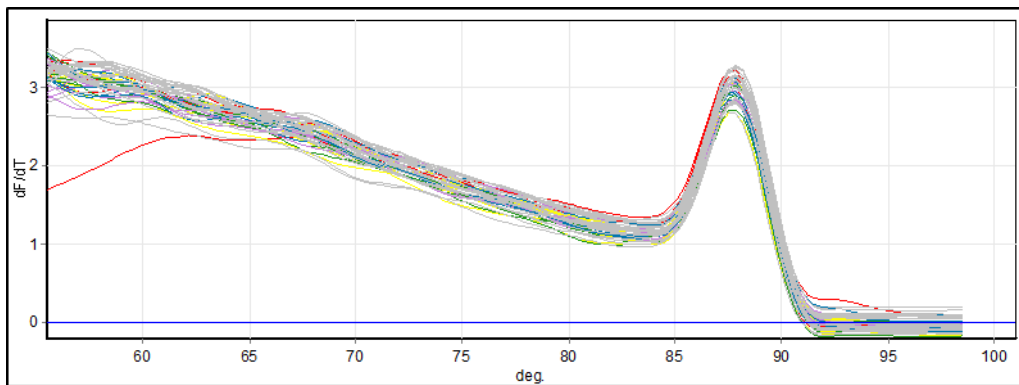


Figure- 31: Melting curves for *M. tuberculosis* wild-type strain including No-RT and gDNA standard samples using RT2661 primers from acid stress experiment

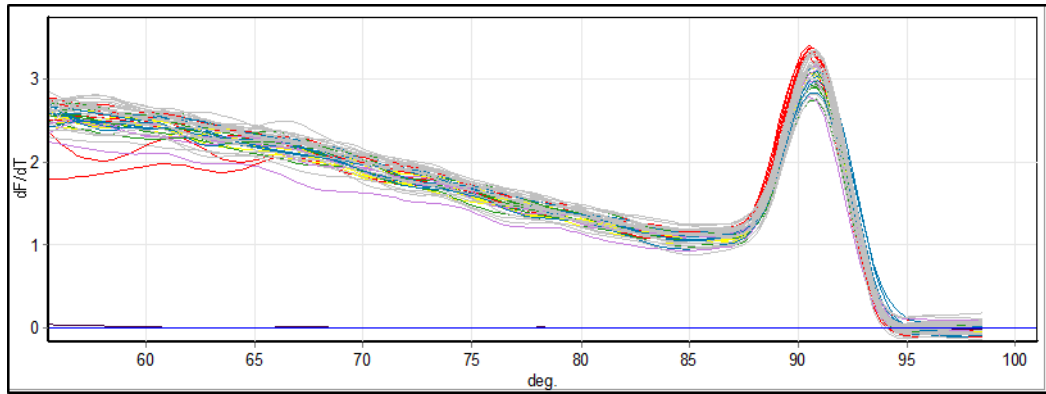


Figure- 32: Melting curves for *M. tuberculosis* wild-type strain including No-RT and gDNA standard samples using RT2662 primers from acid stress experiment

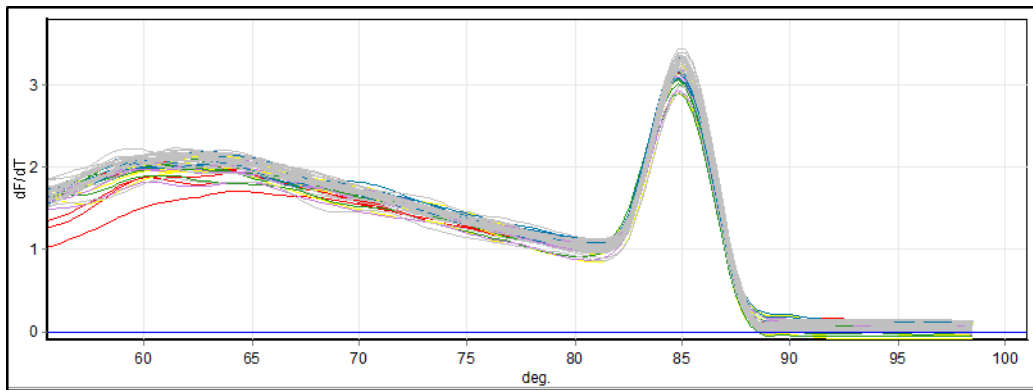


Figure- 33: Melting curves for *M. tuberculosis* wild-type strain including No-RT and gDNA standard samples using RT12659 primers from acid stress experiment

f) CONFIRMATION OF OVER-EXPRESSING STRAINS OF *cmr* AND *cmr* MUTANT VARIANT (*cmr*_{C2A}) IN *M. TUBERCULOSIS* (CHAPTER 5)

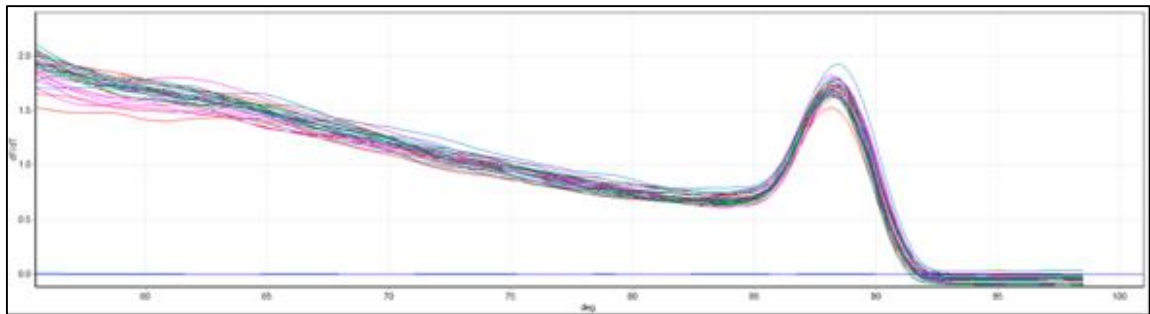


Figure- 34: Melting curves for *cmr* and *cmr*_{C2A} over-expressing and control strains including No-RT and gDNA standard samples using MYCO 16s primers

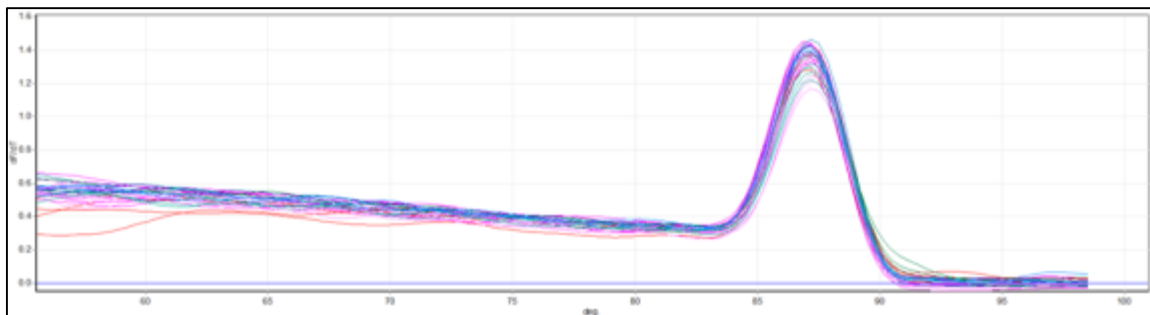


Figure- 35: Melting curves for *cmr* and *cmr*_{C2A} over-expressing and control strains including No-RT and gDNA standard samples using RT1675 primers

g) NITROSATIVE STRESS EXPERIMENTS

Samples presented in different colours as follow; gDNA standards (Red lines), *M. tuberculosis* H37Rv (Dark pink), Δcmr (Dark Green) and Δcmr_{com} (Purple).

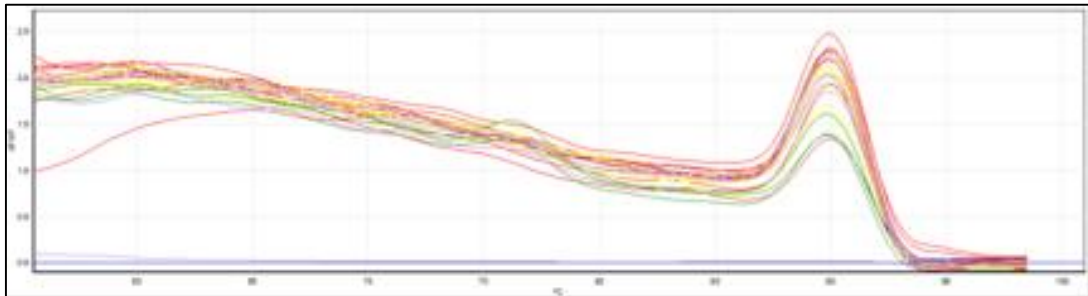


Figure- 36: Melting curves for *M. tuberculosis* wild-type, *cmr* deletion and complemented strains and gDNA standard samples using MYCO 16S primers from nitrosative stress experiment

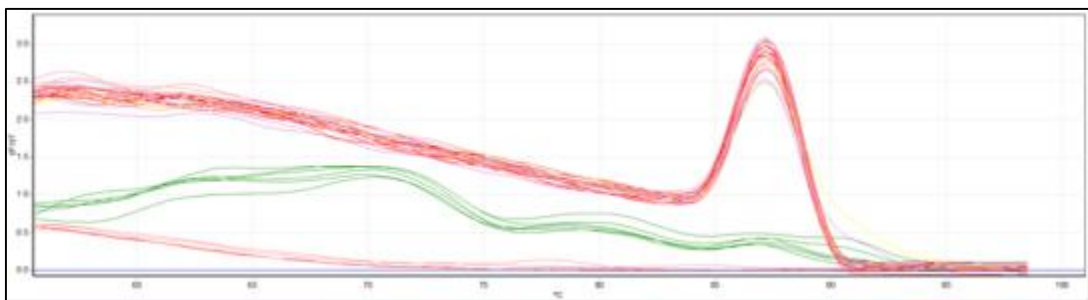


Figure- 37: Melting curves for *M. tuberculosis* wild-type, *cmr* deletion (green lines) and complemented strains and gDNA standard samples using RT1675 primers from nitrosative stress experiment

Appendix 8. **TARGET GENE COPY NUMBERS AND RELATIVE EXPRESSION VALUES**

Nutrient Starvation (n=6)		mRNA transcripts	
		<i>rv2661c</i>	ncRv12659
Exponential Growth	Copy numbers \pm SD	$(1.03X \pm 1.08) X10^6$	$(6.44X \pm 5.37) X10^5$
	Relative expression \pm SEM	$(7.5 \pm 2.30) X10^{-4}$	$(3.99 \pm 1.28) X10^{-4}$
Nutrient starvation- 24 hours	Copy numbers \pm SD	$(1.37X \pm 2.05) X10^5$	$(2.98X \pm 1.42) X10^6$
	Relative expression \pm SEM	$(2.39 \pm 1.36) X10^{-4}$	$3.6X10^{-3} \pm 9.9X10^{-4}$
Nutrient starvation- 96 hours	Copy numbers \pm SD	$(4.28X \pm 5.73) X10^4$	$2.33X10^6 \pm 8.53X10^5$
	Relative expression \pm SEM	$(5.4 \pm 2.1) X10^{-5}$	$(3.94 \pm 1.04) X10^{-3}$

Table- 1: Average target copy numbers generated and expression values of *rv2661c* and ncRv12659 post 24 and 96 hours during nutrient starvation relative to *16S*

5mM H ₂ O ₂ (n=2)		mRNA transcripts			
		<i>rv2660c</i>	<i>rv2661c</i>	<i>rv2662</i>	ncRv12659
Exponential Growth	Copy numbers \pm SD	$3.64X10^4 \pm 5.83X10^3$	$(3.89 \pm 2.06) X10^4$	$(2.27 \pm 1.25) X10^4$	$3.02X10^5 \pm 6.97X10^4$
	Relative expression \pm SEM	$(2.33 \pm 1.77) X10^{-6}$	$(1.92 \pm 1.18) X10^{-6}$	$(2.10 \pm 1.91) X10^{-6}$	$(2.41 \pm 2.06) X10^{-5}$
Oxidative stress- 40mins	Copy numbers \pm SD	$(3.89 \pm 2.5) X10^4$	$(8.34 \pm 4.77) X10^3$	$(5.05 \pm 1.1) X10^3$	$4.04X10^5 \pm 3.3X10^4$
	Relative expression \pm SEM	$(5.27 \pm 2.33) X10^{-6}$	$1.13X10^{-6} \pm 4.19X10^{-7}$	$(7.0 \pm 1.35) X10^{-7}$	$5.56X10^{-5} \pm 1.03X10^{-6}$

Table- 2: Average target copy numbers generated and expression values of *rv2660c*, *rv2661c*, *rv2662* and ncRv12659 post 40 minutes exposure to 5mM H₂O₂ relative to *16S*

25mM H ₂ O ₂ (n=3)		mRNA transcripts			
		<i>rv2660c</i>	<i>rv2661c</i>	<i>rv2662</i>	ncRv12659
Exponential Growth	Copy numbers ± SD	790±635	4901±3455	223±76	(6.67± 4.8) X10 ⁴
	Relative expression ± SEM	(8.18± 5.29) X10 ⁻⁶	1.20 X10 ⁻⁴ ± 9.2 X10 ⁻⁵	(3.85± 3.16) X10 ⁻⁶	(6.15± 4.19) X10 ⁻⁴
Oxidative stress-40mins	Copy numbers ± SD	604±673	5188±1555	304±187	(2.94± 1.58) X10 ⁴
	Relative expression ± SEM	(2.86± 2.35) X10 ⁻⁵	(2.09± 1.05) X10 ⁻⁴	(1.21± 1.2) X10 ⁻⁵	(8.53± 6.78) X10 ⁻⁴
Oxidative stress-4hours	Copy numbers ± SD	702±650	1964±821	94±47	(5.95± 5.36) X10 ⁴
	Relative expression ± SEM	1.96 X10 ⁻⁵ ± 9.87 X10 ⁻⁶	1.36 X10 ⁻⁴ ± 7.10 X10 ⁻⁵	(3.66± 3.60) X10 ⁻⁶	(4.63± 4.54) X10 ⁻³

Table- 3: Average target copy numbers generated and expression values of *rv2660c*, *rv2661c*, *rv2662* and ncRv12659 post 40 minutes and 4 hours exposure to 25 mM H₂O₂ relative to 16S

Acid pH5.3 (n=2)		mRNA transcripts		
		<i>rv2660c</i>	<i>rv2662</i>	ncRv12659
Exponential Growth	Copy numbers ± SD	1.31 X10 ⁵ ± 3.18 X10 ⁴	8.23 X10 ⁴ ± 6.32 X10 ³	2.53 X10 ⁵ ± 8.94 X10 ³
	Relative expression ± SEM	(1.7± 1.15) X10 ⁻⁴	1.44 X10 ⁻⁴ ± 4.5 X10 ⁻⁵	(4.84±1.28) X10 ⁻⁴
Acid stress-2 hours	Copy numbers ± SD	(3.56± 2.32) X10 ⁴	(1.46± 1.42) X10 ⁴	(6.37± 6.07) X10 ⁵
	Relative expression ± SEM	(2.91± 2.53) X10 ⁻⁴	(1.35± 1.24) X10 ⁻⁴	0.01± (1.85 X10 ⁻³)
Oxidative stress-4hours	Copy numbers ± SD	(7.85± 4.71) X10 ⁴	(2.01± 1.37) X10 ⁴	(6.17± 1.23) X10 ⁵
	Relative expression ± SEM	(3.45± 2.53) X10 ⁻⁵	(8.07± 5.63) X10 ⁻⁶	(3.80± 3.21) X10 ⁻⁴

Table- 4: Average target copy numbers generated and expression values of *rv2660c*, *rv2661c*, *rv2662* and ncRv12659 post 2 and 4 hours exposure to acidic pH of 5.3 relative to 16S

100μM NO donor		mRNA transcripts	
		Wild-type	Δcmr_{com}
Exponential Growth	Copy numbers \pm SD	$1.51 \times 10^4 \pm 6224$	$5.97 \times 10^3 \pm 2605$
	Relative expression \pm SD	$(7.96 \pm 5.71) \times 10^{-5}$	$(9.02 \pm 7.93) \times 10^{-5}$
Nitrosative stress- 40mins	Copy numbers \pm SD	$1.98 \times 10^4 \pm 2673$	$7.56 \times 10^3 \pm 8141$
	Relative expression \pm SD	$(2.61 \pm 2.51) \times 10^{-4}$	$(3.70 \pm 3.26) \times 10^{-5}$

Table- 5: Average target copy numbers and expression values generated post 40 minutes exposure to 100μM NO donor 6-methoxy-5-pyrimidin-4-yl pyrrolidine-1-carbodithiate relative to 16S

Appendix 9. **Publication**

REFERENCES

- AAGAARD, C., HOANG, T., DIETRICH, J., CARDONA, P. J., IZZO, A., DOLGANOV, G., SCHOOLNIK, G. K., CASSIDY, J. P., BILLESKOV, R. & ANDERSEN, P. 2011. A multistage tuberculosis vaccine that confers efficient protection before and after exposure. *Nat Med*, 17, 189-94.
- ADAMS, L., DINAUER, M., MORGENSTERN, D. & KRAHENBUHL, J. 1997. Comparison of the roles of reactive oxygen and nitrogen intermediates in the host response to *Mycobacterium tuberculosis* using transgenic mice. *Tubercle and Lung Disease*, 78, 237-246.
- AGARWAL, N., LAMICHHANE, G., GUPTA, R., NOLAN, S. & BISHAI, W. R. 2009. Cyclic AMP intoxication of macrophages by a *Mycobacterium tuberculosis* adenylate cyclase. *Nature*, 460, 98-102.
- AGARWAL, N., RAGHUNAND, T. R. & BISHAI, W. R. 2006. Regulation of the expression of whiB₁ in *Mycobacterium tuberculosis*: role of cAMP receptor protein. *Microbiology*, 152, 2749-2756.
- AINSA, J., MARTIN, C., CABEZA, M., DE LA CRUZ, F. & MENDIOLA, M. 1996. Construction of a family of *Mycobacterium*/*Escherichia coli* shuttle vectors derived from pAL5000 and pACYC184: their use for cloning an antibiotic-resistance gene from *Mycobacterium fortuitum*. *Gene*, 176, 23-26.
- AKHTER, Y., TUNDUP, S. & HASNAIN, S. E. 2007. Novel biochemical properties of a CRP/FNR family transcription factor from *Mycobacterium tuberculosis*. *International Journal of Medical Microbiology*, 297, 451-457.
- ALBRETHSEN, J., AGNER, J., PIERSMA, S. R., HØJRUP, P., PHAM, T. V., WELDINGH, K., JIMENEZ, C. R., ANDERSEN, P. & ROSENKRANDS, I. 2013. Proteomic profiling of *Mycobacterium tuberculosis* identifies nutrient-starvation-responsive toxin-antitoxin systems. *Molecular & Cellular Proteomics*, 12, 1180-1191.
- ALEXANDER, K. A., LAVER, P. N., VAN HELDEN, P. D., WARREN, R. M. & GEY VAN PITTIUS, N. C. 2010. Novel *Mycobacterium tuberculosis* complex pathogen, *M. mungi*.
- ANDERSEN, P. & DOHERTY, T. M. 2005. Opinion: The success and failure of BCG--implications for a novel tuberculosis vaccine. *Nature reviews. Microbiology*, 3, 656.
- ARNVIG, K. & YOUNG, D. 2012. Non-coding RNA and its potential role in *Mycobacterium tuberculosis* pathogenesis. *RNA Biol*, 9, 427-36.
- ARNVIG, K. B., COMAS, I., THOMSON, N. R., HOUGHTON, J., BOSHOFF, H. I., CROUCHER, N. J., ROSE, G., PERKINS, T. T., PARKHILL, J. & DOUGAN, G. 2011. Sequence-based analysis uncovers an abundance of non-coding RNA in the total transcriptome of *Mycobacterium tuberculosis*. *PLoS Pathog*, 7, e1002342.
- ARNVIG, K. B., CORTES, T. & YOUNG, D. B. 2014. Noncoding RNA in Mycobacteria. *Microbiology Spectrum*, 2.
- ARNVIG, K. B. & YOUNG, D. B. 2009. Identification of small RNAs in *Mycobacterium tuberculosis*. *Molecular microbiology*, 73, 397-408.

- ASENSIO, J. G., MAIA, C., FERRER, N. L., BARILONE, N., LAVAL, F., SOTO, C. Y., WINTER, N., DAFFÉ, M., GICQUEL, B. & MARTÍN, C. 2006. The virulence-associated two-component PhoP-PhoR system controls the biosynthesis of polyketide-derived lipids in *Mycobacterium tuberculosis*. *Journal of Biological Chemistry*, 281, 1313-1316.
- AUGENSTREICH, J., ARBUÉS, A., SIMEONE, R., HAANAPPEL, E., WEGENER, A., SAYES, F., LE CHEVALIER, F., CHALUT, C., MALAGA, W. & GUILHOT, C. 2017. ESX-1 and phthiocerol dimycocerosates of *Mycobacterium tuberculosis* act in concert to cause phagosomal rupture and host cell apoptosis. *Cellular microbiology*.
- AVERILL, B. A. & ELDREDGE, P. 2012. Principles of general chemistry. *Creative Commons*.
- BALASUBRAMANIAN, V., PAVELKA, M., BARDAROV, S. S., MARTIN, J., WEISBROD, T. R., MCADAM, R. A., BLOOM, B. R. & JACOBS, W. 1996. Allelic exchange in *Mycobacterium tuberculosis* with long linear recombination substrates. *Journal of bacteriology*, 178, 273-279.
- BARDAROV, S. 1997. Conditionally replicating mycobacteriophages: a system for transposon delivery to *Mycobacterium tuberculosis*. *Proc. Natl Acad. Sci. USA*, 94, 10961-10966.
- BARDAROV, S., BARDAROV JR, S., JR., PAVELKA JR, M. S., JR., SAMBANDAMURTHY, V., LARSEN, M., TUFARIELLO, J., CHAN, J., HATFULL, G. & JACOBS JR, W. R., JR. 2002. Specialized transduction: an efficient method for generating marked and unmarked targeted gene disruptions in *Mycobacterium tuberculosis*, *M. bovis* BCG and *M. smegmatis*. *Microbiology*, 148, 3007-17.
- BARRY, C. E., BOSHOFF, H. I., DARTOIS, V., DICK, T., EHRT, S., FLYNN, J., SCHNAPPINGER, D., WILKINSON, R. J. & YOUNG, D. 2009. The spectrum of latent tuberculosis: rethinking the biology and intervention strategies. *Nature reviews. Microbiology*, 7, 845-855.
- BARRY, C. E., CRICK, D. C. & MCNEIL, M. R. 2007. Targeting the formation of the cell wall core of *M. tuberculosis*. *Infectious Disorders-Drug Targets (Formerly Current Drug Targets-Infectious Disorders)*, 7, 182-202.
- BARTEK, I., RUTHERFORD, R., GRUPPO, V., MORTON, R., MORRIS, R., KLEIN, M., VISCONTI, K., RYAN, G., SCHOOLNIK, G. & LENAERTS, A. 2009. The DosR regulon of *M. tuberculosis* and antibacterial tolerance. *Tuberculosis*, 89, 310-316.
- BARTEK, I., WOOLHISER, L., BAUGHN, A., BASARABA, R., JACOBS, W., LENAERTS, A. & VOSKUIL, M. 2014. *Mycobacterium tuberculosis* Lsr2 is a global transcriptional regulator required for adaptation to changing oxygen levels and virulence. *MBio*, 5, e01106-14.
- BASARABA, R. J., DAILEY, D. D., MCFARLAND, C. T., SHANLEY, C. A., SMITH, E. E., MCMURRAY, D. N. & ORME, I. M. 2006. Lymphadenitis as a major element of disease in the guinea pig model of tuberculosis. *Tuberculosis*, 86, 386-394.
- BASTOS, R. G., BORSUK, S., SEIXAS, F. K. & DELLAGOSTIN, O. A. 2009. Recombinant *Mycobacterium bovis* BCG. *Vaccine*, 27, 6495-6503.
- BEDARD, K. & KRAUSE, K.-H. 2007. The NOX family of ROS-generating NADPH oxidases: physiology and pathophysiology. *Physiological Reviews*, 87, 245-313.

- BELISLE, J. T. & SONNENBERG, M. G. 1998. Isolation of Genomic DNA from Mycobacteria. *In*: PARISH, T. & STOKER, N. G. (eds.) *Mycobacteria Protocols*. Totowa, NJ: Humana Press.
- BESRA, G. S. 1998. Preparation of cell-wall fractions from mycobacteria. *Mycobacteria Protocols*, 91-107.
- BESRA, G. S. & CHATTERJEE, D. 1994. Lipids and carbohydrates of *Mycobacterium tuberculosis*. *Tuberculosis*. American Society of Microbiology.
- BETTS, J. C., LUKEY, P. T., ROBB, L. C., MCADAM, R. A. & DUNCAN, K. 2002. Evaluation of a nutrient starvation model of *Mycobacterium tuberculosis* persistence by gene and protein expression profiling. *Molecular Microbiology*, 43, 717-731.
- BIAU, D. J., KERNÉIS, S. & PORCHER, R. 2008. Statistics in brief: the importance of sample size in the planning and interpretation of medical research. *Clinical Orthopaedics and Related Research*, 466, 2282-2288.
- BIKETOV, S., MUKAMOLOVA, G. V., POTAPOV, V., GILENKOV, E., VOSTROKNUTOVA, G., KELL, D. B., YOUNG, M. & KAPRELYANTS, A. S. 2000. Culturability of *Mycobacterium tuberculosis* cells isolated from murine macrophages: a bacterial growth factor promotes recovery. *FEMS Immunology & Medical Microbiology*, 29, 233-240.
- BILLESKOV, R., TAN, E. V., CANG, M., ABALOS, R. M., BURGOS, J., PEDERSEN, B. V., CHRISTENSEN, D., AGGER, E. M. & ANDERSEN, P. 2016. Testing the H56 vaccine delivered in 4 different adjuvants as a BCG-booster in a non-human primate model of tuberculosis. *PLoS One*, 11, e0161217.
- BLEVINS, S. M. & BRONZE, M. S. 2010. Robert Koch and the 'golden age' of bacteriology. *International Journal of Infectious Diseases*, 14, e744-e751.
- BLOKPOEL, M. C., MURPHY, H. N., O'TOOLE, R., WILES, S., RUNN, E. S., STEWART, G. R., YOUNG, D. B. & ROBERTSON, B. D. 2005. Tetracycline-inducible gene regulation in mycobacteria. *Nucleic Acids Research*, 33, e22-e22.
- BOACHIE-ADJEI, O. & SQUILLANTE, R. G. 1996. Tuberculosis of the spine. *The Orthopedic clinics of North America*, 27, 95-103.
- BOON, C. & DICK, T. 2002. *Mycobacterium bovis* BCG response regulator essential for hypoxic dormancy. *Journal of Bacteriology*, 184, 6760-6767.
- BOON, C. & DICK, T. 2012. How *Mycobacterium tuberculosis* goes to sleep: the dormancy survival regulator DosR a decade later. *Future Microbiology*, 7, 513-518.
- BOSHOFF, H. I. & BARRY, C. E. 2005. Tuberculosis—metabolism and respiration in the absence of growth. *Nature Reviews Microbiology*, 3, 70-80.
- BRAIAN, C., SVENSSON, M., BRIGHENTI, S., LERM, M. & PARASA, V. R. 2015. A 3D Human Lung Tissue Model for Functional Studies on *Mycobacterium tuberculosis* Infection. *J Vis Exp*.
- BRETL, D. J., DEMETRIADOU, C. & ZAHRT, T. C. 2011. Adaptation to environmental stimuli within the host: two-component signal transduction systems of *Mycobacterium tuberculosis*. *Microbiology and Molecular Biology Reviews*, 75, 566-582.
- BROSCH, R., GORDON, S. V., MARMIESSE, M., BRODIN, P., BUCHRIESER, C., EIGLMEIER, K., GARNIER, T., GUTIERREZ, C., HEWINSON, G. & KREMER, K.

2002. A new evolutionary scenario for the *Mycobacterium tuberculosis* complex. *Proceedings of the National Academy of Sciences*, 99, 3684-3689.
- BROWN, A. C. & PARISH, T. 2006. Instability of the acetamide-inducible expression vector pJAM2 in *Mycobacterium tuberculosis*. *Plasmid*, 55, 81-86.
- BUSTIN, S., BENES, V., NOLAN, T. & PFAFFL, M. 2005. Quantitative real-time RT-PCR—a perspective. *Journal of Molecular Endocrinology*, 34, 597-601.
- BUSTIN, S. A., BENES, V., GARSON, J. A., HELLEMANS, J., HUGGETT, J., KUBISTA, M., MUELLER, R., NOLAN, T., PFAFFL, M. W. & SHIPLEY, G. L. 2009. The MIQE guidelines: minimum information for publication of quantitative real-time PCR experiments. *Clinical Chemistry*, 55, 611-622.
- BUTLER, R. E., BRODIN, P., JANG, J., JANG, M.-S., ROBERTSON, B. D., GICQUEL, B. & STEWART, G. R. 2012. The balance of apoptotic and necrotic cell death in *Mycobacterium tuberculosis* infected macrophages is not dependent on bacterial virulence. *PLoS One*, 7, e47573.
- CAMACHO, L. R., ENSERGUEIX, D., PEREZ, E., GICQUEL, B. & GUILHOT, C. 1999. Identification of a virulence gene cluster of *Mycobacterium tuberculosis* by signature-tagged transposon mutagenesis. *Molecular Microbiology*, 34, 257-267.
- CAMUS, J.-C., PRYOR, M. J., MÉDIGUE, C. & COLE, S. T. 2002. Re-annotation of the genome sequence of *Mycobacterium tuberculosis* H37Rv. *Microbiology*, 148, 2967-2973.
- CANETTI, G. 1955. The tubercle bacillus in the pulmonary lesion of man: histobacteriology and its bearing on the therapy of pulmonary tuberculosis. Springer Publishing Company.
- CARDONA, P.-J. 2007. New insights on the nature of latent tuberculosis infection and its treatment. *Inflammation & Allergy-Drug Targets (Formerly Current Drug Targets-Inflammation & Allergy)*, 6, 27-39.
- CHADHA, V. 1997. Global trends of tuberculosis-an epidemiological review. *NTI Bulletin*, 33, 11-18.
- CHAITANKAR, V., KARAKÜLAH, G., RATNAPRIYA, R., GIUSTE, F. O., BROOKS, M. J. & SWAROOP, A. 2016. Next generation sequencing technology and genomewide data analysis: Perspectives for retinal research. *Progress in Retinal and Eye Research*, 55, 1-31.
- CHAUHAN, A., MADIRAJU, M. V., FOL, M., LOFTON, H., MALONEY, E., REYNOLDS, R. & RAJAGOPALAN, M. 2006. *Mycobacterium tuberculosis* cells growing in macrophages are filamentous and deficient in FtsZ rings. *Journal of Bacteriology*, 188, 1856-1865.
- CHEAH, E. S., MALKIN, J., FREE, R. C., LEE, S.-M., PERERA, N., WOLTMANN, G., PATEL, H., KIMMITT, P. T., SMITH, R. J. & RAJAKUMAR, K. 2010. A two-tube combined Taqman/SYBR Green assay to identify mycobacteria and detect single global lineage-defining polymorphisms in *Mycobacterium tuberculosis*. *The Journal of Molecular Diagnostics*, 12, 250-256.
- CHENGALROYEN, M. D., BEUKES, G. M., GORDHAN, B. G., STREICHER, E. M., CHURCHYARD, G., HAFNER, R., WARREN, R., OTWOMBE, K., MARTINSON, N. & KANA, B. D. 2016. Detection and quantification of differentially culturable tubercle bacteria in sputum from patients with tuberculosis. *American Journal of Respiratory and Critical Care Medicine*, 194, 1532-1540.

- CHOI, H.-S., RAI, P. R., CHU, H. W., COOL, C. & CHAN, E. D. 2002. Analysis of nitric oxide synthase and nitrotyrosine expression in human pulmonary tuberculosis. *American Journal of Respiratory and Critical Care Medicine*, 166, 178-186.
- CHOLO, M., BOSHOFF, H., STEEL, H., COCKERAN, R., MATLOLA, N., DOWNING, K., MIZRAHI, V. & ANDERSON, R. 2006. Effects of clofazimine on potassium uptake by a Trk-deletion mutant of *Mycobacterium tuberculosis*. *Journal of Antimicrobial Chemotherapy*, 57, 79-84.
- CHOUDHARY, E., BISHAI, W. & AGARWAL, N. 2014. Expression of a subset of heat stress induced genes of *Mycobacterium tuberculosis* is regulated by 3',5'-cyclic AMP. *PLoS One*, 9, e89759.
- CHOUDHARY, E., THAKUR, P., PAREEK, M. & AGARWAL, N. 2015. Gene silencing by CRISPR interference in mycobacteria. *Nature Communications*, 6.
- CINGOLANI, P. 2012. snpEff: Variant effect prediction.
- CIRILLO, J. D., BARLETTA, R. G., BLOOM, B. R. & JACOBS, W. R., JR. 1991. A novel transposon trap for mycobacteria: isolation and characterization of IS1096. *J Bacteriol*, 173, 7772-80.
- COLANGELI, R., HAQ, A., ARCUS, V. L., SUMMERS, E., MAGLIOZZO, R. S., MCBRIDE, A., MITRA, A. K., RADJAINIA, M., KHAJO, A., JACOBS, W. R., JR., SALGAME, P. & ALLAND, D. 2009. The multifunctional histone-like protein Lsr2 protects mycobacteria against reactive oxygen intermediates. *Proc Natl Acad Sci U S A*, 106, 4414-8.
- COLANGELI, R., HELB, D., VILCHÈZE, C., HAZBÓN, M. H., LEE, C.-G., SAFI, H., SAYERS, B., SARDONE, I., JONES, M. B. & FLEISCHMANN, R. D. 2007. Transcriptional regulation of multi-drug tolerance and antibiotic-induced responses by the histone-like protein Lsr2 in *M. tuberculosis*. *PLoS Pathogens*, 3, e87.
- COLE, S., BROSCH, R., PARKHILL, J., GARNIER, T., CHURCHER, C., HARRIS, D., GORDON, S., EIGLMEIER, K., GAS, S. & BARRY, C. R. 1998. Deciphering the biology of *Mycobacterium tuberculosis* from the complete genome sequence. *Nature*, 393, 537-544.
- COLE, S. T. 1998. Deciphering the biology of *Mycobacterium tuberculosis* from the complete genome sequence. *Nature*, 393, 537-544.
- CONG, L., RAN, F. A., COX, D., LIN, S., BARRETTO, R., HABIB, N., HSU, P. D., WU, X., JIANG, W. & MARRAFFINI, L. A. 2013. Multiplex genome engineering using CRISPR/Cas systems. *Science*, 339, 819-823.
- COOPER, A. M., SEGAL, B. H., FRANK, A. A., HOLLAND, S. M. & ORME, I. M. 2000. Transient loss of resistance to pulmonary tuberculosis in p47 phox^{-/-} mice. *Infection and Immunity*, 68, 1231-1234.
- CORTES, T., SCHUBERT, O. T., ROSE, G., ARNVIG, K. B., COMAS, I., AEBERSOLD, R. & YOUNG, D. B. 2013. Genome-wide mapping of transcriptional start sites defines an extensive leaderless transcriptome in *Mycobacterium tuberculosis*. *Cell Rep*, 5, 1121-31.
- COX, M. P., PETERSON, D. A. & BIGGS, P. J. 2010. SolexaQA: At-a-glance quality assessment of Illumina second-generation sequencing data. *BMC Bioinformatics*, 11, 485.
- CRUBÉZY, E., LUDES, B., POVEDA, J.-D., CLAYTON, J., CROUAU-ROY, B. & MONTAGNON, D. 1998. Identification of *Mycobacterium* DNA in an Egyptian

- Pott's disease of 5400 years old. *Comptes Rendus de l'Académie des Sciences - Series III - Sciences de la Vie*, 321, 941-951.
- CUNNINGHAM-BUSSEL, A., ZHANG, T. & NATHAN, C. F. 2013. Nitrite produced by *Mycobacterium tuberculosis* in human macrophages in physiologic oxygen impacts bacterial ATP consumption and gene expression. *Proceedings of the National Academy of Sciences*, 110, E4256-E4265.
- CURRY, J. M., WHALAN, R., HUNT, D. M., GOHIL, K., STROM, M., RICKMAN, L., COLSTON, M. J., SMERDON, S. J. & BUXTON, R. S. 2005. An ABC transporter containing a forkhead-associated domain interacts with a serine-threonine protein kinase and is required for growth of *Mycobacterium tuberculosis* in mice. *Infection and Immunity*, 73, 4471-4477.
- DANIEL, J., DEB, C., DUBEY, V. S., SIRAKOVA, T. D., ABOMOELAK, B., MORBIDONI, H. R. & KOLATTUKUDY, P. E. 2004. Induction of a novel class of diacylglycerol acyltransferases and triacylglycerol accumulation in *Mycobacterium tuberculosis* as it goes into a dormancy-like state in culture. *Journal of Bacteriology*, 186, 5017-5030.
- DANIEL, J., MAAMAR, H., DEB, C., SIRAKOVA, T. D. & KOLATTUKUDY, P. E. 2011. *Mycobacterium tuberculosis* uses host triacylglycerol to accumulate lipid droplets and acquires a dormancy-like phenotype in lipid-loaded macrophages. *PLoS Pathogens*, 7, e1002093.
- DANIEL, T. M. 2006. The history of tuberculosis. *Respiratory Medicine*, 100, 1862-1870.
- DANNENBERG JR, A. M. & ROOK, G. A. 1994. Pathogenesis of pulmonary tuberculosis: an interplay of tissue-damaging and macrophage-activating immune responses—dual mechanisms that control bacillary multiplication. *Tuberculosis*. American Society of Microbiology.
- DAVIS, J. M., CLAY, H., LEWIS, J. L., GHORI, N., HERBOMEL, P. & RAMAKRISHNAN, L. 2002. Real-time visualization of mycobacterium-macrophage interactions leading to initiation of granuloma formation in zebrafish embryos. *Immunity*, 17, 693-702.
- DEB, C., LEE, C.-M., DUBEY, V. S., DANIEL, J., ABOMOELAK, B., SIRAKOVA, T. D., PAWAR, S., ROGERS, L. & KOLATTUKUDY, P. E. 2009. A novel in vitro multiple-stress dormancy model for *Mycobacterium tuberculosis* generates a lipid-loaded, drug-tolerant, dormant pathogen. *PLoS One*, 4, e6077.
- DEJESUS, M. A., GERRICK, E. R., XU, W., PARK, S. W., LONG, J. E., BOUTTE, C. C., RUBIN, E. J., SCHNAPPINGER, D., EHRT, S. & FORTUNE, S. M. 2017. Comprehensive essentiality analysis of the *Mycobacterium tuberculosis* genome via saturating transposon mutagenesis. *MBio*, 8, e02133-16.
- DELTCHEVA, E., CHYLINSKI, K., SHARMA, C. M., GONZALES, K., CHAO, Y., PIRZADA, Z. A., ECKERT, M. R., VOGEL, J. & CHARPENTIER, E. 2011. CRISPR RNA maturation by trans-encoded small RNA and host factor RNase III. *Nature*, 471, 602-607.
- DEN HENGST, C. D. & BUTTNER, M. J. 2008. Redox control in actinobacteria. *Biochimica et Biophysica Acta (BBA)-General Subjects*, 1780, 1201-1216.
- DEPRISTO, M. A., BANKS, E., POPLIN, R., GARIMELLA, K. V., MAGUIRE, J. R., HARTL, C., PHILIPPAKIS, A. A., DEL ANGEL, G., RIVAS, M. A. & HANNA, M. 2011. A framework for variation discovery and genotyping using next-generation DNA sequencing data. *Nature Genetics*, 43, 491-498.

- DIETRICH, J., AAGAARD, C., LEAH, R., OLSEN, A. W., STRYHN, A., DOHERTY, T. M. & ANDERSEN, P. 2005. Exchanging ESAT6 with TB10.4 in an Ag85B fusion molecule-based tuberculosis subunit vaccine: efficient protection and ESAT6-based sensitive monitoring of vaccine efficacy. *J Immunol*, 174, 6332-9.
- DOBSON, G., MINNIKIN, D. E., MINNIKIN, S. M., PARLETT, J. H., GOODFELLOW, M., RIDELL, M. & MAGNUSSON, M. 1985. Systematic analysis of complex mycobacterial lipids. *Society for Applied Bacteriology. Technical Series*, 237-265.
- DOMENECH, P. & REED, M. B. 2009. Rapid and spontaneous loss of phthiocerol dimycocerosate (PDIM) from *Mycobacterium tuberculosis* grown in vitro: implications for virulence studies. *Microbiology*, 155, 3532-3543.
- DOS VULTOS, T., MÉDERLÉ, I., ABADIE, V., PIMENTEL, M., MONIZ-PEREIRA, J., GICQUEL, B., REYRAT, J.-M. & WINTER, N. 2006. Modification of the mycobacteriophage Ms6 attP core allows the integration of multiple vectors into different tRNA ala T-loops in slow-and fast-growing mycobacteria. *BMC Molecular Biology*, 7, 47.
- DRAGHICI, S., KHATRI, P., EKLUND, A. C. & SZALLASI, Z. 2006. Reliability and reproducibility issues in DNA microarray measurements. *Trends in Genetics : TIG*, 22, 101-109.
- DRUMM, J. E., MI, K., BILDER, P., SUN, M., LIM, J., BIELEFELDT-OHMANN, H., BASARABA, R., SO, M., ZHU, G., TUFARIELLO, J. M., IZZO, A. A., ORME, I. M., ALMO, S. C., LEYH, T. S. & CHAN, J. 2009. *Mycobacterium tuberculosis* universal stress protein Rv2623 regulates bacillary growth by ATP-Binding: requirement for establishing chronic persistent infection. *PLoS Pathogens*, 5, e1000460.
- DUNN, P. L. & NORTH, R. 1996. Persistent infection with virulent but not avirulent *Mycobacterium tuberculosis* in the lungs of mice causes progressive pathology. *Journal of Medical Microbiology*, 45, 103-109.
- ECONOMIC, U. N. D. O., AFFAIRS, S. & DIVISION, P. 2015. World Population Prospects: The 2015 Revision, Key Findings and Advance Tables. *Working Paper, No. ESA/P/WP. 241*.
- EHLERS, S. & SCHAIBLE, U. E. 2012. The Granuloma in Tuberculosis: Dynamics of a Host-Pathogen Collusion. *Frontiers in Immunology*, 3, 411.
- EHRT, S., GUO, X. V., HICKEY, C. M., RYOU, M., MONTELEONE, M., RILEY, L. W. & SCHNAPPINGER, D. 2005. Controlling gene expression in mycobacteria with anhydrotetracycline and Tet repressor. *Nucleic Acids Research*, 33, e21-e21.
- EHRT, S. & SCHNAPPINGER, D. 2006. Controlling gene expression in mycobacteria. *Future Microbiology*, 1, 177-184.
- EHRT, S. & SCHNAPPINGER, D. 2009. Mycobacterial survival strategies in the phagosome: defence against host stresses. *Cell Microbiol*, 11, 1170-8.
- EL-NAJJAR, M., AL-SHIYAB, A. & AL-SARIE, I. 1996. Cases of tuberculosis at'Ain Ghazal, Jordan. *Paléorient*, 123-128.
- EL-ROBH, M. S. & BUSBY, S. J. 2002. The *Escherichia coli* cAMP receptor protein bound at a single target can activate transcription initiation at divergent promoters: a systematic study that exploits new promoter probe plasmids. *Biochemical Journal*, 368, 835-843.

- ESMAIL, H., BARRY, C. E., YOUNG, D. B. & WILKINSON, R. J. 2014. The ongoing challenge of latent tuberculosis. *Philosophical Transactions of the Royal Society B: Biological Sciences*, 369.
- EUROPEAN CONCERTED ACTION ON NEW GENERATION GENETIC MARKERS AND TECHNIQUES FOR THE EPIDEMIOLOGY AND CONTROL OF TUBERCULOSIS 2006. Beijing/W genotype *Mycobacterium tuberculosis* and drug resistance. *Emerg Infect Dis*, 12, 736-43.
- FALGUERAS, J., LARA, A. J., FERNÁNDEZ-POZO, N., CANTÓN, F. R., PÉREZ-TRABADO, G. & CLAROS, M. G. 2010. SeqTrim: a high-throughput pipeline for pre-processing any type of sequence read. *BMC Bioinformatics*, 11, 38.
- FALLOW, A., DOMENECH, P. & REED, M. B. 2010. Strains of the East Asian (W/Beijing) Lineage of *Mycobacterium tuberculosis* Are DosS/DosT-DosR Two-Component Regulatory System Natural Mutants. *Journal of Bacteriology*, 192, 2228-2238.
- FEINER, R., ARGOV, T., RABINOVICH, L., SIGAL, N., BOROVOK, I. & HERSKOVITS, A. A. 2015. A new perspective on lysogeny: prophages as active regulatory switches of bacteria. *Nat Rev Micro*, 13, 641-650.
- FINE, P. E. 1995. Variation in protection by BCG: implications of and for heterologous immunity. *Lancet*, 346, 1339-45.
- FIRMANI, M. A. & RILEY, L. W. 2002. Reactive nitrogen intermediates have a bacteriostatic effect on *Mycobacterium tuberculosis* in vitro. *Journal of Clinical Microbiology*, 40, 3162-3166.
- FLYNN, J., CHAN, J. & LIN, P. 2011. Macrophages and control of granulomatous inflammation in tuberculosis. *Mucosal Immunology*, 4, 271.
- FLYNN, J. L. 2006. Lessons from experimental *Mycobacterium tuberculosis* infections. *Microbes and Infection*, 8, 1179-1188.
- FLYNN, J. L. & CHAN, J. 2001. Tuberculosis: latency and reactivation. *Infection and Immunity*, 69, 4195-4201.
- FLYNN, J. L., SCANGA, C. A., TANAKA, K. E. & CHAN, J. 1998. Effects of aminoguanidine on latent murine tuberculosis. *The Journal of Immunology*, 160, 1796-1803.
- FORRELLAD, M. A., KLEPP, L. I., GIOFFRÉ, A., SABIO Y GARCIA, J., MORBIDONI, H. R., SANTANGELO, M. D. L. P., CATALDI, A. A. & BIGI, F. 2013. Virulence factors of the *Mycobacterium tuberculosis* complex. *Virulence*, 4, 3-66.
- FORTI, F., CROSTA, A. & GHISOTTI, D. 2009. Pristinamycin-inducible gene regulation in mycobacteria. *Journal of Biotechnology*, 140, 270-277.
- FORTUNE, S., JAEGER, A., SARRACINO, D., CHASE, M., SASSETTI, C., SHERMAN, D., BLOOM, B. & RUBIN, E. 2005. Mutually dependent secretion of proteins required for mycobacterial virulence. *Proceedings of the National Academy of Sciences of the United States of America*, 102, 10676-10681.
- FRITH, J. 2014. History of tuberculosis. Part 1-phthisis, consumption and the white plague. *Journal of Military and Veterans Health*, 22, 29.
- GALAGAN, J. E., MINCH, K., PETERSON, M., LYUBETSKAYA, A., AZIZI, E., SWEET, L., GOMES, A., RUSTAD, T., DOLGANOV, G. & GLOTOVA, I. 2013. The *Mycobacterium tuberculosis* regulatory network and hypoxia. *Nature*, 499, 178-183.

- GALILI, E., WEINSTEIN-EVRON, M., HERSHKOVITZ, I., GOPHER, A., KISLEV, M., LERNAU, O., KOLSKA-HORWITZ, L. & LERNAUT, H. 1993. Atlit-Yam: A prehistoric site on the sea floor off the Israeli coast. *Journal of Field Archaeology*, 20, 133-157.
- GARTON, N. J., CHRISTENSEN, H., MINNIKIN, D. E., ADEGBOLA, R. A. & BARER, M. R. 2002. Intracellular lipophilic inclusions of mycobacteria in vitro and in sputum. *Microbiology*, 148, 2951-2958.
- GARTON, N. J., WADDELL, S. J., SHERRATT, A. L., LEE, S.-M., SMITH, R. J., SENNER, C., HINDS, J., RAJAKUMAR, K., ADEGBOLA, R. A. & BESRA, G. S. 2008. Cytological and transcript analyses reveal fat and lazy persistor-like bacilli in tuberculous sputum. *PLoS Med*, 5, e75.
- GAUTAM, U. S., MCGILLIVRAY, A., MEHRA, S., DIDIER, P. J., MIDKIFF, C. C., KISSEE, R. S., GOLDEN, N. A., ALVAREZ, X., NIU, T. & RENGARAJAN, J. 2015a. DosS is required for the complete virulence of *Mycobacterium tuberculosis* in mice with classical granulomatous lesions. *American Journal of Respiratory Cell and Molecular Biology*, 52, 708-716.
- GAUTAM, U. S., MEHRA, S. & KAUSHAL, D. 2015b. In-vivo gene signatures of *Mycobacterium tuberculosis* in C3HeB/FeJ mice. *PloS One*, 10, e0135208.
- GAWRONSKI, J. D., WONG, S. M., GIANNOUKOS, G., WARD, D. V. & AKERLEY, B. J. 2009. Tracking insertion mutants within libraries by deep sequencing and a genome-wide screen for Haemophilus genes required in the lung. *Proceedings of the National Academy of Sciences*, 106, 16422-16427.
- GAZDIK, M. A., BAI, G., WU, Y. & MCDONOUGH, K. A. 2009. Rv1675c (cmr) regulates intramacrophage and cyclic AMP-induced gene expression in *Mycobacterium tuberculosis*-complex mycobacteria. *Mol Microbiol*, 71, 434-48.
- GAZI, M. A., KIBRIA, M. G., MAHFUZ, M., ISLAM, M. R., GHOSH, P., AFSAR, M. N. A., KHAN, M. A. & AHMED, T. 2016. Functional, structural and epitopic prediction of hypothetical proteins of *Mycobacterium tuberculosis* H37Rv: An in silico approach for prioritizing the targets. *Gene*, 591, 442-455.
- GENGENBACHER, M. & KAUFMANN, S. H. 2012. *Mycobacterium tuberculosis*: success through dormancy. *FEMS Microbiology Reviews*, 36, 514-532.
- GENGENBACHER, M., RAO, S. P., PETHE, K. & DICK, T. 2010. Nutrient-starved, non-replicating *Mycobacterium tuberculosis* requires respiration, ATP synthase and isocitrate lyase for maintenance of ATP homeostasis and viability. *Microbiology*, 156, 81-87.
- GETAHUN, H., GUNNEBERG, C., GRANICH, R. & NUNN, P. 2010. HIV infection—associated tuberculosis: the epidemiology and the response. *Clinical Infectious Diseases*, 50, S201-S207.
- GETAHUN, H., HARRINGTON, M., O'BRIEN, R. & NUNN, P. 2007. Diagnosis of smear-negative pulmonary tuberculosis in people with HIV infection or AIDS in resource-constrained settings: informing urgent policy changes. *The Lancet*, 369, 2042-2049.
- GLOBAL TB ALLIANCE. *TB Alliance* [Online]. Available: <https://www.tballiance.org/> [Accessed 20th August 2017].
- GOMEZ, J. E. & MCKINNEY, J. D. 2004. *M. tuberculosis* persistence, latency, and drug tolerance. *Tuberculosis*, 84, 29-44.

- GONZALO-ASENSIO, J., MALAGA, W., PAWLIK, A., ASTARIE-DEQUEKER, C., PASSEMAR, C., MOREAU, F., LAVAL, F., DAFFÉ, M., MARTIN, C. & BROSCHE, R. 2014. Evolutionary history of tuberculosis shaped by conserved mutations in the PhoPR virulence regulator. *Proceedings of the National Academy of Sciences*, 111, 11491-11496.
- GORDHAN, B. G., SMITH, D. A., KANA, B. D., BANCROFT, G. & MIZRAHI, V. 2006. The carbon starvation-inducible genes Rv2557 and Rv2558 of *Mycobacterium tuberculosis* are not required for long-term survival under carbon starvation and for virulence in SCID mice. *Tuberculosis*, 86, 430-437.
- GOREN, M. B., BROKL, O. & SCHAEFER, W. B. 1974. Lipids of putative relevance to virulence in *Mycobacterium tuberculosis*: correlation of virulence with elaboration of sulfatides and strongly acidic lipids. *Infection and Immunity*, 9, 142-149.
- GOULD, T. A., VAN DE LANGEMHEEN, H., MUÑOZ-ELÍAS, E. J., MCKINNEY, J. D. & SACCHETTINI, J. C. 2006. Dual role of isocitrate lyase 1 in the glyoxylate and methylcitrate cycles in *Mycobacterium tuberculosis*. *Molecular Microbiology*, 61, 940-947.
- GOVENDER, L., ABEL, B., HUGHES, E. J., SCRIBA, T. J., KAGINA, B. M., DE KOCK, M., WALZL, G., BLACK, G., ROSENKRANDS, I. & HUSSEY, G. D. 2010. Higher human CD4 T cell response to novel *Mycobacterium tuberculosis* latency associated antigens Rv2660 and Rv2659 in latent infection compared with tuberculosis disease. *Vaccine*, 29, 51-57.
- GRIFFIN, J. E., GAWRONSKI, J. D., DEJESUS, M. A., IOERGER, T. R., AKERLEY, B. J. & SASSETTI, C. M. 2011. High-resolution phenotypic profiling defines genes essential for mycobacterial growth and cholesterol catabolism. *PLoS Pathogens*, 7, e1002251.
- GUIRADO, E. & SCHLESINGER, L. S. 2013. Modeling the *Mycobacterium tuberculosis* Granuloma – the Critical Battlefield in Host Immunity and Disease. *Frontiers in Immunology*, 4, 98.
- GUPTA, M., NAYYAR, N., CHAWLA, M., SITARAMAN, R., BHATNAGAR, R. & BANERJEE, N. 2016. The Chromosomal parDE2 Toxin–Antitoxin System of *Mycobacterium tuberculosis* H37Rv: Genetic and Functional Characterization. *Frontiers in Microbiology*, 7.
- GUPTA, U. & KATOCH, V. 2005. Animal models of tuberculosis. *Tuberculosis*, 85, 277-293.
- GUTIERREZ, M. C., BRISSE, S., BROSCHE, R., FABRE, M., OMAÏS, B., MARMIESSE, M., SUPPLY, P. & VINCENT, V. 2005. Ancient origin and gene mosaicism of the progenitor of *Mycobacterium tuberculosis*. *PLoS Pathogens*, 1, e5.
- HAAS, D. & DES PREZ, R. 1995. *Mycobacterium tuberculosis*. Principles and Practice of Infectious Diseases, 4th ed. New York: Churchill Livingstone Inc.
- HAMMOND, R. J., BARON, V. O., ORAVCOVA, K., LIPWORTH, S. & GILLESPIE, S. H. 2015. Phenotypic resistance in mycobacteria: is it because I am old or fat that I resist you? *Journal of Antimicrobial Chemotherapy*, 70, 2823-2827.
- HANING, K., CHO, S. H. & CONTRERAS, L. M. 2014. Small RNAs in mycobacteria: an unfolding story. *Front Cell Infect Microbiol*, 4, 96.
- HARPER, J., SKERRY, C., DAVIS, S. L., TASNEEN, R., WEIR, M., KRAMNIK, I., BISHAI, W. R., POMPER, M. G., NUERMBERGER, E. L. & JAIN, S. K. 2011. Mouse model

- of necrotic tuberculosis granulomas develops hypoxic lesions. *Journal of Infectious Diseases*, jir786.
- HAWGOOD, B. J. 2007. Albert Calmette (1863–1933) and Camille Guérin (1872–1961): the C and G of BCG vaccine. *Journal of Medical Biography*, 15, 139-146.
- HE, H., YANG, H. & DENG, Y. 2015. *Mycobacterium tuberculosis* dormancy-associated antigen of Rv2660c induces stronger immune response in latent *Mycobacterium tuberculosis* infection than that in active tuberculosis in a Chinese population. *Eur J Clin Microbiol Infect Dis*, 34, 1103-9.
- HERSHKOVITZ, I., DONOGHUE, H. D., MINNIKIN, D. E., MAY, H., LEE, O. Y.-C., FELDMAN, M., GALILI, E., SPIGELMAN, M., ROTHSCHILD, B. M. & BAR-GAL, G. K. 2015. Tuberculosis origin: the Neolithic scenario. *Tuberculosis*, 95, S122-S126.
- HERZOG, H. 1998. History of tuberculosis. *Respiration*, 65, 5-15.
- HICKEY, M. J., ARAIN, T. M., SHAWAR, R. M., HUMBLE, D. J., LANGHORNE, M. H., MORGENROTH, J. N. & STOVER, C. K. 1996. Luciferase in vivo expression technology: use of recombinant mycobacterial reporter strains to evaluate antimycobacterial activity in mice. *Antimicrobial Agents and Chemotherapy*, 40, 400-407.
- HISERT, K. B., KIRKSEY, M. A., GOMEZ, J. E., SOUSA, A. O., COX, J. S., JACOBS, W. R., NATHAN, C. F. & MCKINNEY, J. D. 2004. Identification of *Mycobacterium tuberculosis* counterimmune (cim) mutants in immunodeficient mice by differential screening. *Infection and Immunity*, 72, 5315-5321.
- HOANG, T., AAGAARD, C., DIETRICH, J., CASSIDY, J. P., DOLGANOV, G., SCHOOLNIK, G. K., LUNDBERG, C. V., AGGER, E. M. & ANDERSEN, P. 2013. ESAT-6 (EsxA) and TB10.4 (EsxH) Based Vaccines for Pre- and Post-Exposure Tuberculosis Vaccination. *PLoS One*, 8, e80579.
- HOUBEN, R. M. & DODD, P. J. 2016. The global burden of latent tuberculosis infection: a re-estimation using mathematical modelling. *PLoS Medicine*, 13, e1002152.
- HOUGHTON, J. 2015. *The Regulatory Role of sRNAs in Mycobacterium tuberculosis*. Doctor of Philosophy, University College London.
- HOUGHTON, J., CORTES, T., SCHUBERT, O., ROSE, G., RODGERS, A., CROIX, M. D. S., AEBERSOLD, R., YOUNG, D. B. & ARNVIG, K. B. 2013. A small RNA encoded in the Rv2660c locus of *Mycobacterium tuberculosis* is induced during starvation and infection. *PloS One*, 8, e80047.
- HU, X., LI, X., HUANG, L., CHAN, J., CHEN, Y., DENG, H. & MI, K. 2015a. Quantitative proteomics reveals novel insights into isoniazid susceptibility in mycobacteria mediated by a universal stress protein. *Journal of Proteome Research*, 14, 1445-1454.
- HU, Y. & COATES, A. R. 2009. Acute and persistent *Mycobacterium tuberculosis* infections depend on the thiol peroxidase TpX. *PLoS One*, 4, e5150.
- HU, Y., LIU, A., ORTEGA-MURO, F., ALAMEDA-MARTIN, L., MITCHISON, D. & COATES, A. 2015b. High-dose rifampicin kills persisters, shortens treatment duration, and reduces relapse rate in vitro and in vivo. *Frontiers in Microbiology*, 6, 641-641.

- HUGHES, P., MARSHALL, D., REID, Y., PARKES, H. & GELBER, C. 2007. The costs of using unauthenticated, over-passaged cell lines: how much more data do we need? *Biotechniques*, 43, 575.
- HUNTER, R. L. 2016. Tuberculosis as a three-act play: A new paradigm for the pathogenesis of pulmonary tuberculosis. *Tuberculosis*, 97, 8-17.
- HUSSON, R., JAMES, B. & YOUNG, R. 1990. Gene replacement and expression of foreign DNA in mycobacteria. *Journal of Bacteriology*, 172, 519-524.
- HUTCHISON, C. A., PETERSON, S. N., GILL, S. R., CLINE, R. T., WHITE, O., FRASER, C. M., SMITH, H. O. & VENTER, J. C. 1999. Global transposon mutagenesis and a minimal Mycoplasma genome. *Science*, 286, 2165-2169.
- IGNARRO, L. J. 1989. Endothelium-derived nitric oxide: actions and properties. *The FASEB Journal*, 3, 31-36.
- IGNATOV, D. V., SALINA, E. G., FURSOV, M. V., SKVORTSOV, T. A., AZHIKINA, T. L. & KAPRELYANTS, A. S. 2015. Dormant non-culturable *Mycobacterium tuberculosis* retains stable low-abundant mRNA. *BMC Genomics*, 16, 954.
- IM, J.-G., ITOH, H., LEE, K. S. & HAN, M. C. 1995. CT-pathology correlation of pulmonary tuberculosis. *Critical reviews in diagnostic imaging*, 36, 227-285.
- IMLAY, J. A. 2008. Cellular defenses against superoxide and hydrogen peroxide. *Annu. Rev. Biochem.*, 77, 755-776.
- IMLAY, J. A. 2013. The molecular mechanisms and physiological consequences of oxidative stress: lessons from a model bacterium. *Nature Reviews Microbiology*, 11, 443-454.
- IONA, E., PARDINI, M., GAGLIARDI, M. C., COLONE, M., STRINGARO, A. R., TELONI, R., BRUNORI, L., NISINI, R., FATTORINI, L. & GIANNONI, F. 2012. Infection of human THP-1 cells with dormant *Mycobacterium tuberculosis*. *Microbes Infect*, 14, 959-67.
- IONA, E., PARDINI, M., MUSTAZZOLU, A., PICCARO, G., NISINI, R., FATTORINI, L. & GIANNONI, F. 2016. *Mycobacterium tuberculosis* gene expression at different stages of hypoxia-induced dormancy and upon resuscitation. *Journal of Microbiology*, 54, 565-572.
- JAIN, P., HSU, T., ARAI, M., BIERMANN, K., THALER, D. S., NGUYEN, A., GONZÁLEZ, P. A., TUFARIELLO, J. M., KRIAKOV, J. & CHEN, B. 2014. Specialized transduction designed for precise high-throughput unmarked deletions in *Mycobacterium tuberculosis*. *MBio*, 5, e01245-14.
- JAMWAL, S. V., MEHROTRA, P., SINGH, A., SIDDIQUI, Z., BASU, A. & RAO, K. V. 2016. Mycobacterial escape from macrophage phagosomes to the cytoplasm represents an alternate adaptation mechanism. *Scientific Reports*, 6, 23089.
- JIA, Q., HU, X., SHI, D., ZHANG, Y., SUN, M., WANG, J., MI, K. & ZHU, G. 2016. Universal stress protein Rv2624c alters abundance of arginine and enhances intracellular survival by ATP binding in mycobacteria. *Scientific Reports*, 6.
- JINEK, M., CHYLINSKI, K., FONFARA, I., HAUER, M., DOUDNA, J. A. & CHARPENTIER, E. 2012. A programmable dual-RNA-guided DNA endonuclease in adaptive bacterial immunity. *Science*, 337, 816-821.
- JONES-LÓPEZ, E. C., NAMUGGA, O., MUMBOWA, F., SSEBIDANDI, M., MBABAZI, O., MOINE, S., MBOOWA, G., FOX, M. P., REILLY, N., AYAKAKA, I., KIM, S., OKWERA, A., JOLOBA, M. & FENNELLY, K. P. 2013. Cough Aerosols of

- Mycobacterium tuberculosis* Predict New Infection. A Household Contact Study. *American Journal of Respiratory and Critical Care Medicine*, 187, 1007-1015.
- JOSEPH, J., SAUBI, N., PEZZAT, E. & GATELL, J. M. 2006. Progress towards an HIV vaccine based on recombinant Bacillus Calmette–Guérin: failures and challenges. *Expert Review of Vaccines*, 5, 827-838.
- JOSHI, S. M., PANDEY, A. K., CAPITE, N., FORTUNE, S. M., RUBIN, E. J. & SASSETTI, C. M. 2006. Characterization of mycobacterial virulence genes through genetic interaction mapping. *Proceedings of the National Academy of Sciences*, 103, 11760-11765.
- KAHRAMANOGLU, C., CORTES, T., MATANGE, N., HUNT, D. M., VISWESWARIAH, S. S., YOUNG, D. B. & BUXTON, R. S. 2014. Genomic mapping of cAMP receptor protein (CRPMt) in *Mycobacterium tuberculosis*: relation to transcriptional start sites and the role of CRPMt as a transcription factor. *Nucleic Acids Research*.
- KANDASAMY, S. & NARAYANAN, S. 2014. The PknI and DacB2 double deletion mutant of *Mycobacterium tuberculosis* leads to alteration of cell morphology and susceptibility to antibiotics. *BMC Infectious Diseases*, 14, E22.
- KANNO, A. I., GOULART, C., ROFATTO, H. K., OLIVEIRA, S. C., LEITE, L. C. & MCFADDEN, J. 2016. New Recombinant *Mycobacterium bovis* BCG Expression Vectors: Improving Genetic Control over Mycobacterial Promoters. *Applied and Environmental Microbiology*, 82, 2240-2246.
- KAPOPOULOU, A., LEW, J. M. & COLE, S. T. 2011. The MycoBrowser portal: A comprehensive and manually annotated resource for mycobacterial genomes. *Tuberculosis*, 91, 8-13.
- KAPRELYANTS, A. S., GOTTSCHAL, J. C. & KELL, D. B. 1993. Dormancy in non-sporulating bacteria. *FEMS Microbiology Letters*, 104, 271-285.
- KARAKOUSIS, P. C., YOSHIMATSU, T., LAMICHHANE, G., WOOLWINE, S. C., NUERMBERGER, E. L., GROSSET, J. & BISHAI, W. R. 2004. Dormancy phenotype displayed by extracellular *Mycobacterium tuberculosis* within artificial granulomas in mice. *Journal of Experimental Medicine*, 200, 647-657.
- KAUFMANN, S. H. 2002. Protection against tuberculosis: cytokines, T cells, and macrophages. *Annals of the Rheumatic Diseases*, 61, ii54-ii58.
- KAUFMANN, S. H. 2003. Immune response to tuberculosis: experimental animal models. *Tuberculosis*, 83, 107-111.
- KAUR, P., AGARWAL, S. & DATTA, S. 2009. Delineating Bacteriostatic and Bactericidal Targets in Mycobacteria Using IPTG Inducible Antisense Expression. *PLoS One*, 4, e5923.
- KELKAR, D. S., KUMAR, D., KUMAR, P., BALAKRISHNAN, L., MUTHUSAMY, B., YADAV, A. K., SHRIVASTAVA, P., MARIMUTHU, A., ANAND, S. & SUNDARAM, H. 2011. Proteogenomic analysis of *Mycobacterium tuberculosis* by high resolution mass spectrometry. *Molecular & Cellular Proteomics*, 10, M111. 011627.
- KERR, J. H. & BARRETT, T. L. 1917. *Atypical mycobacterial diseases*.
- KIM, S. O., MERCHANT, K., NUDELMAN, R., BEYER, W. F., JR., KENG, T., DEANGELO, J., HAUSLADEN, A. & STAMLER, J. S. 2002. OxyR. *Cell*, 109, 383-396.

- KIMBALL, E., KOVACS, E., CLARK, M. & SCHNEIDER, C. 1995. Activation of cytokine production and adhesion molecule expression on THP-1 myelomonocytic cells by macrophage colony-stimulating factor in combination with interferon-gamma. *Journal of Leukocyte Biology*, 58, 585-594.
- KIRKSEY, M. A., TISCHLER, A. D., SIMÉONE, R., HISERT, K. B., UPLEKAR, S., GUILHOT, C. & MCKINNEY, J. D. 2011. Spontaneous phthiocerol dimycocerosate-deficient variants of *Mycobacterium tuberculosis* are susceptible to gamma interferon-mediated immunity. *Infection and Immunity*, 79, 2829-2838.
- KLINKENBERG, L. G., SUTHERLAND, L. A., BISHAI, W. R. & KARAKOUSHIS, P. C. 2008. Metronidazole lacks activity against *Mycobacterium tuberculosis* in an in vivo hypoxic granuloma model of latency. *Journal of Infectious Diseases*, 198, 275-283.
- KLOPPER, M., WARREN, R. M., HAYES, C., GEY VAN PITTIUS, N. C., STREICHER, E. M., MULLER, B., SIRGEL, F. A., CHABULA-NXIWENI, M., HOOSAIN, E., COETZEE, G., DAVID VAN HELDEN, P., VICTOR, T. C. & TROLLIP, A. P. 2013. Emergence and spread of extensively and totally drug-resistant tuberculosis, South Africa. *Emerg Infect Dis*, 19, 449-55.
- KOECK, J. L., FABRE, M., SIMON, F., DAFFÉ, M., GARNOTEL, E., MATAN, A., GÉRÔME, P., BERNATAS, J. J., BUISSON, Y. & POURCEL, C. 2011. Clinical characteristics of the smooth tubercle bacilli '*Mycobacterium canettii*' infection suggest the existence of an environmental reservoir. *Clinical Microbiology and Infection*, 17, 1013-1019.
- KOLB, A., BUSBY, S., BUC, H., GARGES, S. & ADHYA, S. 1993. Transcriptional regulation by cAMP and its receptor protein. *Annual Review of Biochemistry*, 62, 749-797.
- KONG, H., DONG, C. & XIONG, S. 2014. A novel vaccine p846 encoding Rv3615c, Mtb10.4, and Rv2660c elicits robust immune response and alleviates lung injury induced by *Mycobacterium* infection. *Hum Vaccin Immunother*, 10, 378-90.
- KÖRNER, H., SOFIA, H. J. & ZUMFT, W. G. 2003. Phylogeny of the bacterial superfamily of Crp-Fnr transcription regulators: exploiting the metabolic spectrum by controlling alternative gene programs. *FEMS Microbiology Reviews*, 27, 559-592.
- KRAMNIK, I. & BEAMER, G. Mouse models of human TB pathology: roles in the analysis of necrosis and the development of host-directed therapies. *Seminars in immunopathology*, 2016. Springer, 221-237.
- KROGH, A., LARSSON, B., VON HEIJNE, G. & SONNHAMMER, E. L. 2001. Predicting transmembrane protein topology with a hidden Markov model: application to complete genomes. *Journal of Molecular Biology*, 305, 567-580.
- KULKA, K., HATFULL, G. & OJHA, A. K. 2012. Growth of *Mycobacterium tuberculosis* biofilms. *JoVE (Journal of Visualized Experiments)*, e3820-e3820.
- KUMAR, A., DESHANE, J. S., CROSSMAN, D. K., BOLISSETTY, S., YAN, B.-S., KRAMNIK, I., AGARWAL, A. & STEYN, A. J. C. 2008. Heme Oxygenase-1-derived Carbon Monoxide Induces the *Mycobacterium tuberculosis* Dormancy Regulon. *The Journal of Biological Chemistry*, 283, 18032-18039.

- KUMAR, A., TOLEDO, J. C., PATEL, R. P., LANCASTER, J. R. & STEYN, A. J. 2007. *Mycobacterium tuberculosis* DosS is a redox sensor and DosT is a hypoxia sensor. *Proceedings of the National Academy of Sciences*, 104, 11568-11573.
- LAMICHHANE, G., ZIGNOL, M., BLADES, N. J., GEIMAN, D. E., DOUGHERTY, A., GROSSET, J., BROMAN, K. W. & BISHAI, W. R. 2003. A postgenomic method for predicting essential genes at subsaturation levels of mutagenesis: application to *Mycobacterium tuberculosis*. *Proceedings of the National Academy of Sciences*, 100, 7213-7218.
- LE DANTEC, C., WINTER, N., GICQUEL, B., VINCENT, V. & PICARDEAU, M. 2001. Genomic sequence and transcriptional analysis of a 23-kilobase mycobacterial linear plasmid: evidence for horizontal transfer and identification of plasmid maintenance systems. *Journal of Bacteriology*, 183, 2157-2164.
- LEE, C., LEE, S. M., MUKHOPADHYAY, P., KIM, S. J., LEE, S. C., WOO-SUNG, A., YU, M.-H., STORZ, G. & RYU, S. E. 2004. Redox regulation of OxyR requires specific disulfide bond formation involving a rapid kinetic reaction path. *Nature Structural & Molecular Biology*, 11, 1179.
- LEE, J. Y. 2015. Diagnosis and Treatment of Extrapulmonary Tuberculosis. *Tuberculosis and Respiratory Diseases*, 78, 47-55.
- LEE, M. H., PASCOPELLA, L., JACOBS, W. R. & HATFULL, G. F. 1991. Site-specific integration of mycobacteriophage L5: integration-proficient vectors for *Mycobacterium smegmatis*, *Mycobacterium tuberculosis*, and bacille Calmette-Guerin. *Proceedings of the National Academy of Sciences*, 88, 3111-3115.
- LEE, W., VANDERVEN, B. C., FAHEY, R. J. & RUSSELL, D. G. 2013. Intracellular *Mycobacterium tuberculosis* exploits host-derived fatty acids to limit metabolic stress. *Journal of Biological Chemistry*, 288, 6788-6800.
- LEISTIKOW, R. L., MORTON, R. A., BARTEK, I. L., FRIMPONG, I., WAGNER, K. & VOSKUIL, M. I. 2010. The *Mycobacterium tuberculosis* DosR regulon assists in metabolic homeostasis and enables rapid recovery from nonrespiring dormancy. *Journal of Bacteriology*, 192, 1662-1670.
- LENAERTS, A. J., HOFF, D., ALY, S., EHLERS, S., ANDRIES, K., CANTARERO, L., ORME, I. M. & BASARABA, R. J. 2007. Location of persisting mycobacteria in a Guinea pig model of tuberculosis revealed by r207910. *Antimicrobial Agents and Chemotherapy*, 51, 3338-3345.
- LESIC, B., LÉPINE, F., DÉZIEL, E., ZHANG, J., ZHANG, Q., PADFIELD, K., CASTONGUAY, M.-H., MILOT, S., STACHEL, S. & TZIKA, A. A. 2007. Inhibitors of pathogen intercellular signals as selective anti-infective compounds. *PLoS Pathogens*, 3, e126.
- LEW, J. M., KAPOPOULOU, A., JONES, L. M. & COLE, S. T. 2011. TubercuList—10 years after. *Tuberculosis*, 91, 1-7.
- LI, H. & DURBIN, R. 2009. Fast and accurate short read alignment with Burrows–Wheeler transform. *Bioinformatics*, 25, 1754-1760.
- LIFE TECHNOLOGIES 2012. *Real Time PCR Handbook*, Life Technologies Corporation.
- LILLEBAEK, T., DIRKSEN, A., BAESS, I., STRUNGE, B., THOMSEN, V. Ø. & ANDERSEN, Å. B. 2002. Molecular evidence of endogenous reactivation of *Mycobacterium tuberculosis* after 33 years of latent infection. *The Journal of Infectious Diseases*, 185, 401-404.

- LIM, E. M., RAUZIER, J., TIMM, J., TORREA, G., MURRAY, A., GICQUEL, B. & PORTNOI, D. 1995. Identification of *Mycobacterium tuberculosis* DNA sequences encoding exported proteins by using phoA gene fusions. *Journal of Bacteriology*, 177, 59-65.
- LIN, P. L., DIETRICH, J., TAN, E., ABALOS, R. M., BURGOS, J., BIGBEE, C., BIGBEE, M., MILK, L., GIDEON, H. P., RODGERS, M., COCHRAN, C., GUINN, K. M., SHERMAN, D. R., KLEIN, E., JANSSEN, C., FLYNN, J. L. & ANDERSEN, P. 2012. The multistage vaccine H56 boosts the effects of BCG to protect cynomolgus macaques against active tuberculosis and reactivation of latent *Mycobacterium tuberculosis* infection. *J Clin Invest*, 122, 303-14.
- LIN, X., XU, S., YANG, Y., WU, J., WANG, H., SHEN, H. & WANG, H. 2009. Purification and characterization of anthranilate synthase component I (TrpE) from *Mycobacterium tuberculosis* H37Rv. *Protein Expression and Purification*, 64, 8-15.
- LIPWORTH, S., HAMMOND, R., BARON, V., HU, Y., COATES, A. & GILLESPIE, S. 2016. Defining dormancy in mycobacterial disease. *Tuberculosis*, 99, 131-142.
- LOBUE, P. A. & CASTRO, K. G. 2012. Is It Time to Replace the Tuberculin Skin Test With a Blood Test? *JAMA*, 308, 241-242.
- LOEBEL, R., SHORR, E. & RICHARDSON, H. 1933. The influence of adverse conditions upon the respiratory metabolism and growth of human tubercle bacilli. *Journal of Bacteriology*, 26, 167.
- LORENZ, M. C. & FINK, G. R. 2002. Life and Death in a Macrophage: Role of the Glyoxylate Cycle in Virulence. *Eukaryotic Cell*, 1, 657-662.
- LOW, K. L., RAO, P. S. S., SHUI, G., BENDT, A. K., PETHE, K., DICK, T. & WENK, M. R. 2009. Triacylglycerol Utilization Is Required for Regrowth of In Vitro Hypoxic Nonreplicating *Mycobacterium bovis* Bacillus Calmette-Guerin. *Journal of Bacteriology*, 191, 5037-5043.
- LUABEYA, A. K., KAGINA, B. M., TAMERIS, M. D., GELDENHUYS, H., HOFF, S. T., SHI, Z., KROMANN, I., HATHERILL, M., MAHOMED, H., HANEKOM, W. A., ANDERSEN, P., SCRIBA, T. J., SCHOEMAN, E., KROHN, C., DAY, C. L., AFRICA, H., MAKHETHE, L., SMIT, E., BROWN, Y., SULIMAN, S., HUGHES, E. J., BANG, P., SNOWDEN, M. A., MCCLAIN, B. & HUSSEY, G. D. 2015. First-in-human trial of the post-exposure tuberculosis vaccine H56:IC31 in *Mycobacterium tuberculosis* infected and non-infected healthy adults. *Vaccine*, 33, 4130-40.
- LUNDBERG, J. O., WEITZBERG, E., COLE, J. A. & BENJAMIN, N. 2004. Nitrate, bacteria and human health. *Nature Reviews Microbiology*, 2, 593.
- MACMICKING, J., XIE, Q.-W. & NATHAN, C. 1997a. Nitric oxide and macrophage function. *Annual Review of Immunology*, 15, 323-350.
- MACMICKING, J. D., NORTH, R. J., LACOURSE, R., MUDGETT, J. S., SHAH, S. K. & NATHAN, C. F. 1997b. Identification of nitric oxide synthase as a protective locus against tuberculosis. *Proceedings of the National Academy of Sciences*, 94, 5243-5248.
- MACMICKING, J. D., TAYLOR, G. A. & MCKINNEY, J. D. 2003. Immune control of tuberculosis by IFN- γ -inducible LRG-47. *Science*, 302, 654-659.
- MAGNUSSON, L. U., FAREWELL, A. & NYSTRÖM, T. 2005. ppGpp: a global regulator in *Escherichia coli*. *Trends in Microbiology*, 13, 236-242.

- MAHENTHIRALINGAM, E., DRAPER, P., DAVIS, E. O. & COLSTON, M. J. 1993. Cloning and sequencing of the gene which encodes the highly inducible acetamidase of *Mycobacterium smegmatis*. *Microbiology*, 139, 575-583.
- MAKSYMUIK, C., IOERGER, T., BALAKRISHNAN, A., BRYK, R., RHEE, K., SACCHETTINI, J. & NATHAN, C. 2015. Comparison of transposon and deletion mutants in *Mycobacterium tuberculosis*: The case of rv1248c, encoding 2-hydroxy-3-oxoadipate synthase. *Tuberculosis*, 95, 689-694.
- MALHOTRA, V., SHARMA, D., RAMANATHAN, V., SHAKILA, H., SAINI, D. K., CHAKRAVORTY, S., DAS, T. K., LI, Q., SILVER, R. F. & NARAYANAN, P. 2004. Disruption of response regulator gene, *devR*, leads to attenuation in virulence of *Mycobacterium tuberculosis*. *FEMS Microbiology Letters*, 231, 237-245.
- MANGANELLI, R., DUBNAU, E., TYAGI, S., KRAMER, F. R. & SMITH, I. 1999. Differential expression of 10 sigma factor genes in *Mycobacterium tuberculosis*. *Molecular Microbiology*, 31, 715-724.
- MANTOUX, M. C. 1912. La voie intradermique en tuberculinothérapie. *Presse Med*, 20, 146-148.
- MATSUI, M., TOMITA, M. & KANAI, A. 2013. Comprehensive computational analysis of bacterial CRP/FNR superfamily and its target motifs reveals stepwise evolution of transcriptional networks. *Genome Biology and Evolution*, 5, 267-282.
- MATSUO, K. & YASUTOMI, Y. 2011. *Mycobacterium bovis* bacille Calmette-Guerin as a vaccine vector for global infectious disease control. *Tuberculosis Research and Treatment*, 2011.
- MAURIN, M. & RAOULT, D. 2001. Use of Aminoglycosides in Treatment of Infections Due to Intracellular Bacteria. *Antimicrobial Agents and Chemotherapy*, 45, 2977-2986.
- MAYER, K. H. & HAMILTON, C. D. 2010. Synergistic Pandemics: Confronting the Global HIV and Tuberculosis Epidemics. *Clinical Infectious Diseases*, 50, S67-S70.
- MAZUREK, G. H. & VILLARINO, M. E. 2002. Guidelines for using the QuantiFERON®-TB test for diagnosing latent *Mycobacterium tuberculosis* infection. *Morbidity and Mortality Weekly Report*, 51.
- MCADAM, R. A. 1995. In vivo growth characteristics of leucine and methionine auxotrophic mutants of *Mycobacterium bovis* BCG generated by transposon mutagenesis. *Infect. Immun.*, 63, 1004-1012.
- MCCUNE, R. M., FELDMANN, F. M. & MCDERMOTT, W. 1966. Microbial persistence: II. Characteristics of the sterile state of tubercle bacilli. *The Journal of Experimental Medicine*, 123, 469.
- MCGILLIVRAY, A., GOLDEN, N. A. & KAUSHAL, D. 2015. The *Mycobacterium tuberculosis* Clp Gene Regulator Is Required for in Vitro Reactivation from Hypoxia-induced Dormancy. *The Journal of Biological Chemistry*, 290, 2351-2367.
- MCKENNA, A., HANNA, M., BANKS, E., SIVACHENKO, A., CIBULSKIS, K., KERNYTSKY, A., GARIMELLA, K., ALTSHULER, D., GABRIEL, S. & DALY, M. 2010. The Genome Analysis Toolkit: a MapReduce framework for analyzing next-generation DNA sequencing data. *Genome Research*, 20, 1297-1303.

- MCKINNEY, J. D., ZU BENTRUP, K. H., MUÑOZ-ELÍAS, E. J., MICZAK, A., CHEN, B., CHAN, W.-T., SWENSON, D., SACCHETTINI, J. C., JACOBS, W. R. & RUSSELL, D. G. 2000. Persistence of *Mycobacterium tuberculosis* in macrophages and mice requires the glyoxylate shunt enzyme isocitrate lyase. *Nature*, 406, 735-738.
- MCLAUGHLIN, B., CHON, J. S., MACGURN, J. A., CARLSSON, F., CHENG, T. L., COX, J. S. & BROWN, E. J. 2007. A mycobacterium ESX-1–secreted virulence factor with unique requirements for export. *PLOS Pathogens*, 3, e105.
- MEDICAL RESEARCH COUNCIL STREPTOMYCIN IN TUBERCULOSIS TRIALS COMMITTEE 1948. Streptomycin treatment for pulmonary tuberculosis. *BMJ*, 2, 769-82.
- MEHRA, S., FOREMAN, T. W., DIDIER, P. J., AHSAN, M. H., HUDOCK, T. A., KISSEE, R., GOLDEN, N. A., GAUTAM, U. S., JOHNSON, A. M., ALVAREZ, X., RUSSELL-LODRIGUE, K. E., DOYLE, L. A., ROY, C. J., NIU, T., BLANCHARD, J. L., KHADER, S. A., LACKNER, A. A., SHERMAN, D. R. & KAUSHAL, D. 2015. The DosR Regulon Modulates Adaptive Immunity and Is Essential for *Mycobacterium tuberculosis* Persistence. *Am J Respir Crit Care Med*, 191, 1185-96.
- MEHTA, M., RAJMANI, R. S. & SINGH, A. 2016. *Mycobacterium tuberculosis* WhiB3 responds to Vacuolar pH-induced changes in mycothiol redox potential to modulate phagosomal maturation and virulence. *Journal of Biological Chemistry*, 291, 2888-2903.
- MELLARS, P. 2006. Going east: new genetic and archaeological perspectives on the modern human colonization of Eurasia. *Science*, 313, 796-800.
- MENDOZA-CORONEL, E. & CASTANON-ARREOLA, M. 2016. Comparative evaluation of in vitro human macrophage models for mycobacterial infection study. *Pathog Dis*, 74.
- MIDDLEBROOK, G., DUBOS, R. J. & PIERCE, C. 1947. Virulence and morphological characteristics of mammalian tubercle bacilli. *J. Exp. Med.*, 86, 175-183.
- MIGLIORI, G. B., DE IACO, G., BESOZZI, G., CENTIS, R. & CIRILLO, D. M. 2007. First tuberculosis cases in Italy resistant to all tested drugs. *Euro Surveill*, 12, E070517.1.
- MILES, A., MISRA, S. & IRWIN, J. 1938. The estimation of the bactericidal power of the blood. *Journal of Hygiene*, 38, 732-749.
- MILLÁN-LOU, M. I., LÓPEZ-CALLEJA, A. I., COLMENAREJO, C., LEZCANO, M. A., VITORIA, M. A., DEL PORTILLO, P., OTAL, I., MARTÍN, C. & SAMPER, S. 2013. Global study of IS6110 in a successful *Mycobacterium tuberculosis* strain: clues for deciphering its behavior and for its rapid detection. *Journal of Clinical Microbiology*, 51, 3631-3637.
- MINNIKIN, D. E., KREMER, L., DOVER, L. G. & BESRA, G. S. 2002. The Methyl-Branched Fortifications of *Mycobacterium tuberculosis*. *Chemistry & Biology*, 9, 545-553.
- MIOTTO, P., FORTI, F., AMBROSI, A., PELLIN, D., VEIGA, D. F., BALAZSI, G., GENNARO, M. L., DI SERIO, C., GHISOTTI, D. & CIRILLO, D. M. 2012. Genome-wide discovery of small RNAs in *Mycobacterium tuberculosis*. *PLoS One*, 7, e51950.

- MITCHISON, D. A. 2005. The diagnosis and therapy of tuberculosis during the past 100 years. *American Journal of Respiratory and Critical Care Medicine*, 171, 699-706.
- MO, Y., QUANQUIN, N. M., VECINO, W. H., RANGANATHAN, U. D., TESFA, L., BOURN, W., DERBYSHIRE, K. M., LETVIN, N. L., JACOBS, W. R. & FENNELLY, G. J. 2007. Genetic alteration of *Mycobacterium smegmatis* to improve mycobacterium-mediated transfer of plasmid DNA into mammalian cells and DNA immunization. *Infection and Immunity*, 75, 4804-4816.
- MODJARRAD, K. & VERMUND, S. H. 2010. Effect of treating co-infections on HIV-1 viral load: a systematic review. *The Lancet Infectious Diseases*, 10, 455-463.
- MOORES, A., RIESCO, A. B., SCHWENK, S. & ARNVIG, K. B. 2017. Expression, maturation and turnover of DrrS, an unusually stable, DosR regulated small RNA in *Mycobacterium tuberculosis*. *PloS One*, 12, e0174079.
- MORIYA, H. 2015. Quantitative nature of overexpression experiments. *Molecular Biology of the Cell*, 26, 3932-3939.
- MUKAMOLOVA, G. V., TURAPOV, O., MALKIN, J., WOLTMANN, G. & BARER, M. R. 2010. Resuscitation-promoting factors reveal an occult population of tubercle bacilli in sputum. *American Journal of Respiratory and Critical Care Medicine*, 181, 174-180.
- MUKAMOLOVA, G. V., YANOPOLSKAYA, N. D., KELL, D. B. & KAPRELYANTS, A. S. 1998. On resuscitation from the dormant state of *Micrococcus luteus*. *Antonie van Leeuwenhoek*, 73, 237-243.
- MUNOZ-ELIAS, E. J., UPTON, A. M., CHERIAN, J. & MCKINNEY, J. D. 2006. Role of the methylcitrate cycle in *Mycobacterium tuberculosis* metabolism, intracellular growth, and virulence. *Mol Microbiol*, 60, 1109-22.
- NAHID, P. & DALEY, C. L. 2006. Prevention of tuberculosis in HIV-infected patients. *Current Opinion in Infectious Diseases*, 19, 189-193.
- NAMOUCHE, A., GÓMEZ-MUÑOZ, M., FRYE, S. A., MOEN, L. V., ROGNES, T., TØNJUM, T. & BALASINGHAM, S. V. 2016. The *Mycobacterium tuberculosis* transcriptional landscape under genotoxic stress. *BMC Genomics*, 17, 791.
- NAVEEN, G. & PEERAPUR, B. V. 2012. Comparison of the Lowenstein-Jensen medium, the Middlebrook 7H10 medium and MB/BacT for the isolation of *Mycobacterium tuberculosis* (MTB) from clinical specimens. *Journal of Clinical and Diagnostic Research: JCDR*, 6, 1704.
- NAYAK, S. & ACHARJYA, B. 2012. Mantoux test and its interpretation. *Indian Dermatology Online Journal*, 3, 2-6.
- NIKIYAN, H., VASILCHENKO, A. & DERYABIN, D. 2010. Humidity-dependent bacterial cells functional morphometry investigations using atomic force microscope. *International Journal of Microbiology*, 2010.
- NYKA, W. 1974. Studies on the effect of starvation on mycobacteria. *Infection and Immunity*, 9, 843-850.
- O'CONNOR, B. D., WOLTMANN, G., PATEL, H., TURAPOV, O., HALDAR, P. & MUKAMOLOVA, G. V. 2015. Can resuscitation-promoting factors be used to improve culture rates of extra-pulmonary tuberculosis? *The International Journal of Tuberculosis and Lung Disease*, 19, 1556-1557.

- O'GARRA, A., REDFORD, P. S., MCNAB, F. W., BLOOM, C. I., WILKINSON, R. J. & BERRY, M. P. 2013. The immune response in tuberculosis. *Annual Review of Immunology*, 31, 475-527.
- OJHA, A. K., BAUGHN, A. D., SAMBANDAN, D., HSU, T., TRIVELLI, X., GUERARDEL, Y., ALAHARI, A., KREMER, L., JACOBS, W. R. & HATFULL, G. F. 2008. Growth of *Mycobacterium tuberculosis* biofilms containing free mycolic acids and harbouring drug-tolerant bacteria. *Molecular Microbiology*, 69, 164-174.
- OJHA, A. K., MUKHERJEE, T. K. & CHATTERJI, D. 2000. High intracellular level of guanosine tetraphosphate in *Mycobacterium smegmatis* changes the morphology of the bacterium. *Infection and Immunity*, 68, 4084-4091.
- ORME, I. 1988. A Mouse Model of the Recrudescence of Latent Tuberculosis in the Elderly. *Age*, 18, 24.
- ORME, I. M., ANDERSEN, P. & BOOM, W. H. 1993. T cell response to *Mycobacterium tuberculosis*. *Journal of Infectious Diseases*, 167, 1481-1497.
- ORMEROD, L. P. 2005. Multidrug-resistant tuberculosis (MDR-TB): epidemiology, prevention and treatment. *British Medical Bulletin*, 73-74, 17-24.
- PAI, M., DENKINGER, C. M., KIK, S. V., RANGAKA, M. X., ZWERLING, A., OXLADE, O., METCALFE, J. Z., CATTAMANCHI, A., DOWDY, D. W. & DHEDA, K. 2014. Gamma interferon release assays for detection of *Mycobacterium tuberculosis* infection. *Clinical Microbiology Reviews*, 27, 3-20.
- PANDEY, A. K., RAMAN, S., PROFF, R., JOSHI, S., KANG, C.-M., RUBIN, E. J., HUSSON, R. N. & SASSETTI, C. M. 2009. Nitrile-inducible gene expression in mycobacteria. *Tuberculosis*, 89, 12-16.
- PANG, X., VU, P., BYRD, T. F., GHANNY, S., SOTEROPOULOS, P., MUKAMOLOVA, G. V., WU, S., SAMTEN, B. & HOWARD, S. T. 2007. Evidence for complex interactions of stress-associated regulons in an *mprAB* deletion mutant of *Mycobacterium tuberculosis*. *Microbiology*, 153, 1229-1242.
- PAPAVINASASUNDARAM, K., CHAN, B., CHUNG, J.-H., COLSTON, M. J., DAVIS, E. O. & AV-GAY, Y. 2005. Deletion of the *Mycobacterium tuberculosis pknH* gene confers a higher bacillary load during the chronic phase of infection in BALB/c mice. *Journal of Bacteriology*, 187, 5751-5760.
- PARISH, T., MAHENTHIRALINGAM, E., DRAPER, P., DAVIS, E. O. & COLSTON, E. O. 1997. Regulation of the inducible acetamidase gene of *Mycobacterium smegmatis*. *Microbiology*, 143, 2267-2276.
- PARISH, T., SMITH, D. A., KENDALL, S., CASALI, N., BANCROFT, G. J. & STOKER, N. G. 2003a. Deletion of two-component regulatory systems increases the virulence of *Mycobacterium tuberculosis*. *Infection and Immunity*, 71, 1134-1140.
- PARISH, T., SMITH, D. A., ROBERTS, G., BETTS, J. & STOKER, N. G. 2003b. The *senX3-regX3* two-component regulatory system of *Mycobacterium tuberculosis* is required for virulence. *Microbiology*, 149, 1423-1435.
- PARISH, T. & STOKER, N. G. 1997. Development and use of a conditional antisense mutagenesis system in mycobacteria. *FEMS Microbiology Letters*, 154, 151-157.
- PARISH, T. & STOKER, N. G. 2000a. *glnE* Is an Essential Gene in *Mycobacterium tuberculosis*. *Journal of Bacteriology*, 182, 5715-5720.
- PARISH, T. & STOKER, N. G. 2000b. Use of a flexible cassette method to generate a double unmarked *Mycobacterium tuberculosis tlyA plcABC* mutant by gene replacement. *Microbiology*, 146, 1969-1975.

- PARK, H. D., GUINN, K. M., HARRELL, M. I., LIAO, R., VOSKUIL, M. I., TOMPA, M., SCHOOLNIK, G. K. & SHERMAN, D. R. 2003. Rv3133c/dosR is a transcription factor that mediates the hypoxic response of *Mycobacterium tuberculosis*. *Mol Microbiol*, 48, 833-43.
- PASHLEY, C. A., PARISH, T., MCADAM, R. A., DUNCAN, K. & STOKER, N. G. 2003. Gene replacement in mycobacteria by using incompatible plasmids. *Applied and Environmental Microbiology*, 69, 517-523.
- PECCIA, J., WERTH, H. M., MILLER, S. & HERNANDEZ, M. 2001. Effects of relative humidity on the ultraviolet induced inactivation of airborne bacteria. *Aerosol Science & Technology*, 35, 728-740.
- PELICIC, V., JACKSON, M., REYRAT, J.-M., JACOBS, W. R., GICQUEL, B. & GUILHOT, C. 1997. Efficient allelic exchange and transposon mutagenesis in *Mycobacterium tuberculosis*. *Proceedings of the National Academy of Sciences*, 94, 10955-10960.
- PELLIN, D., MIOTTO, P., AMBROSI, A., CIRILLO, D. M. & DI SERIO, C. 2012. A genome-wide identification analysis of small regulatory RNAs in *Mycobacterium tuberculosis* by RNA-Seq and conservation analysis. *PLoS One*, 7, e32723.
- PEÑA, J. C. & HO, W.-Z. 2015. Monkey models of tuberculosis: lessons learned. *Infection and immunity*, 83, 852-862.
- PETERSEN, T. N., BRUNAK, S., VON HEIJNE, G. & NIELSEN, H. 2011. SignalP 4.0: discriminating signal peptides from transmembrane regions. *Nature Methods*, 8, 785-786.
- PICARDEAU, M., LE DANTEC, C. & VINCENT, V. 2000. Analysis of the internal replication region of a mycobacterial linear plasmid. *Microbiology*, 146, 305-313.
- PICCARO, G., GIANNONI, F., FILIPPINI, P., MUSTAZZOLU, A. & FATTORINI, L. 2013. Activities of drug combinations against *Mycobacterium tuberculosis* grown in aerobic and hypoxic acidic conditions. *Antimicrobial Agents and Chemotherapy*, 57, 1428-1433.
- PICCAZZO, R., PAPARO, F. & GARLASCHI, G. 2014. Diagnostic accuracy of chest radiography for the diagnosis of tuberculosis (TB) and its role in the detection of latent TB infection: a systematic review. *The Journal of Rheumatology Supplement*, 91, 32-40.
- PIDDINGTON, D. L., KASHKOULI, A. & BUCHMEIER, N. A. 2000. Growth of *Mycobacterium tuberculosis* in a defined medium is very restricted by acid pH and Mg(2+) levels. *Infect Immun*, 68, 4518-22.
- PODINOVSKAIA, M., LEE, W., CALDWELL, S. & RUSSELL, D. G. 2013. Infection of macrophages with *Mycobacterium tuberculosis* induces global modifications to phagosomal function. *Cell Microbiol*, 15, 843-59.
- PRIMM, T. P., ANDERSEN, S. J., MIZRAHI, V., AVARBOCK, D., RUBIN, H. & BARRY, C. E. 2000. The stringent response of *Mycobacterium tuberculosis* is required for long-term survival. *Journal of Bacteriology*, 182, 4889-4898.
- QI, L. S., LARSON, M. H., GILBERT, L. A., DOUDNA, J. A., WEISSMAN, J. S., ARKIN, A. P. & LIM, W. A. 2013. Repurposing CRISPR as an RNA-guided platform for sequence-specific control of gene expression. *Cell*, 152, 1173-1183.

- QUENARD, F., FOURNIER, P. E., DRANCOURT, M. & BROUQUI, P. 2017. Role of second-line injectable antituberculosis drugs in the treatment of MDR/XDR tuberculosis. *International Journal of Antimicrobial Agents*.
- RAFFETSEDER, J., PIENAAR, E., BLOMGRAN, R., EKLUND, D., BRODIN, V. P., ANDERSSON, H., WELIN, A. & LERM, M. 2014. Replication rates of *Mycobacterium tuberculosis* in human macrophages do not correlate with mycobacterial antibiotic susceptibility. *PLoS One*, 9, e112426.
- RAMACHANDRA, L., NOSS, E., BOOM, W. H. & HARDING, C. V. 2001. Processing of *Mycobacterium tuberculosis* antigen 85B involves intraphagosomal formation of peptide-major histocompatibility complex II complexes and is inhibited by live bacilli that decrease phagosome maturation. *Journal of Experimental Medicine*, 194, 1421-1432.
- RAMAGE, H. R., CONNOLLY, L. E. & COX, J. S. 2009. Comprehensive functional analysis of *Mycobacterium tuberculosis* toxin-antitoxin systems: implications for pathogenesis, stress responses, and evolution. *PLoS Genetics*, 5, e1000767.
- RAMAN, S., SONG, T., PUYANG, X., BARDAROV, S., JACOBS, W. R. & HUSSON, R. N. 2001. The alternative sigma factor SigH regulates major components of oxidative and heat stress responses in *Mycobacterium tuberculosis*. *Journal of Bacteriology*, 183, 6119-6125.
- RANGANATHAN, S., BAI, G., LYUBETSKAYA, A., KNAPP, G. S., PETERSON, M. W., GAZDIK, M., GOMES, A. L., GALAGAN, J. E. & MCDONOUGH, K. A. 2015. Characterization of a cAMP responsive transcription factor, Cmr (Rv1675c), in TB complex mycobacteria reveals overlap with the DosR (DevR) dormancy regulon. *Nucleic Acids Res.*
- RAO, S. P., ALONSO, S., RAND, L., DICK, T. & PETHE, K. 2008. The protonmotive force is required for maintaining ATP homeostasis and viability of hypoxic, nonreplicating *Mycobacterium tuberculosis*. *Proceedings of the National Academy of Sciences*, 105, 11945-11950.
- RAVIGLIONE, M. C. & DITIUI, L. 2013. Setting new targets in the fight against tuberculosis. *Nature Medicine*, 19, 263-263.
- REDDY, M. C., PALANINATHAN, S. K., BRUNING, J. B., THURMAN, C., SMITH, D. & SACCHETTINI, J. C. 2009. Structural insights into the mechanism of the allosteric transitions of *Mycobacterium tuberculosis* cAMP receptor protein. *Journal of Biological Chemistry*, 284, 36581-36591.
- REED, M. B., GAGNEUX, S., DERIEMER, K., SMALL, P. M. & BARRY, C. E. 2007. The W-Beijing lineage of *Mycobacterium tuberculosis* overproduces triglycerides and has the DosR dormancy regulon constitutively upregulated. *Journal of Bacteriology*, 189, 2583-2589.
- RHEE, K. Y., DE CARVALHO, L. P. S., BRYK, R., EHRT, S., MARRERO, J., PARK, S. W., SCHNAPPINGER, D., VENUGOPAL, A. & NATHAN, C. 2011. Central carbon metabolism in *Mycobacterium tuberculosis*: an unexpected frontier. *Trends in Microbiology*, 19, 307-314.
- RICKMAN, L., SCOTT, C., HUNT, D. M., HUTCHINSON, T., MENÉNDEZ, M. C., WHALAN, R., HINDS, J., COLSTON, M. J., GREEN, J. & BUXTON, R. S. 2005. A member of the cAMP receptor protein family of transcription regulators in *Mycobacterium tuberculosis* is required for virulence in mice and controls

- transcription of the *rpfA* gene coding for a resuscitation promoting factor. *Molecular Microbiology*, 56, 1274-1286.
- RINDI, L., FATTORINI, L., BONANNI, D., IONA, E., FREER, G., TAN, D., DEHÒ, G., OREFICI, G. & GARZELLI, C. 2002. Involvement of the *fadD33* gene in the growth of *Mycobacterium tuberculosis* in the liver of BALB/c mice. *Microbiology*, 148, 3873-3880.
- ROBERTS, D. M., LIAO, R. P., WISEDCHAISRI, G., HOL, W. G. & SHERMAN, D. R. 2004. Two sensor kinases contribute to the hypoxic response of *Mycobacterium tuberculosis*. *Journal of Biological Chemistry*, 279, 23082-23087.
- ROCK, J. M., HOPKINS, F. F., CHAVEZ, A., DIALLO, M., CHASE, M. R., GERRICK, E. R., PRITCHARD, J. R., CHURCH, G. M., RUBIN, E. J. & SASSETTI, C. M. 2017. Programmable transcriptional repression in mycobacteria using an orthogonal CRISPR interference platform. *Nature Microbiology*, 2, 16274.
- RODRÍGUEZ, J. G., HERNÁNDEZ, A. C., HELGUERA-REPETTO, C., AYALA, D. A., GUADARRAMA-MEDINA, R., ANZÓLA, J. M., BUSTOS, J. R., ZAMBRANO, M. M., GONZÁLEZ-Y-MERCHAND, J. & GARCÍA, M. J. 2014. Global adaptation to a lipid environment triggers the dormancy-related phenotype of *Mycobacterium tuberculosis*. *MBio*, 5, e01125-14.
- ROHDE, K. H., ABRAMOVITCH, R. B. & RUSSELL, D. G. 2007. *Mycobacterium tuberculosis* invasion of macrophages: linking bacterial gene expression to environmental cues. *Cell Host Microbe*, 2, 352-64.
- ROHDE, K. H., VEIGA, D. F., CALDWELL, S., BALÁZSI, G. & RUSSELL, D. G. 2012. Linking the transcriptional profiles and the physiological states of *Mycobacterium tuberculosis* during an extended intracellular infection. *PLoS Pathog*, 8, e1002769.
- RUSSELL, D. G., VANDERVEN, B., GLENNIE, S., MWANDUMBA, H. & HEYDERMAN, R. 2009. The macrophage marches on its phagosome: dynamic assays of phagosome function. *Nature Reviews. Immunology*, 9, 594-600.
- RUSSELL, D. G., VANDERVEN, B. C., LEE, W., ABRAMOVITCH, R. B., KIM, M. J., HOMOLKA, S., NIEMANN, S. & ROHDE, K. H. 2010. *Mycobacterium tuberculosis* wears what it eats. *Cell Host Microbe*, 8, 68-76.
- RUSTAD, T. R., HARRELL, M. I., LIAO, R. & SHERMAN, D. R. 2008. The enduring hypoxic response of *Mycobacterium tuberculosis*. *PLoS One*, 3, e1502.
- RUSTAD, T. R., SHERRID, A. M., MINCH, K. J. & SHERMAN, D. R. 2009. Hypoxia: a window into *Mycobacterium tuberculosis* latency. *Cellular Microbiology*, 11, 1151-1159.
- RYABOVA, O. B., KHMEL'NITSKAYA, E. Y., MAKAROV, V. A., ALEKSEEVA, L. M., GRIGOR'EV, N. B. & GRANIK, V. G. 2005. 4-(N,N-Dialkylthiocarbamoylthio)-5-nitropyrimidines as new potential nitric oxide donors. *Russian Chemical Bulletin*, 54, 2873-2879.
- RYABOVA, O. B., MAKAROV, V. A., CHERNYSHEV, V. V. & GRANIK, V. G. 2004. Synthesis and thermal transformations of 5-nitropyrimidin-4-yl dialkyldithiocarbamates. *Russian Chemical Bulletin*, 53, 882-888.
- SABERI, F., KAMALI, M., NAJAFI, A., YAZDANPARAST, A. & MOGHADDAM, M. M. 2016. Natural antisense RNAs as mRNA regulatory elements in bacteria: a review on function and applications. *Cellular & Molecular Biology Letters*, 21, 6.

- SACHDEVA, P., MISRA, R., TYAGI, A. K. & SINGH, Y. 2010. The sigma factors of *Mycobacterium tuberculosis*: regulation of the regulators. *The FEBS Journal*, 277, 605-626.
- SAIKOLAPPAN, S., ESTRELLA, J., SASINDRAN, S. J., KHAN, A., ARMITIGE, L. Y., JAGANNATH, C. & DHANDAYUTHAPANI, S. 2012. The fbpA/sapM double knock out strain of *Mycobacterium tuberculosis* is highly attenuated and immunogenic in macrophages. *PLoS One*, 7, e36198.
- SAINI, D. K., MALHOTRA, V., DEY, D., PANT, N., DAS, T. K. & TYAGI, J. S. 2004. DevR–DevS is a bona fide two-component system of *Mycobacterium tuberculosis* that is hypoxia-responsive in the absence of the DNA-binding domain of DevR. *Microbiology*, 150, 865-875.
- SAIYUR RAMSUGIT, M. P. 2014. *Mycobacterium tuberculosis* Pili Promote Adhesion to and Invasion of THP-1 Macrophages. *Jpn. J. Infect. Dis.*, 67, 476-478.
- SAKULA, A. 1982. Robert Koch: centenary of the discovery of the tubercle bacillus, 1882. *Thorax*, 37, 246-251.
- SALGAME, P., GEADAS, C., COLLINS, L., JONES-LÓPEZ, E. & ELLNER, J. J. 2015. Latent tuberculosis infection–revisiting and revising concepts. *Tuberculosis*, 95, 373-384.
- SALINA, E. G., MOLLENKOPF, H. J., KAUFMANN, S. H. & KAPRELYANTS, A. S. 2009. *M. tuberculosis* Gene Expression during Transition to the "Non-Culturable" State. *Acta Naturae*, 1, 73-7.
- SANTOS, C. L., CORREIA-NEVES, M., MORADAS-FERREIRA, P. & MENDES, M. V. 2012. A walk into the LuxR regulators of Actinobacteria: phylogenomic distribution and functional diversity. *PLoS One*, 7, e46758.
- SANYI, R. 2016. Studies into the Role of Two Mycobacterial Proteins in Stress Response and Survival Inside Macrophages. University of Leicester.
- SARATHY, J., DARTOIS, V., DICK, T. & GENGENBACHER, M. 2013. Reduced drug uptake in phenotypically resistant nutrient-starved nonreplicating *Mycobacterium tuberculosis*. *Antimicrob Agents Chemother*, 57, 1648-53.
- SARBYBAEVA, A. 2015. Investigation of mycobacterial survival in non-permissive growth conditions. Doctor of Philosophy, Leicester.
- SASSETTI, C. M., BOYD, D. H. & RUBIN, E. J. 2003. Genes required for mycobacterial growth defined by high density mutagenesis. *Molecular Microbiology*, 48, 77-84.
- SASSETTI, C. M. & RUBIN, E. J. 2003. Genetic requirements for mycobacterial survival during infection. *Proceedings of the National Academy of Sciences*, 100, 12989-12994.
- SAVARY, B., VASU, P. & LORENCE, A. 2011. Recombinant Gene Expression, Reviews and Protocols. Lorence, A. 3rd, Humana Press. New York, NY.
- SCANGA, C. A., MOHAN, V., JOSEPH, H., YU, K., CHAN, J. & FLYNN, J. L. 1999. Reactivation of latent tuberculosis: variations on the Cornell murine model. *Infection and Immunity*, 67, 4531-4538.
- SCHAIBLE, U. E., COLLINS, H. L. & KAUFMANN, S. H. E. 1998. Confrontation between Intracellular Bacteria and the Immune System. *Advances in Immunology*, 71, 267-377.
- SCHNAPPINGER, D. & EHRT, S. 2014. Regulated Expression Systems for Mycobacteria and Their Applications. *Microbiology Spectrum*, 2.

- SCHNAPPINGER, D. & EHRT, S. 2016. A broader spectrum of tuberculosis. *Nat Med*, 22, 1076-1077.
- SCHNAPPINGER, D., EHRT, S., VOSKUIL, M. I., LIU, Y., MANGAN, J. A., MONAHAN, I. M., DOLGANOV, G., EFRON, B., BUTCHER, P. D., NATHAN, C. & SCHOOLNIK, G. K. 2003. Transcriptional Adaptation of *Mycobacterium tuberculosis* within Macrophages: Insights into the Phagosomal Environment. *J Exp Med*, 198, 693-704.
- SCHNAPPINGER, D., SCHOOLNIK, G. K. & EHRT, S. 2006. Expression profiling of host pathogen interactions: how *Mycobacterium tuberculosis* and the macrophage adapt to one another. *Microbes Infect*, 8, 1132-40.
- SCHREUDER, L. J. & PARISH, T. 2014. *Mycobacterium tuberculosis* DosR is required for activity of the PmbtB and PmbtI promoters under hypoxia. *PLoS One*, 9, e107283.
- SEELIGER, J. C., TOPP, S., SOGI, K. M., PREVITI, M. L., GALLIVAN, J. P. & BERTOZZI, C. R. 2012. A riboswitch-based inducible gene expression system for mycobacteria. *PLoS One*, 7, e29266.
- SELWYN, P. A., HARTEL, D., LEWIS, V. A., SCHOENBAUM, E. E., VERMUND, S. H., KLEIN, R. S., WALKER, A. T. & FRIEDLAND, G. H. 1989. A prospective study of the risk of tuberculosis among intravenous drug users with human immunodeficiency virus infection. *New England Journal of Medicine*, 320, 545-550.
- SHI, L., SOHASKEY, C. D., PFEIFFER, C., DATTA, P., PARKS, M., MCFADDEN, J., NORTH, R. J. & GENNARO, M. L. 2010. Carbon flux rerouting during *Mycobacterium tuberculosis* growth arrest. *Molecular Microbiology*, 78, 1199-1215.
- SHILOH, M. U., MANZANILLO, P. & COX, J. S. 2008. *Mycobacterium tuberculosis* senses host-derived carbon monoxide during macrophage infection. *Cell Host & Microbe*, 3, 323-330.
- SHIRES, K. & STEYN, L. 2001. The cold-shock stress response in *Mycobacterium smegmatis* induces the expression of a histone-like protein. *Molecular Microbiology*, 39, 994-1009.
- SHLEEVA, M., MUKAMOLOVA, G., TELKOV, M., BEREZINSKAIA, T., SYROESHKIN, A., BIKETOV, S. & KAPRELIANTS, A. 2002. Formation of nonculturable *Mycobacterium tuberculosis* and their regeneration. *Mikrobiologiya*, 72, 76-83.
- SHLEEVA, M. O., KUDYKINA, Y. K., VOSTROKNUTOVA, G. N., SUZINA, N. E., MULYUKIN, A. L. & KAPRELYANTS, A. S. 2011. Dormant ovoid cells of *Mycobacterium tuberculosis* are formed in response to gradual external acidification. *Tuberculosis*, 91, 146-154.
- SIA, J. K., GEORGIEVA, M. & RENGARAJAN, J. 2015. Innate Immune Defenses in Human Tuberculosis: An Overview of the Interactions between *Mycobacterium tuberculosis* and Innate Immune Cells. *J Immunol Res*, 2015, 747543.
- SIDDIQ, S. H. & RUSCH-GERDES, S. 2006. Section I: principle of procedure. *MGI TTM Procedure Manual*.
- SIGUIER, P., GOURBEYRE, E. & CHANDLER, M. 2014. Bacterial insertion sequences: their genomic impact and diversity. *FEMS microbiology reviews*, 38, 865-891.
- SIKRI, K. & TYAGI, J. S. 2013. The evolution of *Mycobacterium tuberculosis* dormancy models. *Curr. Sci*, 105, 607-616.

- SILVA MIRANDA, M., BREIMAN, A., ALLAIN, S., DEKNUYDT, F. & ALTARE, F. 2012. The tuberculous granuloma: an unsuccessful host defence mechanism providing a safety shelter for the bacteria? *Clinical and Developmental Immunology*, 2012.
- SILVA, M. T. 2012. Classical labeling of bacterial pathogens according to their lifestyle in the host: inconsistencies and alternatives. *Frontiers in Microbiology*, 3.
- SIMEONE, R., SAYES, F., SONG, O., GRÖSCHEL, M. I., BRODIN, P., BROSCHE, R. & MAJLESSI, L. 2015. Cytosolic access of *Mycobacterium tuberculosis*: critical impact of phagosomal acidification control and demonstration of occurrence in vivo. *PLoS Pathogens*, 11, e1004650.
- SINGH, R., SINGH, M., ARORA, G., KUMAR, S., TIWARI, P. & KIDWAI, S. 2013. Polyphosphate deficiency in *Mycobacterium tuberculosis* is associated with enhanced drug susceptibility and impaired growth in guinea pigs. *J Bacteriol*, 195, 2839-51.
- SIRAKOVA, T. D., THIRUMALA, A. K., DUBEY, V. S., SPRECHER, H. & KOLATTUKUDY, P. E. 2001. The *Mycobacterium tuberculosis* *pk2* gene encodes the synthase for the hepta- and octamethyl-branched fatty acids required for sulfolipid synthesis. *Journal of Biological Chemistry*, 276, 16833-16839.
- SMEULDERS, M. J., KEER, J., SPEIGHT, R. A. & WILLIAMS, H. D. 1999. Adaptation of *Mycobacterium smegmatis* to stationary phase. *Journal of Bacteriology*, 181, 270-283.
- SMITH, L. J., BOCHKAREVA, A., ROLFE, M. D., HUNT, D. M., KAHRAMANOGLOU, C., BRAUN, Y., RODGERS, A., BLOCKLEY, A., COADE, S., LOUGHEED, K. E. A., HAFNEH, N. A., GLENN, S. M., CRACK, J. C., LE BRUN, N. E., SALDANHA, J. W., MAKAROV, V., NOBELI, I., ARNVIG, K., MUKAMOLOVA, G. V., BUXTON, R. S. & GREEN, J. 2017. Cmr is a redox-responsive regulator of DosR that contributes to *M. tuberculosis* virulence. *Nucleic Acids Research*, 45, 6600-6612.
- SOHASKEY, C. D. 2008. Nitrate enhances the survival of *Mycobacterium tuberculosis* during inhibition of respiration. *Journal of Bacteriology*, 190, 2981-2986.
- SOHASKEY, C. D. & WAYNE, L. G. 2003. Role of narK2X and narGHJ1 in hypoxic upregulation of nitrate reduction by *Mycobacterium tuberculosis*. *Journal of Bacteriology*, 185, 7247-7256.
- SONNHAMMER, E. L., VON HEIJNE, G. & KROGH, A. A hidden Markov model for predicting transmembrane helices in protein sequences. *ISMB*, 1998. 175-182.
- SOTO-RAMIREZ, M. D., AGUILAR-AYALA, D. A., GARCIA-MORALES, L., RODRIGUEZ-PEREDO, S. M., BADILLO-LOPEZ, C., RIOS-MUÑIZ, D. E., MEZA-SEGURA, M. A., RIVERA-MORALES, G. Y., LEON-SOLIS, L. & CERNA-CORTES, J. F. 2017. Cholesterol plays a larger role during *Mycobacterium tuberculosis* in vitro dormancy and reactivation than previously suspected. *Tuberculosis*, 103, 1-9.
- SPIEGEL, D. A., SINGH, G. K. & BANSKOTA, A. K. 2005. Tuberculosis of the musculoskeletal system. *Techniques in Orthopaedics*, 20, 167-178.
- SRIVASTAVA, S., ERNST, J. D. & DESVIGNES, L. 2014. Beyond macrophages: the diversity of mononuclear cells in tuberculosis. *Immunological Reviews*, 262, 179-192.

- STAHL, D. A. & URBANCE, J. 1990. The division between fast-and slow-growing species corresponds to natural relationships among the mycobacteria. *Journal of Bacteriology*, 172, 116-124.
- STALLINGS, C. L., STEPHANOU, N. C., CHU, L., HOCHSCHILD, A., NICKELS, B. E. & GLICKMAN, M. S. 2009. CarD is an essential regulator of rRNA transcription required for *Mycobacterium tuberculosis* persistence. *Cell*, 138, 146-159.
- STAPLETON, M., HAQ, I., HUNT, D. M., ARNVIG, K. B., ARTYMIUK, P. J., BUXTON, R. S. & GREEN, J. 2010. *Mycobacterium tuberculosis* cAMP Receptor Protein (Rv3676) Differs from the *Escherichia coli* Paradigm in Its cAMP Binding and DNA Binding Properties and Transcription Activation Properties. *The Journal of Biological Chemistry*, 285, 7016-7027.
- STAPLETON, M. R., SMITH, L. J., HUNT, D. M., BUXTON, R. S. & GREEN, J. 2012. *Mycobacterium tuberculosis* WhiB1 represses transcription of the essential chaperonin GroEL2. *Tuberculosis*, 92, 328-332.
- STERNE, J., RODRIGUES, L. & GUEDES, I. 1998. Does the efficacy of BCG decline with time since vaccination? *The International Journal of Tuberculosis and Lung Disease*, 2, 200-207.
- STOKES, R. W. & DOXSEE, D. 1999. The receptor-mediated uptake, survival, replication, and drug sensitivity of *Mycobacterium tuberculosis* within the macrophage-like cell line THP-1: a comparison with human monocyte-derived macrophages. *Cellular Immunology*, 197, 1-9.
- STORZ, G., VOGEL, J. & WASSARMAN, K. M. 2011. Regulation by small RNAs in bacteria: expanding frontiers. *Molecular Cell*, 43, 880-891.
- STOVER, C. K., BANSAL, G. P., HANSON, M. S., BURLEIN, J., PALASZYNSKI, S., YOUNG, J., KOENIG, S., YOUNG, D., SADZIENE, A. & BARBOUR, A. 1993. Protective immunity elicited by recombinant bacille Calmette-Guerin (BCG) expressing outer surface protein A (OspA) lipoprotein: a candidate Lyme disease vaccine. *Journal of Experimental Medicine*, 178, 197-209.
- STOVER, C. K., DE LA CRUZ, V. F., FUERST, T. R., BURLEIN, J. E., BENSON, L. A., BENNETT, L. T., BANSAL, G. P., YOUNG, J. F., LEE, M. H., HATFULL, G. F., SNAPPER, S. B., BARLETTA, R. G., JACOBS, W. R. & BLOOM, B. R. 1991. New use of BCG for recombinant vaccines. *Nature*, 351, 456-460.
- STUCKI, D. & GAGNEUX, S. 2013. Single nucleotide polymorphisms in *Mycobacterium tuberculosis* and the need for a curated database. *Tuberculosis (Edinburgh, Scotland)*, 93, 30-39.
- STURGILL-KOSZYCKI, S., SCHLESINGER, P. H., CHAKRABORTY, P., HADDIX, P. L., COLLINS, H. L., FOK, A. K., ALLEN, R. D., GLUCK, S. L., HEUSER, J. & RUSSELL, D. G. 1994. Lack of acidification in *Mycobacterium* phagosomes produced by exclusion of the vesicular proton-ATPase. *Science*, 263, 678-682.
- SUPPLY, P., MARCEAU, M., MANGENOT, S., ROCHE, D., ROUANET, C., KHANNA, V., MAJLESSI, L., CRISCUOLO, A., TAP, J. & PAWLIK, A. 2013. Genomic analysis of smooth tubercle bacilli provides insights into ancestry and pathoadaptation of *Mycobacterium tuberculosis*. *Nature Genetics*, 45, 172-179.
- SUREKA, K., DEY, S., DATTA, P., SINGH, A. K., DASGUPTA, A., RODRIGUE, S., BASU, J. & KUNDU, M. 2007. Polyphosphate kinase is involved in stress-induced mprAB-sigE-rel signalling in mycobacteria. *Molecular Microbiology*, 65, 261-276.

- TALAAT, A. M., LYONS, R., HOWARD, S. T. & JOHNSTON, S. A. 2004. The temporal expression profile of *Mycobacterium tuberculosis* infection in mice. *Proceedings of the National Academy of Sciences of the United States of America*, 101, 4602-4607.
- TALAAT, A. M., REIMSCHUESSEL, R., WASSERMAN, S. S. & TRUCKSIS, M. 1998. Goldfish, *Carassius auratus*, a Novel Animal Model for the Study of *Mycobacterium marinum* Pathogenesis. *Infection and Immunity*, 66, 2938-2942.
- TAN, M. P., SEQUEIRA, P., LIN, W. W., PHONG, W. Y., CLIFF, P., NG, S. H., LEE, B. H., CAMACHO, L., SCHNAPPINGER, D., EHRT, S., DICK, T., PETHE, K. & ALONSO, S. 2010. Nitrate respiration protects hypoxic *Mycobacterium tuberculosis* against acid- and reactive nitrogen species stresses. *PLoS One*, 5, e13356.
- TAN, S. & RUSSELL, D. G. 2015. Trans-species communication in the *Mycobacterium tuberculosis*-infected macrophage. *Immunol Rev*, 264, 233-48.
- TB ALLIANCE. 2017. *EU Leaders Urge Funding of Critically-needed New Tools against Drug-resistant Tuberculosis* [Online]. Available: <https://www.tballiance.org/news/eu-leaders-urge-funding-critically-needed-new-tools-against-drug-resistant-tuberculosis> [Accessed 20th July 2017].
- TEKAIA, F., GORDON, S., GARNIER, T., BROSCHE, R., BARRELL, B. & COLE, S. 1999. Analysis of the proteome of *Mycobacterium tuberculosis in silico*. *Tubercle and Lung Disease*, 79, 329-342.
- THERMO SCIENTIFIC 2008. 260/280 and 260/230 Ratios. *Thermo Scientific-Nanodrop products*. 4th ed. Wilmington, Delaware USA.
- THEUS, S. A., CAVE, M. D. & EISENACH, K. D. 2004. Activated THP-1 Cells: an Attractive Model for the Assessment of Intracellular Growth Rates of *Mycobacterium tuberculosis* Isolates. *Infection and Immunity*, 72, 1169-1173.
- THIERRY, D., CAVE, M., EISENACH, K., CRAWFORD, J., BATES, J., GICQUEL, B. & GUESDON, J. 1990. IS6110, an IS-like element of *Mycobacterium tuberculosis* complex. *Nucleic Acids Research*, 18, 188-188.
- TORTOLI, E., BENEDETTI, M., FONTANELLI, A. & SIMONETTI, M. T. 2002. Evaluation of automated BACTEC MGIT 960 system for testing susceptibility of *Mycobacterium tuberculosis* to four major antituberculous drugs: comparison with the radiometric BACTEC 460TB method and the agar plate method of proportion. *Journal of Clinical Microbiology*, 40, 607-610.
- TSOLAKI, A. G., HIRSH, A. E., DERIEMER, K., ENCISO, J. A., WONG, M. Z., HANNAN, M., AMAN, K., KATO-MAEDA, M. & SMALL, P. M. 2004. Functional and evolutionary genomics of *Mycobacterium tuberculosis*: insights from genomic deletions in 100 strains. *Proceedings of the National Academy of Sciences of the United States of America*, 101, 4865-4870.
- TSUCHIYA, S., YAMABE, M., YAMAGUCHI, Y., KOBAYASHI, Y., KONNO, T. & TADA, K. 1980. Establishment and characterization of a human acute monocytic leukemia cell line (THP-1). *International Journal of Cancer*, 26, 171-176.
- TUBERCULIST. 2017. Available: <http://tuberculist.epfl.ch/> [Accessed 20th July 2017].
- TULKENS, P. M. 1990. Intracellular pharmacokinetics and localization of antibiotics as predictors of their efficacy against intraphagocytic infections. *Scand J Infect Dis Suppl*, 74, 209-217.

- TURAPOV, O., GLENN, S., KANA, B., MAKAROV, V., ANDREW, P. W. & MUKAMOLOVA, G. V. 2014. The In Vivo Environment Accelerates Generation of Resuscitation-Promoting Factor-Dependent Mycobacteria. *American Journal of Respiratory and Critical Care Medicine*, 190, 1455-1457.
- UDWADIA, Z. F., AMALE, R. A., AJBANI, K. K. & RODRIGUES, C. 2012. Totally drug-resistant tuberculosis in India. *Clin Infect Dis*, 54, 579-81.
- UPLEKAR, S., ROUGEMONT, J., COLE, S. T. & SALA, C. 2013. High-resolution transcriptome and genome-wide dynamics of RNA polymerase and NusA in *Mycobacterium tuberculosis*. *Nucleic Acids Research*, 41, 961-977.
- VAN DISSEL, J. T., AREND, S. M., PRINS, C., BANG, P., TINGSKOV, P. N., LINGNAU, K., NOUTA, J., KLEIN, M. R., ROSENKRANDS, I. & OTTENHOFF, T. H. 2010. Ag85B-ESAT-6 adjuvanted with IC31[®] promotes strong and long-lived *Mycobacterium tuberculosis* specific T cell responses in naïve human volunteers. *Vaccine*, 28, 3571-3581.
- VAN INGEN, J., RAHIM, Z., MULDER, A., BOEREE, M. J., SIMEONE, R., BROSCH, R. & VAN SOOLINGEN, D. 2012. Characterization of *Mycobacterium orygis* as *M. tuberculosis* complex subspecies. *Emerging Infectious Diseases*, 18, 653.
- VAN VLACK, E. R. & SEELIGER, J. C. 2015. Using riboswitches to regulate gene expression and define gene function in mycobacteria. *Methods Enzymol*, 550, 251-65.
- VASILIADIS, E. S., GRIVAS, T. B. & KASPIRIS, A. 2009. Historical overview of spinal deformities in ancient Greece. *Scoliosis*, 4, 6.
- VELAYATI, A. A., MASJEDI, M. R., FARNIA, P., TABARSI, P., GHANA VI, J., ZIAZARIFI, A. H. & HOFFNER, S. E. 2009. Emergence of new forms of totally drug-resistant tuberculosis bacilli: super extensively drug-resistant tuberculosis or totally drug-resistant strains in Iran. *Chest*, 136, 420-425.
- VON PIQUET, C. 1909. Frequency of tuberculosis in childhood. *Journal of the American Medical Association*, 52, 675-678.
- VOSKUIL, M. I., BARTEK, I. L., VISCONTI, K. & SCHOOLNIK, G. K. 2011. The response of *Mycobacterium tuberculosis* to reactive oxygen and nitrogen species. *Front Microbiol*, 2, 105.
- VOSKUIL, M. I., SCHNAPPINGER, D., VISCONTI, K. C., HARRELL, M. I., DOLGANOV, G. M., SHERMAN, D. R. & SCHOOLNIK, G. K. 2003. Inhibition of respiration by nitric oxide induces a *Mycobacterium tuberculosis* dormancy program. *J Exp Med*, 198, 705-13.
- VOSKUIL, M. I., VISCONTI, K. C. & SCHOOLNIK, G. K. 2004. *Mycobacterium tuberculosis* gene expression during adaptation to stationary phase and low-oxygen dormancy. *Tuberculosis (Edinb)*, 84, 218-27.
- WADDELL, S. J., STABLER, R. A., LAING, K., KREMER, L., REYNOLDS, R. C. & BESRA, G. S. 2004. The use of microarray analysis to determine the gene expression profiles of *Mycobacterium tuberculosis* in response to anti-bacterial compounds. *Tuberculosis*, 84, 263-274.
- WALKER, T. M., IP, C. L., HARRELL, R. H., EVANS, J. T., KAPATAI, G., DEDICOAT, M. J., EYRE, D. W., WILSON, D. J., HAWKEY, P. M. & CROOK, D. W. 2013. Whole-genome sequencing to delineate *Mycobacterium tuberculosis* outbreaks: a retrospective observational study. *The Lancet Infectious Diseases*, 13, 137-146.

- WANG, Z., GERSTEIN, M. & SNYDER, M. 2009. RNA-Seq: a revolutionary tool for transcriptomics. *Nature Reviews Genetics*, 10, 57-63.
- WAYNE, L. & HAYES, L. 1998. Nitrate reduction as a marker for hypoxic shutdown of *Mycobacterium tuberculosis*. *Tubercle and Lung Disease*, 79, 127-132.
- WAYNE, L. G. 1996. In Vitro Model of Hypoxically Induced Non Replicating Persistence of *Mycobacterium Tuberculosis*. *Methods in Molecular Medicine: Mycobacterium Tuberculosis Protocol*. New York: Humana Press Inc.
- WAYNE, L. G. & HAYES, L. G. 1996. An in vitro model for sequential study of shutdown of *Mycobacterium tuberculosis* through two stages of nonreplicating persistence. *Infect Immun*, 64, 2062-9.
- WAYNE, L. G. & SOHASKEY, C. D. 2001. Nonreplicating persistence of *Mycobacterium tuberculosis* 1. *Annual Reviews in Microbiology*, 55, 139-163.
- WAYNE, L. G. & SRAMEK, H. A. 1994. Metronidazole is bactericidal to dormant cells of *Mycobacterium tuberculosis*. *Antimicrobial Agents and Chemotherapy*, 38, 2054-2058.
- WEI, J.-R. & RUBIN, E. J. 2008. The many roads to essential genes. *Tuberculosis*, 88, S19-S24.
- WHALEN, C., HORSBURGH, C. R., HOM, D., LAHART, C., SIMBERKOFF, M. & ELLNER, J. 1995. Accelerated course of human immunodeficiency virus infection after tuberculosis. *American Journal of Respiratory and Critical Care Medicine*, 151, 129-135.
- WHO 2002. An Expanded DOTS Framework for Effective Tuberculosis Control. Geneva: World Health Organization.
- WHO 2007. Use of liquid TB culture and drug susceptibility testing (DST) in low and medium income settings. Geneva: World Health Organization.
- WHO. 2015. WHO- BCG (Tuberculosis) [Online]. World Health Organisation. Available: <http://www.who.int/biologicals/areas/vaccines/bcg/Tuberculosis/en/> [Accessed 20th July 2017].
- WHO 2016. Global tuberculosis report 2016. World Health Organisation.
- WHO. 2017. TB drug resistance types [Online]. World Health Organisation. Available: <http://www.who.int/tb/areas-of-work/drug-resistant-tb/types/en/> [Accessed 20th July 2017].
- WHO 2014 Global strategy and targets for tuberculosis prevention, care and control after 2015. World Health Organisation.
- WHO, S. T. P. 2010. The global plan to stop TB 2011-2015: transforming the fight towards elimination of tuberculosis. World Health Organization, Stop TB Partnership.
- WILLIAMS, E. P., LEE, J.-H., BISHAI, W. R., COLANTUONI, C. & KARAKOUSIS, P. C. 2007. *Mycobacterium tuberculosis* SigF Regulates Genes Encoding Cell Wall-Associated Proteins and Directly Regulates the Transcriptional Regulatory Gene *phoY1*. *Journal of Bacteriology*, 189, 4234-4242.
- WILSON, M., DERISI, J., KRISTENSEN, H.-H., IMBODEN, P., RANE, S., BROWN, P. O. & SCHOOLNIK, G. K. 1999. Exploring drug-induced alterations in gene expression in *Mycobacterium tuberculosis* by microarray hybridization. *Proceedings of the National Academy of Sciences*, 96, 12833-12838.
- WIRTH, T., HILDEBRAND, F., ALLIX-BÉGUEC, C., WÖLBELING, F., KUBICA, T., KREMER, K., VAN SOOLINGEN, D., RÜSCH-GERDES, S., LOCHT, C. &

- BRISSE, S. 2008. Origin, spread and demography of the *Mycobacterium tuberculosis* complex. *PLoS Pathogens*, 4, e1000160.
- WITNEY, A. A., COSGROVE, C. A., ARNOLD, A., HINDS, J., STOKER, N. G. & BUTCHER, P. D. 2016. Clinical use of whole genome sequencing for *Mycobacterium tuberculosis*. *BMC Medicine*, 14, 46.
- WOOLHISER, L., TAMAYO, M. H., WANG, B., GRUPPO, V., BELISLE, J. T., LENAERTS, A. J., BASARABA, R. J. & ORME, I. M. 2007. In vivo adaptation of the Wayne model of latent tuberculosis. *Infect Immun*, 75, 2621-5.
- WOOLHISER, L. K., HOFF, D. R., MARIETTA, K. S., ORME, I. M. & LENAERTS, A. J. 2009. Testing of experimental compounds in a relapse model of tuberculosis using granulocyte-macrophage colony-stimulating factor gene-disrupted mice. *Antimicrobial Agents and Chemotherapy*, 53, 306-308.
- WU, M.-L., GENGENBACHER, M. & DICK, T. 2016. Mild nutrient starvation triggers the development of a small-cell survival morphotype in mycobacteria. *Frontiers in Microbiology*, 7.
- XIE, Z., SIDDIQI, N. & RUBIN, E. J. 2005. Differential antibiotic susceptibilities of starved *Mycobacterium tuberculosis* isolates. *Antimicrobial Agents and Chemotherapy*, 49, 4778-4780.
- XU, J., LAINE, O., MASCIOCCHI, M., MANORANJAN, J., SMITH, J., DU, S. J., EDWARDS, N., ZHU, X., FENSELAU, C. & GAO, L. Y. 2007. A unique *Mycobacterium* ESX-1 protein co-secreted with CFP-10/ESAT-6 and is necessary for inhibiting phagosome maturation. *Molecular Microbiology*, 66, 787-800.
- YAMAMOTO, K., ARAI, H., ISHII, M. & IGARASHI, Y. 2011. Trade-off between oxygen and iron acquisition in bacterial cells at the air-liquid interface. *FEMS Microbiology Ecology*, 77, 83-94.
- YATES, T. A., KHAN, P. Y., KNIGHT, G. M., TAYLOR, J. G., MCHUGH, T. D., LIPMAN, M., WHITE, R. G., COHEN, T., COBELENS, F. G., WOOD, R., MOORE, D. A. J. & ABUBAKAR, I. 2016. The transmission of *Mycobacterium tuberculosis* in high burden settings. *The Lancet Infectious Diseases*, 16, 227-238.
- YE, J., COULOURIS, G., ZARETSKAYA, I., CUTCUTACHE, I., ROZEN, S. & MADDEN, T. L. 2012. Primer-BLAST: A tool to design target-specific primers for polymerase chain reaction. *BMC Bioinformatics*, 13, 134.
- YI, Z., FU, Y., YANG, C., LI, J., LUO, X., CHEN, Q., ZENG, W., JIANG, S., JIANG, Y. & HE, Y. 2007. Recombinant *M. smegmatis* vaccine targeted delivering IL-12/GLS into macrophages can induce specific cellular immunity against *M. tuberculosis* in BALB/c mice. *Vaccine*, 25, 638-648.
- YIHAO, D., HONGYUN, H. & MAODAN, T. 2015. Latency-associated protein Rv2660c of *Mycobacterium tuberculosis* augments expression of proinflammatory cytokines in human macrophages by interacting with TLR2. *Infectious Diseases*, 47, 168-177.
- ZELANTE, T., FALLARINO, F., BISTONI, F., PUCETTI, P. & ROMANI, L. 2009. Indoleamine 2, 3-dioxygenase in infection: the paradox of an evasive strategy that benefits the host. *Microbes and Infection*, 11, 133-141.
- ZHANG, M., GONG, J., LIN, Y. & BARNES, P. F. 1998. Growth of Virulent and Avirulent *Mycobacterium tuberculosis* Strains in Human Macrophages. *Infection and Immunity*, 66, 794-799.

- ZHANG, Y. J., IOERGER, T. R., HUTTENHOWER, C., LONG, J. E., SASSETTI, C. M., SACCHETTINI, J. C. & RUBIN, E. J. 2012. Global assessment of genomic regions required for growth in *Mycobacterium tuberculosis*. *PLoS Pathog*, 8, e1002946.
- ZHANG, Y. J., REDDY, M. C., IOERGER, T. R., ROTHCHILD, A. C., DARTOIS, V., SCHUSTER, B. M., TRAUNER, A., WALLIS, D., GALAVIZ, S., HUTTENHOWER, C., SACCHETTINI, J. C., BEHAR, S. M. & RUBIN, E. J. 2013. Tryptophan biosynthesis protects mycobacteria from CD4 T-cell-mediated killing. *Cell*, 155, 1296-308.
- ZHAO, S., FUNG-LEUNG, W.-P., BITTNER, A., NGO, K. & LIU, X. 2014. Comparison of RNA-Seq and Microarray in Transcriptome Profiling of Activated T Cells. *PLoS One*, 9, e78644.
- ZHENG, M., ÅSLUND, F. & STORZ, G. 1998. Activation of the OxyR transcription factor by reversible disulfide bond formation. *Science*, 279, 1718-1722.
- ZIMMERMAN, M. R. 1979. Pulmonary and osseous tuberculosis in an Egyptian mummy. *Bulletin of the New York Academy of Medicine*, 55, 604.
- ZUMLA, A., GEORGE, A., SHARMA, V., HERBERT, R. H. N., OF ILTON, B. M., OXLEY, A. & OLIVER, M. 2015. The WHO 2014 global tuberculosis report—further to go. *The Lancet Global Health*, 3, e10-e12.